PhD Thesis

School of Chemistry

Cardiff University

Direct synthesis of hydrogen peroxide using monometallic and bimetallic Pd based catalysts supported on TiO_2

Thesis submitted in accordance with the requirements of Cardiff
University for the degree of Doctor of Philosophy by:

Dávid Kovačič

2022

Summary

This thesis explores the direct synthesis of hydrogen peroxide (H_2O_2) from molecular hydrogen and oxygen using Pd-based supported catalysts, under conditions considered unfavourable to H_2O_2 stability, namely in the absence of external additives and at ambient temperature. The direct synthesis of H_2O_2 represents an attractive, more atomically efficient, and environmentally friendly alternative to the current industrial route to H_2O_2 via the anthraquinone oxidation process. However, several issues must be addressed before the direct synthesis process can be considered industrially viable. The main challenge of the process is associated with poor H_2O_2 selectivity of the highly active catalysts as they often display high rates of H_2O_2 degradation, through hydrogenation and decomposition pathway. To inhibit unwanted side reaction and increase selectivity of the catalyst, acid and halide additives are often applied to reaction solution, which leads to additional costs affiliated with removal of these additives, corrosion of the reactor vessel, and metal leaching from the catalyst; which decreases the lifetime and activity of the catalyst. In recent years a growing library of catalysts that display high H_2O_2 selectivity have been reported; however, these earlier studies have utilised complicated catalyst synthesis procedures and still rely on high precious metal loading and the use of sub-ambient temperatures to improve H_2O_2 stability. The aim of this work is focused on utilising conditions that are more likely to be industrially applicable and could result in a decrease in overall process costs. Additionally, novel catalysts were designed and synthesised with a focus on more effective and efficient utilisation of precious metals.

The first part of this work sets out to optimise catalyst formulation and reaction conditions with a focus on monometallic Pd catalysts, prepared by an industrially relevant wet impregnation procedure. It was previously shown that monometallic Pd catalysts are highly active towards synthesis of H_2O_2, although they also typically demonstrate high activity towards competitive degradation reactions. The optimal metal loaded catalyst produced in the work achieved high H_2O_2 synthesis activity of 65 $mol_{H2O2}\ kg_{cat}^{-1}\ h^{-1}$, with no activity to the subsequent degradation of H_2O_2, while avoiding costly secondary metals or the need for external additives previously required to improve catalytic performance. The activity of the catalyst can be attributed to highly dispersed PdO species with mean particle size of 0.7 nm.

The second part of this work is centred around bimetallic supported catalysts and how the addition of secondary metals (Au, Sn, Ni) affect catalytic performance towards H_2O_2 synthesis. The addition of secondary metals to monometallic Pd catalyst is well known to significantly enhance synthesis activity and selectivity of the catalyst towards H_2O_2 and inhibit sequential degradation reactions. To the date, AuPd supported catalyst have been extensively studied in the direct synthesis of H_2O_2, achieving enhanced catalytic performance through synergistic effects and avoiding the requirement of external additives typically required for Pd-only catalyst. In a similar manner to AuPd systems, SnPd and NiPd catalysts have been reported to achieve high H_2O_2 synthesis activities. However, these catalysts have been hindered by the need for extensive and complicated preparation procedures and have typically utilised high metal loadings. Within this work, it is demonstrated that it is possible to synthesise SnPd and NiPd catalysts with high activities of 111 mol_{H2O2} kg_{cat}^{-1} h^{-1} and 55 mol_{H2O2} kg_{cat}^{-1} h^{-1}, respectively, offering comparable synthesis activities to well established AuPd catalysts, under reaction conditions that are unfavourable to H_2O_2 stability.

Acknowledgments

I would like to express my deep gratitude to my research supervisor Professor Graham Hutchings, who provided me in a first place with the opportunity to conduct this research as a member of the Cardiff Catalysis Institute. His guidance, support, and encouragement through my PhD was invaluable.

I extend my deepest gratitude to my co-supervisors. Firstly, Dr Richard Lewis for mentoring me throughout my entire PhD, his willingness to help at any time or give advice as well as his invaluable help during writing of this thesis and for his corrections. Dr Jennifer K. Edwards for her valuable input and advice during experimental work. This thesis would not have been possible without both of your help and therefore thank you so much.

My deepest gratitude goes to Haldor Topsøe and Martin Skov Skjøth-Rasmussen who collaborated on this project and their advice, knowledge and support were vital for progression of my PhD thesis. I would like to thank Dr Qian He and Dr Thomas Davies for the fantastic STEM and TEM images of my catalyst and for the training on the equipment. Dr Ryan Wand and PhD candidate Liqun Kang for their expertise, EXAFS and XANES characterisation of my catalysts. I would like to extend my gratitude to Dr David Morgan for the XPS analysis of the catalysts, his expertise and his time and patience to show me how to use the equipment.

I gratefully acknowledge the staff in the chemistry department at Cardiff University, in particular Steve Morris and Dr Greg Shaw who were always willing to help, when technical issues occurred. I would like to thank all the PhD students and postdocs that I had the privilege to work with, you have all made this experience thoroughly enjoyable. Huge thank you go to hydrogen peroxide team, for the laugh and encouragement. Thanks to you 0.90 was the best place in the University. Special thanks go to Caitlin who started this journey with me and since then she was always there every step of the way.

Most importantly I would like to thank my family and friends who have been a constant support and an inspiration to me, not just during my PhD, but in everything I do. They have always been there for me when I needed them, and I will always be grateful. To my parents and sister, who always encouraged me to keep going and supported me no matter how difficult the task was. To Darren who supported me during the difficult times, especially during the pandemic and who was always there with words of support and kindness. Thank you all for making this journey unforgettable.

Table of Contents

Chapter 3 - The Direct Synthesis of H_2O_2 Using Supported Monometallic….. Palladium Catalysts …………………………………………………….………... 63

Chapter 4 - The Direct Synthesis of H_2O_2 Using Supported Bimetallic Catalysts…... 131

Chapter 5 - Conclusion and future work ……………………………...…. 168

Chapter 1

Introduction

This chapter outlines principles of catalysis along with the use and production of H_2O_2, and developments in the direct synthesis of H_2O_2.

1.1 Overview

H_2O_2 is a widely used chemical with many industrial applications, with the estimated production of 4.5 million metric tonnes of H_2O_2 in 2020.[1,2] The only degradation product of its use is H_2O and therefore H_2O_2 is used in many environmentally friendly processes in chemical industry, replacing chlorine-based bleaches or toxic oxidizing agents. On the industrial scale, H_2O_2 is manufactured via anthraquinone oxidation process (AO).[3,4] IG Farbenindustrie in Germany operated the first commercial plant in early 1940s. This process involves hydrogenation and subsequent oxidation of an alkyl anthraquinone, followed by liquid–liquid extraction to recover H_2O_2. Despite H_2O_2 being considered as environmentally friendly chemical, the AO process itself cannot be considered as a green chemical process, as it uses complex organic solvents, and so only large scale production is economically viable and large quantities of waste are generated.[5]

The direct synthesis of H_2O_2 from hydrogen and oxygen in the presence of a catalyst offers a cleaner, more atom-efficient alternative to the current commercial production and overcomes the extensive disadvantages of the anthraquinone process. Despite extensive research carried out for the last 100 years, there is still no industrial process based on the direct synthesis approach, due to a couple main drawbacks.[6] The first one is that H_2/O_2 gas mixtures are explosive over a wide range of concentrations (5-95 v/v% for H_2 in O_2) and in order to operate in safe conditions, the reaction is carried out below the lower explosive limit.[7] To achieve this condition, the reagent gases have to be diluted in inert gases such as N_2 or CO_2[5,8,9]. The second drawback is that catalysts active for the direct synthesis reaction (1) are almost always active for the parallel combustion of H_2 and O_2 (2) and subsequent hydrogenation (3) and decomposition (4) of H_2O_2, as shown in Figure 1.1.

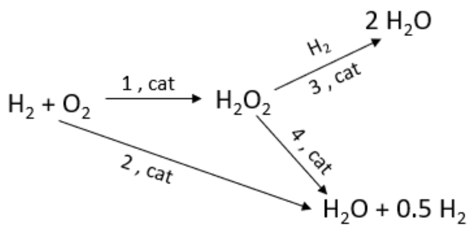

Figure 0.1: Reaction pathways of direct synthesis of hydrogen peroxide.

All side reactions are thermodynamically more favoured than the synthesis reaction, and they can be catalysed by the same catalyst. Formation of water affects the selectivity of the catalyst towards H_2O_2 and decreases effectiveness of hydrogen utilization. To commercialize the direct synthesis process, it is necessary to obtain selectivity towards H_2O_2 above 95% and the catalyst must have minimal or no activity for the unwanted competing reactions.

$$H_2 + O_2 \rightarrow H_2O_2 \qquad \Delta H^\circ_{298K} = -135.9\ \mathrm{kJ\ mol^{-1}}\ , \Delta G^\circ_{298K} = -120.4\ \mathrm{kJ\ mol^{-1}} \tag{1}$$

$$H_2 + O_2 \rightarrow H_2O + 0.5\ O_2 \qquad \Delta H^\circ_{298K} = -241.6\ \mathrm{kJ\ mol^{-1}}\ , \Delta G^\circ_{298K} = -237.2\ \mathrm{kJ\ mol^{-1}} \tag{2}$$

$$H_2O_2 + H_2 \rightarrow 2H_2O \qquad \Delta H^\circ_{298K} = -211.5\ \mathrm{kJ\ mol^{-1}}\ , \Delta G^\circ_{298K} = -354.0\ \mathrm{kJ\ mol^{-1}} \tag{3}$$

$$H_2O_2 \rightarrow H_2O + 0.5O_2 \qquad \Delta H^\circ_{298K} = -105.8\ \mathrm{kJ\ mol^{-1}}\ , \Delta G^\circ_{298K} = -116.8\ \mathrm{kJ\ mol^{-1}} \tag{4}$$

The design of the catalysts for direct synthesis of H_2O_2 needs consider a balance between synthesis activity and H_2O_2 selectivity, as well as selection of reaction condition, solvent system, and choice of diluent. Research into the direct synthesis of H_2O_2 has focused on Pd based catalysts.[6,11,12] Bimetallic AuPd catalysts have been extensively studied as combining Pd with Au enhances catalyst synthesis activity, and can affect subsequential degradation reactions.[13] It was reported that addition of different secondary metals such as Sn, Ni, Sb or Zn can modify the electronic structure or geometric surface of Pd catalysts, resulting in increased H_2O_2 selectivity.[14–18]

Reaction conditions play a crucial role in the amount of H_2O_2 produced during a reaction. It was shown that different catalysts may have different optimal reaction conditions that can significantly affect synthesis activity of the catalyst.[19] Hutchings and co-workers identified low reaction temperatures (2°C) and short reaction times (0.5 h) as the key factors that favour high selectivity towards H_2O_2.[20–22] Use of CO_2 as diluent can increase stability of H_2O_2, as it dissolves in the solvent leading to the formation of carbonic acid under the reaction conditions, which act as a promoter for direct synthesis of H_2O_2.[23]

In this work, catalyst design and conditions for direct synthesis of H_2O_2 has been investigated. The first part of the work focuses on use of monometallic Pd catalyst. Catalyst design and reaction conditions have been optimised to maximise synthesis activity as well as minimise the degradation activity of the catalyst at ambient temperature, which is the temperature preferred for industrial applications.

The second part of this work is concerned with direct synthesis of H_2O_2 using bimetallic AuPd, SnPd and NiPd catalysts supported on TiO_2. Catalyst design was investigated to improve synthesis activity using optimised reaction conditions obtained in the previous work. To maximise H_2O_2 concentration obtained during the reaction different reaction times and amount of gas replacement reaction were used. Addition of a cheaper secondary metal such as Sn or Ni presents a cheaper alternative to well established AuPd catalysts.

1.2 Definition of catalysis

1.2.1 Basic concepts of catalysis

The importance of catalysis in modern society is undeniable and it is crucial to every area of daily life. Approximately 85% of all products manufactured involve catalysis in their production chain, with applications in areas such as energy, transport, healthcare or environment.[24] These catalytic processes involve the production of fuels, bulk and fine chemicals, pharmaceuticals, new materials, but also prevention of pollution formation and decreasing contamination in natural sources. Chemical processes using catalyst have estimated economic impact of 30-40% global GDP.[25]

A catalyst is a substance that converts reactants, through a series of steps, in which the catalyst participates and is recovered in its original form at the end of the cycle. A catalyst accelerates a chemical reaction but does not change the thermodynamics. Catalysts vary from atoms and molecules to large structures such as zeolites or enzymes. In homogeneous catalysis, reactants and products are all present in the same phase. Biocatalysis uses enzymes, a large protein with a shape-specific active sites as a highly specific and efficient catalysts. In heterogeneous catalysis, the catalyst exists in a different phase to that of the reactants; the catalyst is usually solid, and the reactants are either liquids or gases.

Figure 1.2 compares the potential energy of a general non-catalytic and catalytic reaction. The non-catalytic reaction only proceeds when reactants collide with sufficient energy to overcome the substantial energy barrier. The catalytic reaction offers an alternative but much more complex path consisting of multiple steps. The first step is a diffusion of reactants through the boundary layer surrounding the catalyst particle. Next, this is followed by interparticle diffusion, in which reactants move to active sites. In the next step, reactants adsorb onto active sites of the catalyst. Next, this is followed by reactions involving formation of intermediates and products. This step requires an energy barrier, called the activation energy (ΔE_{cat}), to be overcome. However, the activation energy of a catalysed reaction is lower than the activation energy of the uncatalyzed reaction. In the final series of steps, products are desorbed from the catalyst sites, followed by intraparticle diffusion and then products are diffused across the boundary layer into the bulk.

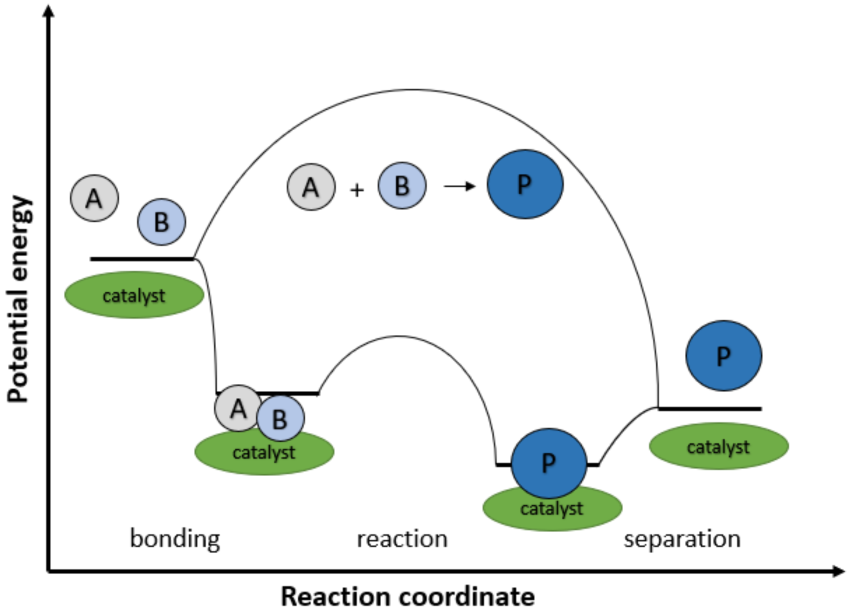

Figure 0.2: Potential energy diagram of a heterogeneous catalytic reaction.

As shown in Figure 1.2, the activation energy of the catalytic reaction is significantly smaller than that of the uncatalyzed reaction and therefore the rate of the catalysed reaction is larger than uncatalyzed one. However, the overall change in Gibbs free energy (ΔG) is the same for the catalysed and uncatalyzed reaction. The Gibbs free energy can be defined as the thermodynamic function of a system that is equal to the enthalpy (H) minus the product of the absolute temperature (T) and entropy (S), and an exact definition of G is therefore given by:

$$\Delta G = \Delta H - T\Delta S \quad (5)$$

If the heat is released during the reaction, the reaction is exothermic and the change in enthalpy is negative ($\Delta H < 0$). A chemical reaction with negative free energy ($\Delta G < 0$) is called exergonic and is associated with release of free energy. This type of reaction is spontaneous and can proceed without any energy input. In contrast, an endothermic reaction ($\Delta H>0$) consumes heat, and a reaction with positive $\Delta G > 0$ is called endergonic and needs an energy input to take place. A catalyst should provide good selectivity towards the desired products and minimal production of undesired by-products of the reaction. The catalyst should have a good accessibility of active sites for the reactants and products. The stability of the catalyst at desired reaction conditions is a very important factor and adequate rates of reaction at chosen reaction conditions are required, so that high yields of product are obtained.

1.2.2 Nanoparticle catalysis

The International Organisation for Standardisation defined nanoparticle as an object with any dimensions in the nanoscale – size range from approximately 1 nm to 100 nm. Commission of the European Union defined nanomaterial as material with one or more external dimensions in the size range of 1 nm to 100 nm.[128] Due to a high potential, nanoparticles have been applied in different areas such as catalysis, electrocatalysis, filters, sensors, nanoscale electronics, cosmetics, fuel cells, environment, energy, optoelectronics and water purification.[129-131]

The nanoparticles (NPs) have properties distinctly different from their bulk and molecular counterparts. The laws of classical physics cannot be used for most of the phenomena that occur on a surface with a diameter of less than 10 nm, and as a result electronic, optical and magnetic properties of the materials, in this range will change. The quantum size effects become more significant when the de-Broglie wavelength of valence electrons (λ) and the size of the particle (d) are of the same order.[131]

Aggregation of the NPs presents a major challenge to the preparation and performance of NPs catalysts. This can be addressed by using support or media for dispersion in order to obtain a high surface area. It is highly desirable to reduce the amount of metal in metal-based catalysts to reduce the cost or potential toxicity of the catalyst. Fine sized nanocrystals have an increase in surface to volume (A/V) ratios leading to higher catalytic activity compared to larger crystals of the same mass present on the surface.

Large specific surface area of nanoparticles is an important property for the reactivity, solubility, sintering performance, etc.[132] Smaller particles have more edges and kinks than larger particles, which also contributes to different reactivity of NPs compared to larger particles.[133] Small NPs can also provide a tremendous driving force for diffusion especially at elevated temperatures and can reduce the incipient melting temperature.[134]

1.2.3 Concept of green chemistry

The concept of green chemistry refers to the "to design of chemical products and processes to reduce or eliminate the use and generation of hazardous substances."[27] The main aim of green chemistry is the reduction of hazards across all stages of a life cycle of chemical product or process. Risk may rise from the nature of the materials used in the process or the chemical process itself, as well as the final products and their disposal. The twelve principles of green chemistry were developed by Paul Anastas and John Warner in 1998 and they serve as a guiding framework for developing greener and more sustainable processes and products.[28] The 12 principles are:

1. Prevention.
2. Atom economy.
3. Less hazardous chemicals synthesis.
4. Designing safer chemicals.
5. Safer solvents and auxiliaries.
6. Design for energy efficiency.
7. Use of renewable feedstock.
8. Reduce derivatives.
9. Catalysis.
10. Design for degradation.
11. Real time analysis for pollution prevention.
12. Inherently safer chemistry for accident prevention.

1.3 Hydrogen peroxide

Hydrogen peroxide is one of the cleanest and most versatile chemicals available, with many industrial applications.[29] As an oxidising agent, H_2O_2 is effective over the whole pH range. It has also a high active oxygen content and is considered to be one of the greenest chemicals, since water is the only degradation product.[30] H_2O_2 is a more efficient oxidizing agent than many other industrially used oxidants, such as nitric acid and sodium hypochlorite as shown in Table 1.1.[5]

Table 1.1: Common industrial oxidants, their active oxygen content, and by-products.[5]

Oxidant	Active oxygen [% w/w]	By-product
H_2O_2	47.1	H_2O

*t*BuOOH	17.8	*t*BuOH
HNO_3	25.0	NO_x, N_2O, N_2
N_2O	36.4	N_2
NaClO	21.6	NaCl
$NaClO_2$	35.6	NaCl
NaBrO	13.4	NaBr

One of the most important industrial applications of H_2O_2 is use in paper and pulp bleaching, as well as textile industry and in the manufacture of chemicals such as sodium perborate and sodium percarbonate.[31–33] In the paper and pulp bleaching sector, H_2O_2 is applied in chemical and mechanical pulp bleaching and also can be used in the bleaching of recycled paper. Its use represents an environmental approach to this process, replacing chlorine-based bleaches and reduces the cost of the production and provides improved quality.[32,33] H_2O_2 is also widely used for the treatment of a whole range of natural and synthetic fibres. It has replaced sodium hypochlorite bleaches due to its lack of toxicity, while its noncorrosive nature results in a high degree of brightness and does not result in fibre damage.[34] The main applications of H_2O_2 are summarised in Figure 1.3.

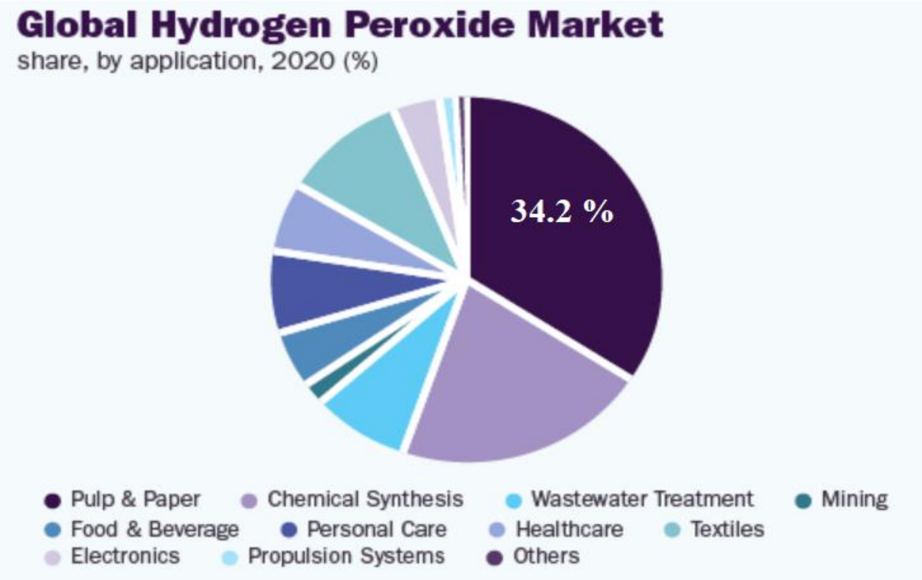

Figure 1.3: Industrial applications of H_2O_2 in 2020.[35]

Environmental applications of H_2O_2 includes waste water and industrial process water treatment, since H_2O_2 can efficiently destroy thiocyanate, chlorine, organic matter and remove sulphides and hydrogen sulphide present in the industrial wastewater.[36–39] Advanced oxidation processes (AOP) use H_2O_2 to generate high reactive hydroxyl radicals to treat various refinery effluents and waste water from chemical and pharmaceutical synthesis.[1,40] Nitrogen oxides, such as nitric oxide and nitrogen dioxide, are major pollutants in atmosphere, which can be removed using H_2O_2 as a part of the scrubbing solution.[41,42]

Several applications of H_2O_2 are also found in cosmetics as an antimicrobial agent, in hair colouring to lighten the hair, oxygenate stains on teeth to increase whiteness, as a green oxidant for the production of numerous valuable compounds. High purity H_2O_2 is used as oxidizing and cleaning agent in the manufacture of semiconductors and in the production of circuit boards.

There is increasing demand for H_2O_2 as there is a potential application in large volume chemical synthesis, such as the epoxidation[43,44] of propylene to propylene oxide or ammoximation of cyclohexanone to its corresponding oxime.[45] Propene oxide, mainly used for the production of polyurethane, polyether polyols and propene glycols, is produced by two different industrial processes: the chlorhydrin process[46] and the hydroperoxidation process.[43] Due to the negative impact of chlorhydrin on the environment, the hydroperoxidation process is mainly used for production of propene oxide. However, co-products are produced in a volume approximately 3 times larger than that of propene oxide, so the economy of this process primarily depends on the marketability of co-products.[5,43] Eco-friendly process of H_2O_2 to propylene oxide (HPPO) is using H_2O_2 as an oxidizing agent in a single step propylene epoxidation over TS-1 catalyst with water as the only by-product.[5,47]

1.4 Industrial manufacture of H_2O_2

Since its discovery by Louis Jacques Thenard in 1818[5], H_2O_2 has become an extremely valuable commodity with many applications. Thenard's process produced low concentrations of aqueous H_2O_2 by reaction of barium peroxide with nitric acid and addition of hydrochloric acid can significantly improve this process.[29] This process is considered as the first commercial manufacture of aqueous H_2O_2 and was still used until the middle of 20th century. Thenard's process to obtain H_2O_2 is summarised in equations 6-8:

$$\mathrm{BaO_2 + 2\,HCl \rightarrow BaCl_2 + H_2O_2} \tag{6}$$

$$\mathrm{BaCl_2 + H_2SO_4 \rightarrow BaSO_4 + 2\,HCl} \tag{7}$$

$$\mathrm{BaO_2 + H_2SO_4 \rightarrow BaSO_4 + H_2O_2} \tag{8}$$

However, some drawbacks were associated with Thenard's process. Mainly, only small concentration of H_2O_2 (3% mass/mass, aqueous) is manufactured using BaO_2, resulting in high production costs. Further, the isolated H_2O_2 had very poor stability due to large volume of impurities.

In 1853 Meidinger discovered electrolytical formation of H_2O_2 from aqueous sulphuric acid, which addressed the disadvantages of the process discovered by Thenard.[48] Berthelot later showed that the intermediate formed during electrolytical formation of H_2O_2 was peroxodisulfuric acid. H_2SO_5 was subsequently hydrolysed to H_2O_2 and sulphuric acid. [48] The electrolytical formation of H_2O_2 is shown in equations 9-12:

$$2\ \mathrm{H_2SO_4} \rightarrow \mathrm{H_2S_2O_8} + \mathrm{H_2} \tag{9}$$

$$\mathrm{H_2S_2O_8} + \mathrm{H_2O} \rightarrow \mathrm{H_2SO_5} + \mathrm{H_2SO_4} \tag{10}$$

$$\mathrm{H_2SO_5} + \mathrm{H_2O} \rightarrow \mathrm{H_2O_2} + \mathrm{H_2SO_4} \tag{11}$$

$$2\mathrm{H_2O} \rightarrow \mathrm{H_2O_2} + \mathrm{H_2} \tag{12}$$

In 1901, Manchot discovered that under alkaline conditions autoxidizable compounds such as hydroquinones or hydrazobenzenes react quantitatively to form peroxides.[49] Production of H_2O_2 via alternating oxidation and reduction of hydrazobenzenes was proposed by Walton and Filson in 1932.[50] The alkaline autoxidation of hydrazobenzenes obtaining sodium peroxide was developed by Pfleiderer and was further developed by Riedl, who employed polynuclear hydroquinones.

Currently, most of the H_2O_2 is industrially produced by an anthraquinone auto oxidation process (AO process). This process was developed by Hans-Joachium Riedl and George Pfleiderer of BASF in 1939 and consist of sequential hydrogenation and oxidation of an alkylanthraquinone precursor dissolved in a mixture of organic solvents.[51] A 2-alkylanthraquinone (AQ), usually ethylanthraquinone, is hydrogenated using a nickel or palladium catalyst to form a anthrahydroquinone (AHQ). The AHQ dissolved in an organic solution is then separated from the catalyst. The anthraquinone is reformed by oxidation with air and H_2O_2 is produced as a by-product.[5] A simplified diagram of the process is illustrated in Figure 1.4, and the main reactions involved in the synthesis are shown in Figure 1.5.

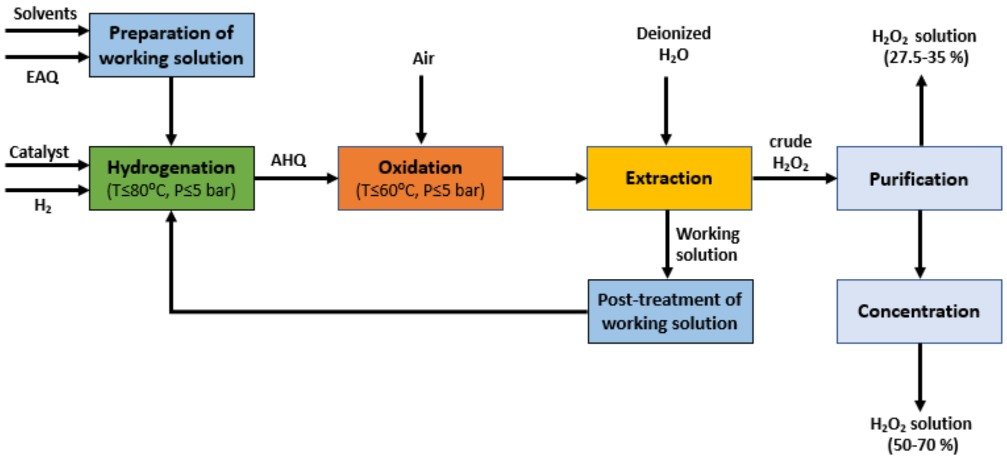

Figure 0.4: Schematic diagram of AO process for the production of H_2O_2.[3]

In the next step H_2O_2 is extracted from the working solution by demineralized water to produce a solution that is usually 30% by weight of H_2O_2. As a final treatment, the aqueous solution is then distilled to remove impurities and increase the concentration of hydrogen peroxide up to 50-70 wt. %. The water content in the working organic solution is reduced and the anthraquinone by-products are reactivated or replaced by fresh anthraquinone.[52,53]

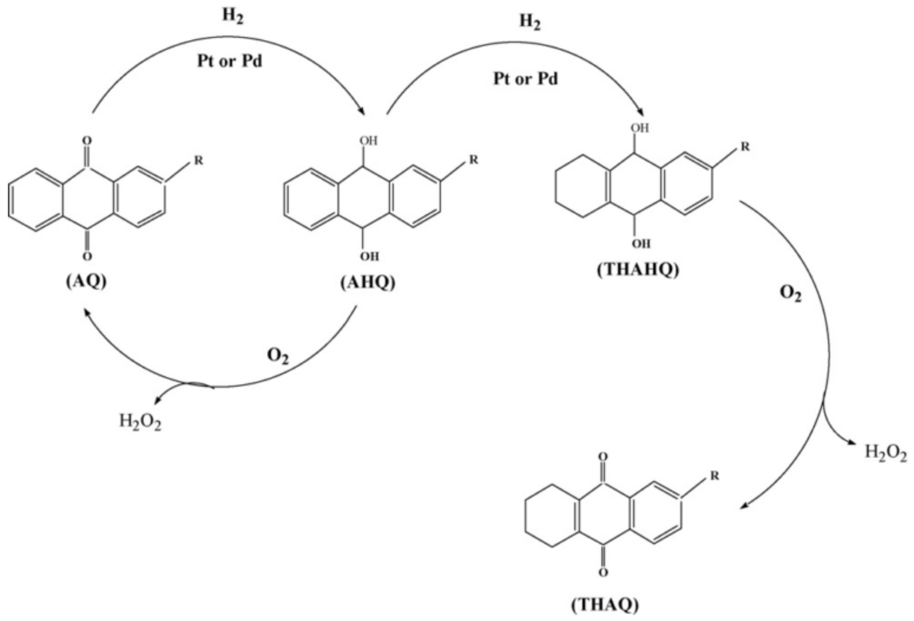

Figure 0.5: Main reactions involved in anthraquinone process.[54]

Due to the high yield of H_2O_2 per cycle, the AO process has been industrially used for several decades and currently over 95 % of H_2O_2 is produced by this process.[55] However, this process can be hardly considered as environmentally friendly. The main disadvantages of the process are its use of complex organic solvents as the working solution, deactivation of the hydrogenation catalyst and replacement of nonactive derivatives of anthraquinone formed during the reaction. The separation steps involve the removal of organic impurities from the H_2O_2 product and reduction of water content.[5,52] The anthraquinone process is only economically viable via large scale production and highly concentrated solutions of H_2O_2 (70 wt. %) are obtained. Most applications use solutions with low concentration of H_2O_2, around 2 to 8 wt. %.[8] Furthermore, transportation and storage of concentrated solutions can be hazardous and additives must be applied to stabilize them.[5,8,10,54]

1.5 Palladium based catalysts in the synthesis of H_2O_2

Since the first patent granted in 1914 to Henkel and Weber, the direct synthesis of H_2O_2 has been an area of great research interest. This patent describes the use of Pd catalysts, demonstrating the possibility to achieve high concentrations of H_2O_2[6]. Still centuries later, Pd based catalysts are at the centre of investigation and most of the important developments in direct synthesis are based upon these catalysts.[6,56–60] In early work for the direct synthesis of H_2O_2, mixtures of gases within the explosive region were exploited. Working within this region led to formation of concentrated solutions of H_2O_2. Gosser and Schwartz obtained solutions with high concentration of H_2O_2 (>35 wt.%) over supported Pd catalysts at elevated pressures.[61] However, commercial operation in these process conditions would be extremely dangerous due to high possibility of explosion.[6,9] Typically, diluted mixtures of H_2/O_2 have been utilised, which present much safer working conditions but also leads to lower concentrations of produced H_2O_2.[9,10,60] The contact between H_2 and O_2 could be prevented by a catalytic membrane, which would allow use of pure gases and result in higher concentration of produced H_2O_2.[62]

The mechanism and the kinetics of H_2O_2 synthesis and degradation have been studied extensively.[57,58,63–66] It has been assumed that the formation of H_2O_2 takes place via a two-step hydrogenation mechanism.[58,64,67,68] In the direst synthesis of H_2O_2 multiple reactions take place simultaneously. These reactions can be divided into four groups:

1. Production of H_2O_2 from H_2 and O_2
2. Production of H_2O from H_2 and O_2
3. Decomposition of H_2O
4. Reduction of H_2O_2 by H_2

Bimolecular reactions occur between liquid-phase species, as H^+, and chemisorbed surface intermediates. The possible elementary steps are shown below in Figure 1.6, in which * represents empty site, X* represents an adsorbate bound to a single Pd atom and X** denotes an intermediate adsorbed in an η^2 configuration.

$$H_2 + 2^* \underset{k_{-1}}{\overset{k_1}{\rightleftarrows}} 2H^* \tag{13}$$

$$H^* \underset{k_{-2}}{\overset{k_2}{\rightleftarrows}} H^+ + e^- + {}^* \tag{14}$$

$$O_2 + {}^{**} \underset{k_{-3}}{\overset{k_3}{\rightleftarrows}} O_2{}^{**} \tag{15}$$

$$O_2^{**} + H^+ + e\text{-} \underset{k_{-4}}{\overset{k_4}{\rightleftarrows}} OOH^{**} \tag{16}$$

$$OOH^{**} + H^+ + e\text{-} \underset{k_{-5}}{\overset{k_5}{\rightleftarrows}} H_2O_2^{**} \tag{17}$$

$$H_2O_2^{**} \underset{k_{-6}}{\overset{k_6}{\rightleftarrows}} H_2O_2 + {}^{**} \tag{18}$$

$$O_2^{**} \overset{k_7}{\rightarrow} 2O^* \tag{19}$$

$$OOH^{**} \overset{k_8}{\rightarrow} OH^* + O^* \tag{20}$$

$$O^* + H^* \overset{k_9}{\rightarrow} OH^* + {}^* \tag{21}$$

$$OH^* + H^* \overset{k_{10}}{\longrightarrow} H_2O^* + {}^* \tag{22}$$

$$H_2O^* \underset{k_{-11}}{\overset{k_{11}}{\rightleftarrows}} H_2O + {}^* \tag{23}$$

$$H_2O_2^{**} \underset{k_{-12}}{\overset{k_{12}}{\rightleftarrows}} 2OH^* \tag{24}$$

Scheme 1.1: Proposed series of elementary steps during direct synthesis of H_2O_2 Pd clusters. *is an empty site, X* represents an adsorbate bound to a single Pd atom, X** denotes an intermediate adsorbed in an η^2 configuration, the equilibrium arrows (⇄) indicate that an elementary step is quasi-equilibrated, and k_x is the rate constant for elementary step x.[58]

These elementary steps are based on two assumptions:

1. The free energy of H_2 and O_2 adsorption is negligible under saturation conditions.
2. The rates of adsorption and desorption of the H_2O_2 species are greater than measured turnover rates.

First step (13) in the proposed scheme (Scheme 1.1) represents dissociative adsorption of H_2 followed by heterolytic H^* oxidation (Step 14). Step 15 shows molecular adsorption of O_2 on Pd cluster. Subsequently, the $O_2{}^{**}$ intermediate in step 15 undergoes either quasi-equilibrated proton−electron transfer (Step 16) to form hydroperoxyl OOH^{**}, or irreversibly cleaves the

O−O bond (Step 19) to form chemisorbed oxygen atoms O^*. In a case of formation of OOH^{**}, this step is followed by proton electron transfer (Step 17) forming adsorbed $H_2O_2^{**}$ molecule that is desorbed in the step 18. Irreversible O-O bond cleavage in O_2^{**} (Step 19), OOH^{**} (Step 20) and $H_2O_2^{**}$(Step 24) is followed by hydrogenation of O^* and OH^* species in steps 21 and 22, to form H_2O^* that desorbs in step 23. As shown in Scheme 1.1, multiple steps are proposed to take place during formation of H_2O_2. Steps 16 and 17 represents proton-electron transfer mechanism as the primary pathway for H_2O_2 formation, and cleavage of the O-O bond in steps 19 and 20 is mainly responsible for H_2O formation.[58,68]

One of the first reaction mechanisms of direct synthesis of H_2O_2 from H_2 and O_2 over a Pd based catalyst was proposed by Pospelova *et al.*[69] In this three-step mechanism, H_2 molecules dissociate on the surface of the Pd catalyst. Then, adsorbed O_2 molecules react with H atoms forming HO_2 adsorbed intermediate species. In the last step these intermediates react with H atoms and form H_2O_2 molecules on the surface of the catalyst.

Lunsford *et al.* carried out experiments using a mixture of $^{16}O_2$ and $^{18}O_2$ to see whether a dissociated form of O_2 is involved in formation of H_2O_2. Raman spectroscopy was used to determine the isotopic distribution in the product and results showed that only $H_2{}^{16}O_2$ were present. This result suggested that H_2O_2 is derived from a diatomic form of O_2 that is adsorbed on the Pd.[56] This observation is consistent with the proposed mechanism by Pospelova *et al*. Based on the catalytic cycle proposed by Stahl *et al.*[70], Lunsford *et al.* proposed a catalytic cycle for direct synthesis of H_2O_2 over Pd/SiO_2 in 0.1 N HCl, as illustrated in Figure 1.6.[66] Colloidal palladium is formed from a Pd/ SiO_2 catalyst in the presence of HCl during the direct synthesis process. Pd^0 reacts with O_2 in the presence of chloride ions to form a dichloroperoxopalladium(II) complex. This complex subsequently reacts with H_3O^+ forming H_2O_2 and $PdCl_4^{2-}$. In the next step, $PdCl_4^{2-}$ is reduced back to colloidal state by H_2 and HCl is also formed in this step.

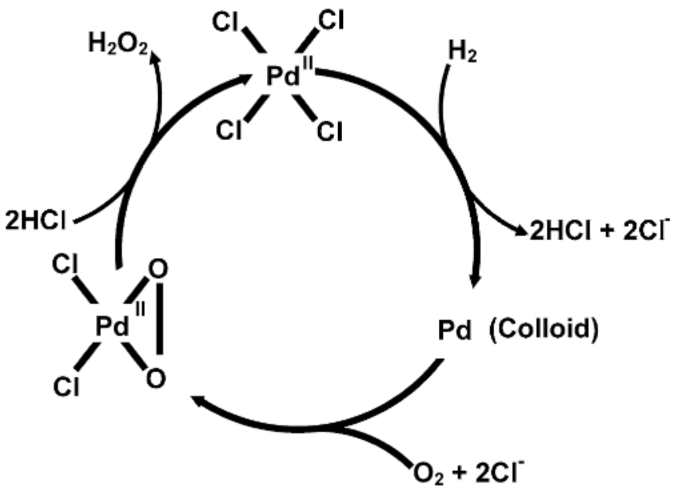

Figure 1.6: Proposed catalytic cycle for direct synthesis of H_2O_2 formation over Pd.[66]

Yoshizava *et al.* investigated the direct synthesis of H_2O_2 on Pd and Pd/Au catalysts by theoretical calculation using first-principle DFT methods.[64] In this mechanism it was assumed that the starting geometry for H addition to O_2 molecule was superoxo precursor state. Next, the OOH intermediate is formed. In the superoxo state the oxygen molecule accepts an electron from the surface[71] and reacts as a monoradical with atomic H. In the second step, the intermediate reacts with the second H situated over the nearest 3-fold position. During this process, the competitive reaction of O_2 dissociation occurs leading to formation of H_2O. This dissociation may be blocked by presence of surface Au. Todorovic and Meyer conducted a comparative density functional study of direct synthesis of H_2O_2 on different metal surfaces.[72] They concluded that O_2 must be adsorbed molecularly on the metal surface and therefore that active and selective H_2O_2 catalyst must have a high energy barrier to O_2 dissociation. In contrast, H_2 must adsorb dissociatively with a low energy barrier.

Similar conclusions were obtained by Abate *et al.*, with their proposed reaction scheme illustrated in Figure 1.7.[73] Here, the O_2 molecule is considered to chemisorb onto a Pd particle without dissociation. In the next step, protonation from external H^+ occurs, followed by reaction with a H_2 that is not chemisorbed. This leads to formation of H_2O_2 and finally H^+ is restored. In contrary, more energetic sites such as edges, corners or defects of Pd clusters, will dissociatively chemisorb O_2. For the high selectivity towards H_2O_2 only non-chemisorbed H_2 is required. The presence of chemisorbed H_2 will lead to production of H_2O, via the direct reaction with O or OH species. Radical pathways could be inhibited by promoters such as halide ions.

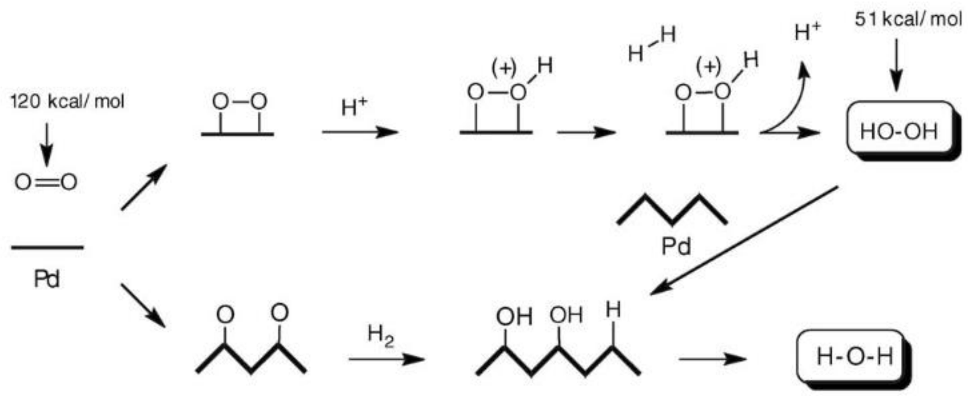

Figure 1.7: Direct synthesis of H_2O_2 mechanism over Pd catalyst proposed by Adate et al.[73]

Flaherty *et al.* reported a mechanistic study of steady state H_2O_2 and H_2O formation as function of reactant pressure and solvent properties.[58,67] They showed that H_2O_2 was only produced in presence of protic solvents (water, methanol) and no H_2O_2 was detected in tested aprotic solvents (acetonitrile, dimethyl sulfoxide and propylene carbonate). Based on these observations, they suggested a reaction mechanism, shown in Figure 1.8, in which protic solvents, such as water or methanol may participate directly in H_2O_2 formation. According to the proposed mechanism, the protic solvent introduces low barrier pathways for O_2^* reduction. H_2 is necessary as reductant. Protons are formed by heterolytic oxidation of H_2 and shuttled via oxonium species during reduction of O_2 to H_2O_2.

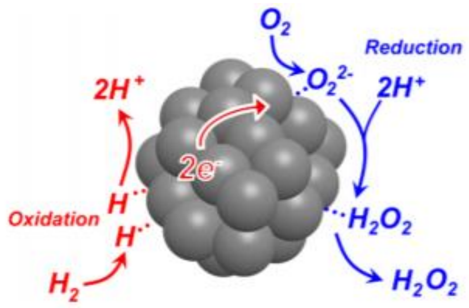

Figure 1.8 Direct synthesis of H_2O_2 mechanism over Pd clusters proposed by Flaherty et al.[58]

Zhou *et al.* claimed that the selective exposition of specific desired crystal phases or faces of the noble metal on the support was found to be a critical factor for improvement of the catalyst and its activity.[74] They proposed that, for selective formation of H_2O_2, the {110} facet of Pd has desired atomic configuration. On the other hand, {100} and {111} facets have higher probability of H_2O formation, decreasing the selectivity towards H_2O_2. Kim *et al.* suggested that the Pd {111} facet is more favourable than {100} in H_2O_2 synthesis, because the {100} Pd facet is superior in dissociation of O-O bond in O_2, OOH and H_2O_2.[75]

Tian *et al.* performed Density functional theory (DFT) calculations to study the direct synthesis of H_2O_2 on {111}, {100} and {110} surfaces.[76] Their results showed that the atomic densities decrease in order Pd {111}, Pd {100} and Pd {110}. In addition, the order of the OOH dissociation barriers is Pd {111}>Pd {100}>Pd {110} and the order of the O_2 dissociation barriers is Pd {111}>Pd {110}>Pd {100}. Among the studied Pd surfaces, Pd {111} showed the highest density of surface atoms, the lowest surface energy and this surface exhibits the highest selectivity towards H_2O_2. Iwamoto *et al.* calculated using DFT that less saturated sites, such as corners and edges, are more likely to result in H_2O production, while more saturated sites like Pd{111} are beneficial to produce H_2O_2.[77]

Lunsford *et al.* have shown that Pd supported on micro spheroidal silica is an effective source of colloidal Pd, suggesting that colloidal Pd is the principal catalytic component for direct synthesis of H_2O_2.[56,78] Their results showed that the rate of H_2O_2 production is proportional to the Pd colloid concentration.[11] The Pd particles dissolved into Pd^{2+} complexes ($PdCl_4^{2-}$) and redistributed as nanometre sized Pd colloids in the presence of HCl, as shown in Figure 1.6. The Pd is believed to be distributed between its several states based on partial pressure of H_2 and O_2 and are responsible for different rates in H_2O_2 production.[56] The rates of H_2O_2 over colloidal Pd were constant for 3-5 h, but afterwards the rates, as well as concentration of colloids, were continuously decreasing. The attempt to stabilize colloids was made using sodium citrate or polyvinyl alcohol without success.[11]

Choudary *et al.* extensively investigated the oxidation state of Pd species through modification of catalyst support (ZrO_2, Ga_2O_3, CeO_2, SiO_2, H-β, ThO_2, CeO_2, ZrO_2, BPO_4, Al_2O_3), the use of additives (KBr, KCl, KF, H_3PO_4) and precious metal additives (Au, Rh, Ru).[79–84] When Pd was presented in Pd^0 (reduced form), higher conversion of H_2 were achieved compared to PdO state (oxidized form). However, Pd presented as PdO had considerably higher selectivity towards H_2O_2 formation.[85] In addition, the decomposition activity of the oxidized form was found to be an order of magnitude less than the reduced form, which may be attributed to the higher propensity for H_2O_2 adsorption on reduced sites.[85] For example, almost no H_2O_2 was formed and low selectivity was achieved when Al_2O_3 was used as a support over reduced Pd. However, once the catalyst was oxidised (static air, 500 °C, 3 h), higher yields of H_2O_2 were obtained with selectivity around 37% and significantly lower decomposition activity. Similar results were obtained over a whole range of supports as illustrated in Figure 1.9. In conclusion, the presence of bulk or sub-surface PdO makes the supported Pd catalyst more selective and active towards H_2O_2 formation.[80] This was in agreement with observations made by Hutchings and co-workers, who concluded that for high selectivity of H_2O_2 it is essential that Pd is present in the cationic form.[9]

As shown in Figure 1.9, the choice of support plays significant role for direct synthesis of H_2O_2 and can affect the conversion, yield and selectivity.[79,84] A strong influence of the calcination temperature on the H_2O_2 formation activity was observed upon different catalyst supports. The best catalyst performance (except PdO/CeO_2) was achieved when the catalyst was calcined at 400 °C. The variation in catalysts activity with different calcination temperatures may be due to change in Pd particle size, which is strongly influenced by calcination temperature and due to catalyst support interaction. Both the H_2O_2 decomposition and hydrogenation rates increased with increasing calcination temperature, while the H_2O_2 formation rate was decreasing. [84]

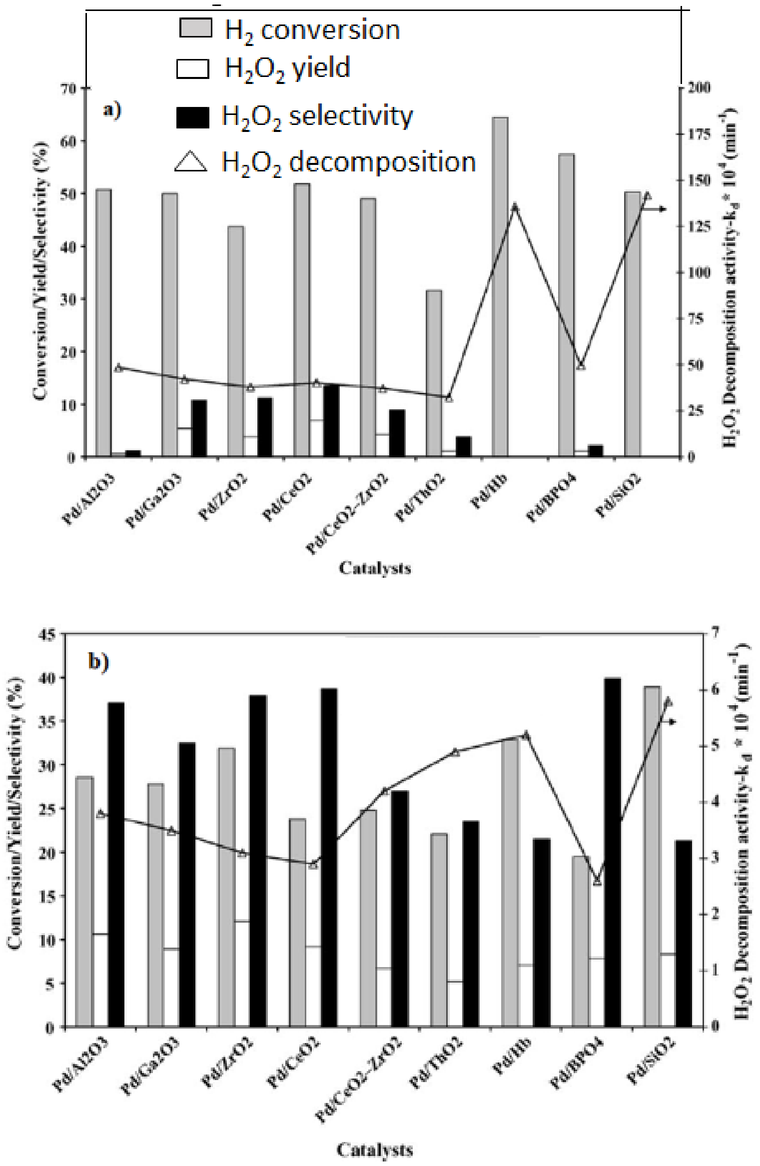

Figure 1.9. Results of the direct oxidation of H_2 to H_2O_2 over different reduced (a) and oxidized (b) Pd catalysts (Pd loading = 2.5 wt.%). Reaction conditions: reaction medium = 0.03 M H_3PO_4, volume of reaction medium = 150 cm^3, amount of catalyst = 0.5 g, reaction temperature = 25 °C, H_2 concentration in O_2= 4.6 mol% and reaction period = 3 h.[79]

Landon *et al.* identified low reaction temperatures (1-2 °C) and short reaction times to be key factors for obtaining high selectivity towards H_2O_2.[20] As shown in Figure 1.10, reaction time is an important factor affecting formation of H_2O_2. The H_2 conversion increased with increasing reaction time. At low H_2 conversion (short reaction time), the 0.6 wt.%Pd/sulfonated carbon showed high selectivity towards H_2O_2, suggesting that the catalyst is highly selective at low temperature and at short reaction time. A selectivity of less than 20% was obtained at 30 ºC after 30 min, due to increased decomposition of H_2O_2 and combustion of H_2 and O_2 to H_2O. This loss in selectivity was partially suppressed by the addition of HBr (1.8×10^{-5} M) as an additive. One of the main limitations of direct synthesis of H_2O_2 is the low concentration of H_2 in reaction solution due to the requirement of working outside H_2/O_2 explosive region (5-95 v/v % for H_2 in O_2). Landon *et al.* addressed this limitation by using supercritical CO_2 as a solvent, as ensuring complete miscibility of supercritical CO_2 and H_2 could result in elimination of gas/liquid mass transfer limitations. However, at the elevated temperature (35 ºC), rapid decomposition of H_2O_2 occurred resulting in minimal H_2O_2 formation over the Pd based catalysts.[20,86]

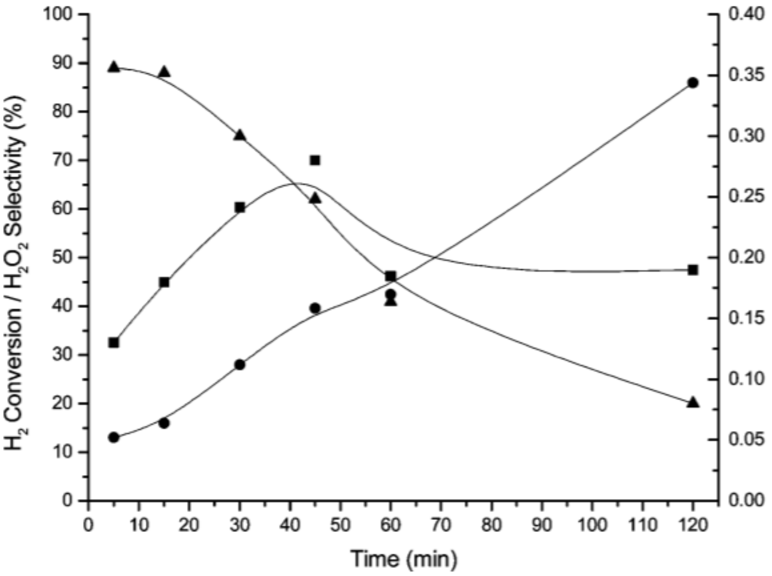

Figure 1.10: Effect of reaction time on the direct synthesis of H_2O_2 using 0.6 wt.% Pd/sulfonated carbon, ● H_2 conversion, ▲ H_2O_2 selectivity, ■ H_2O_2 yield. Reaction conditions: 0.05 g catalyst, 2.9 g H_2O, 5.6g methanol, gas mixture: 5% H_2/CO_2 and 25% O_2/CO_2, total pressure 3.7 MPa, H_2:O_2 ratio 1:2, 1200 rpm, 1 ºC.[20]

Hutchings and co-workers also investigated monometallic Pd catalysts on various supports.[87,88] Carbon based catalysts showed the highest H_2O_2 synthesis activity and the lowest hydrogenation activity. The differences in catalysts towards H_2O_2 synthesis, hydrogenation, and decomposition activity, as shown in Table 1.2, were mainly attributed to the isoelectric point of the support. The use of basic supports lead to the catalysis of unwanted subsequential hydrogenation and decomposition reactions.[87]

Table 1.2: Effect of support on H_2O_2 synthesis, hydrogenation, and decomposition over monometallic Pd-supported catalysts.[87]

Catalyst	**H_2O_2 productivity $[mol_{H_2O_2}kg_{cat}^{-1}h^{-1}]^a$**	**H_2O_2 hydrogenation $[mol_{H_2O_2}kg_{cat}^{-1}h^{-1}]^b$**	**H_2O_2 decomposition $[mol_{H_2O_2}kg_{cat}^{-1}h^{-1}]^c$**
5%Pd/Al_2O_3	9	200	24
5%Pd/TiO_2	30	288	247
5%Pd/MgO	29	582	405
5%Pd/C	55	135	118

[a] **Rate of H_2O_2 production determined after reaction:** 5% H_2/CO_2 and 25% O_2/CO_2,1:2H_2/O_2 at 3.7 MPa, 5.6 g MeOH, 2.9 g H_2O, 0.01 g catalyst and 1200 rpm). [b] **Rate of hydrogenation of H_2O_2 calculated from H_2O_2 hydrogenated using reaction conditions**: 4 wt.% H_2O_2 in solvent (5.6 g MeOH, 2.22 g H_2O and 0.68 g 50% H_2O_2), 0.01 g catalyst, 2.9 MPa 5%H_2/CO_2, 2°C, 1200 rpm. [c] **Rate of decomposition of H_2O_2 calculated from H_2O_2 decomposed using reaction conditions:** 4 wt.% H_2O_2 in solvent (5.6 g MeOH, 2.22 g H_2O and 0.68 g 50% H_2O_2), 0.01 g catalyst, 2°C, 1200 rpm.

1.6 Gold based catalysts in the synthesis of H_2O_2

Until recent years, Au has been overlooked as a catalyst and any indications of activity of the Au were often attributed to impurities rather than Au itself.[9,89] As the perception of Au being the most noble of metals, it was considered unlikely that it could provide any chemical activity. Au catalysts are now established as an effective gas phase oxidation catalyst under mild condition. Use of these catalysts include carbon monoxide oxidation and oxidation of hydrocarbons and organic materials as well as water gas shift reaction.[90–92]

Haruta *et al*. demonstrated that Au can be highly active as a catalyst.[93] Novel Au catalysts were prepared by coprecipitation on various metal oxides and showed to be highly active for the oxidation of carbon monoxide (CO). This discovery led to further examination of Au as active catalyst for oxidations and hydrogenations. They also demonstrated activity of Au/SiO_2 for H_2O_2 formation.[94]

Ishihara *et al.* showed that Au supported on SiO_2 is active for direct synthesis of H_2O_2 without the addition of halogen additives.[95] No H_2O_2 formation was observed over analogous Pd, Pt or Ag catalysts. They also concluded that the nature of the metal oxide support had great influence on H_2O_2 formation. No H_2O_2 formation was observed using basic supports as MgO or Al_2O_3, however, use of acidic supports as SiO_2, ZrO_2 or ZMS-5 led to yield of H_2O_2. The highest rate of H_2O_2 formation was achieved with the 1%Au/SiO_2 catalyst. The addition of small amounts of Pd (up to 0.1wt.%) resulted in an increased formation of H_2O_2 due to improved H_2 activation capability.[95] Olivera *et al.* predicted that Au could be more active than Pd, Pt and Ag for the production of H_2O_2 from H_2 and O_2, based on a theoretical study of involved reactions.[96]

Hutchings and co-workers were among first to show that Au catalysts are very selective for the direct synthesis of H_2O_2.[20,86] Initially supercritical CO_2 (3.5ºC, 9.7MPa) was used as a reaction medium to overcome problems with H_2 diffusion, shown in previous studies over monometallic Pd catalysts. Enhanced solubility of H_2 was expected in supercritical CO_2. With this approach, low rates of H_2O_2 formation were observed. It was considered that H_2O_2 at this elevated temperature was relatively unstable due to high rates of H_2O_2 decomposition and hydrogenation. These observations led authors to carry out experiments at significantly lower temperatures. Significant increases in the rate of H_2O_2 synthesis was observed when experiments were carried out at 2 ºC and with methanol as solvent. The Au/Al_2O_3 (2 $mol_{H_2O_2}kg_{cat}^{-1}h^{-1}$) catalyst showed higher synthesis activity than a monometallic Pd/Al_2O_3 counterpart (0.3 $mol_{H_2O_2}kg_{cat}^{-1}h^{-1}$), under these reaction conditions. However, the more interesting observation was that the supported Au-Pd (1:1 by wt/wt.) produced 3 times more H_2O_2 than monometallic analogues.[20,86]

In a view of these findings, a series of monometallic Au catalysts was prepared over different supports by Hutchings and co-workers and were investigated for direct synthesis of H_2O_2 at low temperatures using a CH_3OH/H_2O solvent. As shown in Table 1.3, in all cases catalysts showed low rates of H_2O_2 formation with insufficient level of produced H_2O_2 to determine H_2 selectivity with any accuracy. It is apparent from result, that TiO_2 was a far more effective support compared to the rest of the catalysts.

Table 1.3: Effect of support on H_2O_2 synthesis, hydrogenation, and decomposition over monometallic Pd-supported catalysts.[87]

Catalyst	**H_2O_2 productivity [$mol_{H_2O_2}kg_{cat}^{-1}h^{-1}$]^a**	**H_2O_2 hydrogenation [$mol_{H_2O_2}kg_{cat}^{-1}h^{-1}$]^b**	**H_2O_2 decomposition [$mol_{H_2O_2}kg_{cat}^{-1}h^{-1}$]^c**
5%Au/Al_2O_3	2.6	229	18
5%Au/TiO_2	7	71	24
5%Au/MgO	0	100	12
5%Au/C	1	0	0

[a] **Rate of H_2O_2 production determined after reaction:** 5% H_2/CO_2 and 25% O_2/CO_2,1:2H_2/O_2 at 3.7 MPa, 5.6 g MeOH, 2.9 g H_2O, 0.01 g catalyst and 1200 rpm). [b] **Rate of hydrogenation of H_2O_2 calculated from H_2O_2 hydrogenated using reaction conditions**: 4 wt.% H_2O_2 in solvent (5.6 g MeOH, 2.22 g H_2O and 0.68 g 50% H_2O_2), 0.01 g catalyst, 2.9 MPa 5%H_2/CO_2, 2°C, 1200 rpm. [c] **Rate**

of decomposition of H_2O_2 calculated from H_2O_2 decomposed using reaction conditions: 4 wt.% H_2O_2 in solvent (5.6 g MeOH, 2.22 g H_2O and 0.68 g 50% H_2O_2), 0.01 g catalyst, 2°C, 1200 rpm.

1.7 Bimetallic AuPd catalysts in the synthesis of H_2O_2

Hutchings and co-workers were one of the first to report that alloying Au with Pd resulted in a dramatic enhancement in catalyst activity towards H_2O_2 formation through a synergistic effect, and this effect was further extensively investigated.[9] As shown in Table 1.4, the monometallic Au catalysts showed a low rate of H_2O_2 production. The combination of Au-Pd led to more effective catalysts than the Au and Pd only catalysts. The enhancement was not only in productivity but also in H_2O_2 selectivity compared to monometallic Pd analogues.

Table 1.4: Formation of H_2O_2 using monometallic Au,Pd and Au-Pd supported catalysts.[9]

Catalyst	H_2O_2 productivity $[mol_{H_2O_2} kg_{cat}^{-1} h^{-1}]^a$	H_2 selectivity [%]
5%Au/C	1	n.d
2.5%Au-2.5%Pd/C	110	80
5%Pd/C	55	34
5%Au/TiO_2	7	n.d
2.5%Au-2.5%Pd/TiO_2	64	70
5%Pd/TiO_2	30	21

Reaction conditions: a) Synthesis reaction: 0.01g catalyst, 2.9 g of water, 5.6 g of methanol, 5%H_2/CO_2 (2.9MPa) and 25%O_2/CO_2 (1.1 MPa), 0.5 h, 2°C, 1200 rpm

They further reported the importance of catalyst heat treatment and its effect on catalyst stability and reusability, with calcination at 400 °C resulting in fully stable and reusable catalysts. As shown in Table 1.5, a significant loss of Pd and Au after reaction was observed without heat treatment at 400 °C, and upon re-use of the catalyst further loss was observed.

Table 1.5: Effect of heat treatment on Au and Pd remaining on the catalysts after multiple reaction cycles.[97]

Catalyst	Pre-treatment	run	Au remaining [%]	Pd remaining [%]
2.5wt.%Au-2.5wt.%Pd/TiO_2	Air, 25 °C	1	20	10
	Air, 25 °C	2	8	5
2.5wt.%Au-2.5wt.%Pd/TiO_2	Air, 400 °C	1	100	100
	Air, 400 °C	2	100	100

2.5wt.%Au-2.5wt.%Pd/Al_2O_3	Air, 25 °C	1	25	21
	Air, 25 °C	2	20	15
2.5wt.%Au-2.5wt.%Pd/Al_2O_3	Air, 400 °C	1	100	100
	Air, 400 °C	2	100	100

Reaction condition: 420 psi 5% H_2/CO_2 +150 psi 25% O_2/CO_2, 2 °C, solvent (5.6 g MeOH and 2.9 g H_2O), H_2:O_2 molar ratio = 1:2, 3.7MPa, stirring 1200 rpm.

During the calcination process of AuPd catalysts supported on metal oxide, an Au-core Pd-shell morphology is typically formed (Figure 1.11).[9] As the core-shell structure is formed, the catalyst simultaneously becomes less active and more stable. However, the formation of core-shell morphologies was not observed for analogous C supported catalysts. Instead, bimodal distribution of alloys was observed, with smaller alloys being Pd-rich and larger particles(<20nm) Au-rich.[98]

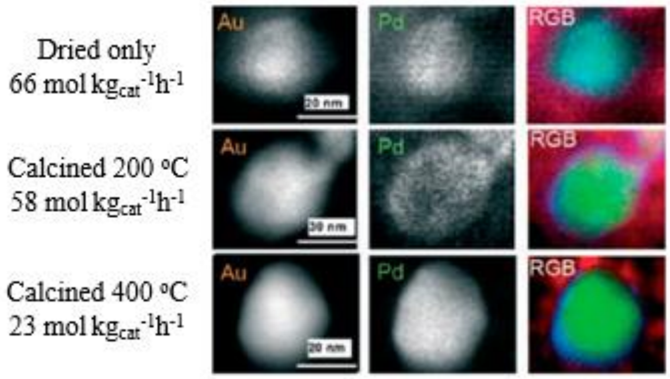

Figure 1.11: HAADF image showing development of the core-shell structure in 2.5 wt.%Au-2.5 wt.%Pd/Al_2O_3 catalyst. Individual Au and Pd maps are combined in the red/green/blue (RGB) image: Au green, Pd blue, Al_2O_3 red. Top row, dried at 120 °C; middle row, calcined at 200 °C; bottom row, calcined at 400 °C with respective H_2O_2 productivities with reaction conditions given in Table 1.5.[7]

Han *et al.* aimed to establish the relationship between Au content and enhancement in performance of AuPd alloy catalysts for direct synthesis of H_2O_2 in a micro tri-phase reactor at 10 ^oC.[99] The rate of H_2O_2 formation increased with increasing Au content up to Pd:Au ratio 1:1.6 (atomic), and then dropped down by almost 50% with further increase in Au content up to Pd:Au ratio of 1:3.4. Selectivity towards H_2O_2 increased also with increasing Au content from 12%, obtained over the monometallic Pd catalyst to 62% obtained over $Pd_1Au_{3.4}$ catalyst. Based on the evidence, it was suggested that the existence of electron density transfer between Pd and Au atoms in the alloys surface was key in achieving improved catalytic performance. The introduction of Au into the Pd catalyst resulted in change of the surface structure of the catalysts through geometric effects and reconstruction of the surface composition, for example, finely tuning the Pd-Pd bond length, as well as modification of electronic structure of Pd.

Choudhary and co-workers have also investigated the effect of an Au additive on catalyst activity compared to monometallic Pd catalysts supported on ZrO_2.[79] They report that the addition of small quantities of Au (Au/Pd ratio = 0.02) increased catalytic performance. However, with further addition of Au, rates of H_2O_2 synthesis were markedly lower. It was suggested that small amount of Au might supress side reaction, but higher amount of Au resulted in higher decomposition activity.

Gudrazi *et al.* investigated the effect of Au in AuPd catalysts supported on activated carbon cloth at high pressure (38 bar) and 0 ºC using methanol as a solvent.[100] All bimetallic AuPd catalysts were found to be more selective towards H_2O_2 formation than monometallic counterparts. The effect of Au:Pd ratio was also investigated over 5 wt.%AuPd/C, with 1:4 ratio being the most active for H_2O_2 formation, and Au:Pd ratio of 2:1 ratio resulting in the highest H_2 selectivity among studied catalyst. The heat treatment of the catalyst was shown to be crucial as it has two opposite effects on the catalyst performance: affecting the Pd oxidation state; and damaging the oxygen containing surface functional groups, with both factors leading to an increase in the selectivity of the catalyst.

1.8 Bimetallic catalysts in the synthesis of H_2O_2

Hutchings and co-workers demonstrated that subjecting SnPd supported on TiO_2 to oxidation-reduction-oxidation (ORO) treatment resulted in highly active and selective catalysts under sub-ambient temperatures (2 ºC).[14] Three different structures were identified in the catalyst: amorphous SnO_x films on the TiO_2 particles, small Pd species associated with the SnO_x films, and larger PdSn nanoparticles. It was suggested that during heat treatment the small Pd-rich particles responsible for H_2O_2 degradation are encapsulated in an SnO_x layer by generating strong metal support interactions (SMSIs). No loss in catalytic activity was reported with subsequential use of catalyst in up to 5 gas replacement reactions (after the reaction, a reactor was de-gassed, charged with the same amount of reagent gases and followed by another synthesis reaction; detailed procedure is described in Section 2), with a H_2O_2 concentration of 0.56 wt.% obtained at the end of 5th gas replacement. A series of bimetallic catalysts using Ni, Zn, Ga, In and Co were also subjected to the ORO heath treatment, with test results showing no degradation towards H_2O_2 but significantly lower synthesis activities compared to the SnPd counterpart. In contrast, the same suppression of H_2O_2 degradation was not observed for a corresponding AuPd/TiO_2 catalyst subjected to this heat treatment procedure. It was concluded that the second metal oxide added to the Pd and TiO_2 system has to show no degradation activity towards H_2O_2 when in oxide form, form an alloy or mixed oxide phase with Pd, and encapsulate small Pd-rich particles by SMSIs for the heath treatment to result in a decrease in degradation activity of the catalyst.

Li *et al.* investigated a series of PdSn nanocrystals with a hollow structure using facile solvent-thermal method.[101] The introduction of Sn played an important role on the morphology evolution and composition control of the hollow SnPd nanocrystals. In order to inhibit the high H_2O_2 degradation activity of these catalysts, a rapid thermal treatment process (350 ^{o}C, 6 min) was applied, resulting in an effective inhibition of H_2O_2 degradation, while the synthesis activity of the catalysts increased gradually with treatment time. Due to the short heat treatment time, morphology and composition of the crystals were not affected. The observed low selectivity of the catalysts in a water-methanol solvent was attributed to combustion of H_2. Interestingly, by using water as the only solvent, an increase in H_2 selectivity from 15 % to 80 % was reported at 0 ^{o}C. This was attributed to lower solubility of reagent gases, limiting degradation of H_2O_2. As a result of the rapid heat treatment, a drastic reduction in Pd^0 proportion was obtained with more than 95 % of Pd species present as Pd^{2+}, which was concluded to have a major contribution for the H_2O_2 degradation inhibition. The enhancement of synthesis activity and inhibition of degradation activity is also attributed to the ensemble effect of PdSn alloys as well as Pd/SnO_x and PdO/SnO_x interface. The authors reported that presence of SnO_x is extremely beneficial for obtaining high slectivities, as SnO_x can achieve a weak activation of O_2 without cleaving the bond between O atoms, and therefore H_2O_2 is rapidly generated at Pd/SnO_x and PdO/SnO_x interface.[102,103]

Wang *et al.* prepared different bimetallic PdM (M: Ni, Zn, Ga, In, Sn, Pb) nanocrystal catalysts by adsorbing metal nanocrystal from colloidal solution in chloroform on the acid pre-treated $TiO_{2.}$[15] Among the studied metals, addition of Sn and Ga showed a significant increase in H_2O_2 synthesis activity by 3 and 2 times respectively, compared to monometallic Pd counterpart. Analogous catalysts including In, Ni and Zn showed no significant change in synthesis activity and the addition of Pb resulted in a decrease in synthesis activity compared to monometallic Pd counterpart. Random distribution of Pd and M (Ni, Zn, Ga and In) was attributed to the nanocrystals while an intermetallic Pd_2Sn phase was distinguished on XRD patterns. It was reported that both Pd electronic structure and geometric surface structure was modified by addition of secondary metal. High synthesis activity of 180 $mol_{H2O2}\,kg_{cat}^{-1}\,h^{-1}$and selectivity of 51 % was achieved over $Sn_{0.62}Pd_{0.38}$/TiO_2 (atomic composition). However, significant leaching of Pd (39 %) was observed after the reaction in ethanol and, due to the large reaction volume, only low H_2O_2 concentrations below 0.08% were achieved. Introduction of small quantities of Ga and In resulted in decreased degradation activity and enhanced selectivity of the catalyst.[104]

A significant improvement in H_2O_2 synthesis activity through the introduction of Ni into Pd based catalyst has been reported by Maity and Eswaramoorthy.[105] A Ni containing Pd catalyst showed 3-times higher activity for the direct synthesis of H_2O_2 than the corresponding monometallic Pd catalyst or the AuPd counterpart. Nanostructured catalysts were prepared by borohydride reduction method without any support and experiments were carried out at atmospheric pressure and 10 ^{o}C. The NiPd catalyst showed H_2 selectivity of 95 % and H_2O_2 concentration of 1.2 wt.% was achieved after 72 h. However, the presence of 0.1 M HCl was required to synthetise any H_2O_2. During the reaction, a reorganisation of Ni atoms from a random distribution into ordered nanoalloy domains as well as increase in particle size from 15 to 30 nm, was suggested by authors. It was concluded that the higher synthesis activity and high selectivity of NiPd catalysts is due to modification of Pd electronic structure by Ni.[106,107]

Gu *et al.* reported that the addition of small amounts of Ag (0.012 – 0.07 wt.%) to a Pd/C catalyst caused a decrease in H_2O_2 synthesis activity compared to monometallic Pd/C, but also suppressed degradation activity of the catalyst.[108] As a result, lower H_2 conversions and higher H_2 selectivities were obtained. The optimised 0.83 wt.%Pd- 0.18 wt.%Ag/C catalyst offered H_2O_2 synthesis activity of 58 $mol_{H2O2}\ kg_{cat}^{-1}\ h^{-1}$ and H_2 selectivity of 71 %. The enhancement in catalyst performance was attributed to dilution of Pd by Ag in the alloy surfaces, leading to less contiguous Pd ensembles and more monomer Pd sites on the surface, which effectively prevents formation of H_2O. The addition of Ag elevated the fraction of Pd^{2+} as a result of electronic interactions between Pd and Ag. Moreover, the decreased activity was attributed to the reduced adsorption capacity of reagent gases due to the Ag additive.

The addition of a small amount of Sb to Pd/TiO_2 (Sb:Pd atomic ratio 1:80 to 1:20) was also reported to enhance H_2 selectivity and decrease degradation activity of the catalyst compared to monometallic Pd/TiO_2.[17] Ding *et al.* showed H_2 selectivities up to 73 % and a decrease in degradation activity can be achieved by finely tunning Sb:Pd ratio. A decrease in both, synthesis and degradation activity were observed with an increase in Sn content compared to monometallic Pd counterpart. Interestingly, no synthesis activity was obtained when the Sb:Pd atomic ratio was 1:2. The role of Sb on the active sites of Pd catalyst was attributed to isolating contiguous Pd sites via the formation of Sb-Pd bimetallic sites, coating the Pd surface via formation of Sb_2O_3 layer and an increase in Pd^{2+} species on the surface. The authors proposed the reaction mechanism, showed in Figure 1.12, in which Pd-Sb sites were formed and the Pd nanoparticles were diluted. The isolated Pd sites surrounded by Sb were considered to be responsible for the non-dissociative activation of O_2 and selective formation of H_2O_2, while the contiguous Pd ensembles are more favourable for H_2O formation. The Sb located on the surface inhibits H_2 adsorption and therefore decrease the degradation and synthesis activity compared to monometallic Pd catalyst.

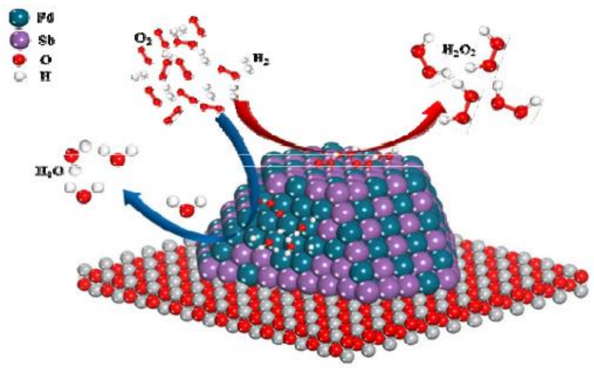

Figure 1.12: Direct synthesis of H_2O_2 over Pd-Sb/TiO_2 catalyst.[17]

The highly selective synthesis of H_2O_2 in a semi-batch reactor over a Te promoted Pd/TiO_2 catalyst in acidified ethanol reaction medium has been reported by Tian *et al.*[109] A selectivity towards H_2O_2 of near to 100 % was obtained by carefully controlling the Te:Pd atomic ratio to 1:100. Increasing Te content resulted in a decrease in Pd-Pd coordination due to a decrease in particle size and a dilution effect of Te. Highly dispersed clusters of isolated Pd atoms were observed with Te:Pd atomic ratios 4:17 and higher. The formation of Pd-Te sites blocks contiguous Pd domains, and Te introduction was shown to significantly weaken dissociative activation of O_2. DFT results suggested that the terrace Pd-Te sites present a higher activation barrier for O-O bond cleavage than for O-H bond formation. Therefore, a small Pd:Te ratio (1:100) showed abundant surface Pd-Te sites were responsible for inhibiting side reactions and achieving high selectivity. In contrast, reduction of particle size, because of increasing Te:Pd ratio, resulted in an increase of low-coordinated active sites at edges and corners. These active sites are more active for dissociative activation of O_2 than terrace Pd or Pd-Te sites. A high concentration of Te on the surface significantly hinders adsorption of reagent gases, causing inertness of the catalysts. Therefore, the ratio of Te:Pd needs to be carefully considered to maximise the effect of the secondary metal. The different active sites and their effect on H_2O_2 formation are summarised in Figure 1.13.

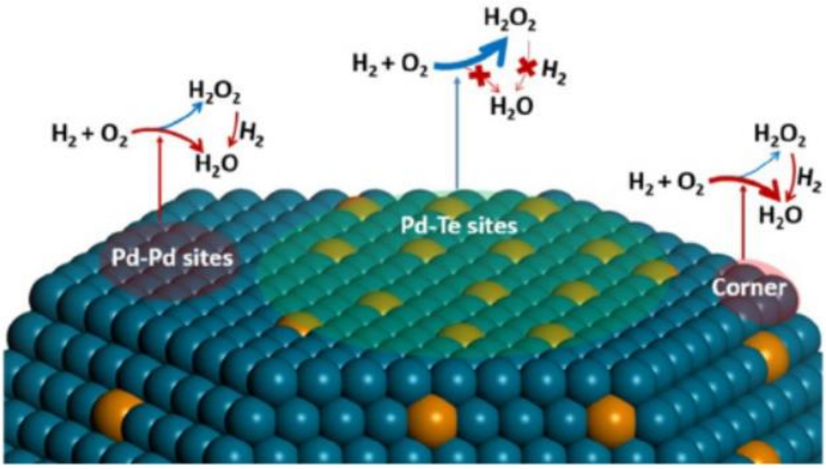

Figure 1.13: Effect of different active sites of Pd-Te/TiO_2 catalyst on the direct synthesis of H_2O_2.[109] Blue and brown spheres are Pd and Te atoms, respectively.

Wang *et al*. reported that addition of Zn can also significantly improve the catalytic performance of monometallic Pd catalysts.[18] By introducing high content of Zn (5 wt.%) to 1 wt.%Pd/Al_2O_3, the synthesis activity was enhanced 3 times compared to monometallic Pd counterpart, with increase in selectivity towards H_2O_2 from 64 to 78 % in 0.03 M H_2SO_4/MeOH solution at 2 ºC. However, a significant increase in hydrogenation activity (almost 2 times) was observed over this PdZn catalyst compared to the monometallic Pd counterpart. This suggests that the increase in selectivity was observed due to significantly enhancement in synthesis activity rather than inhibition of H_2O formation. The function of Zn addition on the H_2O_2 synthesis was attributed to the geometric effect and the electronic effect in the bimetallic PdZn catalysts. A smaller particle size and higher Pd dispersion was shown over PdZn catalysts than monometallic Pd analogue. The adsorption capacity of PdZn catalysts towards reagent gases was increased due to the addition of Zn resulting in more adsorption sites compared to monometallic Pd catalyst. The increased adsorption capacity correlates with increased synthesis and hydrogenation activity of the catalyst. An increase in Pd^0 fraction was observed with increasing Zn metal loading, which can also explain increased synthesis and hydrogenation activity of the catalyst.

1.9 The effect of additives on direct synthesis of H_2O_2

Studies by Pospelova in the early 1960s showed that the addition of acids, such as HCl and HNO_3, results in higher productivities of H_2O_2 over Pd based catalysts by suppressing the base catalysed decomposition.[8]

Choudhary *et al.* investigated the role of halide additives for promoting direct synthesis of H_2O_2 over reduced Pd catalysts in an aqueous reaction medium.[82,83,85,110–119] The halides were introduced as potassium halides in the reaction medium, The absence of halide in the reaction medium resulted in low H_2O_2 formation rates, but also showed high activity of catalysts to H_2O_2 decomposition and hydrogenation.[115,117] The addition of fluoride anions (introduced as KF) caused even further increase in decomposition and hydrogenation of H_2O_2 with no increase in synthesis activity. Iodide anions (introduced as KI) caused almost complete deactivation of catalysts due to poisoning caused by strong coordinating ability to Pd. On the other hand, addition of chloride and bromide anions decrease the activity towards side reactions and in addition increase formation of H_2O_2, with Br^- anions being the most effective halide additive. Similar conclusions were reached over oxidised Pd catalysts; however, the effect was smaller compared to reduced counterparts.[85,110,114,115,117] This promotion effect was only observed in presence of acid (protons), showing the essential role of acid in reaction medium. Without the presence of acid in the reaction medium, the presence of identical concentrations of halide anions result in low formation of H_2O_2 and also high decomposition activity as shown in Table 1.6.[119]

Table 1.6: Formation and decomposition of H_2O_2 at 27°C and atmospheric pressure over Pd/C catalyst in in the presence and absence of mineral acid with or without halide additive.[120]

Catalyst	**Halide additive [a] (mmol/dm^3)**	**H_2 conversion [b] (%)**		**H_2O_2 decomposition [c] (%)**
		Total	**To H_2O_2**	
Acid in the reaction medium: H_3PO_4 (0.03 mol/dm^3)				
Pd/C	none	57.2	1.5	61.4
	KF [2.7]	58.3	0.0	72.5
	KCl [2.7]	52.3	15.4	5.4
	KBr [2.7]	36.2	11.5	2.8
	KI [2.7]	<5.0	0.0	<1.0
Absence of mineral acid				
Pd/C	none	48.5	0.0	100
	KF [2.7]	-	-	100
	KCl [2.7]	43.8	0.0	68.5
	KBr [2.7]	38.5	0.0	18.0
	KI [2.7]	-	-	32.5

[a] Value given in square brackets corresponds to the concentration of halide in the aqueous reaction medium.

[b] Reaction period is 3h.

[c] Reaction period is 1h.

Figure 1.14 illustrates the effect of halide additives with or without addition of acid using a Pd/Al_2O_3 catalyst. In the absence of acid, or in the acidic medium without Cl^- or Br^- anions, decomposition of H_2O_2 is the dominant reaction (Figure 1.14 a). The addition of non-halo acid resulted in formation of H_2O_2 over oxidised form of catalyst, but also decomposition and hydrogenation of H_2O_2 (Figure 1.14 b). In the presence of acid and Cl^- or Br^-, both a promotion in H_2O_2 formation and suppression of H_2O_2 decomposition is observed, with hydrogenation of H_2O_2 being the main side reaction (Figure 1.14 c).[121] However, significant leaching of Pd from the catalyst was also observed in the presence of higher concentration of halide anions (≥25 mmol/dm^3) and/or acid (≥0.3 mol/dm^3).[113,119,122] No significant leaching was observed in presence of H_2O and H_3PO_4. PO_4^{3-} ions can also stabilise H_2O_2.[121]

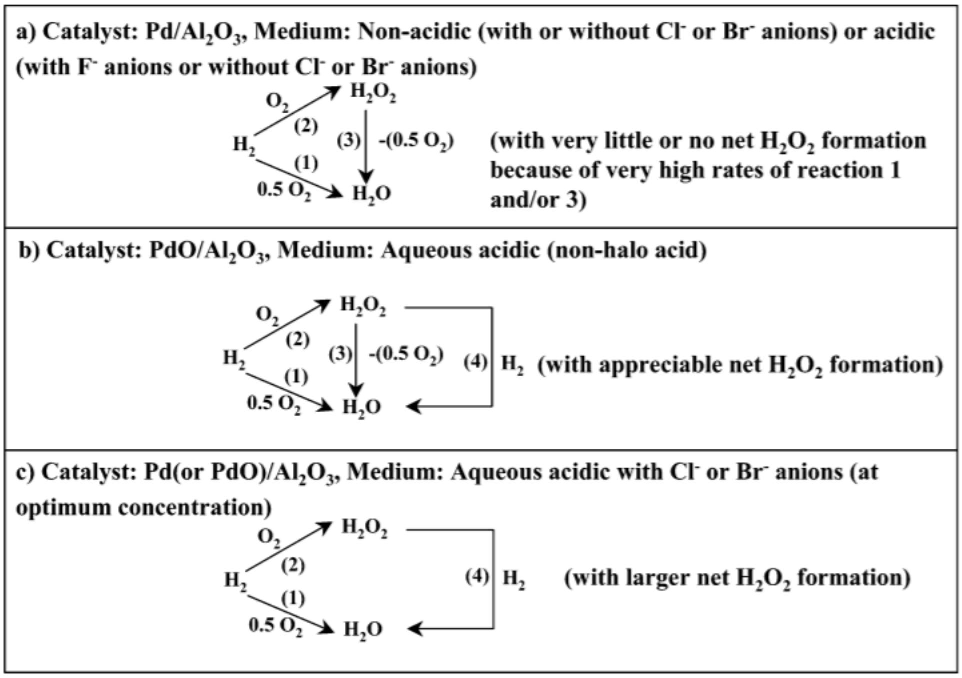

Figure 1.14: Reaction scheme of direct synthesis of H_2O_2 over Pd/Al_2O_3 catalyst in aqueous reaction solution with or without addition of halide anions and/or protons. [(1) H_2 combustion, (2) H_2O_2 formation, (3) H_2O_2 decomposition and (4) H_2O_2 hydrogenation] proposed by Choudhary *et al.*[121]

Choudhary *et al*. proposed that anions can adsorb on catalytic surfaces and act as poisons or modifiers of electronic properties of surface Pd (via Pd-halide interaction) resulting in the reduction of dissociative adsorption of O_2, reduction of H_2O_2 dissociation and inhibition of H_2O_2 hydrogenation. At higher than optimal concentrations of halide anions (the optimal concentration depends on the catalyst used and the promoters used), more active sites were blocked or modified, which further decreases the decomposition activity but also decreases the catalytic activity and formation of H_2O_2.[113] The presence of a second halogen in the acidic reaction medium causes a strong synergistic effect, enhancing H_2O_2 formation rate and selectivity.[112,116,123] This effect is expected to arise from the modification of the electronic properties of Pd, due to the interaction of two different anions with different electronegativity and electron affinity. The synergistic effect was most noticeable for the combination of fluoride and iodide anions. This is interesting considering that addition of fluoride anions previously only increased side reactions and addition of only iodide anions resulted in decreased activity of the catalyst for all reactions.[116] The halide ions can be incorporated directly into the catalyst or deposited on the support prior Pd deposition. The same beneficial promotion effect was observed as with direct addition to reaction medium.[112,118,123]

The addition of non-halo acids (with no addition of halide) such as H_2SO_4, H_3PO_4, H_3BO_3 or HNO_3 had no effect on formation of H_2O_2 but resulted in large decrease in H_2O_2 decomposition activity, however, halo acids showed a stronger effect on the direct synthesis reactions.[110,111,119] The presence of HCl (0.1M) caused a large decrease in H_2 conversion and a significant increase in H_2O_2 formation and selectivity; however, the addition of HBr and HI (0.1M) cased deactivation of the catalyst for the H_2O_2 formation and degradation. All non-halo acids performed in a similar manner, showing the importance of protons in decreasing the decomposition rate of H_2O_2 with little to no effect on H_2O_2 formation. However, in the presence of HCl, the improvement in selectivity was observed, suggesting that for selective formation of H_2O_2 both proton (decreasing the decomposition activity) and Cl^-(increasing H_2O_2 formation) are needed. Deactivation of the catalyst using 0.1M HBr and HI was result of catalyst poisoning poisoning. The effect of an acid additive on the H_2O_2 decomposition over Pd/C is illustrated in Figure 1.15, which shows the significant difference between non-halo and halo acids.

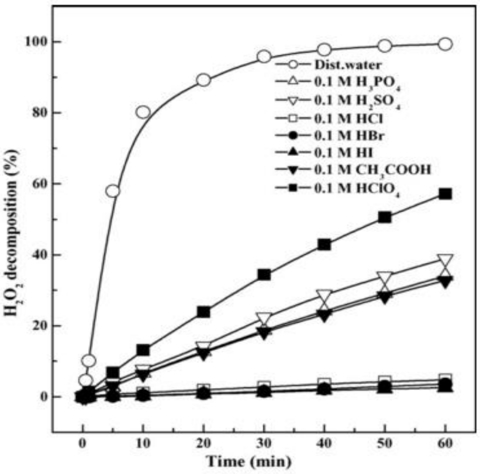

Figure 0.15: The effect of acids on decomposition activity of hydrogen peroxide over 5 wt.% Pd/C catalyst at 25°C in an aqueous reaction medium.[122]

Edwards *et al.* also investigated the addition of promoters such as NaBr and H_3PO_4, using CO_2 as a diluent for H_2 and O_2 reactant gases.[23] The decrease in synthesis activity from 64 mol_{H2O2} kg_{cat}^{-1} h^{-1} to 53 mol_{H2O2} kg_{cat}^{-1} h^{-1} was observed in presence of NaBr and H_3PO_4 over 2.5 wt.% Au- 2.5 wt.% Pd/TiO_2, compared to activity with no additives. This can be related to possible blocking with anions of catalyst sites active for formation of H_2O_2. The role of CO_2 was further investigated by comparison to N_2 as diluent. As shown in Table 1.7 the use of N_2, as the gaseous diluent resulted in significantly lower rates of H_2O_2 formation. The carbonic acid formed upon dissolution of CO_2 in reaction medium acts as *in situ* promoter stabilizing H_2O_2. Upon depressurizing the reactor, CO_2 is degassed from the solution and hence there is no need to remove acidic promoter.

Table ***1.7: Effect of gas diluent on synthesis of H_2O_2.*** [23]

Catalyst	Pre-treatment	Productivity [$mol_{H2O2}\ kg_{cat}^{-1}\ h^{-1}$]
2.5wt.%Au-2.5wt.%Pd/TiO_2	Air, 400°C, 3h	64[a]
2.5wt.%Au-2.5wt.%Pd/TiO_2	Air, 400°C, 3h	29[b]
2.5wt.%Au-2.5wt.%Pd/C	Air, 400°C, 3h	110[a]
2.5wt.%Au-2.5wt.%Pd/C	Air, 400°C, 3h	10[b]

[a] **Reaction condition:** 420 psi 5% H_2/CO_2 +150 psi 25% O_2/CO_2, 2 °C, solvent (5.6 g MeOH and 2.9 g H_2O), H_2:O_2 molar ratio = 1:2, 3.7MPa, stirring 1200 rpm**.** [b] **Reaction condition:** N_2 used as diluent: 5% H_2/Ar (290 pisg) + 10% O_2/He (290 psig), 2 °C, solvent (5.6 g MeOH and 2.9 g H_2O), H2:O2 molar ratio = 1:2, 3.7 MPa, stirring 1200 rpm.

Instead of adding acid promoters into the reaction medium, Edwards *et al*. investigated the effect of initial acid pre-treatment of catalyst supports using 2% HNO_3.[124] For Au-Pd catalysts on oxide supports, acid pre-treatment led to a decrease in combined decomposition and hydrogenation activity. However, when pre-treated carbon was used as support for Au-Pd nanoparticles, the degradation of H_2O_2 was switched off completely, resulting in a catalyst with high H_2O_2 formation rate and H_2 selectivity (> 98%). The acid pre-treatment decreases the size of the alloy nanoparticles, and it was suggested that these smaller nanoparticles decorate and inhibit the sites for decomposition reaction. Interestingly, no enhancement in activity was observed over Pd/C catalyst pre-treated in similar manner. HNO_3 and CH_3COOH were the most effective acids for this type of pre-treatment. On the other hand, acids like HCl and H_3PO_4, that were shown as efficient additives for direct synthesis of H_2O_2, resulted in an increase in H_2O_2 formation but also a significant decrease in H_2 selectivity.[124] Similar enhancements in catalyst activity were observed over Au-Pd catalyst supported on TiO_2.[13] No enhancement was observed, when the support was treated after metal deposition and neither did addition of HNO_3 or HCl during metal impregnation.[13]

1.10 Effect of calcination temperature on catalyst performance

Catalyst heat treatment has been shown to be the essential feature controlling catalyst stability and re-usability.[9,125] Uncalcined bimetallic catalysts were reported to offer higher synthesis activity and conversions compared to calcined counterparts.[126] However, these catalysts were also shown to be unstable, and non-re-usable with a significant loss in active metal content as previously shown in Table 1.5. It was suggested that the higher synthesis activity of uncalcined catalysts can be contributed to leached Pd as it can act as active homogenous catalyst. [88]

Hutchings and co-workers showed that catalysts calcined at lower temperatures are much more active than catalyst calcined at 400°C, upon first use, as shown in Figure 1.16.[23] However, on subsequent re-use catalysts calcined at temperatures below 400°C were much less active, due to loss of Pd and Au on use. Catalysts calcined at 400°C were stable and showed no detectable leaching of metals. During the calcination process of AuPd catalysts supported on metal oxide, the core-shell structure is formed with Pd-rich shell and Au-rich core.[9]

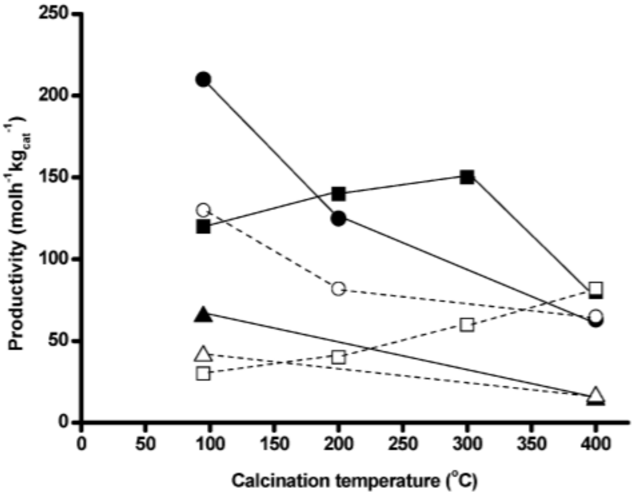

Figure 1.16.: Effect of calcination temperature on the formation of hydrogen peroxide using standard reaction conditions. Key: ▲ 2.5 wt% Au–2.5 wt% Pd/Al2O3; ■ 2.5 wt% Au–2.5 wt% Pd/SiO2; ● 2.5 wt% Au–2.5 wt% Pd/TiO2; closed and open symbols represent first and second use, respectively.[23]

Freakley *et al.* developed a heat treatment cycle consisting of 3 steps in which a catalyst is calcined at 500 °C in static air, reduced at 200 °C in H_2/Ar, and re-calcined at 400 °C in static air.[14] This extensive heat treatment, illustrated in Figure 1.17, resulted in highly selective, stable, and reusable $SnPd/TiO_2$ catalysts. All three steps were shown to be necessary and the same results were not obtained when the reduction step was replaced with another oxidation treatment. It was suggested, that during the heat treatment, amorphous layers of SnO_x encapsulated the small Pd-rich nanoparticles, with high hydrogenation activity resulting in high selectivity of the catalyst.

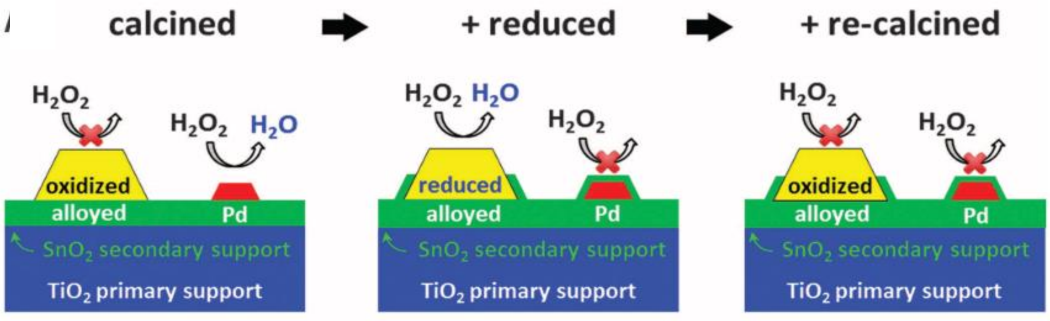

Figure 1.17: Proposed mechanism for switching off H_2O_2 hydrogenation by small Pd-rich NPs through a strong metal-support interaction (SMSI).[14]

Cybula *et al.* demonstrated that calcination temperature affected the structure of AuPd nanoparticles supported on TiO_2 as well as surface properties of support.[127] The increase in calcination temperature caused shrinking of the support surface area, growth of crystal size and slight transformation from anatase to rutile phase. The catalyst calcined at 350 °C showed a nanoparticle core was Au rich and a shell contained mostly Pd. Increasing the calcination temperature up to 700 °C resulted in alloying of the metals and increase in particle size. The structure of the catalyst changed from core-shell to a island like structure with areas of different composition, and ends in fully alloyed system at 700 °C. The increase of calcination temperature caused re-distribution and segregation of metal particles on the support, and is illustrated trough HAADF images combined with elemental mapping in Figure 1.18.

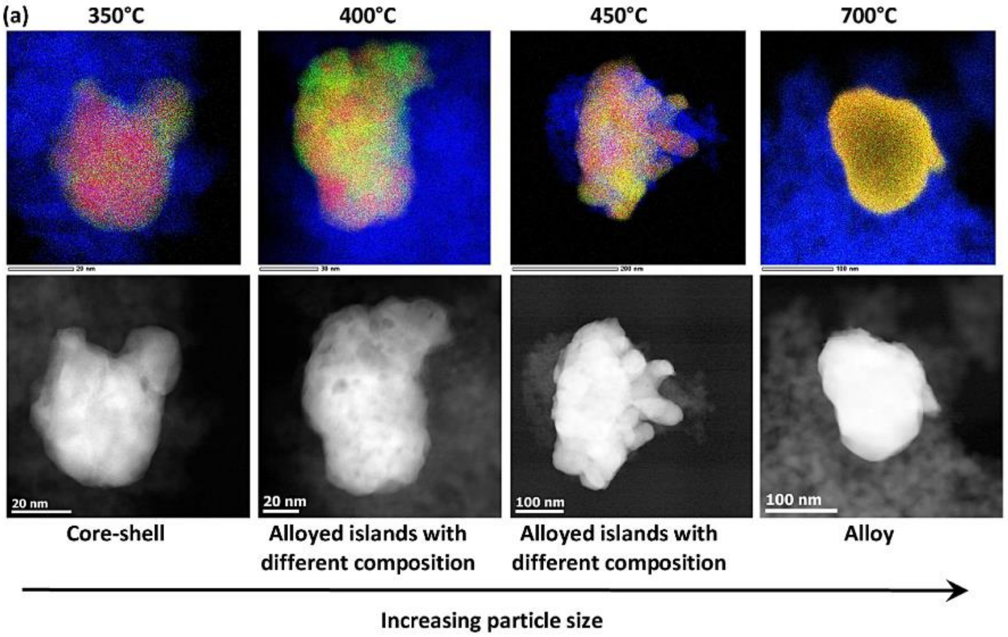

Figure 1.18: HAADF images combined with mappings of Au, Pd and Ti (blue is Ti, red is Au and green is Pd) calcined at 350, 400, 450 and 700 °C.[127]

Li *et al.* demonstrated the importance of heat treatment over hollow SnPd nanocrystals supported on TiO_2.[9] Catalysts with no heat treatment showed extremely high degradation activities towards H_2O_2 of 2400 $mol_{H2O2}\ kg_{cat}^{-1}\ h^{-1}$. In order to inhibit the conversion of H_2O_2 to H_2O, a thermal treatment process was applied to these catalysts. To avoid a particle aggregation, the treatment process was carried out at 350 °C for a short time. After only 6 min of heat treatment, no degradation activity was observed and significant increase in catalyst activity from 100 to 160 $mol_{H2O2}\ kg_{cat}^{-1}\ h^{-1}$ was achieved. Due to the low treatment time, the composition and morphology of the nanocrystals were largely maintained.[101]

In order to optimize preparation procedure, Menegazzo *et al.* investigated the effect of the calcination temperature on the catalyst performance of 1.5 wt.%Pd/SiO_2 catalyst.[12] The uncalcined catalyst showed the highest initial H_2 selectivity (75%) with declining trend with the reaction time. The catalysts calcined at 300°C, 500°C, 600°C demonstrated the same synthesis activity and H_2 selectivities at around 60 %, which remained unchanged with reaction time up to 300 min. These results indicated that calcination from 300 °C to 600 °C does not significantly influence the catalyst properties. Similar synthesis activity was observed over an uncalcined sample. In contrast, catalysts calcined at 800 °C showed both the lowest synthesis activity and selectivity towards H_2O_2 among studied catalysts. The authors concluded that calcination is essential for production of stable and re-usable catalyst. Catalysts calcined at 500 °C showed no change in synthesis activity and selectivity upon re-use, while no synthesis activity was observed over re-used uncalcined catalyst due to leaching of Pd.

1.11 Thesis aims

The direct synthesis of H_2O_2 represents an attractive, more atomically efficient, and environmentally friendly alternative to the current industrial anthraquinone process. However, the main challenge of the process is a poor H_2O_2 selectivity of the highly active catalysts as they often display high rates of H_2O_2 degradation, through hydrogenation and decomposition pathway.

The aims of the thesis are outlined below:

1) The synthesis reactions were carried out at ambient temperature eliminating the need of cooling down the reactor set up and no acidic or halide additives were used, which may result in decrease of the process cost. The catalyst design was focused on more effective and efficient utilisation of precious metals to maximize the amount of produced H_2O_2 per mol of precious metal. The protocol for catalyst preparation was created to enable large scale production with minimal operational cost.

2) Investigate bimetallic supported catalysts and how the addition of secondary metal (Au, Sn, Ni) effects catalyst synthesis and degradation activity towards H_2O_2. Catalyst design of bimetallic catalyst was caried out to investigate if SnPd and NiPd catalysts can present a cheaper alternative to well established and studied AuPd catalyst. To maximise the concentration of H_2O_2 obtained during the reaction, different reaction conditions were also investigated.

The PhD project is collaboration between Cardiff University and Haldor Topsøe and therefore work is mainly focused on utilising conditions that are more likely to be industrially applicable. The preferences of the industrial partner were to use temperature that does not require extensive cooling and use of TiO_2 as main catalyst support. Catalyst preparation method and reaction conditions were optimised to minimise the overall process cost.

1.12 References

1 Evonik, *The Modern Chemist's Guide to Hydrogen Peroxide and Peracetic Acid*, 2018.

2 Market Research , April 2021, Hydrogen Peroxide, www.marketresearch.com/Global-Industry-Analysts-v1039/Hydrogen-Peroxide-14447679/, (accessed 1 March 2022).

3 Q. Chen, *Chem. Eng. Process. Process Intensif.*, 2008, **47**, 787–792.

4 T. Nishimi, T. Kamachi, K. Kato, T. Kato and K. Yoshizawa, *European J. Org. Chem.*, 2011, 4113–4120.

5 J. M. Campos-Martin, G. Blanco-Brieva and J. L. G. Fierro, *Angew. Chemie - Int. Ed.*, 2006, **45**, 6962–6984.

6 W. Weber and T. Assiertons, *US Pat., Pat. 1108752.*

7 J. K. Edwards and G. J. Hutchings, *Angew. Chemie - Int. Ed.*, 2008, **47**, 9192–9198.

8 J. K. Edwards, S. J. Freakley, R. J. Lewis, J. C. Pritchard and G. J. Hutchings, *Catal. Today*, 2015, **248**, 3–9.

9 J. K. Edwards, S. J. Freakley, A. F. Carley, C. J. Kiely and G. J. Hutchings, *Acc. Chem. Res.*, 2013, **47**, 845–854.

10 J. K. Edwards and G. J. Hutchings, *Angew. Chemie - Int. Ed.*, 2008, **47**, 9192–9198.

11 D. P. Dissanayake and J. H. Lunsford, *J. Catal.*, 2002, **206**, 173–176.

12 F. Menegazzo, M. Signoretto, G. Frison, F. Pinna, G. Strukul, M. Manzoli and F. Boccuzzi, *J. Catal.*, 2012, **290**, 143–150.

13 J. K. Edwards, E. Ntainjua N, A. F. Carley, A. A. Herzing, C. J. Kiely and G. J. Hutchings, *Angew. Chemie Int. Ed.*, 2009, **48**, 8512–8515.

14 S. J. Freakley, Q. He, J. H. Harrhy, L. Lu, D. A. Crole, D. J. Morgan, E. N. Ntainjua, J. K. Edwards, A. F. Carley, A. Y. Borisevich, C. J. Kiely and G. J. Hutchings, 2015, **351**, 279–296.

15 S. Wang, D. E. Doronkin, M. Hähsler, X. Huang, D. Wang, J. D. Grunwaldt and S. Behrens, *ChemSusChem*, 2020, **13**, 3243–3251.

16 S. Han, Y. Liu, J. Li, R. Li, F. Yuan and Y. Zhu, *Catal. 2018, 8.*

17 D. Ding, X. Xu, P. Tian, X. Liu, J. Xu and Y. F. Han, *Cuihua Xuebao/Chinese J. Catal.*, 2018, **39**, 673–681.

18 S. Wang, K. Gao, W. Li and J. Zhang, *Appl. Catal. A Gen.*, 2017, **531**, 89–95.

19 M. Piccinini, J. K. Edwards, J. A. Moulijn and G. J. Hutchings, *Catal. Sci. Technol.*, 2012, **2**, 1908–1913.

20 P. Landon, P. J. Collier, A. F. Carley, D. Chadwick, A. J. Papworth, A. Burrows, C. J. Kiely and G. J. Hutchings, *Phys. Chem. Chem. Phys.*, 2003, **5**, 1917–1923.

21 D. A. Crole, S. J. Freakley, J. K. Edwards and G. J. Hutchings, *Proc. R. Soc. A Math. Phys. Eng. Sci.*, , DOI:10.1098/rspa.2016.0156.

22 A. Santos, R. J. Lewis, G. Malta, A. G. R. Howe, D. J. Morgan, E. Hampton, P. Gaskin and G. J. Hutchings, *Ind. Eng. Chem. Res.*, 2019, **58**, 12623–12631.

23 J. K. Edwards, A. Thomas, A. F. Carley, A. A. Herzing, C. J. Kiely and G. J. Hutchings, *Green Chem.*, 2008, **10**, 388–39.

24 M. R. Gogate, *Chem. Eng. Commun.*, 2017, **204**, 1–27.

25 BASF, Management's Report, 2018.

26 I. Chorkendorff and H. Niemantsverdriet, *Concepts of Modern Catalysis and Kinetics*, Wiley-VCH, Weinheim, Germany, 2003.

27 P. Anastas and N. Eghbali, *Chem. Soc. Rev.*, 2010, **39**, 301–312.

28 Anastas, P. T.; Warner, J. C. Green Chemistry: Theory and Practice, Oxford University Press: New York, 1998.

29 C. W. Jones, *Introduction to the Preparation and Properties of Hydiogen Peroxide*, 1999.

30 S. J. Freakley, M. Piccinini, J. K. Edwards, E. N. Ntainjua, J. A. Moulijn and G. J. Hutchings, *ACS Catal.*, 2013, **3**, 487–501.

31 The Essential Chemical Industry, 6 November 2016, Production of hydrogen peroxide, http://www.essentialchemicalindustry.org/chemicals/hydrogen-peroxide.html,

32 Mordor Intelligence, Hydrogen Peroxide Market - Growth, Trends, COVID-19 Impact, and Forecast (2022 - 2027), 2021.

33 Evonik, 2022, Hydrogen peroxide, Application areas, 2020.

34 Evonik, Applications of hydrogen peroxide for textile industry, 2020.

35 Grand View Research, April 2021, Hydrogen Peroxide Market Size, Share & Trends Analysis Report By Function (Oxidant, Disinfectant, Bleaching), By Application (Healthcare, Wastewater Treatment), By Region, And Segment Forecasts, 2021 - 2028, 2019.

36 A. A. Batoeva, M. R. Sizykh and D. G. Aseev, *Catal. Ind.*, 2010, **2**, 67–71.

37 J.E. Schiller, Removal of cyanide and metals from mineral processing waste water, Report of Investigation 8836, United States, 1983.

38 A.M Shams El Din, R.A. Mohammed, *Desalination,1998*, **115,** 145-153

39 R. Mikutta, M. Kleber, K. Kaiser and R. Jahn, *Soil Sci. Soc. Am. J.*, 2005, **69**, 120–135.

40 C. B. Chidambara Raj and L. H. Quen, *Chem. Eng. Sci.*, 2005, **60**, 5305–5311.

41 USP Technoligies, Nitrogen Oxides (NOx) Abatement with Hydrogen Peroxide, 2020.

42 J. M. Haywood and C. D. Cooper, *J. Air Waste Manag. Assoc.*, 1998, **48**, 238–246.

43 S. B. Shin and D. Chadwick, *Ind. Eng. Chem. Res.*, 2010, **49**, 8125–8134.

44 E. Klemm, E. Dietzsch, T. Schwarz, T. Kruppa, A. L. De Oliveira, F. Becker, G. Markowz, S. Schirrmeister, R. Schütte, K. J. Caspary, F. Schüth and D. Hönicke, *Ind. Eng. Chem. Res.*, 2008, **47**, 2086–2090.

45 X. Liang, Z. Mi, Y. Wang, L. Wang, X. Zhang and T. Liu, *Chem. Eng. Technol.*, 2004, **27**, 176–180.

46 T. A. Nijhuis, M. Makkee, J. A. Moulijn and B. M. Weckhuysen, *Ind. Eng. Chem. Res.*, 2006, **45**, 3447–3459.

47 F. Schmidt, M. Bernhart, H. Morell and M. Pascaly, Evonik Industries, April 2014, HPPO Process Technology A novel route to propylene oxide without coproducts, https://www.teknoscienze.com/Contents/Riviste/PDF/chimica_2_2014_RGB_33-37.pdf, (accessed 20 May 2020).

48 C. W. Jones and J. H. Clark, *J. Chem. Inf. Model.*, 1999, 53, 56.

49 W. Manchot, *Justus Liebig's Ann. der Chemie*, 1901, **314**, 177–199.

50 J. H. Walton and G. W. Filson, *J. Am. Chem. Soc.*, 1932, **54**, 3228–3229.

51 H.-J. Rledl and G. Pfleiderer, US Patent, 2158525,1939.

52 Evonik, *The Modern Chemist's Guide to Hydrogen Peroxide and Peracetic Acid*, 2018.

53 G. Goor, Hydrogen Peroxide: Manufacture and Industrial Use for Production of Organic Chemicals, Catalysis by Metal Complexes, vol 9. Springer, 1992.

54 C. Samanta, *Appl. Catal. A Gen.*, 2008, **350**, 133–149.

55 D. A. Crole, R. Underhill, J. K. Edwards, G. Shaw, S. J. Freakley, G. J. Hutchings and R. J. Lewis, *Philos. Trans. R. Soc. A Math. Phys. Eng. Sci.*, 2020, **378,** 1-11.

56 D. P. Dissanayake and J. H. Lunsford, *J. Catal.*, 2003, **214**, 113–120.

57 J. S. Adams, A. Chemburkar, P. Priyadarshini, T. Ricciardulli, Y. Lu, V. Maliekkal, A. Sampath, S. Winikoff, A. M. Karim, M. Neurock and D. W. Flaherty, *Science*, 2021, **371**, 626–632.

58 N. M. Wilson and D. W. Flaherty, *J. Am. Chem. Soc.*, 2016, **138**, 574–586.

59 L. Ouyang, P. F. Tian, G. J. Da, X. C. Xu, C. Ao, T. Y. Chen, R. Si, J. Xu and Y. F. Han, *J. Catal.*, 2015, **321**, 70–80.

60 P. Tian, L. Ouyang, X. Xu, C. Ao, X. Xu, R. Si, X. Shen, M. Lin, J. Xu and Y.-F. Han, *J. Catal.*, 2017, **349**, 30–40.

61 L. W. Gosser and J. T. Schwarts, *United State Pat. 4772458*.

62 S. Abate, S. Melada, G. Centi, S. Perathoner, F. Pinna and G. Strukul, *Catal. Today*, 2006, **117**, 193–198.

63 Y. Voloshin and A. Lawal, *Appl. Catal. A Gen.*, 2009, **353**, 9–16.

64 A. Staykov, T. Kamachi, T. Ishihara and K. Yoshizawa, *J. Phys. Chem. C*, 2008, **112**, 19501–19505.

65 Y. Voloshin and A. Lawal, *Chem. Eng. Sci.*, 2010, **65**, 1028–1036.

66 S. Chinta and J. H. Lunsford, *J. Catal.*, 2004, 225, 249–255.

67 D. W. Flaherty, *ACS Catal.*, 2018, **8**, 1520–1527.

68 E. Ntainjua N., J. K. Edwards, A. F. Carley, J. A. Lopez-Sanchez, J. A. Moulijn, A. a. Herzing, C. J. Kiely and G. J. Hutchings, *Green Chem.*, 2008, **10**, 1162.

69 T. Pospelova and N. Kobozev, *Russ. J. Phys. Chem.*, 1961, **35**, 535.

70 S. S. Stahl, J. L. Thorman, R. C. Nelson and M. A. Kozee, *J. Am. Chem. Soc.*, 2001, **123**, 7188–7189.

71 K. Honkala and K. Laasonen, *J. Chem. Phys.*,2001,**115**, 2297-2302.

72 R. Todorovic and R. J. Meyer, *Catal. Today*, 2011, **160**, 242–248.

73 S. Abate, G. Centi, S. Melada, S. Perathoner, F. Pinna and G. Strukul, *Catal. Today*, 2005, **104**, 323–328.

74 B. Zhou and L.-K. Lee, United States Patent 6168775, 2001.

75 S. Kim, D. W. Lee and K. Y. Lee, *J. Mol. Catal. A Chem.*, 2014, **391**, 48–54.

76 P. Tian, L. Ouyang, X. Xu, J. Xu and Y. F. Han, *Cuihua Xuebao/Chinese J. Catal.*, 2013, **34**, 1002–1012.

77 T. Deguchi and M. Iwamoto, *J. Phys. Chem. C*, 2013, **117**, 18540–18548.

78 S. Chinta and J. H. Lunsford, *J. Catal.*, 2004, **225**, 249–255.

79 V. R. Choudhary, C. Samanta and T. V. Choudhary, *Appl. Catal. A Gen.*, 2006, **308**, 128–133.

80 V. R. Choudhary, A. G. Gaikwad and S. D. Sansare, *Catal. Letters*, 2002, **83**, 235–239.

81 A. G. Gaikwad, S. D. Sansare and V. R. Choudhary, *J. Mol. Catal. A Chem.*, 2002, **181**, 143–149.

82 C. Samanta and V. R. Choudhary, *Chem. Eng. J.*, 2008, **136**, 126–132.

83 V. R. Choudhary and P. Jana, *Catal. Commun.*, 2008, **9**, 2371–2375.

84 V. R. Choudhary and P. Jana, *Catal. Commun.*, 2008, **9**, 1624–1629.

85 V. R. Choudhary, C. Samanta and T. V. Choudhary, *Catal. Commun.*, 2007, **8**, 1310–1316.

86 P. Landon, P. J. Collier, A. J.Papworth, C. J. Kiely and G. J. Hutchings, *Chem. Commun.*, 2002, 2058–2059.

87 E. N. Ntainjua, J. K. Edwards, A. F. Carley, J. A. Lopez-Sanchez, J. A. Moulijn, A. A. Herzing, C. J. Kiely and G. J. Hutchings, *Green Chem.*, 2008, **10**, 1162–1169.

88 J. K. Edwards, A. Thomas, B. E. Solsona, P. Landon, A. F. Carley and G. J. Hutchings, *Catal. Today*, 2007, **122**, 397–402.

89 A. S. K. Hashmi and G. J. Hutchings, *Angew. Chemie - Int. Ed.*, 2006, **45**, 7896–7936.

90 M. Haruta, *CATTECH*, 2002, **6**, 102–115.

91 G. J. Hutchings and M. Haruta, *Appl. Catal. A Gen.*, 2005, **291**, 2–5.

92 F. Mohr, Ed., *Gold Chemistry*, Wiley, 2009.

93 M. Haruta, N. Yamada, T. Kobayashi and S. Iijima, *J. Catal.*, 1989, **115**, 301–309.

94 M. Okumura, Y. Kitagawa, K. Yamagcuhi, T. Akita, S. Tsubota and M. Haruta, *Chem. Lett.*, 2003, **32**, 822–823.

95 T. Ishihara, Y. Ohura, S. Yoshida, Y. Hata, H. Nishiguchi and Y. Takita, *Appl. Catal. A Gen.*, 2005, **291**, 215–221.

96 P. P. Olivera, E. M. Patrito and H. Sellers, *Sourface Sci.*, 1994, **313**, 25–40.

97 J. K. Edwards, A. F. Carley, A. A. Herzing, C. J. Kiely and G. J. Hutchings, *Faraday Discuss.*, 2008, **138**, 225–239.

98 J. K. Edwards, B. Solsona, E. N. N, A. F. Carley, A. a Herzing, C. J. Kiely and G. J. Hutchings, 2009, 1037–1041.

99 Y. F. Han, Z. Zhong, K. Ramesh, F. Chen, L. Chen, T. White, Q. Tay, S. N. Yaakub and Z. Wang, *J. Phys. Chem. C*, 2007, **111**, 8410–8413.

100 D. Gudarzi, W. Ratchananusorn, I. Turunen, M. Heinonen and T. Salmi, *Catal. Today*, 2015, **248**, 58–68.

101 F. Li, Q. Shao, M. Hu, Y. Chen and X. Huang, *ACS Catal.*, 2018, **8**, 3418–3423.

102 Y. Liu, A. Ishihara, S. Mitsushima, N. Kamiya and K. Ota, *J. Electrochem. Soc.*, 2007, **154**, B664.

103 N. Garino, A. Sacco, M. Castellino, J. A. Muñoz-Tabares, A. Chiodoni, V. Agostino, V. Margaria, M. Gerosa, G. Massaglia and M. Quaglio, *ACS Appl. Mater. Interfaces*, 2016, **8**, 4633–4643.

104 S. Wang, R. J. Lewis, D. E. Doronkin, D. J. Morgan, J. D. Grunwaldt, G. J. Hutchings and S. Behrens, *Catal. Sci. Technol.*, 2020, **10**, 1925–1932.

105 S. Maity and M. Eswaramoorthy, *J. Mater. Chem. A*, 2016, **4**, 3233–3237.

106 C. Zhu, D. Wen, M. Oschatz, M. Holzschuh, W. Liu, A. K. Herrmann, F. Simon, S. Kaskel and A. Eychmüller, *Small*, 2015, **11**, 1430–1434.

107 N. J. S. Costa, M. Guerrero, V. Collière, É. Teixeira-Neto, R. Landers, K. Philippot and L. M. Rossi, *ACS Catal.*, 2014, **4**, 1735–1742.

108 J. Gu, S. Wang, Z. He, Y. Han and J. Zhang, *Catal. Sci. Technol.*, 2016, **6**, 809–817.

109 P. Tian, X. Xu, C. Ao, D. Ding, W. Li, R. Si, W. Tu, J. Xu and Y. F. Han, *ChemSusChem*, 2017, **10**, 3342–3346.

110 V. R. Choudhary, C. Samanta and P. Jana, *Appl. Catal. A Gen.*, 2007, **332**, 70–78.

111 V. R. Choudhary, C. Samanta and P. Jana, *Ind. Eng. Chem. Res.*, 2007, **46**, 3237–3242.

112 V. R. Choudhary and P. Jana, *Appl. Catal. A Gen.*, 2009, **352**, 35–42.

113 V. R. Choudhary and C. Samanta, *J. Catal.*, 2006, **238**, 28–38.

114 C. Samanta and V. R. Choudhary, *Appl. Catal. A Gen.*, 2007, **326**, 28–36.

115 C. Samanta and V. R. Choudhary, *Catal. Commun.*, 2007, **8**, 2222–2228.

116 V. R. Choudhary and P. Jana, *J. Catal.*, 2007, **246**, 434–439.

117 C. Samanta and V. R. Choudhary, *Catal. Commun.*, 2007, **8**, 73–79.

118 C. Samanta and V. R. Choudhary, *Appl. Catal. A Gen.*, 2007, **330**, 23–32.

119 V. R. Choudhary, C. Samanta and P. Jana, *Appl. Catal. A Gen.*, 2007, **317**, 234–243.

120 V. R. Choudhary and C. Samanta, *J. Catal.*, 2006, **238**, 28–38.

121 V. R. Choudhary, Y. V. Ingole, C. Samanta and P. Jana, *Ind. Eng. Chem. Res.*, 2007, **46**, 8566–8573.

122 V. R. Choudhary, C. Samanta and T. V. Choudhary, *J. Mol. Catal. A Chem.*, 2006, **260**, 115–120.

123 V. R. Choudhary and P. Jana, *Appl. Catal. A Gen.*, 2007, **329**, 79–85.

124 J. K. Edwards, B. Solsona, E. N. N, A. F. Carley, A. A. Herzing, C. J. Kiely and G. J. Hutchings, *Science*, 2009, **323**, 1037–1041.

125 J. K. Edwards, J. Pritchard, M. Piccinini, G. Shaw, Q. He, A. F. Carley, C. J. Kiely and G. J. Hutchings, *J. Catal.*, 2012, **292**, 227–238.

126 J. K. Edwards, B. E. Solsona, P. Landon, A. F. Carley, A. Herzing, C. J. Kiely and G. J. Hutchings, *J. Catal.*, 2005, **236**, 69–79.

127 A. Cybula, J. B. Priebe, M. M. Pohl, J. W. Sobczak, M. Schneider, A. Zielińska-Jurek, A. Brückner and A. Zaleska, *Appl. Catal. B Environ.*, 2014, **152–153**, 202–211.

128 The European Commision, Commission Recommendation of 18 October 2011 on the definition of nanomaterialT, *Official Journal of the European Union*,2011.

129 D. Astruc, *Nanoparticles and Catalysis, 2008, WILEY-VCH Verlag GmbH & Co. KGaA, Weinheim.*

130 F. Valentini, V. Biagiotti, C. Lete, G. Palleschi and J. Wang, *Sensors Actuators, B Chem.*, 2007, **128**, 326–333.

131 A. Z. Moshfegh, *J. Phys. D. Appl. Phys.*, 2009, **42,**

132 R. Schlögl and S. B. Abd Hamid, *Angew. Chemie - Int. Ed.*, 2004, **43**, 1628–1637.

133 C. T. Campbell, *Science*, 2004, **306**, 234–235.

134 C. P. Poole and F. J. Owens, *Introduction to Nanotechnology*, 2003, John Wiley & Sons.

Chapter 2

Experimental

This Chapter outlines the chemicals, experimental procedure used for catalysts preparation, testing and characterization used and discussed in this thesis.

2.1 Materials used

This Section outlines the chemicals used during the work within this thesis, and the suppliers used, with the purity of the various chemicals in parenthesis.

$PdCl_2$ - Merck (99.999% trace metal basis)
$Pd(NO_3)_2.2H_2O$ - Merck (40 % Pd basis)
$HAuCl_4.3H_2O$ - Merck (99 % trace metal basis)
$SnCl_4.5H_2O$ - Merck (98 % trace metal basis)
$NiCl_2.6H_2O$ - Merck (99.9 % trace metal basis)
TiO_2 - Degussa p25 (99.5 % trace metal basis, 20-30 nm particle size)
TiO_2 - Merck, anatase (99.7% trace metal basis, <25 nm particle size)
TiO_2 - Merck, rutile (99.5% trace metal basis, <100 nm particle size)
SiO_2 - Merck (99.5% trace metal basis, 5-15 nm particle size)
Al_2O_3 - Merck (99% trace metal basis, <50 nm particle size)
ZrO_2 - Merck (99% trace metal basis, <100 nm)
CH_3OH - Fischer Scientific (HPLC Grade)
H_2O - Fischer Scientific (HPLC Grade)
H_2O_2 – Honeywell Fluka (50 wt.%, stabilised)
$(NH_4)_2Fe(SO_4)_2.6H_2O$ - Fischer Scientific (0.06 M)
$Ce(SO_4)_2$ - Sigma Aldrich (> 98 %)

2.2 Catalyst preparation by wet impregnation

2.2.1 Monometallic catalysts

Monometallic Pd, Au, Sn and Ni catalysts were prepared by wet co-impregnation of the appropriate support with solutions of $PdCl_2$, $HAuCl_4$, $SnCl_2$ and $NiCl_2$, using an excess of solvent (deionised H_2O). The catalysts were prepared to have a nominal metal content of 0.5 wt.%, unless stated otherwise.

A typical catalyst preparation procedure of 0.5wt.%Pd /TiO_2 was carried out according to the following procedure, which is a modification of procedure previously published by Edwards *et al.*[1]

$PdCl_2$ (Merck, 0.883 mL, 6 mg.mL^{-1}) was added into a 50 mL round-bottom flask fitted with a magnetic stirrer bar. The volume of the solution was adjusted using deionized water to a total volume of 16 mL and heated to 65 °C with stirring (800 rpm) in a thermostatically controlled oil bath. TiO_2 (Evonik Degussa, P25,1.99 g) support was then added to the solution, and mixture was heated to 95°C. The slurry was stirred for 16 h until all the water evaporated leaving a dry solid. The catalyst was ground into fine powder and then 0.5 g of catalyst was calcined in static air (400 °C, 3 h, ramp rate of 20°C.min^{-1}) if not stated differently. Calcining only 0.5 g of catalyst at once ensured that the layer of catalyst in calcination boat was thin and heat treatment was even.

A similar procedure was followed when $Pd(NO_3)_2$ was used as Pd precursor. $Pd(NO_3)_2.2H_2O$ (Merck, 0.025 g) was added into a 50 mL round-bottom flask fitted with a magnetic stirrer bar and dissolved in 16 ml of deionised H_2O and heated to 65 °C with stirring. The rest of the procedure was identical to the one mentioned above.

2.2.2 Bimetallic catalysts.

Bimetallic AuPd, SnPd and NiPd catalysts were prepared by wet impregnation of the appropriate support with solutions of $PdCl_2$, $HAuCl_4$, $SnCl_2$ and $NiCl_2$, using an excess of solvent (deionised H_2O). The catalysts were prepared to have a nominal metal content of 0.5 wt.%, unless stated otherwise.

A typical catalyst preparation procedure of 0.25 wt.%Au-0.25 wt.%Pd /TiO_2 was carried out according to the following procedure, which is a modification of procedure previously published by Edwards *et al.*[1]

$HAuCl_4.3H_2O$ (Strem Chemicals, 0.41 mL, 12.25 mg.mL^{-1}) and $PdCl_2$ (Merck, 0.883 mL, 6 mg.mL^{-1}) were added into a 50 mL round-bottom flask fitted with a magnetic stirrer bar. The volume of the solution was adjusted using deionized water to a total volume of 16 mL and heated to 65 °C with stirring. A TiO_2 (Evonik Degussa, P25,1.99 g) support was then added to the solution, and mixture was heated to 95°C. The slurry was stirred for 16 h until all the water evaporated leaving a dry solid. The catalyst was grund into fine powder and then 0.5 g of catalyst was calcined in static air (400 °C, 3 h with a ramp rate of 20 °C min^{-1}) if not stated differently.

2.3 Catalyst testing

2.3.1 Direct synthesis of hydrogen peroxide

Catalytic activity toward the direct synthesis of H_2O_2 from H_2 and O_2 was determined using a Parr Instruments stainless-steel autoclave (equipped with overhead stirrer and temperature/pressure sensors) with a nominal volume of 50 mL, equipped with a PTFE 50 ml liner and maximum working pressure of 14 MPa, as shown in Figure 2.1. During a standard H_2O_2 synthesis reaction the autoclave was charged with HPLC standard CH_3OH (5.6 g), HPLC standard H_2O (2.9 g), and catalyst (0.01 g). The charged autoclave was then purged 3 times with 5% H_2/CO_2 (0.7 MPa) to get rid of residual air from reactor vessel. The autoclave was pressurized with 2.9 MPa 5% H_2/CO_2 and 1.1 MPa 25% O_2/CO_2 to give a total reaction pressure of 4 MPa. The reaction gas contains CO_2 as a diluent, which has been shown to form carbonic acid *in situ* by dissolving in the solvent at elevated pressure, lowering the pH of the reaction solution, stabilising the H_2O_2 that was formed and suppressing the subsequent degradation reactions.[2,3] The reaction mixture was stirred at 1200 rpm for 0.5 h at ambient temperature. If the reaction was carried out at different temperature than ambient, temperature was first adjusted by cooling the reactor vessel using ice bath prior to the start of the reaction. The reaction starts once the reactor starts stirring. After the reaction was completed, a gaseous sample was collected and analysed by gas chromatography when necessary. Once the gas sample was collected, the remaining reagent gas was vented, and the catalyst was removed from the solvent by filtration. Aliquots of the solvent were titrated against a $Ce(SO_4)_2$ solution with a known concentration and acidified with 2% H_2SO_4 using ferroin as an indicator. The concentration of the $Ce(SO_4)_2$ solution was standardized by titration of a known amount of $(NH_4)_2Fe(SO_4)_2.6H_2O$, using ferroin as an indicator.[6]

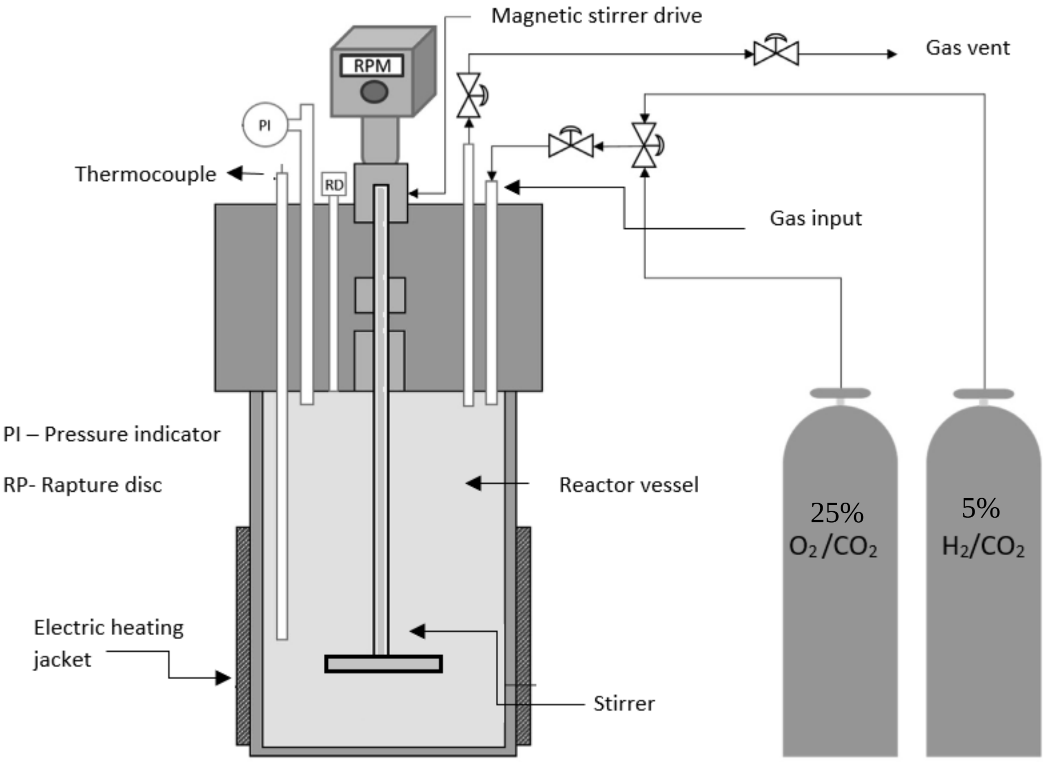

Figure 2.1: Schematic representation of the high-pressure autoclave used for testing.

To compare the performance of the catalysts, productivity was calculated by normalising the produced amount of H_2O_2 over reaction time and catalysts mass used in reaction and presented as $mol_{H2O2}h^{-1}kg^{-1}$. The following equations were used to calculate productivity and wt.% of H_2O_2. The Equation 2.1 was used to calculate the volume of $Ce(SO_4)_2$ solution required to titre the reaction solution after the reaction. The volume of $Ce(SO_4)_2$ solution of known concentration was then used to calculated the moles of $Ce(SO_4)_2$ used in titration according to Equation 2.2.

$$Volume\ of\ Ce(SO_4)_2\ to\ titrate\ reaction\ solution = \frac{recorded\ titre\ x\ mass\ of\ reaction\ solution}{sample\ mass} \tag{2.1}$$

$$Moles\ of\ Ce(SO_4)_2 = volume\ of\ Ce(SO_4)_2\ \ x\ concentration\ of\ Ce(SO_4)_2 \tag{2.2}$$

In the Equation 2.3, 2 moles of $Ce(SO_4)_2$ react with one mole of H_2O_2 and therefore this ratio was used to calculate moles of H_2O_2 according to Equation 2.4.

$$H_2O_2 + 2Ce(SO_4)_2 \rightarrow Ce_2(SO_4)_3 + H_2SO_4 + O_2 \tag{2.3}$$

$$Moles\ of\ H_2O_2 = \frac{moles\ of\ Ce(SO_4)_2}{2} \tag{2.4}$$

The catalytic activity towards the synthesis of H_2O_2 was presented in terms of productivity or weight percentage (wt. %) in reaction solution . The concentration of H_2O_2 was determined and standardised by the mass of catalyst and time, as shown in Equation 2.5 and Equation 2.6.

$$Productivity = \frac{Moles\ of\ H_2O_2}{mass\ of\ catalyst\ x\ reaction\ time} \tag{2.5}$$

$$wt.\%\ H_2O_2 = \frac{Moles\ of\ H_2O_2\ x\ Molar\ mass\ of\ H_2O_2}{mass\ of\ reaction\ solution} \tag{2.6}$$

2.3.2 Degradation testing

The degradation activity of a catalyst toward H_2O_2, which is the sum of H_2O_2 decomposition and hydrogenation activity, was determined in a manner similar to the direct synthesis activity of a catalyst. The autoclave was charged with CH_3OH (5.6 g), H_2O_2 (50 wt. % 0.68 g), and HPLC standard H_2O (2.21 g), with the solvent composition equivalent to a 4 wt. % H_2O_2 solution. From the solution, 5 aliquots of known mass were removed and titrated with acidified $Ce(SO_4)_2$ solution of known concentration, using ferroin as an indicator to determine an accurate concentration of H_2O_2 at the start of the reaction. Then, catalyst (0.01 g) was added to the solvent. The charged autoclave was then purged 3 times with 5% H_2/CO_2 (100 psi) to get rid of residual air from reactor vessel. The autoclave was pressurized with 2.9 MPa 5% H_2/CO_2. No O_2 was present in the reaction system during degradation testing. The reaction mixture was stirred at 1200 rpm for 0.5 h at ambient temperature. If the reaction was carried out at different temperature than ambient, temperature was first adjusted by cooling the reactor vessel using ice bath prior the start of the reaction. The reaction starts once the reactor starts stirring. After the reaction was completed, the remaining reagent gas is vented, and the catalyst was removed from the solvent by filtration. Again, five aliquots of known mass were titrated against the acidified $Ce(SO_4)_2$ solution using ferroin as an indicator.[6] The degradation activity was calculated as $mol_{H2O2}\ h^{-1} kgcat^{-1}$ along with the percentage of H_2O_2 remaining after the reaction.

2.3.3 Blank degradation testing

A blank degradation reaction, in the absence of a catalyst, was carried out on a regular basis to determine possible reactor contamination. The same procedure was followed as described in Section 2.3.2, however no catalyst was added into reaction solution. In the case of contamination, the reactor was subjected to cleaning process using mineral acids followed by water and TiO_2 washing cycles. A subsequent blank degradation reaction was then carried out before continuing testing with catalyst.

2.3.4 Catalyst re-use

Catalyst reusability was carried out by using standard reaction conditions as stated in Chapter 2.3.1 but the mass of the catalyst was increased to 0.05 g. After the reaction was carried out, the catalyst was removed from the reaction medium via filtration. The catalyst was then dried under vacuum oven at 25 ^{o}C for 16 h. Between reactions, a blank degradation reaction was carried out to make sure that no contamination of the reactor occurred due to the use of increased amount of the catalyst. Following this procedure, a standard synthesis reaction was run as previously described in Section 2.3.1.

2.4 Catalyst characterization

2.4.1 Gas chromatography

Gas chromatography (GC) is a technique used to separate and analyse mixture of chemical compounds. GC uses carrier gas, for example He or N_2, in the separation as mobile phase. The sample is introduced to the GC with syringe or autosampler. After injection into the GC, the sample mixture is first vaporised if required. Based on the concentration, the whole vapourised sample is transferred into the column by the carrier gas, or only portion of the sample can be transferred into column in a split mode and the rest is flushed from the system.[4]

In the analytical column, separation of the sample components take place based on the different interactions with the separation phase.[4] A liquid stationary phase (for example, silicone polymers) is chemically bonded or coated in the column. The vaporized sample is repeatedly dissolved and vaporized in the liquid stationary phase while traveling downstream with the carrier gas.[5] The time of dissolving in the liquid phase and the time of vaporizing will be different for each compound, based on their physicochemical properties and interaction with the column. Once the compounds different than the carrier gas are eluted from the column, the detector converts them into electrical signals which are amplified and sent to a data processor. The data processor analyses the signal from the detector and is able to identify the substances in the sample.[5,6]

There are two types of GC columns available on the market: packed and capillary. A longer column with smaller diameter is suitable for higher resolution analysis, while a larger diameter column can be used if higher resolution is unnecessary.[5] The column is placed in a thermostatically controlled oven, with ranging temperature from ambient to over 400^{o}C. Temperature can remain constant during a separation if needed, or can increase at a determined rate to increase elution.

A thermal conductivity detector (TCD) detects the difference of the thermal conductivity between the sample and the carrier gas. Most of the compounds except carrier gas can be detected using TCD, but the sensitivity is lower compared to other detectors. A flame ionisation detector (FID) burns and ionizes the sample and is used for detection of organic compounds.[5,6] In the mass spectrometer (MS), the compounds are ionized and fragmented using electron or chemical ionization sources. Ionized molecules and fragments are then accelerated through the mass analyser, for example a quadrupole or ion trap, separating the ions based on their different mass-to-charge (*m/z*) ratios.[7]

Catalytic conversion of H_2 and selectivity towards H_2O_2 were determined using a Varian 3800 GC fitted with a thermal conductivity detector and equipped with a Porapak Q column. The following equation was used to calculate H_2 conversion:

$$H_2\ conversion\ [\%] = \frac{mmol_{H_2blank} - mmol_{H_2final}}{mmol_{H_2blank}}\ x\ 100 \qquad (2.7)$$

In order to calculate catalytic conversion as well as selectivity towards H_2O_2, blank synthesis reaction was carried out following procedure as stated in section 2.3.1, with no catalyst present in reaction system. After a reaction, the gas sample was taken and analysed by GC. The amount of H_2 in a blank reaction represents the maximal amount of H_2 in the reactor if no reaction took place, and is used in equation 2.7 as $mmol_{H2\ blank}$. The gas sample was analysed after a standard H_2O_2 synthesis reaction and represents $mmol_{H2final}$ in equation 2.7.

The selectivity towards H_2O_2 (equation 2.8) is calculated as the amount of H_2O_2 present in the reaction system after the reaction, estimated by titration, divided by the theoretical amount of H_2O_2 that could be formed based on H_2 conversion as calculated by equation 2.7.

$$H_2O_2\ selectivity\ [\%] = \frac{H_2O_2\ detectet\ [mmol]}{H_2O_2\ theoretical\ [mmol]}\ x\ 100 \qquad (2.8)$$

The column oven (containing a Porapak Q column) was heated up to 30 ^{o}C for 16 min, which allows separation of H_2, O_2 and CO_2, using Argon as a carrier gas. The retention times of the components analysed during a H_2O_2 synthesis reaction are shown in Table 2.1.

Table 2.1: Retention times of components analysed by GC after synthesis reaction.

Component	Retention time [min]
H_2	1.6
O_2	2.2
CO_2	9.2

2.4.2 X-ray diffraction (XRD)

X-ray diffraction is one of the most frequently applied analytical techniques, widely used for phase identification of a crystalline material.[8] It can be also used to obtain an indication of particle size, measurement of sample purity and identification of fine-grained minerals such as clays, which are difficult to determine optically. It is a non-destructive technique with detection limit approximately a 3 nm crystalline size.[9,10]

XRD is based on constructive interference of monochromatic X-rays and crystalline sample. X-rays are generated by a cathode ray tube by heating a filament to produce electrons, accelerating the electrons toward a target by applying a voltage, and bombarding the target with electrons. When electrons have sufficient energy to dislodge inner shell electrons of the target material, characteristic X-ray spectra are produced consisting of several components, the most common being K_α and K_β. Copper is the most common target material for single-crystal diffraction, with CuK_α radiation = 1.5418 Å. These X-rays are filtered by foils or crystal monochromators to produce monochromatic radiation, collimated to concentrate and directed toward sample. The sample and the detector are rotated, and the intensity of the reflected X-rays is recorded. Once these X-rays hit the sample, they are diffracted by the lattice planes present in the crystalline sample and interference between the diffracted beams can occur as illustrated in Figure 2.2. If an X-ray is diffracted from A and D then, to produce constructive interference, the distance travelled by the beam after it has been diffracted from D must be an integer of the wavelength. The integer is the sum of the path lengths BD and DC, which will depend on the lattice spacing (d) and the angle of incidence of the incoming X-ray beam (θ).[11]

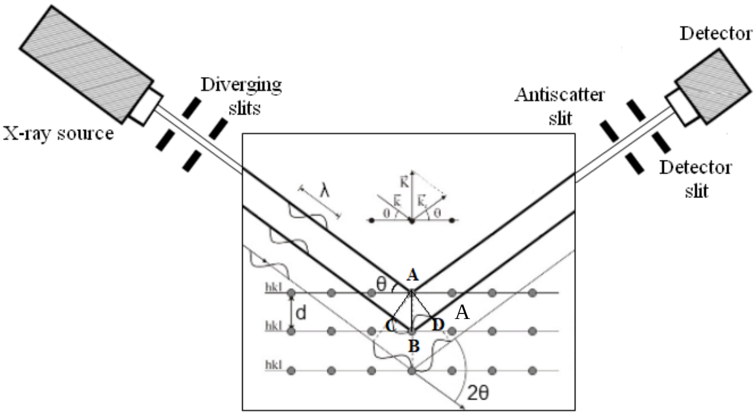

Figure 2.2: Diagram showing the diffraction of X-rays from lattice planes in a crystalline lattice. Where *d* is the lattice spacing and λ is the angle of incidence.[12]

$$n\lambda = BD + DC \tag{2.9}$$

$$BD = DC = d\ sin\theta \tag{2.10}$$

If the angles (2*θ*), under which constructively interfering X-rays leave the crystal, are measured, the Bragg relationship (2.11) gives the corresponding lattice spacings. These spacings are characteristic for a certain compound.[13]

$$n\lambda = 2d\ sin\ \theta\ ; \quad n = 1,2, \ldots \tag{2.11}$$

Where:

λ	is the wavelength of X-rays
d	is the distance between two lattice planes
θ	is the angle between the incoming X-rays and the normal to the reflecting lattice plane
n	is the integer called order of the reflection.

The shape of the reflection can provide information with regard to crystallite size. Larger crystals will produce sharper narrow peaks, while smaller crystals will result in broader peaks. Crystal size can be calculated trough the Sherrer equation (2.12), which relates crystal size to peak width:

$$\langle L \rangle = \frac{K\lambda}{\beta\ cos\theta} \tag{2.12}$$

Where:

$\langle L \rangle$ is a measure for the dimension of the particle in the direction perpendicular to the reflection plane

β is the peak width

K is a constant

XRD is a suitable method for catalyst characterization that gives clear information about crystalline structure and particle size of sufficiently large particles. However, XRD cannot detect particles that are below 3 nm or amorphous, which is a major limitation of this method, since one can overlook phases present and not detected with XRD.

Methodology:

Investigation of the bulk structure of the metal supported catalysts was carried out using a (θ-θ) PANalytical X'pert Pro powder diffractometer using a Cu Kα radiation source operating at 40 KeV and 40 mA. Standard analysis was performed using a 40 min scan between 2θ values of 10-80°, with the samples supported on an amorphous silicon wafer. Diffraction patterns of phases were identified using the ICDD data base.

2.4.3 X-ray photoelectron spectroscopy (XPS)

X-ray photoelectron spectroscopy is a frequently used surface sensitive technique in catalysis providing information on the elemental composition and the oxidation state of species on the surface of the sample to a depth of around 10 nm.[13] XPS is based on the photoelectric effect, whereby a photon of energy hv penetrates the surface and is absorbed by an electron with a binding energy E_b. The kinetic energy of the ejected electron is dependent on energy of the incident X-rays, the work function of the spectrometer, and the binding energy of the core electron, as shown in Figure 2.13. The electron is then ejected with a kinetic energy:

$$E_k = hv - E_b - \varphi \qquad (2.13)$$

Where:

E_k is the kinetic energy of the photoelectron

h is Planck's constant

v is the frequency of the exciting radiation

E_b is the binding energy of the photoelectron with respect to the Fermi level of the sample

φ is the work function of the spectrometer

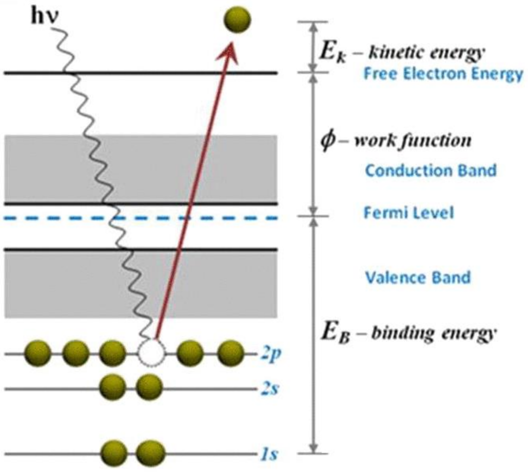

Figure 2.3: Schematic band diagram showing the energy of the photoelectron process.[14]

Each element has a characteristic set of binding energies, which are used to analyse composition of the sample. For a core electron to be emitted, the energy of the incident X-ray must be greater than the binding energy. The binding energy also contains chemical information, because the energy levels of core electrons depends slightly on the oxidation state of the atom. The higher the oxidation state of the sample, the higher the binding energy of its core electrons. The energy of the incident X-ray must be greater than that of the binding energy combined with the work function of the spectrometer. The intensity of photoelectrons is measured as a function of their kinetic energy. The XPS spectrum is usually a plot of intensity of these photoelectrons versus kinetic energy or binding energy.

Methodology:

XPS was performed using a VG EscaLab 220i spectrometer, using a standard Al-Kα X-ray source (300 W) and an analyser pass energy of 20 eV. Samples were mounted using double-sided adhesive tape, and binding energies were referenced to the C 1s binding energy of adventitious carbon contamination, which was taken to be 284.7 eV.

Acknowledgements:

I would like to thank the Cardiff University XPS facility for the access to X-Ray photoelectron spectroscopy (XPS), necessary training to operate the equipment and acquiring data presented in this thesis.

2.4.4 Scanning electron microscopy (SEM).

Scanning electron microscopy is carried out by focusing a high-energy electron beam over the sample surface to detect secondary and backscattering electrons as a function of the position of the primary beam.[8] The signals that derive from electron-sample interactions reveal information about sample morphology, chemical composition, and crystalline structure. The secondary electrons originated from the surface region of the sample and have low energies. Characteristic transitions in the sample can be studied by analysing the energy loss from the primary electrons, which often lose their energy due to subsequent collisions before they emit as secondary electrons. The backscattered electrons come from deeper areas, carrying information on the composition of the sample. Heavy elements are more efficient scatterers and appear brighter in the image.[8] The interaction between the primary electron and the sample in an electron microscope leads to detectable signals and is shown schematically in Figure 2.4.

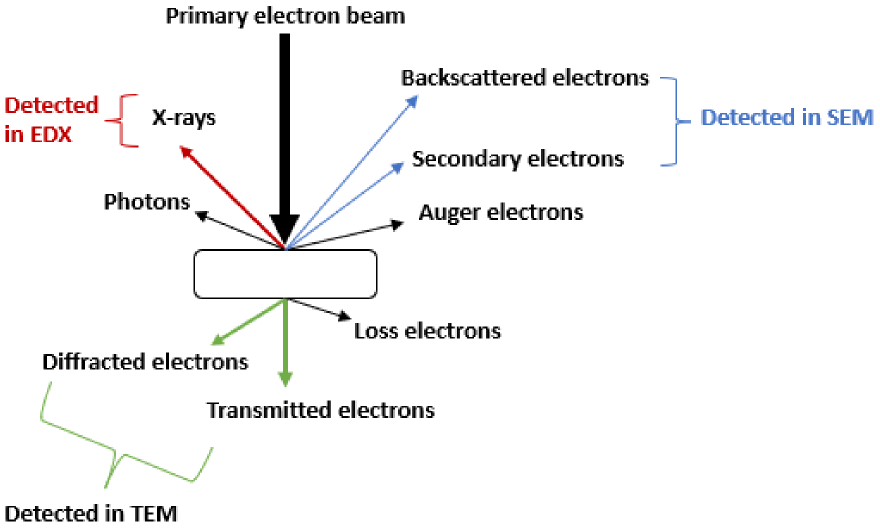

Figure: 2.4 The interaction between the primary electron beam and the sample.[13]

Data are collected over a selected area of the sample surface and a 2-dimensional image is generated. Areas ranging from approximately 1 cm to 5 microns can be imaged in a scanning mode using SEM techniques.

Methodology:

Microscopy was performed on a Tescan Maia3 field emission gun scanning electron microscope (FEG-SEM) operating in the variable pressure Univac mode and using the cooled Peltier stage. The samples were mounted uncoated on 12.5 mm aluminium stubs using adhesive carbon Lite discs. Images were taken at 250 Pa and 5 °C with a beam energy of 15 kV using the Low Vacuum secondary electron Tescan detector (LVSTD)

Acknowledgements:

I would like to thank the Cardiff University electron microscopy facility for the access to scanning electron microscopy (SEM), necessary training to operate the equipment and acquiring some of the data presented in this thesis.

2.4.5 Transmission electron microscopy (TEM)

Transmission electron microscopy (TEM) is a high-resolution imaging technique in which a primary electron beam of the high energy and intensity is generated from an electron gun and is passed through the condenser producing parallel rays, which are directed to the sample on the sample holder. A two-dimensional projection of the sample is formed by transmitted electrons and it is subsequently magnified by the electron optics to produce bright-field image. The dark-field image is formed by diffracted electron beams. Unlike SEM, which gathers the net intensity of secondary electrons in each point of the scan, TEM resolution is only limited by the wavelength of the electron and the quality of the electron optics. Therefore, images on sub-nanometre scale can be collected. The resolution of the TEM is about 0.1 nm.[15] The TEM technique has been applied to investigate the fine structure and elemental information of the catalysts.

Methodology:

Transmission electron microscopy (TEM) and scanning transmission electron microscopy (STEM) were performed on a JEOL JEM-2100 operating at 200 kV. Energy dispersive X-ray analysis (EDX) was done using an Oxford Instruments X-MaxN 80 detector and the data analysed using the Aztec software. samples were prepared by dispersion in ethanol by sonication and deposited on 300 mesh copper grids coated with holey carbon film.

Acknowledgements:

I would like to thank the Cardiff University electron microscopy facility for the access to transmission electron microscopy (TEM), necessary training to operate the equipment and acquiring some of the data presented in this thesis.

2.4.6 Energy dispersive X-ray spectroscopy (EDX)

Energy Dispersive X-Ray Spectroscopy (EDX) is a surface technique used for elemental analysis. An electron beam interacts with the sample, causing an emission of an electron from an inner shell and formation of an electron hole in the electronic structure of the element.[16] The vacancy is filled by an electron from an outer shell, as shown in Figure 2.5.

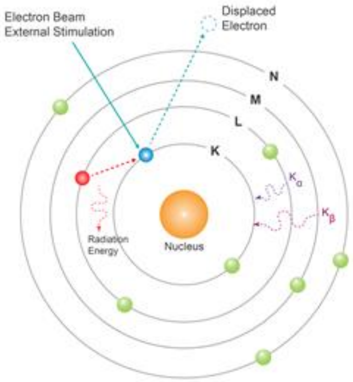

Figure 2.5: Energy Dispersive X-Ray spectroscopy schematic.[17]

The difference in energy between the two shells is released as an X-ray, hitting the detector. The amount of the energy released is individual for each element, which allows the detection of the specific element on the sample.

Methodology:

Transmission electron microscopy (TEM) was performed on a JEOL JEM-2100 operating at 200 kV. Energy dispersive X-ray analysis (EDX) was done using an Oxford Instruments X-MaxN 80 detector and the data analysed using the Aztec software. Samples were prepared via dispersion in ethanol by sonication, and deposited on 300 mesh copper grids coated with holey carbon film.

Acknowledgements:

I would like to thank the Cardiff University electron microscopy facility for the access to electron microscopy, necessary training to operate the equipment and acquiring the data presented in this thesis.

2.4.7 Inductively coupled plasma mass spectrometry (ICP-MS)

Inductively Coupled Plasma (ICP) is an analytical method used for detection and measurement of trace amounts or major concentration of nearly all elements within a sample, utilizing a high temperature plasma discharge as a source of positively charged ions.[19] ICP uses noble gases such as Ar as plasma gas. The argon gas streaming through a torch apparatus is lit, resulting in extremely hot plasma in which the vaporization, dissociation or atomization, excitation and final ionization of the sample components takes place. The temperature of the plasma may exceed 7000 K and is capable of ionizing the atoms of many chemical elements, creating a single-charged ion. The ions are passed into a mass spectrometer where a signal relative to the concentration of various elements is obtained. Calibration of an ICP unit using reference standards is required to obtain exact concentration of the elements. ICP-MS is suited to handle liquid samples as well as gaseous or solid samples, using gas chromatography or laser ablation as sample introduction technique. The schematic of the ICP-MS units is shown in Figure 2.6.

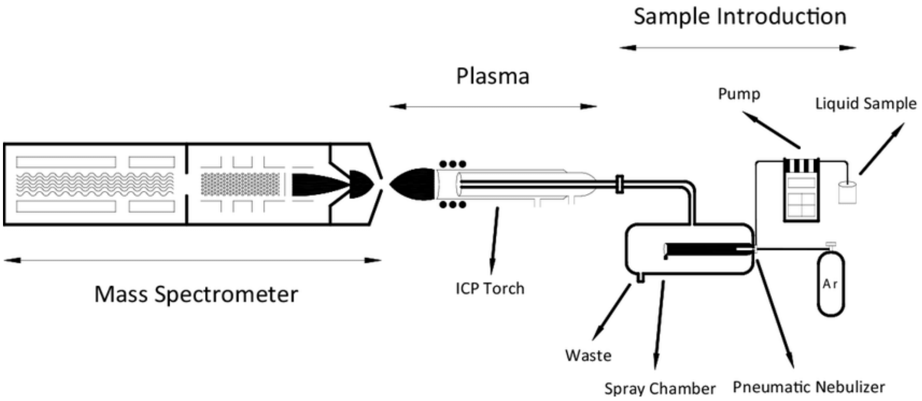

Figure 2.6: Schematic of ICP-MS unit with sample introduction system, torch and mass spectrometer. [20]

Methodology:

Post-reaction solutions were analysed using an Agilent 7900 ICP-MS equipped with I-AS auto sampler. All samples were diluted by a factor of 10 using HPLC grade H_2O. All calibrants were matrix matched and measured against a three-point calibration using certified reference materials purchased from Perkin Elmer and certified internal standards acquired from Agilent.

Acknowledgements:

I would like to thank the Cardiff University for the access to ICP-MS facility and acquiring the data presented in this thesis

2.4.8 Diffuse reflectance infrared Fourier transform spectroscopy (DRIFTS)

When an infrared beam is focused onto fine material, the incident beam can interact with particle by reflecting radiation from the surface without penetrating the particle. True diffuse reflectance results from the penetration of the incident radiation into one or more particles.[21] The light that penetrates is reflected in all directions. The light leaving the surface will pass through a thin layer of the reflecting material and therefore its wavelength content will be modified by optical properties of the matrix, containing structural information of the sample. The type of reflection that the radiation might undergo are illustrated in Figure 2.7. The diffuse reflection can not be optically separated from specular reflection.[22] If the specular reflection component is weak compared to diffuse reflection, then diffuse reflection spectra are very similar to transmission spectra. To minimise contribution from specular reflection, a sample should be ground to a particle size smaller than 10 μm. In the case of a strongly absorbent sample, dilution with a non-absorbent matrix such as KBr is required.

During DRIFTS measurement, the IR energy is directed into a sample cup filled with a mixture of the sample and an IR transparent matrix, such as KBr. The IR radiation interacts with the particles, causing the light to diffuse or scatter. The scattered energy is then directed by an output mirror into the detector of the spectrometer. The altered IR beam is recorded and used to generate a spectrum. To obtain a more accurate measurement, a background signal is collected by measuring only the IR matrix and subtracting from sample spectrum.

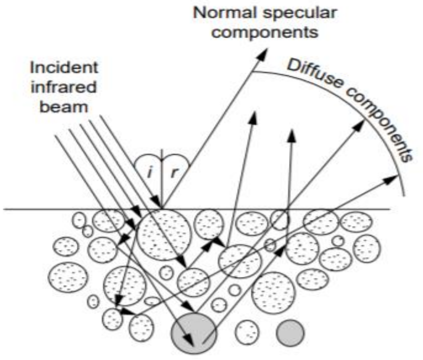

Figure 2.7: Mechanism generating the infrared spectrum of the powder.[22]

Methodology:

DRIFTS measurements were caried out on a Bruker Tensor 27 spectrometer fitted with a mercury cadmium telluride (MCT) detector. A sample was loaded into the Praying Mantis high temperature (HVC-DRP-4) *in situ* cell before exposure to N_2 and then 1% CO/N_2 at a flow rate of 50 $cm^3.min^{-1}$. A background spectrum was obtained using KBr, and measurements were recorded every 1 min at room temperature. Once the CO adsorption bands in the DRIFT spectra ceased to increase in size, the gas feed was changed back to N_2 and measurements were repeated until no change in subsequent spectra was observed.

2.4.9 X-Ray absorption near edge structure (XANES)

X-ray absorption near edge structure (XANES) is a type of an element-specific X-ray absorption spectroscopy (XAS), providing information on the electronic, structural, and magnetic properties of matter.[23] In XANES, absorption of a photon occurs and is followed by an electron excitation from a core state to an empty state. The photon energy has to be equal or higher than the binding energy of this core-level to excite an electron in a given core-level leaving a hole in an inner shell. This vacancy can be filled by an electron from the higher energy state, causing release of energy. The released energy can either undergo a fluorescence emission to release a photon, or it can further excite and eject an electron from a higher energy state. In XANES, the intensities of the light coming through samples are measured as well as the effect of scattering from auger electrons, photoelectrons, and even emitted photon. As shown in Figure 2.8, XANES refers to the absorption fine structure close to an absorption edge, about the 50 eV below and above the absorption edge.[24] EXAFS spectrum typically starts above 50 eV above absorption edge and can extend for 1000 eV.

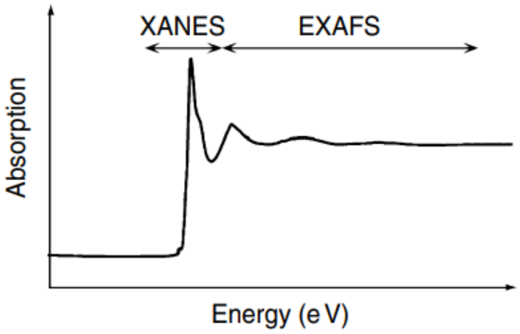

Figure 2.8: Schematic illustration of an X-Ray absorption spectrum.[24]

Methodology:

X-ray Absorption Near Edge Structure (XANES) was measured at Beamline B18 of Diamond Light Source (UK) with a Si (311) double crystal monochromator QXAFS setup. Transmission and fluorescence signals were measured simultaneously via ionisation chambers and 36 element Ge solid state detectors, respectively. Samples were pressed into a 13 mm diameter pellets for measurement. Pd foil and PdO were used for energy shift calibration. The spectrum of each sample was measured three times and merged to improve the signal-noise ratio. XAFS data was analysed by Demeter software package (including Athena and Artemis software). Athena software was used for data extraction and XANES analysis..

Acknowledgement:

The XANES characterisation was carried out by Dr Wang and his research team. We acknowledge the Diamond Light Source B18 beamline for the experiment sessions (SP17377, SP19072 and SP19850).

2.4.10 Extended X-ray absorption fine structure (EXAFS)

Extended X-ray absorption fine structure (EXAFS) contains information about the identity of adjacent atoms, their distance from the excited atom, the degree of disorder in a particular atomic shell and the number of neighbouring atoms in the nearest shell.[25] An EXAFS spectrum corresponds with the oscillating part of the X-ray absorption spectrum, starting at roughly 50 eV and extending to about 1000 eV above the edge as shown previously in Figure 2.8.[26]

In X-ray spectroscopy, an X-ray beam causes the ejection of an electron, usually a core electron, leaving a vacancy in the core shell. As a result of the relaxation, an outer electron to fill that vacancy.[27] To cause ejection of electron, the energy of the X-ray must exceed or be equal to the ionization energy of the electrons in that shell.

The relationship between the intensity of an X-ray beam going into a sample and its intensity leaving the sample after traveling a distance x can be described by the X-ray absorption coefficient μ.[26] The absorption coefficient is given by:

$$\mu = -\frac{d \ln I}{dx} \tag{2.16}$$

Where:

I is the intensity

dx is the distance beam travels

In the monochromatic beam, the energy dependence of the absorption coefficient on the photon energy is collected with the Bragg monochromator. A sharp jump, called the absorption edge, marks the opening of an additional photoabsorption channel when the photon energy reaches one of inner-shell ionization energies of the atom. These edges correspond to the ionization of a core orbital, K-edges describing the excitation of the innermost 1s electron, and L-edges and M-edges referring to the same for higher energy orbitals and vary by atom. A series of downward oscillations will be observed after each edge, corresponding to wave interaction between the ejected photoelectron and electrons surrounding the absorbing atom. The waves emitted from the absorbing atom change paths when they hit neighbouring atoms and, therefore, they are called backscattering. The oscillations are characteristic of the surrounding atoms and their distances from the central atom.

Methodology:

Extended X-ray Absorption Fine structure spectrum (EXAFS) of the Pd K-edge were measured at Beamline B18 of Diamond Light Source (UK) with a Si (311) double crystal monochromator QXAFS setup. Transmission and fluorescence signals were measured simultaneously via ionisation chambers and 36 element Ge solid state detectors, respectively. Samples were pressed into a 13 mm diameter pellets for measurement. Pd foil and PdO were used for energy shift calibration. The spectrum of each sample was measured three times and merged to improve the signal-noise ratio. EXAFS data was analysed by Demeter software package (including Athena and Artemis software) [3]. Artemis software was used to fit the k^2-weighted EXAFS data. The amplitude reduction factors S_0^2 of Pd K-edge was calculated to be 0.86 from EXAFS analysis of Pd foil and used as a fixed parameter for EXAFS fitting.

Acknowledgement:

The EXAFS characterisation was carried out by Dr Wang and his research team. We acknowledge the Diamond Light Source B18 beamline for the experiment sessions (SP17377, SP19072 and SP19850).

2.5 References

1 J. K. Edwards, B. Solsona, P. Landon, A. F. Carley, A. Herzing, M. Watanabe, C. J. Kiely and G. J. Hutchings, *J. Mater. Chem.*, 2005, **15**, 4595–4600.

2 J. K. Edwards, S. J. Freakley, A. F. Carley, C. J. Kiely and G. J. Hutchings, *Acc. Chem. Res.*, 2013, **47**, 845–854.

3 S. J. Freakley, M. Piccinini, J. K. Edwards, E. N. Ntainjua, J. A. Moulijn and G. J. Hutchings, *ACS Catal.*, 2013, **3**, 487–501.

4 M. Lorenzo , Y. Pico, Chapter 2 - Gas chromatography and mass spectroscopy techniques for the detection of chemical contaminants and residues in foods. In: D. Schrenk , A. Cartus , *Chemical Contaminants and Residues in Food (Second Edition)*. Woodhead Publishing Series in Food Science, Technology and Nutrition. Woodhead Publishing; 2017.

5 Shimadzu, *Basics & Fundamentals Gas Chromatography*, 2020.

6 R. L. Grob and E. F. Barry, *Modern Practice of Gas Chromatogramy*, John Wiley & Sons, 4 th., 2004.

7 P. Kusch, Application of gas chromatography/mass spectrometry (GC/MS) and pyrolysis-gas chromatography/mass spectrometry (Py-GC/MS) in failure analysis in the automotive industry. *Eng. Fail. Anal.* 2017;82:726-732.

8 I. Chorkendorff and J. W. Niemantsverdriet, *Concepts of Modern Catalysis and Kinetics*, Wiley-VCH, 2003.

9 L. Ouyang, P. F. Tian, G. J. Da, X. C. Xu, C. Ao, T. Y. Chen, R. Si, J. Xu and Y. F. Han, *J. Catal.*, 2015, **321**, 70–80.

10 P. Tian, L. Ouyang, X. Xu, J. Xu and Y. F. Han, *Cuihua Xuebao/Chinese J. Catal.*, 2013, **34**, 1002–1012.

11 M. M. Woolfson, *An Introduction to X-Ray Crystalography*, Cambridge University Press, Cambridge, 2nd Edition, 1998.

12 C. Charpentier, Investigation of deposition conditions and annealing treatments on sput- tered ZnO:Al thin films: Material properties and application to microcristalline silicon solar cells. Plasma Physics. Ecole Polytechnique X, 2012.

13 J. W. Niemantsverdriet, *Spectroscopy in Catalysis: An Introduction*, John Wiley & Sons, 3rd edn., 2007.

14 R. Gurwitz, R. Cohen and I. Shalish, *J. Appl. Phys.*,2014,**115.**

15 D. J. Smith, *Mater. Today*, 2008, **11**, 30–38.

16 A. Polini and F. Yang, *Nanofiber Compos. Biomed. Appl.*, 2017, 97–115.

17 Particle Technology Labs, Energy Dispersive X-ray Spectroscopy (EDS/EDX),

https://www.particletechlabs.com/analytical-testing/particle-identification-speciation/energy-dispersive-x-ray-spectroscopy-eds-edx, (accessed 20 February 2022).

18 I. Chorkendorff and H. Niemantsverdriet, *Concepts of Modern Catalysis and Kinetics*, Wiley-VCH, Weinheim, Germany, 2003.

19 D. Pröfrock and A. Prange, *Appl. Spectrosc.*, 2012, **66**, 843–868.

20 A. Kashani and J. Mostaghimi, *At. Sprays*, 2010, **20**, 415–433.

21 C. Maria, *Advance Aspects of Spectroscopy*, IntechOpen, 2012.

22 T. Armaroli, T. Bécue and S. Gautier, *Oil Gas Sci. Technol.*, 2004, **59**, 215–237.

23 G. S. Henderson, F. M. F. de Groot and B. J. A. Moulton, *Spectrosc. Methods Mineral. Mater. Sci.*, 2014, 75–138.

24 J. E. Penner-Hahn, *Compr. Coord. Chem. II*, 2003, **2**, 159–186.

25 Z. Cai, F. Li, M. Rong, L. Lin, Q. Yao, Y. Huang, X. Chen and X. Wang, *Introduction*, Elsevier Inc., 2018.

26 L.D. Winefordner, X-Ray Absorption. *Chem. anal*. 1988, **92**, 53-83.

27 M. Newville, *Rev. Mineral. Geochemistry*, 2014, **78**, 33–74.

Chapter 3

The Direct Synthesis of H_2O_2 Using Supported Monometallic Palladium Catalysts

3.1 Introduction

The direct synthesis of H_2O_2 using transition metal supported catalysts offers an attractive and environmentally friendly method in H_2O_2 production to facilitate variety of selective oxidation reactions as well as use as disinfectant or bleaching agent.[1,2] The direct synthesis of H_2O_2 is well studied reaction with the prevalent use of Pd supported catalysts.[3–6] Typical reaction conditions described in literature are as follows: H_2/O_2 reagent gas mixture (concentration of H_2 below 5%, often high concentration of diluent such as CO_2 or N_2), supported metal catalyst, acidified H_2O or alcohol as solvent, promoters such as halides, lower temperatures close to 0^oC or ambient temperature and atmospheric or positive pressure. The complex combination of reaction conditions and additives have significant effect on catalyst synthesis activity and selectivity.

The monometallic Pd catalysts, although highly active towards synthesis of H_2O_2, typically also demonstrate high activity in subsequential degradation pathways. Therefore, a primary challenge is suppressing O-O bond cleavage on Pd nanoparticles. To increase selectivity of the catalyst two common approaches are used: an introduction of secondary metal (Au, Sn, Ni) to monometallic Pd catalyst or the use of promoters and additives (e.g., Cl^-, Br^-) that may inhibit cleavage of O-O bond.[7–13] However, the promoters used in the reaction to enhance selectivity of the catalysts reduce catalyst stability and lifetime. Cost of neutralizing and replacing promoters, as well as corrosion of reactor are some of the issues linked to use of promoters.

To work below the lower explosive limit of H_2 in O_2 (4 mol% H_2 at 1 atm.) significantly limits reaction rates and therefore concentration of H_2O_2 produced. To address this limitation, the choice of solvent plays a crucial role in the direct synthesis of H_2O_2. Due to the low solubility of reagent gases in H_2O, the use of lower alcohols as CH_3OH or C_2H_5OH is preferred. The main role of the solvent considered in many studies was to facilitate transport of the dissolved reagent gases to the active sites.[5,14] However, recent studies suggest that solvent might participate directly in reaction mechanism.[15,16]

In this Chapter, the direct synthesis of H_2O_2 over monometallic Pd catalysts (reaction pathway shown in Chapter 1, Figure 1.1) was investigated. The effect of reaction conditions, such as pressure, gas composition, reaction time and solvent composition was investigated. As shown within this Chapter, the metal loading of the catalyst plays crucial role in the catalyst activity as well as support used. The role of the promoters are also examined. Reusability studies are carried out and changes in catalyst structure after reaction are also investigated. Gas replacement reactions were tested to observe the possibility to maximise the concentration of H_2O_2.

3.2 Results and Discussion

Supported monometallic Pd catalysts were prepared using the standard wet impregnation technique using $PdCl_2$ as the metal precursor and TiO_2 as the support, as outlined in Chapter 2, Section 2.2.1. Each catalyst was prepared at least 3 times and each batch of catalyst was tested at least 3 times for H_2O_2 synthesis and degradation reaction. All H_2O_2 synthesis and degradation testing were carried out according to the procedures discussed previously in Chapter 2, unless otherwise stated. Unless stated otherwise, the reactions were carried out at ambient temperature - temperature of the environment without use if heating/cooling system.. A summary of the testing conditions is given below:

- A blank degradation reaction, in the absence of a catalyst, was carried out on a regular basis to determine possible reactor contamination. In a case of contamination, the reactor was subjected to cleaning process using mineral acids followed by water and TiO_2 washing cycles. A subsequent blank degradation reaction was then carried out before continuing testing with catalyst.
- Standard reaction conditions for H_2O_2 synthesis: 0.01g catalyst, 2.9 g of water, 5.6 g of methanol, 2.9 MPa 5%H_2/CO_2, 1.1 MPa 25%O_2/CO_2, 0.5 h, ambient temperature,1200 rpm.
- H_2O_2 degradation activity was determined from the amount of H_2O_2 that was degraded after reaction under standard reaction conditions: 0.01 g catalyst, 0.68 g H_2O_2, 2.22 g of water, 5.6 g of methanol, 2.9 MPa 5%H_2/CO_2, 0.5 h, ambient temperature, 1200 rpm.

3.2.1 Effect of metal loading on catalytic activity towards the direct synthesis and subsequent degradation of H_2O_2.

Particle size, shape, morphology, metal dispersion and electronic state are some of the many factors that can have significant effect on the catalytic properties of metal supported catalysts in direct synthesis of H_2O_2.[17–24] To investigate the effect of the Pd metal loading on H_2O_2 synthesis and degradation activity, a series of catalysts were prepared with different Pd content (0.0625-5 wt.%) by wet impregnation (methodology described in this Chapter). No activity towards H_2O_2 formation or degradation was observed over bare TiO_2. As shown in Figure 3.1, even a small amount of Pd on the catalyst exhibited activity towards H_2O_2 formation. The lowest metal loading, 0.0625wt.%Pd/TiO_2, showed low H_2O_2 synthesis activity, 6 mol_{H2O2} kg_{cat}^{-1} h^{-1}. Doubling the metal loading up to 0.125wt.%Pd resulted in 4 times higher rate of H_2O_2 formation. The synthesis activity towards H_2O_2 passed through a maximum of 65 mol_{H2O2} kg_{cat}^{-1} h^{-1} with 0.5wt.%Pd/TiO_2. In comparison, synthesis activity of 64 mol_{H2O2} kg_{cat}^{-1} h^{-1} was obtained with the well-studied 2.5wt.%Au-2.5wt.%Pd/TiO_2 catalyst previously prepared by Edwards *et al.*, which is an established catalyst for direct synthesis of H_2O_2 used as benchmark within our research group.[25] Further increase in Pd metal loading resulted in a decrease in synthesis activity. A substantial decrease in catalyst synthesis activity to 30 mol_{H2O2} kg_{cat}^{-1} h^{-1} was observed with 5wt.% metal loading, where the obtained synthesis activity was less than half of the activity achieved by catalysts with 10 times lower metal loading.

In the presence of 4wt.% H_2O_2 in reaction solution (standard degradation reaction), no degradation activity was observed up to 0.5wt.% metal loading. Further increase of Pd loading in the catalyst caused a significant increase in H_2O_2 degradation activity. Degradation activity of 609 mol_{H2O2} kg_{cat}^{-1} h^{-1} was obtained with 5wt.%Pd/TiO_2, which represents around 30% of H_2O_2 in the starting solution. Hutchings and co-workers have previously studied 5wt.%Pd catalysts prepared on various supports with same synthesis activity, obtained with 5wt.%Pd/TiO_2 at 2°C, with the reported hydrogenation value of this catalyst only 288 mol_{H2O2} kg_{cat}^{-1} h^{-1}.[26,27] However, these experiments were carried out at 2°C, with lower reaction temperatures known to inhibit H_2O_2 degradation via hydrogenation and decomposition.

The differences in catalyst activity and reaction conditions between individual testing of the monometallic Pd catalysts with various metal loadings are summarised in Appendix 1. The reaction temperature for both synthesis and degradation reaction is in the range of 22-27 °C; however, as shown in Appendix 1, the activity of the catalyst is not significantly affected by this temperature range.

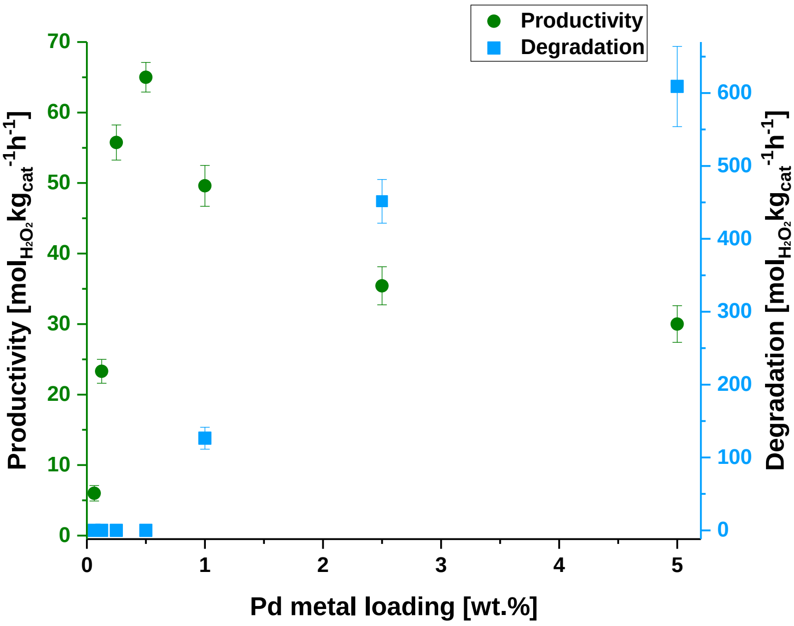

Figure 3.1: ***Synthesis and degradation activity of the monometallic Pd catalysts with various metal loadings.*** **Reaction conditions: a) Synthesis reaction:** 0.01g catalyst, 2.9 g of water, 5.6 g of methanol, 2.9 MPa 5%H_2/CO_2, 1.1 MPa 25%O_2/CO_2, 0.5 h, ambient temperature, 1200 rpm **b) Degradation reaction:** 0.01g catalyst, 0.68 g H_2O_2, 2.22 g of water, 5.6 g of methanol, 2.9 MPa 5%H_2/CO_2, 1.1 MPa 25%O_2/CO_2, 0.5 h, ambient temperature, 1200 rpm.

Based on results shown in Figure 3.1, rates of reaction were calculated using 0.5 h reactions over monometallic Pd catalysts with different metal loading. As shown in Table 3.1, the reaction rate increases with Pd metal loading, with the highest reaction rate observed with 0.25 wt.%Pd/TiO_2 catalyst. Further increase in metal loading resulted in a sharp decrease in reaction rate. In comparison, the highest H_2O_2 concentration and productivity were achieved over 0.5 wt.%Pd/TiO_2 catalyst. These results better illustrate the importance of optimal Pd metal loading on the catalyst activity, and demonstrate how catalysts with low Pd metal loading present cheaper and effective alternative to previously studied catalysts with higher metal loadings.

Table 3.1: Rates of synthesis reaction over studied monometallic Pd catalysts with different metal loading. The reaction rates were calculated after 0.5 h reaction.

Pd metal loading [wt.%]	**Reaction rate [$mol_{H_2O_2}mol_{Pd}^{-1}h^{-1}$]**	**H_2O_2 concentration [wt.%]**	**Productivity [$mol_{H2O2}\,kg_{cat}^{-1}\,h^{-1}$]**
0.0625	1021	0.01	6
0.125	1983	0.05	23

0.25	2373	0.11	56
0.5	1383	0.14	65
1	528	0.10	50
2.5	151	0.07	35
5	64	0.06	30

Reaction conditions: 0.01 g catalyst, 2.9 g of water, 5.6 g of methanol 2.9 MPa 5%H_2/CO_2, 1.1 MPa 25%O_2/CO_2, 5 min, ambient temperature, 1200 rpm.

As shown in Figure 3.2, the increase in Pd metal loading results in increase of H_2 conversion. A sharp increase in H_2 conversion is observed up to 0.5wt.%Pd metal loading, with maximum H_2 conversion of 53%. Further increase in Pd metal loading to 5wt.% shows an increase in H_2 conversion to 73%; however, as also shown in Figure 3.2, very low selectivity towards H_2O_2 is observed at ambient temperature over these catalysts. Selectivity passes through a maximum of 50% with the 0.125wt.% Pd/TiO_2 and then decreases with increasing metal loading up to 1wt.% Pd. No significant decrease in H_2 selectivity is observed with further increase in Pd metal loading to 5wt.%. The low selectivity of the catalysts with higher Pd loading can be attributed to high H_2O_2 degradation activity, resulting in H_2O formation. However, low H_2O_2 selectivity with metal loading up to 0.5wt.% is interesting considering that these catalysts showed no degradation activity in presence of high concentrations of H_2O_2 in reaction solution. The data suggests that the presence of high H_2O_2 concentrations in the reaction solution can inhibit the degradation of H_2O_2 over catalysts with Pd metal loading of up to 0.5 wt.%, as shown in Figure 3.1. This observation is discussed in more detail in Section 3.2.4.

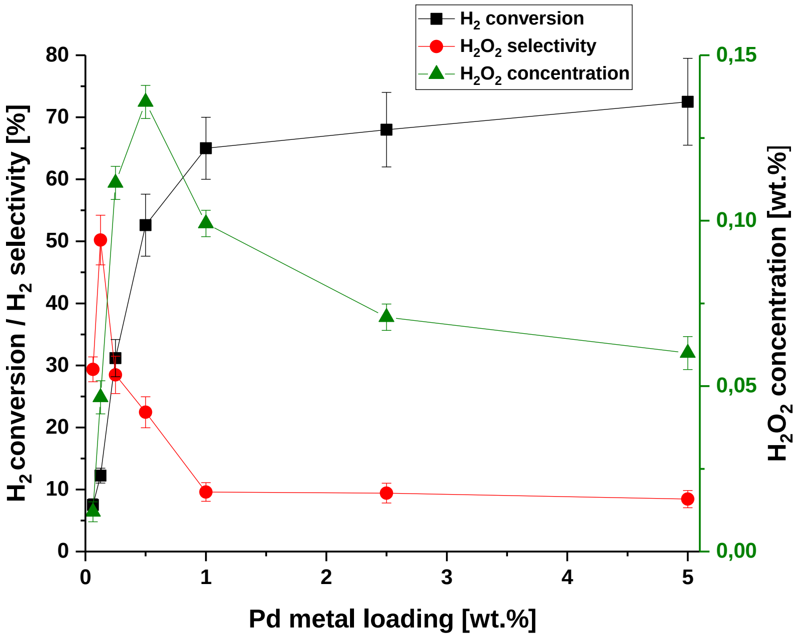

Figure 3.2: **Conversion and selectivity of the monometallic Pd catalysts with various metal loadings. Reaction conditions:** a) Synthesis reaction: 0.01 g catalyst, 2.9 g of water, 5.6 g of methanol, 2.9 MPa 5%H_2/CO_2, 1.1 MPa 25%O_2/CO_2, 0.5 h, ambient temperature, 1200 rpm

The monometallic Pd catalysts with various metal loadings have been digested in aqua regia and analysed by microwave plasma atomic emission spectroscopy (MP-AES) to determine the metal loading of the catalysts. As shown in Table 3.2, the Pd loadings detected by MP-AES are comparable with the theoretical Pd loadings of the catalysts, demonstrating that the catalyst preparation method is effective.

Table 3.2: Concentration of Pd metal detected by MP-AES post digestion in aqua-regia for monometallic Pd catalysts with different metal loading.

Theoretical Pd loading [wt.%]	Pd loading detected by MP-AES [wt.%]
0.0625	0.07
0.125	0.13
0.25	0.23
0.5	0.52
1	1.05
2.5	2.48
5	5.05

Choudhary and co-workers obtained selectivity around 30% over 2.5wt.% Pd catalysts supported on various supports (Al_2O_3, Ga_2O_3, ZrO_2, CeO_2, ThO_2, SiO_2) in 0.03M H_3PO_4 reaction medium.[28] In comparison, only 10 % H_2 selectivity was achieved over 2.5 wt.%Pd/TiO_2 prepared in this work, demonstrating the role of acid stabilisers.

Samanta *et. al* investigated the effect of Pd metal loading over a CeO_2 support at ambient temperature.[29] They report that both H_2O_2 decomposition activity and H_2 conversion increased with increasing Pd loadings in the catalyst, while H_2 selectivity and H_2O_2 yield passed through a maximum of 25% and 10%, respectively, with 1wt.%Pd metal loading; however, in the presence of acid and Br^- anion additives, both H_2 selectivity and H_2O_2 yield increased up to 80% and 20%, respectively. The presence of acid and halide anions were shown to be effective additives for direct synthesis of H_2O_2 by inhibiting the decomposition of H_2O_2 and promoting formation of H_2O_2. Gemo *et al.* demonstrated the strong influence of Pd metal loading on H_2O_2 synthesis over Pd catalysts supported on an acidic microporous resin in the absence of any promoters at 2 °C.[17] A concentration of H_2O_2 up to 14.6 mM was achieved with Pd loading of 0.5wt.%, which represented synthesis activity of 82 $mol_{H2O2}\ kg_{cat}^{-1}\ h^{-1}$ after 0.5h reaction and

H_2 selectivity of 57% was reported. Further increasing the Pd loading resulted in a significant drop in synthesis activity and H_2 selectivity below 20 mol_{H2O2} kg_{cat}^{-1} h^{-1} and 10%, respectively. They concluded that the key factor in controlling catalyst activity and selectivity over investigated monometallic catalysts (supported on commercial ion exchange resin K2621) was the ratio of dissolved H_2 in solvent and Pd supported on catalyst. In comparison, Tian *et al.* showed an opposite trend in synthesis activity over Pd catalysts supported on hydroxyapatite (HAp) at 10 °C in presence of H_2SO_4 used as additive. The highest productivity of 38 mol_{H2O2} kg_{cat}^{-1} h^{-1} was obtained with 5wt.%Pd/Hap and a decrease in synthesis activity was observed with decreasing Pd loading to activity of 10 mol_{H2O2} kg_{cat}^{-1} h^{-1}.[18] The difference in the trends can be attributed to significantly lower H_2 conversions and higher H_2 selectivities obtained over Pd catalysts supported on HAp. For example, H_2 conversion of 18% and H_2 selectivity of 43% was achieved over 5 wt.% Pd/HAp (Tian) while significantly higher H_2 conversion of 73% and lower H_2 selectivity of 8% was obtained with 5 wt.%Pd/TiO_2 (this work). Because of the low H_2 conversion (2%) of 0.5 wt.%Pd/HAp, only small amount of H_2O_2 was produced despite H_2 selectivity of 94% resulting in lower synthesis activity, compared to 5 wt.%Pd/HAp that produced more H_2O_2 but less selectively. In contrast, high H_2 conversion and low H_2O_2 selectivity of the 5 wt.% Pd/TiO_2 translated in the poor catalyst activity compared to the more selective 0.5 wt.%Pd/TiO_2. The higher H_2 selectivity and lower H_2 conversion of the Pd catalysts supported on HAp can be attributed to three factors: a) use of acid additive known for decreasing the degradation activity of the catalyst, b) use of lower reaction temperature, favouring higher H_2 selectivity and c) use of flow reactor set up which decreases the contact time of H_2O_2 and catalyst.

X-ray diffraction was carried out to obtain indication of Pd particle size and investigate any changes to support during the catalyst preparation. XRD patterns of the catalysts with different Pd loading are given in Figure 3.3. Only X-ray diffraction peaks characteristic of TiO_2 (P25) are observed in theses catalysts, with bare TiO_2 was used as the reference. The peaks of Pd (40° Pd(111), 46° Pd(200), 68° Pd(220), 82° Pd(311) and 87° Pd(222)) are not detected by XRD in the 2θ region from 5° to 80°. This might be caused by low percentage of Pd on the catalysts, and the impregnated Pd is highly dispersed on the support, suggesting that there are no larger Pd particles present (>ca 3nm, limit for XRD analysis)[18]. Uncalcined TiO_2 and calcined Pd supported catalysts show peaks for anatase and rutile TiO_2 phases, which suggests no phase transformation occurred after Pd impregnation and subsequent heat treatment. Fernandes Machado *et al.* demonstrated that anatase-rutile phase transformation takes place at 600 °C.[30] No difference in phase constitution or change in surface area is observed after calcination of the samples presented within this work, at 400 °C.

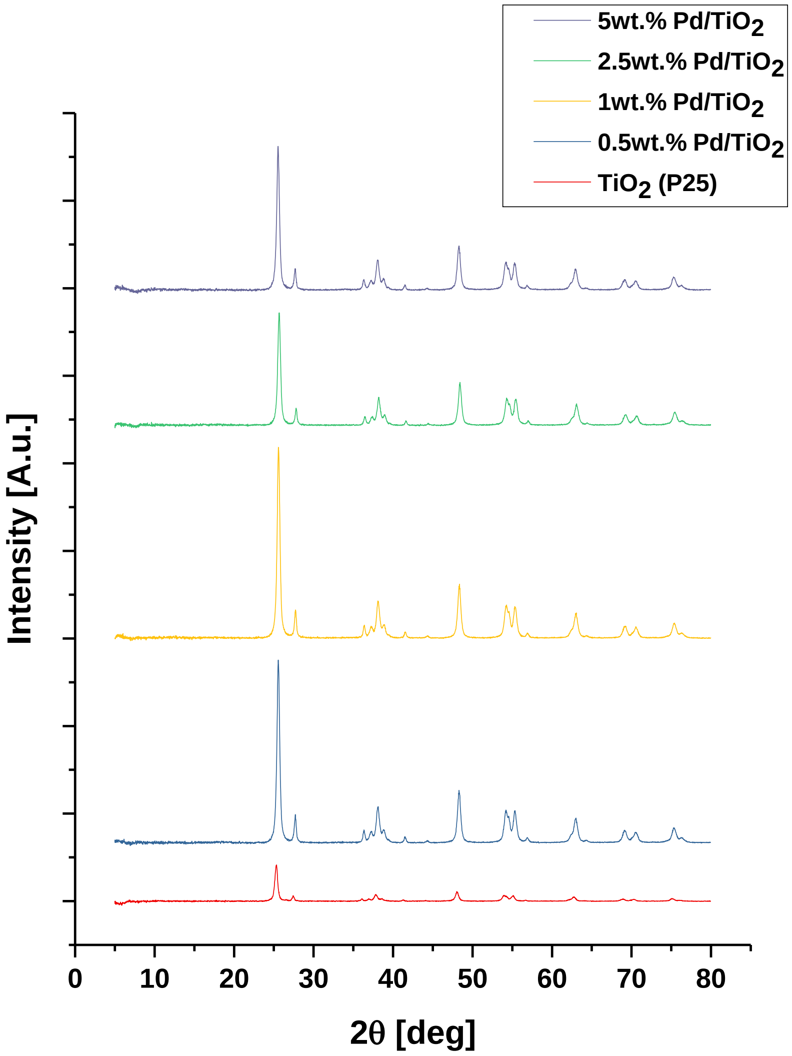

Figure 3.3: XRD patterns of supported Pd catalysts on TiO_2 with different Pd metal loadings.

The observed effect of Pd loading on the H_2O_2 formation and degradation may be attributed to variation on mean particle size with metal loading. Transmission electron microscopy (TEM) characterization was carried out to investigate average particle size of catalysts with different Pd loadings, with TEM micrographs shown in Figure 3.4. No visible particles are observed for 0.5wt.%Pd/TiO_2 and 1wt.%Pd/TiO_2 catalysts. However, analysis by Energy dispersive X-Ray spectroscopy (SEM-EDX), Figure 3.6, shows weak Pd peak suggesting the presence of Pd in both catalysts. This suggest that Pd particles were below detection limit of the TEM equipment (Joel JEM 2100) which is around 1nm. TEM analysis (Figure 3.4c) of 2.5wt.%Pd/TiO_2 shows well dispersed particles, with an average particle diameter of 1.5 nm. As shown in Figure 3.5 a), 88.5% analysed particles have diameter below 2 nm. TEM micrograph (Figure 3.4 d) of 5wt.%Pd/TiO_2 shows a good dispersion of nanoparticles, with an average particle diameter of around 1.7 nm, with particles no larger than 4.2 nm. In contrast, a different trend in particle size was obtained by Gemo *et al.* over monometallic Pd catalysts supported on an acidic microporous resin prepared by ion-exchange/reduction method. The mean particle diameter passed through a maximum with 0.5wt.%Pd metal loading, and decreased with further increase in Pd metal loading. They showed that the catalyst with the biggest Pd nanoparticles (mean particle size of 5.3 nm) resulted in being the most selective catalyst in the series. Tian *et al.* demonstrated that the size of Pd particles could be manipulated by varying the Pd loading. The highest H_2 selectivity of 94% was achieved over 0.5wt.%Pd/HAp, with a mean particle size of 1.4 nm. A further decrease in H_2 selectivity and increase in Pd particle size was observed with increasing metal loading, obtaining 43% H_2 selectivity over 5wt.%Pd/HAp with a mean particle size of 2.6 nm. Interestingly, they also prepared a 3wt.%Pd/HAp catalysts with a mean particle size 22 and 36 nm and showed no change in selectivity when the Pd size was increased above 2.5 nm. In conclusion, they showed that selectivity of the Pd based catalysts can be improved by decreasing Pd particle size in the small range 2.5-1.4 nm. Ouyang *et al.* studied the performance of Pd/TiO_2 catalysts with varying Pd loading for direct synthesis of H_2O_2.[31] They showed that the activity and H_2 selectivity can be significantly improved by changing the Pd loading from 1wt.% - 5wt.%, while keeping similar Pd particle size around 2.4 nm. Because there was no significant difference in the Pd particle size with varying metal loading, they ruled out the effect of Pd particle size on catalyst activity. Instead, they suggested that the configuration of surface Pd atoms is one of the decisive factors affecting the catalyst activity and they showed it can be affected with different metal loadings.

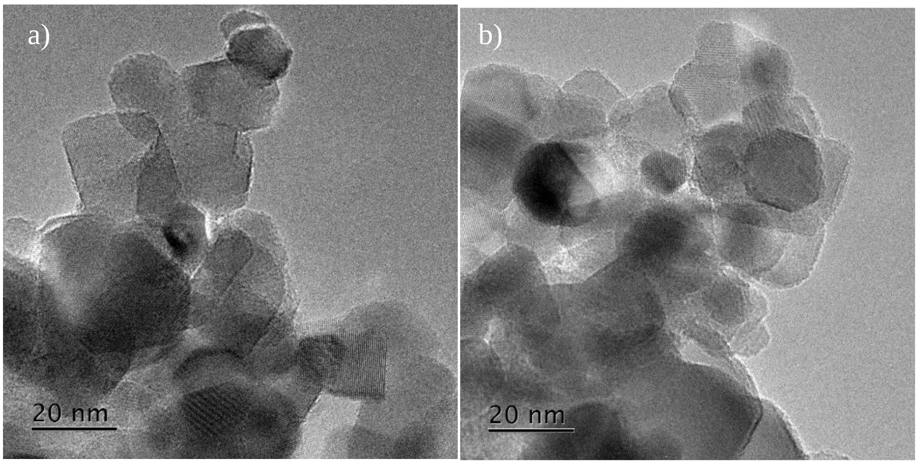

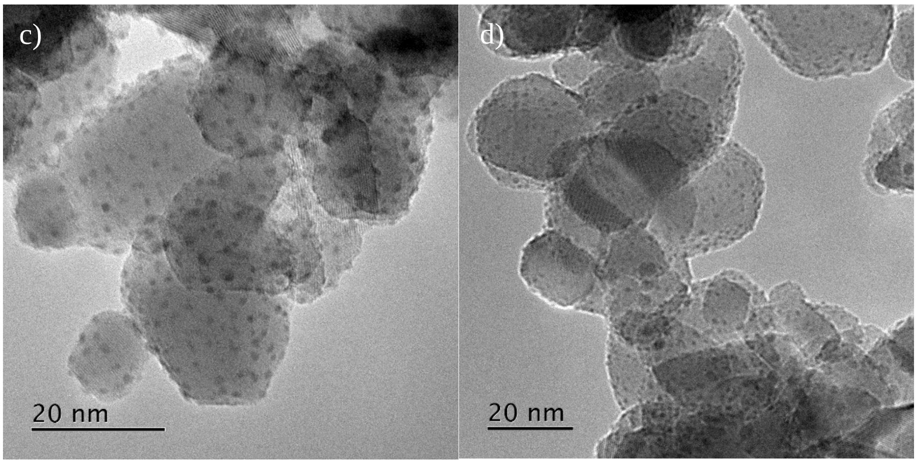

Figure 3.4: ***TEM images of fresh monometallic Pd catalysts with different metal loading:*** a) 0.5wt.%Pd/TiO$_2$; b) 1wt.%Pd/TiO$_2$; c) 2.5wt.%Pd/TiO$_2$; d) 5wt.%Pd/TiO$_2$.

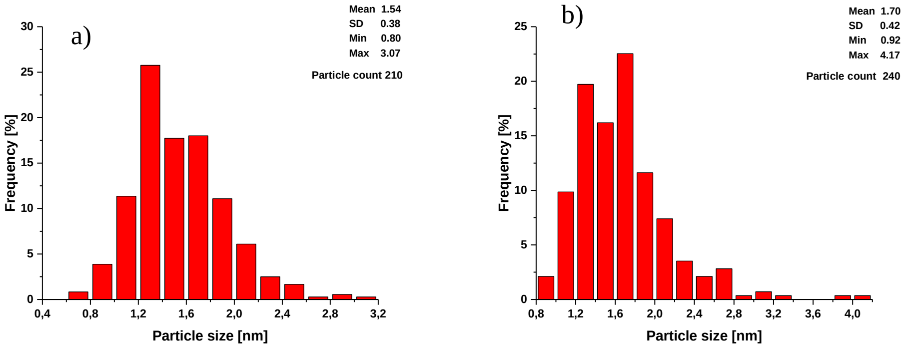

Figure 3.5: ***Particle diameter distribution of the Pd/TiO$_2$ catalysts with different metal loading:*** a) 2.5wt.%Pd/TiO$_2$; b) 5wt.%Pd/TiO$_2$.

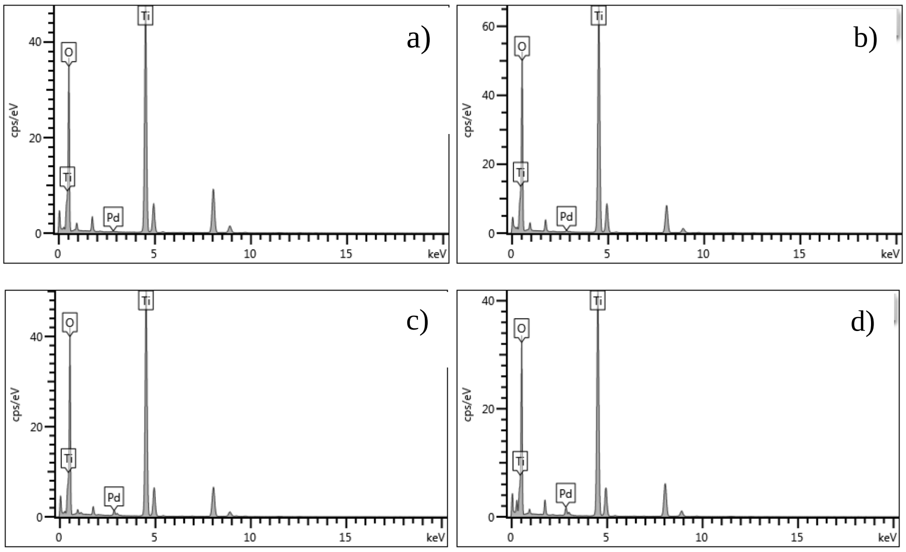

Figure 3.6: ***EDX images of fresh monometallic Pd catalysts with different metal loading:*** a) 0.5wt.%Pd/TiO$_2$; b) 1wt.%Pd/TiO$_2$; c) 2.5wt.%Pd/TiO$_2$; d) 5wt.%Pd/TiO$_2$.

As shown in Figure 3.1, no degradation of H_2O_2 is observed over the 0.5wt.%Pd/TiO_2 catalyst, which is a system that showes no visible particles, suggesting that sub-nanometre particles were present on the catalyst. Higher metal loaded catalysts were observed to have average particle diameters above 1.5 nm and a significant increase in degradation activity towards H_2O_2. This suggests that the sub-nanometre particles have no activity towards degradation of H_2O_2. An increase in particle diameter might result in an increase in degradation activity, as both 2.5wt.%Pd/TiO_2 and 5wt.%Pd/TiO_2 catalysts shows much higher degradation activity compared to the 0.5wt.%Pd/TiO_2 catalyst. However, the difference of 0.2 nm in mean Pd particle diameter observed between 2.5wt.%Pd and 5wt.%Pd catalyst is minor to explicitly attribute as the difference in catalyst activity. Figure 3.7 illustrates the relationship between the catalyst activity for the direct synthesis of H_2O_2 and the Pd particle size proposed by Tian e*t al.*, and is in agreement with observations obtained in this work.[18]

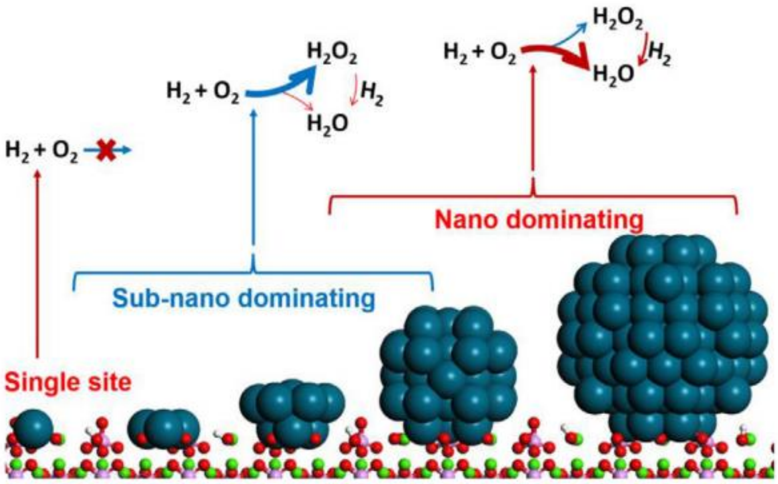

Figure 3.7: Structures of catalysts corresponding to three scales of particle sizes and proposed mechanism for H_2O_2 synthesis. Blue, red, white, purple, and green spheres are palladium, oxygen, hydrogen, phosphorus, and calcium atoms, respectively.[18]

3.2.2 Effect of reaction conditions on the synthesis and degradation activity of 0.5wt.%Pd/TiO_2

Reaction conditions play a crucial role in catalyst performance and fine tuning of these parameters can lead to high synthesis rates of H_2O_2. Landon *et al.* identified low reaction temperature (1-2 °C) and short reaction time as a key factors that favour high selectivity to H_2O_2.[32] Piccinini *et al.* showed that with a AuPd/carbon catalyst the optimum reaction conditions differ for the H_2O_2 synthesis and degradation reactions.[33] By applying an optimal set of synthesis conditions, a dramatic increase in catalyst synthesis activity from 160 mol_{H2O2} kg_{cat}^{-1} h^{-1} to 315 mol_{H2O2} kg_{cat}^{-1} h^{-1} was obtained, and, with optimal degradation conditions, no degradation activity of the catalyst was observed while synthesis activity remained 160

mol_{H2O2} kg_{cat}^{-1} h^{-1}. Crole *et al.* investigated the effect of reaction conditions using H_2O as a solvent and 2.5 wt.% Au – 2.5 wt.% Pd/TiO_2 catalyst at ambient temperature, showing lower synthesis activity due to lower solubility of reagent gases compared to H_2O/CH_3OH solvents and higher reaction temperature.[14] Hutchings and co-workers extensively investigated reaction conditions over various catalysts and showed that use of a higher pressure, a stoichiometric substrate gas ratio, increasing the concentration of CH_3OH to 93% in H_2O/CH_3OH solvent mixture, reducing the solvent volume, and lower reaction temperature all resulted in higher concentration of H_2O_2 being produced.[14,33–35]

Using standard reaction conditions, listed above (Section 3.2) the 0.5wt.%Pd/TiO_2 catalyst showed the greatest synthesis activity, 65 mol_{H2O2} kg_{cat}^{-1} h^{-1} and no degradation activity towards H_2O_2 in presence of 4wt.%H_2O_2. The effect of H_2/O_2 ratio, total pressure and solvent composition are investigated now on the synthesis and degradation activity over this catalyst, to determine if catalytic performance can be enhanced through modification of these reaction parameters.

3.2.2.1 Effect of H_2/O_2 ratio on synthesis and degradation activity of 0.5wt.%Pd/TiO_2

The first variable that was studied was the effect of H_2/O_2 ratio. The variation in H_2/O_2 partial pressure was achieved by controlled addition of two reagent gas mixtures: 5%H_2/CO_2 and 25%O_2/CO_2. All the other variables were kept constant, including total pressure. The CO_2 is used as a diluent to keep the potentially explosive mixture of H_2 and O_2 below the lower explosive limit (4% H_2 by volume). Because pre-mixed mixtures of gases were used, the amount of CO_2 was changing with varying H_2/O_2 ratio, from 78% with no H_2 present in reactor to 94% (molar fraction) with the highest H_2/O_2 ratio applied.

It has been previously showed that CO_2 can act as *in situ* acid promoter.[36,37] Once dissolved in the water-methanol mixtures carbonic acid is formed, lowering the solvent pH and stabilizing H_2O_2. Edwards *et al.* calculated that the pH of the solvent during the reaction using CO_2 will be approximately 4.[25] When they used N_2 as diluent with a solvent acidified with HNO_3 to obtain pH 4, they obtained enhancement in synthesis activity that were directly comparable to that observed when CO_2 was used as diluent. However, it is reasonable to presume that the amount of CO_2 introduced is high enough to lead to complete saturation of the H_2O/CH_3OH solvent ensuring that the pH of the solution is constant regardless of the H_2/O_2 ratio.

Taking the above into account this presumption, Figure 3.8 illustrates the effect of varying H_2/O_2 ratio over 0.5wt.%Pd/TiO_2 at ambient temperature. As H_2O_2 degradation is determine in presence of H_2/CO_2 only, it was not possible to determine the effect of H_2/O_2 ratio on this reaction pathway. Instead, the degradation reaction was carried out with the same amount of H_2/CO_2 that was added to reactor during the synthesis reaction. No degradation activity is observed over the whole range of different H_2 amounts. A low synthesis activity of 7 mol_{H2O2} kg_{cat}^{-1} h^{-1} is obtained at 0.047 H_2:O_2 ratio, and it increases to 31 mol_{H2O2} kg_{cat}^{-1} h^{-1} with increasing the H_2:O_2 ratio to 1.2. Figure 3.8 illustrates a sharp increase in catalyst synthesis activity towards H_2O_2 with increasing content of H_2. Synthesis activity passes a maximum at a ratio of 0.96. The optimal H_2:O_2 ratio is 1:1, which is in agreement with the reaction stoichiometry. At this optimum ratio, the productivity of the catalyst increases from 65 mol_{H2O2} kg_{cat}^{-1} h^{-1} to 70 mol_{H2O2} kg_{cat}^{-1} h^{-1}. Similar observations were made by Hutchings and co-workers, who reported the optimal H_2/O_2 ratio to be 1 using 2.5wt.%Au-2.5wt.%Pd supported on TiO_2 and acid pre-treated C.[33] Santos *et al.* reported the optimal H_2/O_2 to be 0.69 over a 1wt.%Au-Pd/TiO_2 catalyst; however, a H_2/O_2 ratio of 1 was shown to obtain the second highest synthesis activity.[35] For all future experiments, the ratio of 0.53 (standard reaction condition) was chosen due to lower content of H_2 required, but comparable synthesis activity achieved at higher H_2:O_2 ratio. Further increasing the H_2/O_2 ratio results in a decrease in catalyst activity. The dramatic drop in activity is observed once H_2/O_2 ratio reached a value of 2.12 with an activity of 4 mol_{H2O2} kg_{cat}^{-1} h^{-1} observed. The trend observed in Figure 3.8 suggests an effect of limiting reagent gas. At low ratios, H_2 is the limiting gas and at higher ratios the low content of O_2 is limiting factor.

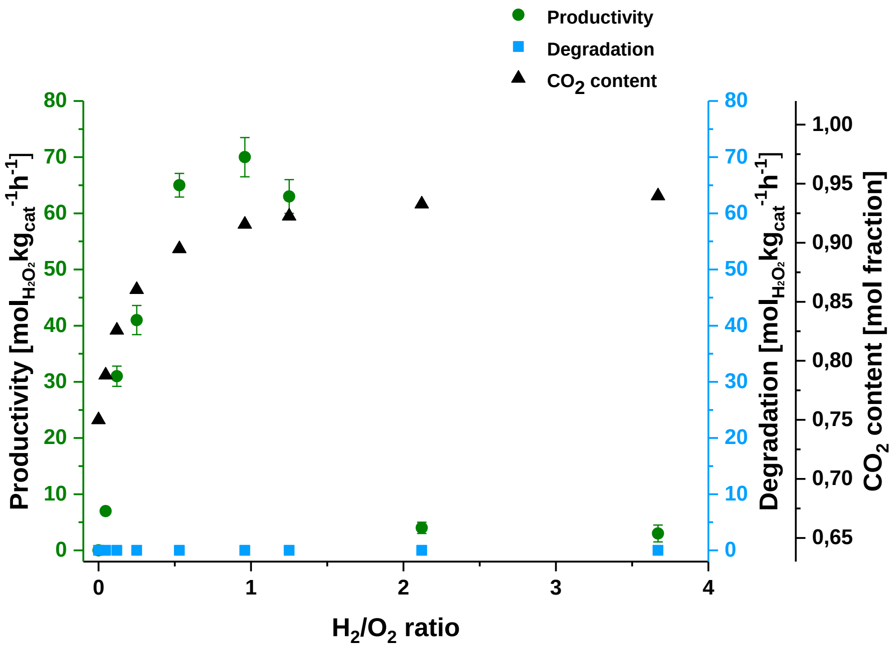

Figure 3.8: ***Synthesis and degradation activity of 0.5wt.%Pd/TiO$_2$ catalysts with various H$_2$/O$_2$ ratio.*** **Reaction conditions: a) Synthesis reaction:** 0.01 g catalyst, 2.9 g of water, 5.6 g of methanol, various H_2/O_2 ratio, total pressure 4 MPa, 0.5 h, ambient temperature, 1200 rpm **b) Degradation reaction:** 0.01 g catalyst, 0.68 g H_2O_2, 2.22 g of water, 5.6 g of methanol, various H_2/CO_2 amount, total pressure 4 MPa, 0.5 h, ambient temperature, 1200 rpm.

Lunsford and co-workers reported that the H_2O_2 formation rate increases in proportion to H_2 pressure and was found to be first order with respect to H_2 and zero order with respect to O_2 in ethanol (0.12 M H_2SO_4) over Pd/SiO_2.[24] Wilson *et al.* showed that formation rate increases with H_2 pressure but does not depend on O_2 pressure in pure methanol.[23] The H_2O_2 formation rate initially showed a linear increase with H_2 pressure in the range of 5 to 150 kPa, and reaches half-order dependence on H_2 pressure up to 400 kPa. The H_2O formation rate shows similar dependency, with weaker dependency on H_2 pressure and no dependency on O_2 pressure.

The data in Figure 3.8 was re-plotted as a function of H_2 molar fraction instead of H_2/O_2 ratio to investigate the effect of partial pressure of H_2 and O_2. The dependency shown in Figure 3.9 is an asymmetrical parabola. This leads to conclusion that at lower partial pressures of O_2 the synthesis activity of catalyst decreases markedly in comparison to lower partial pressure of H_2. This can be explained by considering all the reactions taking place on catalyst surface during direct synthesis: a) formation of H_2O_2, b) formation of H_2O via combustion, c) decomposition of H_2O_2 to H_2O and d) hydrogenation of H_2O_2 by H_2 to H_2O. At higher partial pressure of H_2 the rate of H_2O_2 hydrogenation is likely to be higher due to excess of H_2 and therefore more H_2O_2 is degraded than produced.

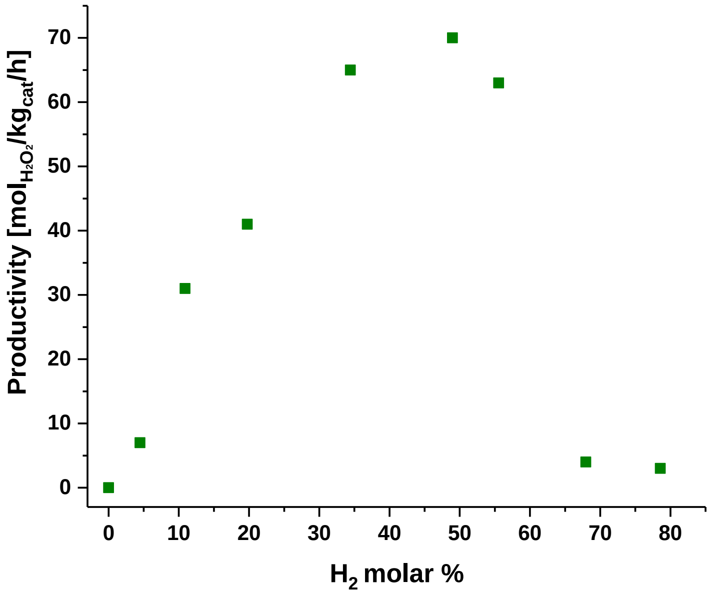

Figure 3.9: ***Synthesis activity of 0.5wt.%Pd/TiO$_2$ catalysts with various H$_2$ content.*** **Reaction conditions: a) Synthesis reaction:** 0.01 g catalyst, 2.9 g of water, 5.6 g of methanol, various H_2/O_2 ratio, total pressure 4 MPa, 0.5 h, ambient temperature, 1200 rpm

Choudhary and co-workers have also investigated this effect and shown that there are strong influences of the H_2/O_2 ratio on H_2 conversion and H_2O_2 formation over a halogenated Pd/Al_2O_3 catalyst.[38] They attributed this influence to two factors: (i) changes in Pd oxidation state during the reaction and (ii) a change in H_2O_2 hydrogenation rate. At high H_2/O_2 ratios, Pd was expected to be present as Pd^0 due to reduction of surface PdO by H_2.[38] Pd^0 was reported to offer higher activity towards H_2O_2 hydrogenation and decomposition than the corresponding PdO catalyst.[6,28]

3.2.2.2 Effect of total pressure on synthesis and degradation activity of 0.5wt.%Pd/TiO$_2$

Within this study, the direct synthesis of H_2O_2 was evaluated in a three phase gas-liquid-solid system and therefore mass transfer limitations may be involved.[5] Mass transfer can be improved by:

a) increasing mass transfer coefficient or reducing the thickness of stagnant film by intensive stirring
b) increasing the surface area of the gas bubbles in feed gas
c) increasing the solubility of the gases by increasing the partial pressure of gases, which implies the use of higher pressures

The total pressure of the system results in an increase of the gas solubility and decreases the bubble size of the fed gas, which will increase mass transfer efficiency.[5,34,39] Consequently, the higher the pressure of H_2 and O_2 is in the gas phase, the higher the concentration of reagent gases is in liquid phase and as a result the concentration of these gases is higher close to catalyst surface.

The effect of total reaction pressure on catalytic activity towards H_2O_2 synthesis and degradation was next investigated, over the 0.5wt.%Pd/TiO$_2$ catalyst. Figure 3.10 shows that the rate of H_2O_2 formation can be increased by increasing the overall pressure in the autoclave. The H_2:O_2 ratio 0.53 is kept constant through the whole series of experiments. No degradation activity is observed over the whole range of total pressures. In this case, only H_2/CO_2 is added into reactor to obtain the desired pressure. As expected, an increase in total pressure results in an increase of H_2O_2 formation rate though the whole range of pressures. At 100 psi (0.7 MPa), only a small H_2O_2 formation rate of 9 $mol_{H2O2}kg_{cat}^{-1}h^{-1}$ is observed. A small increase in synthesis activity is observed at pressures up to 300 psi (2.1 MPa), with productivity of 21 $mol_{H2O2}kg_{cat}^{-1}h^{-1}$. A more significant increase is observed in the pressure range of 400-650 psi (2.8 MPa-4.5 MPa); at 400 psi, synthesis activity of 35 mol_{H2O2} kg_{cat}^{-1} h^{-1} is achieved and the highest activity of 75 mol_{H2O2} kg_{cat}^{-1} h^{-1} is obtained at 650 psi. The pressure of 650 psi is the maximum pressure that could be achieved in our reaction set-up; due to this limitation a pressure of 580 psi (4 MPa) is further used. These results indicate that the reaction rate is controlled by the amount of H_2 and O_2 available in reaction solution.

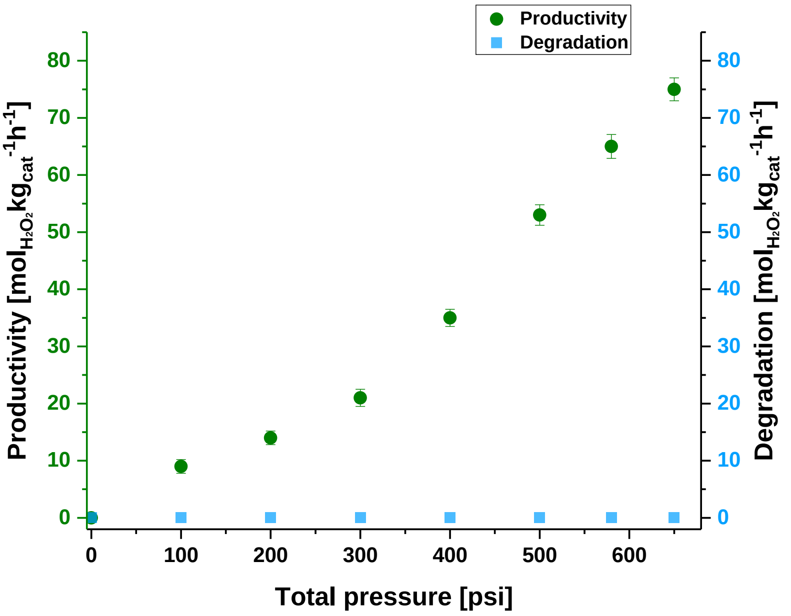

Figure 3.10: ***Synthesis and degradation activity of 0.5wt.%Pd/TiO_2 catalysts with different total pressure.*** **Reaction conditions: a) Synthesis reaction:** 0.01 g catalyst, 2.9 g of water, 5.6 g of methanol, H_2/O_2 ratio 0.53, various total pressure, 0.5 h, ambient temperature, 1200 rpm **b) Degradation reaction:** 0.01 g catalyst, 0.68 g H_2O_2, 2.22 g of water, 5.6 g of methanol, H_2/CO_2 various pressure, 0.5 h, ambient temperature, 1200 rpm.

Moreno *et al.* studied the influence of pressure (0.1-0.9 MPa) in a semi-continuous reactor with CH_3OH as solvent over a commercial Pd/C catalyst.[40] Both H_2O_2 formation and selectivity increases almost linearly with reaction pressure, with highest concentration of H_2O_2 obtained at 0.9 MPa. They concluded that high pressure increases the gas solubility, enhancing mass transfer and therefore increasing reaction rates. Hutchings and co-workers demonstrated that the rate of H_2O_2 synthesis can be increased by increasing the overall pressure using both batch and flow reactors.[33,34] In a batch system, a linear relationship between synthesis rate and reaction pressure was observed for 5wt.%AuPd catalysts supported on TiO_2 and acid pre-treated C. Studies in flow reactor showed an increase in H_2 conversion with increasing reaction pressure, while the selectivity towards H_2O_2 remained constant. These results indicate that the rate of H_2O_2 synthesis and degradation increase proportionally with increasing pressure.[34]

3.2.2.3 Effect of solvent composition on synthesis and degradation activity of 0.5wt.%Pd/TiO_2

The solvent used for the direct synthesis of H_2O_2 has a significant effect on H_2O_2 formation and decomposition.[5,14,41] It is commonly presumed that a primary role of the solvent is to reduce the resistance of mass transfer, by facilitating transport of H_2 and O_2 to the active sites of the catalyst and collect and solubilize the formed H_2O_2.[1,14,33] In the early studies, H_2O was considered to be an ideal solvent because it is non-toxic, non-flammable, highly accessible and miscible with H_2O_2. However, low solubility of reagent gases strongly limits rates of H_2O_2 formation.[1,14,42] Addition of acid and halide promoters is required to obtain high synthesis activity and selectivity in H_2O solvent.[28,43] If the additives are used in the process, they need to be removed from the final solution requiring additional steps in the whole process. The low solubility of the reagent gases in H_2O compared to organic solvents is most often emphasised as a main reason to employ alcohols as co-solvents. Paunovic *et al.* demonstrated that the choice of solvent can not only increase H_2 conversion but can significantly modify selectivity towards H_2O_2.[44] Aprotic polar solvents such as acetone, acetonitrile (MeCN) or DMSO showed very high selectivities, due to possible interaction of solvent and catalyst surface. Indeed, an increase in selectivity from 50% to almost 100% over AuPd/C when MeCN was used as co-solvent in aqueous solvent, compared to H_2O only solvent.[44] The adsorption of surface species onto the unselective sites of Pd surfaces, resulting in blocking of Pd ensembles that are responsible for H_2O formation, was previously showed by Han and Lunsford. Under mild conditions, ethanol reacts with O_2 on the Pd(110) facets, forming acetate ions.[45] Adams *et al.* demonstrated, through combination of kinetic isotope effect (KIE) and density functional theory (DFT) simulations, that CH_3OH is activated on a Pd surface to form chemisorbed hydroxymethyl intermediates ($CH_2OH\text{-}H^*$) that directly transferred electrons and protons to an adsorbed O species.[16] The resulting formaldehyde molecules subsequently regenerated the $CH_2OH\text{-}H^*$ intermediates through heterolytic oxidation of chemisorbed H atoms. In contrast, H_2O molecules heterolytically oxidized H to generate solvated protons and surface electrons that reduce O intermediates.

The effect of the CH_3OH/H_2O composition on catalyst activity is shown in Figure 3.11. In each experiment, the total mass of solvent was kept constant at 8.5 g and the CH_3OH/H_2O composition varied from pure H_2O to pure CH_3OH. It must be noted that in the degradation reaction small amounts of water were aways present, due to the H_2O_2/H_2O mixture used for reaction. In the absence of CH_3OH the synthesis activity is 32 mol_{H2O2} kg_{cat}^{-1} h^{-1}. Further increase in the CH_3OH amount results in a significant increase in H_2O_2 synthesis activity to 63 mol_{H2O2} kg_{cat}^{-1} h^{-1} at a solvent composition of 25% CH_3OH. Only a slight increase in produced H_2O_2 is observed when the amount of CH_3OH was increasing from 25-75%. However, a significant drop in synthesis activity, to 27 mol_{H2O2} kg_{cat}^{-1} h^{-1}, is achieved in a pure methanol solvent. The degradation data shows a more interesting trend. In the absence of CH_3OH, a degradation activity of 84 mol_{H2O2} kg_{cat}^{-1} h^{-1} is obtained in the presence of 4wt.% H_2O_2. With increasing content of CH_3OH, a decrease in degradation is observed and no degradation activity is detected when the concentration of CH_3OH was 50 wt.% and higher.

Hutchings and co-workers reported optimal solvent composition of 80 wt.% CH_3OH in aqueous reaction mixture over a 5wt.%AuPd/TiO_2 catalyst. Addition of methanol was observed to significantly increase the productivity of the catalysts compared to pure H_2O, from 18 mol_{H2O2} kg_{cat}^{-1} h^{-1} to almost 180 mol_{H2O2} kg_{cat}^{-1} h^{-1} at 2°C. They related this increase in synthesis activity to solubility of H_2 and O_2 in the solvent, as H_2 is far more soluble in CH_3OH than in H_2O. They also suggested that the presence of some H_2O is critical for H_2O_2 production enhancement and this could be related to solubility of H_2O_2 in the solvent.[46] In a further study, they suggested that the higher concentrations of H_2 in the liquid phase enables enhanced sequential rate of H_2O_2 hydrogenation and therefore less H_2O_2 was obtained with CH_3OH content higher than 80wt.%.[33] Under the similar reaction conditions, Crole *et al.* also attributed low H_2O_2 synthesis activity of the catalyst to low solubility of H_2 in pure H_2O, and observed an increase in synthesis activity with addition of CH_3OH up to 66 wt.%. They also showed, that at higher CH_3OH composition, hydrogenation of H_2O_2 is the dominant degradation pathway due to increased H_2 solubility.[14] The lower synthesis activity of the 0.5%Pd/TiO_2 catalyst in H_2O-rich solvents can be related to lower solubility of H_2 and O_2 and therefore a lower rate of H_2O_2 formation, and also to the degradation activity of the catalyst occurring at this solvent composition.[37,47–49] An increasing amount of CH_3OH increases reagent gas solubility, which results in a higher rate of H_2O_2 formation up to 80 wt.% of CH_3OH, which is in agreement with results obtained by Hutchings and co-workers.[46] Use of CO_2 as a diluent was shown to have a beneficial effect on H_2O_2 selectivity due to the formation of carbonic acid.[25,36] Solubility of CO_2 is higher in CH_3OH than in water, so the stabilization of H_2O_2 might be improved in CH_3OH rich reaction solution, due to increased formation of carbonic acid.[50] However, the presence of H_2O is still required for the formation of carbonic acid and therefore an optimal CH_3OH/H_2O ratio needs to be applied.[46] Both Piccinini and Crole related the drop in H_2O_2 concentration after optimal solvent composition to increasing degradation activity, due to increasing H_2 solubility.[14,33,46] However, as shown in Figure 3.12, there was no significant change in produced H_2O_2 over a wide CH_3OH concentration range (25-75wt.%), while no degradation activity was observed above 25 wt.% of CH_3OH. Increasing H_2 solubility does not explain this observation; however, this can be explained by the reaction pathway proposed by Adams *et al.*, who showed that CH_3OH and H_2O co-catalyse O_2 reduction by enabling proton-electron transfer reaction.[16] They suggested that, upon increasing the CH_3OH fraction, the surface coverage of CH_2O^* and CH_2OH^* also increases, which can co-catalyse the H_2O_2 formation. At a greater fraction of CH_3OH, less H_2O is available to co-catalyse the CH_2O^* reduction, which results in a decreasing fraction of CH_2OH^*. These findings can explain the trend observed in Figure 3.11. In pure H_2O, H_2O_2 can be produced through heterolytic oxidation of H_2 to produce H_3O^+ ions and electrons that reduce O_2. At a certain concentration of CH_3OH (25wt.%), the surface is saturated with CH_2OH^* intermediates to produce H_2O_2, and, in pure CH_3OH,an absence of H_2O to reduce CH_2O^* to CH_2OH^* results in a decreased synthesis activity of the 0.5wt.%Pd/TiO_2 catalyst.

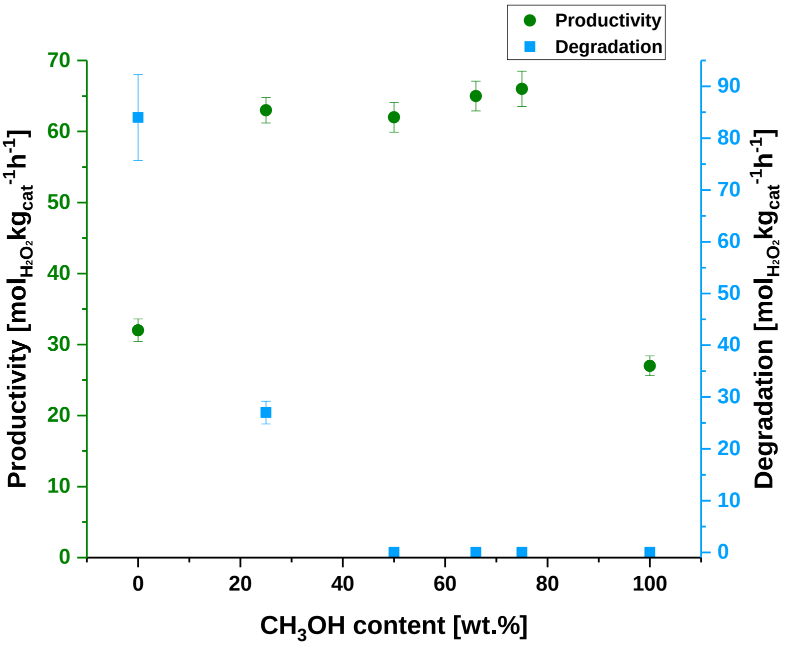

Figure 3.11: ***Synthesis and degradation activity of the 0.5wt.%Pd/TiO₂ catalyst with various water/methanol ratio. Reaction conditions: a) Synthesis reaction:*** *0.01 g catalyst, 8.5 g of solvent, various water/methanol ratio, 2.9 MPa 5%H_2/CO_2, 1.1 MPa 25%O_2/CO_2, 0.5 h, ambient temperature, 1200 rpm* ***b) Degradation reaction:*** *0.01 g catalyst, 0.68 g H_2O_2, various water/methanol ratio, 2.9 MPa 5%H_2/CO_2, 1.1 MPa 25%O_2/CO_2, 0.5 h, ambient temperature, 1200 rpm.*

It was demonstrated that the reaction conditions have a significant effect on the rate of H_2O_2 synthesis and its subsequent degradation when using 0.5.wt.%Pd/TiO_2. Use of higher pressure results in higher amount of H_2O_2 produced, due to a larger amount of dissolved reagent gases. As expected, a stoichiometric substrate ratio shows the highest productivity. An increase in CH_3OH content results in an increase in H_2O_2 synthesis activity and a decrease in H_2O_2

degradation activity when 4wt.% H_2O_2 was present in reaction solution. By optimizing these reaction parameters, high rates of H_2O_2 synthesis can be achieved with 0.5wt.%Pd/TiO_2. These results highlight the need to design the catalysts with reaction conditions in mind.

3.2.3 Further investigation of 0.5wt.%Pd/TiO_2

Extensive investigation by many authors have shown that Pd based catalysts are highly active for the direct synthesis of H_2O_2 from H_2 and O_2; however, they often display low selectivity and high activity towards subsequential activity for degradation of H_2O_2, especially at ambient temperatures and without any additives in reaction medium.[25,38,51] To decrease the degradation activity of monometallic Pd catalysts, the addition of acid and halide promoters or pre-treatment of support before metal impregnation is often required.[38,52] However, additional separation of additives might be required and the use of acids for support pre-treatment will generate acidic waste. A comparison of different monometallic Pd catalysts obtained from literature are summarised in Table 3.3. These results demonstrate how different reaction conditions, reactor systems and the addition of promoters can significantly affect synthesis activity and selectivity of the catalyst. It should be noted that different research groups report results in different units, so results were re-calculated to $mol_{H2O2}kg_{cat}^{-1}h^{-1}$ based on reported data and experimental details.

Table 3.3.: Comparison of synthesis activity and selectivity over Pd catalysts from literature.

Lit. Ref.	**Catalyst**	**Reactor system**	**Liquid phase**	**Gas composition**	**T [°C]**	**P [MPa]**	**Additives**	**Productivity** $[mol_{H2O2}kg_{cat}^{-1}h^{-1}]$	**Selectivity [%]**
This work	0.5wt.%Pd/TiO_2	Batch	CH_3OH/H_2O =1.93	$H_2:O_2:CO_2$ = 1:1.9:24.7	25	4	/	65	23
7	5wt.%Pd/TiO_2	Batch	CH_3OH/H_2O =1.93	$H_2:O_2:CO_2$ = 1:1.9:24.7	2	4	/	30	21
17	0.5wt.%Pd/TiO_2	Batch	CH_3OH	$H_2:O_2:CO_2$ = 1:5:19	2	1.95	/	83	57
13	0.5wt.%Pd/Al_2O_3	Semi-batch	H_2O	H_2: O_2 =1:1	27	0.95	1 mM KCl 0.1 M H_3PO_4	18	34
24	5wt.%Pd/SiO_2	Semi-batch	C_2H_5OH	$H_2:O_2:N_2$ = 1:15:4	10	0.1	0.4 mM HCl	30	60
21	0.5wt.%Pd/1wt.%C-Al_2O_3	Batch	CH_3OH	$H_2:O_2:N_2$ = 1:4:15	20	5	0.03 M H_2SO_4 0.14 mM NaBr	13	49
54	2.5wt.%Pd/ZrO_2 (SO_4^- and Cl^- dopped)	Semi-batch	CH_3OH	$H_2:O_2$ = 1:24	20	0.1	0.03 M H_2SO_4	14	40
18	0.5wt.%Pd/TiO_2	Semi-batch	C_2H_5OH	$H_2:O_2:N_2$ = 1:4:1.7	10	0.1	0.12 mM H_2SO_4	10	94
53	1wt.%Pd/γ-Al_2O_3	Batch	CH_3OH	$H_2:O_2:N_2$ = 1:2:24.7	2	3	0.03M H_2SO_4	85	64
55	1wt.%Pd/C	Batch	CH_3OH	$H_2:O_2:N_2$ = 1:2:24.7	2	3	0.03 M H_2SO_4	64	54
56	3wt.%Pd/TiO_2	Semi-batch	C_2H_5OH	$H_2:O_2:N_2$ = 1:4:1.7	10	0.1	0.12 mM H_2SO_4	76	54
10	Pd (unsupported)	Semi-batch	H_2O	$H_2:O_2$ =1:4	10	0.1	0.1 M HCl 10 mM KBr	15	75

As shown in this Chapter, monometallic Pd catalyst with metal loadings up to 0.5wt.%, prepared by wet impregnation in presence of 4wt.%H_2O_2 in starting solution, shows no degradation activity at ambient temperature with no promoters added during reaction and, therefore, further investigation of this catalyst was carried out to better understand its nature and its low degradation activity. Reusability of the 0.5wt.%Pd/TiO_2 catalyst was tested by applying different post reaction treatments to the catalyst and results are summarized in Table 3.4. After the initial H_2O_2 synthesis reaction, the catalyst was filtered and then exposed to different drying regimes. When the catalyst is dried at room temperate for 24 h, or dried at 110 ºC for 16 h, the synthesis activity decreases upon re-use of the catalyst under standard reaction conditions to 58 mol_{H2O2} kg_{cat}^{-1} h^{-1} and 54 mol_{H2O2} kg_{cat}^{-1} h^{-1}, respectively. Because residual solvent could be still present on the used catalyst surface, or drying the catalyst at higher temperatures might affect the oxidation state of Pd after initial use, the catalyst was dried under vacuum at 25 ºC for 16 h. This treatment shows to be most efficient as the lowest decrease in synthesis activity and the lowest increase in H_2O_2 degradation activity compared to fresh catalyst is observed, and therefore is applied in future reusability studies. Higher rates in synthesis activity is obtained upon re-use compared to other drying treatments. However, in all cases a significant increase in catalyst degradation activity is obtained in presence of 4wt.%H_2O_2 and therefore this change in activity was further explored.

Table 3.4: Re-use of 0.5wt.%Pd/TiO_2 with different post reaction treatments.

Post reaction treatment	**Productivity [mol_{H2O2} kg_{cat}^{-1} h^{-1}]**	**Degradation [mol_{H2O2} kg_{cat}^{-1} h^{-1}]**
As calcined, fresh material	65	0
Used samples		
Dried at ambient temperature	58	390
Dried at 110ºC	54	358
Dried under vacuum at 25ºC	61	331

Reaction conditions: a) Synthesis reaction: 0.01 g catalyst, 2.9 g of water, 5.6 g of methanol, 2.9 MPa 5%H_2/CO_2, 1.1 MPa 25%O_2/CO_2, 0.5 h, ambient temperature, 1200 rpm **b) Degradation reaction:** 0.01 g catalyst, 0.68 g H_2O_2, 2.22 g of water, 5.6 g of methanol, 2.9 MPa 5%H_2/CO_2, 1.1 MPa 25%O_2/CO_2, 0.5 h, ambient temperature, 1200 rpm.

TEM analysis of the 0.5wt.%Pd/TiO_2 catalyst was previously shown in Figure 3.4 a), where no visible Pd particles were observed, suggesting that the particle diameter was below detection limit of the equipment and Pd existed as well dispersed small nanoparticles on the TiO_2 surface. Scanning transmission electron microscopy – high-angle annular dark-field (STEM-HAADF) analysis of the 0.5wt.%Pd/TiO_2 catalyst was carried out to investigate the morphology of the catalysts and can be seen in Figure 3.12. Figure 3.12 a) of the fresh sample indicates sub-nanometres particles with average particle diameter 0.7 nm, with good Pd dispersion, as suggested via the initial TEM studies. STEM-HAADF analysis of the used catalyst, after use in the H_2O_2 synthesis reaction (Figure 3.12 b) revealed an increase in mean particle diameter to 3.9 nm, as shown in Figure 3.13, which suggests the agglomeration of particles during the H_2O_2 synthesis reaction; however, small sub-nanoparticles are also still observed on the sample. An increase in Pd particle diameter after the direct synthesis of H_2O_2 was previously reported by Gemo *et al.* and Tian *et al.*[17,18]

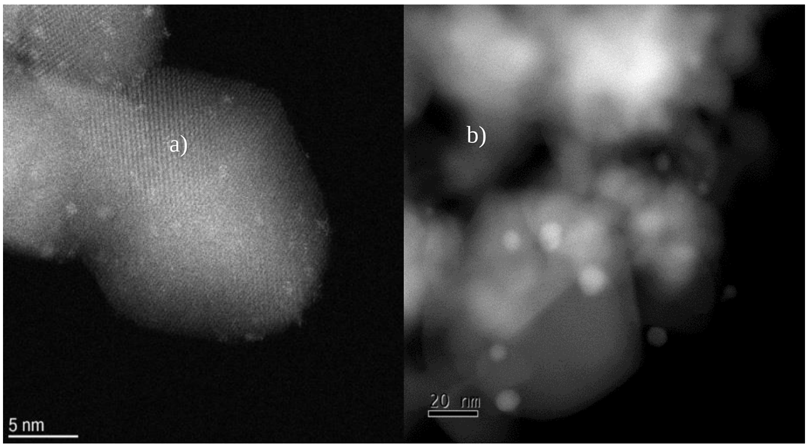

***Figure 3.12: STEM-HAADF images of: a) fresh and b) used 0.5wt.%Pd/TiO_2 catalyst*.** **Acknowledgment:** The STEM-HAADF characterisation was carried out by Dr He and Dr Davies. We acknowledge the Diamond Light Source for the experiment sessions.

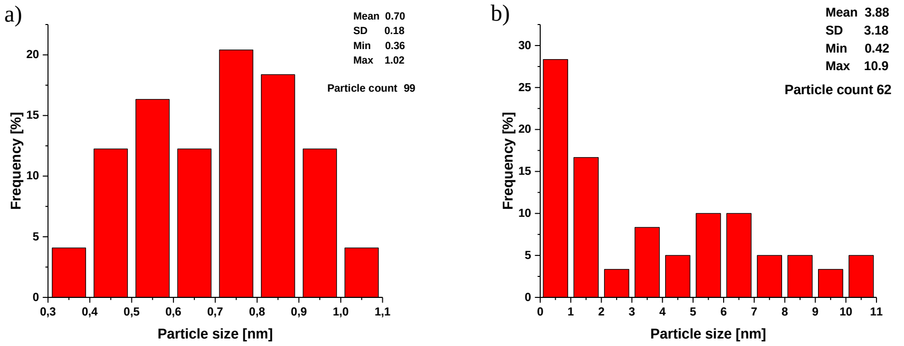

***Figure 3.13: Particle size distribution of 0.5wt.%Pd/TiO_2 of: a) fresh and b) used catalyst*.** Particle sizes are counted using STEEM-HAADF images.

X-ray photoelectron spectroscopy (XPS) was carried out to investigate any change in Pd oxidation state after use in the H_2O_2 synthesis reaction. In the fresh catalyst, Pd species are present as Pd^{2+}, as shown in Figure 3.14. After use in the H_2O_2 synthesis reaction, a shift in Pd binding energy from 336.7 to 335 eV is observed, which suggest that the surface Pd was reduced from Pd^{2+} to Pd^0 (Pd^{2+}:Pd^0 is 1:6.5). Lunsford and co-workers proposed a catalytic cycle in which Pd^0 in a form of colloids reacts with O_2 in presence of Cl ions to form a $PdCl_2O_2$ complex, subsequently reacting with H_3O^+ to form H_2O_2 and $PdCl_4$. The $PdCl_4$ is then reduced back to Pd^0 by H_2, suggesting that Pd is changing oxidation state during formation of H_2O_2.[57] Melada *et al.* also reported reduction of a PdO supported catalyst during thr direct synthesis of H_2O_2, and linked this change in Pd oxidation state to decreasing selectivity of catalysts as reaction proceeded. They suggested that, during reduction of Pd, structural rearrangements might occur, leading to formation of surface defects, which can be related to increased degradation activity of catalyst and decreased selectivity.[58] Adams *et al.* observed that PdO is unreactive in its initial stage and it showed an induction time before H_2O_2 was produced. H_2 readily reduces PdO under reaction conditions, with the core of Pd particles being metallic or hydridic, while O exist on the particle surface. Based on *operando* EXAFS measurements, they concluded that, in CH_3OH, β-PdH_x is stable at most reaction conditions and the oxidation of the nanoparticle surfaces requires much more oxidizing conditions (e.g. 60 kPa H_2, 1000 kPa O_2)[16] However, the partial pressure of O_2 during the synthesis reaction in this study are only 276 kPa, which can explain why Pd is not oxidised back to a Pd^{2+} state during reaction. Reduction of the Pd^{2+} species could explain the increase in degradation activity towards H_2O_2 after re-use of the catalyst, as it has been previously reported that catalysts with a high content of Pd^0 are more active for H_2O_2 degradation than those that exhibit a higher Pd^{2+} content.[51,58–60] Ouyang *et al*. proposed that the synthesis of H_2O_2 should be a consequence of the interaction between Pd and PdO, and should not be assigned to simply pure metallic or oxidised Pd species.[31] Interestingly, this shift in Pd binding energy suggests a reduction of Pd was not observed after the degradation reaction, suggesting that a higher concentration of H_2O_2 retained Pd in Pd^{2+} state. A shift from 336.7 to 337.6 eV was observed, which may indicate a possible Pd-Cl interaction. Choudhary *et al.*[61] and Biniak *et al.*[62] both demonstrated possible use of H_2O_2 as oxidising agent to oxidise Pd to PdO, which could explain why Pd was not reduced to Pd^0 during degradation reaction. Voloshin *et al.* proposed a oxidation and reduction mechanism of Pd by H_2O_2, in which converting Pd^0 to PdO with H_2O_2 is much faster step compared to conversion of PdO to Pd^0 with H_2O_2, due to 6 times higher change of free Gibbs energy.[41]

After use in the H_2O_2 synthesis reaction, a 90% loss of chlorine species were observed compared to un-used sample, based on XPS analysis. Leached halides can act as a promoter for the direct synthesis of H_2O_2 and can also help stabilize produced H_2O_2.[63,64] The loss of Pd from supported catalysts is also a concern in liquid-phase catalysis, with homogeneous Pd species known to be active towards H_2O_2 synthesis.[65] However, ICP-MS analysis of the post-H_2O_2 synthesis reaction solution shows very low levels of Pd leaching, below 14 ppb, which represents less than 0.3% of total Pd content.

An increase in degradation activity towards H_2O_2, from 0 $mol_{H2O2}\ kg_{cat}^{-1}\ h^{-1}$ to 331 $mol_{H2O2}\ kg_{cat}^{-1}\ h^{-1}$, is observed upon re-use of the catalyst. This can be related to an increased mean particle diameter of the used catalyst, as shown by STEM-HAADF, and partial reduction of Pd^{2+} to Pd^0 after the synthesis reaction, as well as loss of Cl species as evidenced by XPS analysis. However, there was no significant change in the activity of the catalyst towards H_2O_2 synthesis upon the re-use, as shown in Table 3.4, when catalyst was dried in vacuum oven.

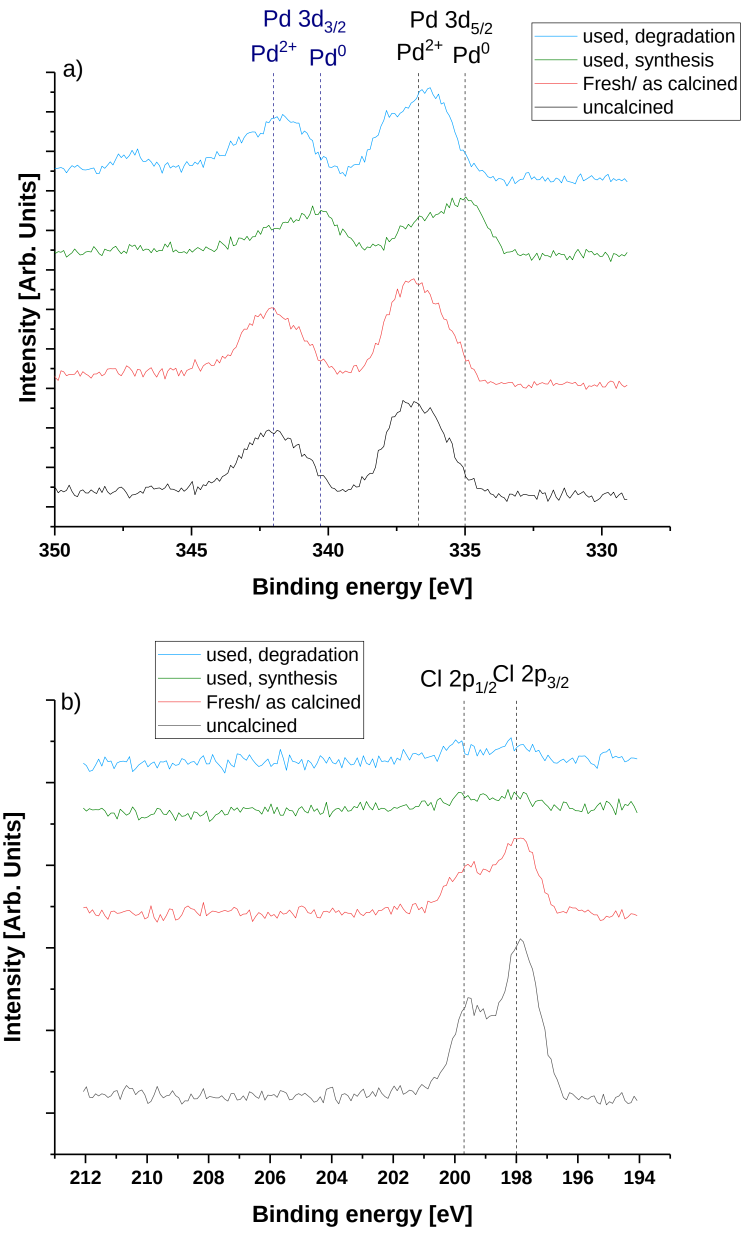

Figure 3.14: a) Pd(3d) and b) Cl(2p) XPS spectra observed for uncalcined, calcined and used 0.5wt.%Pd/TiO_2 catalyst.

To investigate if Cl^- anions present on the catalyst after impregnating Pd on TiO_2, and also Cl^- species leached into reaction solution, have an effect on catalyst activity, 0.5wt.%Pd/TiO_2 was prepared using $Pd(NO_3)_2$ as the Pd precursor. As shown in Table 3.5, a decrease in synthesis activity from 65 to 46 mol_{H2O2} kg_{cat}^{-1} h^{-1} is observed. More importantly, no degradation activity is observed over the catalyst when using $Pd(NO_3)_2$ as the precursor in presence of 4wt.%H_2O_2. These results suggest that choice of Pd precursor can effect catalyst activity, and Cl^- species added as $PdCl_2$ during catalyst preparation might play a role in promoting formation of H_2O_2. However, even in the absence of Cl^- species, no H_2O_2 degradation activity is observed, suggesting that Cl^- species are not required to obtain no degradation activity in presence of 4wt.%H_2O_2.

Table 3.5: Effect of Pd precursor on 0.5wt.%Pd/TiO_2 catalyst activity.

Pd precursor	**Productivity [mol_{H2O2} kg_{cat}^{-1} h^{-1}]**	**Degradation [mol_{H2O2} kg_{cat}^{-1} h^{-1}]**
$PdCl_2$	65	0
$Pd(NO_3)_2$	46	0

Reaction conditions: a) Synthesis reaction: 0.01 g catalyst, 2.9 g of water, 5.6 g of methanol, 2.9 MPa 5% H_2/CO_2, 1.1 MPa 25% O_2/CO_2, 0.5 h, ambient temperature, 1200 rpm **b) Degradation reaction:** 0.01 g catalyst, 0.68 g H_2O_2, 2.22 g of water, 5.6 g of methanol, 2.9 MPa 5% H_2/CO_2, 1.1 MPa 25% O_2/CO_2, 0.5 h, ambient temperature, 1200 rpm.

No H_2O_2 degradation activity in the presence of 4wt.% H_2O_2 over a monometallic Pd catalyst is a unusual observation, particularly in the absence of additives such as halides or acids. Ouyang *et al.*[31] reported hydrogenation activity around 64 mol_{H2O2} kg_{cat}^{-1} h^{-1} over 1wt.% Pd/TiO_2 in acidified C_2H_5OH solution, and Villa *et al.* showed degradation activity of 95 mol_{H2O2} kg_{cat}^{-1} h^{-1} with 1wt.%Pd supported on acid pre-treated carbon nanofibers; both experiments were carried out in presence of H_2O_2. Voloshin *et al.* investigated the kinetics of H_2O_2 decomposition over a Pd/SiO_2 catalyst and demonstrated an increase in the H_2O_2 hydrogenation rate with increasing H_2O_2 concentration in reaction solution.[66]

For industrial application, it would be necessary for H_2O_2 degradation activity to remain low even in the presence of high H_2O_2 concentrations and therefore a series of H_2O_2 degradation experiments were carried out with increasing H_2O_2 concentration; results are summarised in Table 3.6. No degradation activity is observed with increasing concentration of H_2O_2 up to 16 wt.%; this concentration is the maximum possible by replacing the whole H_2O content with the 50 wt.% stock solution of H_2O_2. To achieve higher concentrations, an amount of CH_3OH must be removed, which could affect solubility of the gases and therefore higher concentrations were not tested. No degradation activity, towards H_2O_2 in the presence of highly concentrated H_2O_2 solution, could be a desirable catalyst feature considering 6-8 vol % of H_2O_2 is required for the most industrial applications.[36] Edwards *et al.* previously showed that there is no degradation activity of AuPd supported on pre-treated C catalyst in presence of 14wt.% solution of H_2O_2;[60] however, HNO_3 was used for support pre-treatment and therefore acidic waste was produced, which would require neutralisation, as well as a more complex route to catalyst preparation being required compared to the preparation method used in this work. Freakley *et al.* reported no degradation activity over 3 wt.%Sn – 2 wt.%Pd/TiO_2 in solution up to 8 wt.% H_2O_2, but in the presence of a 16 wt.% H_2O_2 solution degradation activity of over 200 mol_{H2O2} kg_{cat}^{-1} h^{-1} was achieved.[9] The selectivity of 96% was reported for 3 wt.%Sn - 2 wt.%Pd/TiO_2, showing that highly selective catalysts might degrade H_2O_2 at higher concentrations under H_2O_2 synthesis conditions similar to those reported within this work.

Table 3.6: Effect of initial H_2O_2 concentration on 0.5wt.%Pd/TiO_2 catalyst degradation activity.

Concentration of H_2O_2 [wt.%]	**Degradation [mol_{H2O2} kg_{cat}^{-1} h^{-1}]**
4	0
8	0
12	0
16	0
16.3	0

Reaction conditions: Degradation reaction: 0.01 g catalyst, x g H_2O_2, 2.9-x g of water, 5.6 g of methanol, 2.9 MPa 5% H_2/CO_2, 1.1 MPa 25% O_2/CO_2, 0.5 h, ambient temperature, 1200 rpm.

For use in an industrial application, catalyst stability during storage would be preferable to ensure that the catalyst activity remains unchanged. With this in mind, the fresh 0.5wt.%Pd/TiO_2 was repeatedly tested over time, with a change in catalyst activity observed. During this study, where the catalyst (unused) was repeatedly tested over 51 days, the catalyst was stored at room temperature in the dark. Catalytic activity towards the direct synthesis and subsequent degradation of H_2O_2 was evaluated as a function of catalyst age and these results are summarized in Figure 3.15. The catalyst was also characterized by XPS on the same day as synthesis and degradation testing, to relate any changes in catalyst morphology to the observed changes in activity. Initial productivity is 65mol_{H2O2} kg_{cat}^{-1} h^{-1} and a slight increase in synthesis activity is observed after 23 days, rising to 70 mol_{H2O2} kg_{cat}^{-1} h^{-1}.

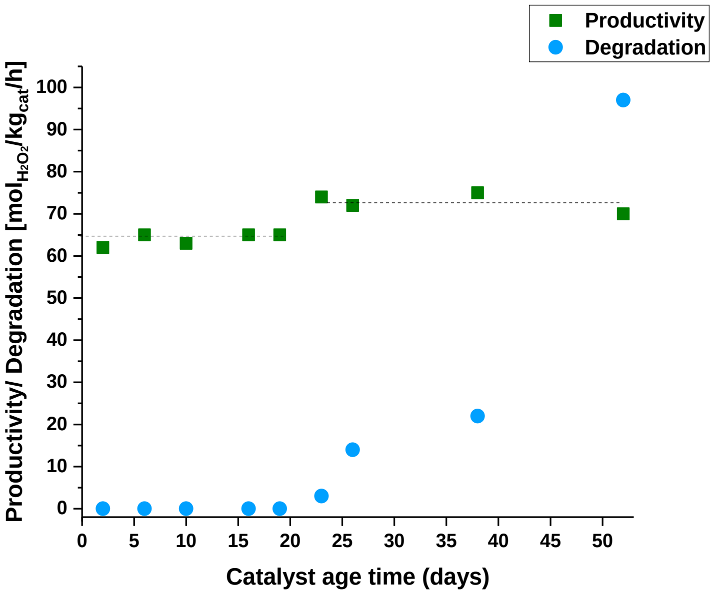

Figure 3.15: H_2O_2 direct synthesis and degradation testing and re-testing over 0.5wt.%Pd/TiO_2 at ambient temperature. **Reaction conditions:** a) H_2O_2 synthesis: 0.01 g catalyst, 2.9 g of water, 5.6 g of methanol 2.9 MPa 5% H_2/CO_2, 1.1 MPa 25% O_2/CO_2, 0.5 h, ambient temperature, 1200 rpm. b) H_2O_2 degradation: 0.01 g catalyst, 0.68 g H_2O_2, 2.9 g of water, 5.6 g of methanol 2.9 MPa 5% H_2/CO_2, 0.5 h, ambient temperature, 1200 rpm.

Initial degradation activity remains at 0 mol_{H2O2} kg_{cat}^{-1} h^{-1} during the first 23 days. Beyond this, the catalyst starts exhibiting degradation activity. After 51 days, degradation activity of 97mol_{H2O2} kg_{cat}^{-1} h^{-1} is observed; notably, H_2O_2 synthesis activity is maintained, despite the rise in degradation activity. The change in both synthesis and degradation activity occurs after the same time, 23 days, suggesting that the changes in activities have the same cause.

STEM-HAADF images of the aged catalyst, (Figure 3.16 a), after storage for 40 days in ambient conditions shows a mean particle diameter of 0.74 nm. As shown in the particle diameter distribution diagram in Figure 3.16 b), a similar particle diameter distribution is observed with both aged and fresh catalysts.

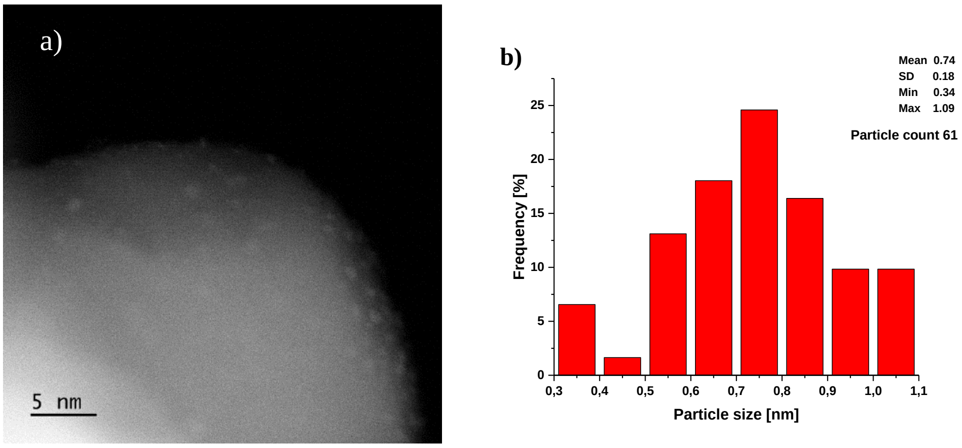

Figure 3.16: a) STEM-HAADF image and b) particle size distribution of aged 0.5wt.%Pd/TiO$_2$ catalyst.

Acknowledgment: The STEM-HAADF characterisation was carried out by Dr He and Dr Davies. We acknowledge the Diamond Light Source for the experiment sessions.

As previously shown, the oxidation state of the metal species plays a crucial role in catalyst activity, with an increase in degradation activity observed upon re-use, when Pd species was reduced from Pd^{2+} to Pd^0. To investigate possible changes in oxidation state, the sample was examined in regular intervals using X-ray photoelectron spectroscopy and the spectra are shown Figure 3.17.

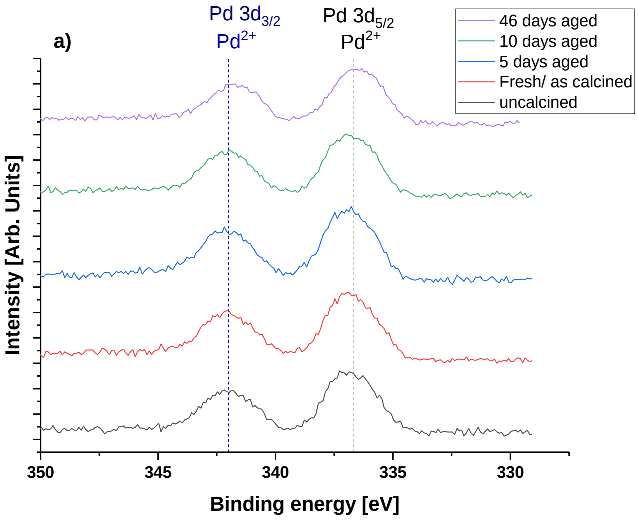

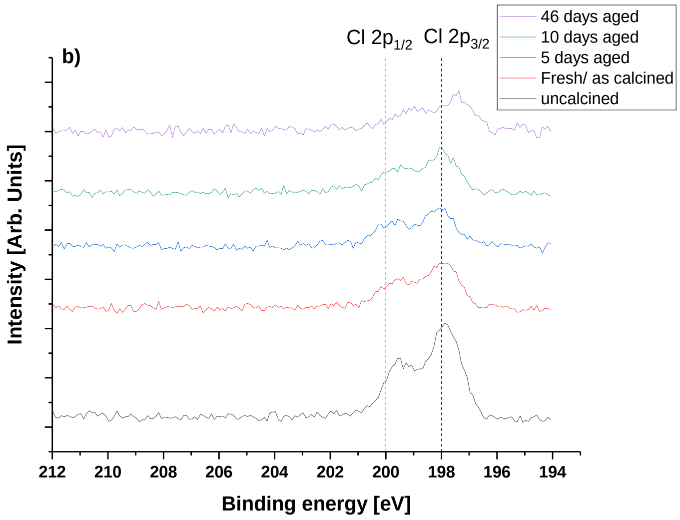

Figure 3.17: a) Pd(3d) and b) Cl(2p) XPS spectra observed for 0.5wt.%Pd/TiO_2 as a function of storage time.

It was observed that Pd in the freshly calcined sample is present on the catalyst surface in cationic form, and there is no significant change observed in oxidation state through time. Similarly, no change in Cl spectra is observed with investigated catalyst after calcination over time. These results show that the change causing an increase in degradation activity are unlikely related to changes in the oxidation state of Pd.

In situ diffusive reflectance infrared Fourier transform spectroscopy of CO adsorption was carried out to determine the surface structure of fresh, aged and used 0.5wt.%Pd/TiO_2 catalysts; using CO as the probe molecule. The peak at 2091 cm^{-1} is assigned to the linear CO bands adsorbed on defects such as corners, edges, steps, and surface kinks with low coordination number.[18] The peaks in a range of 1950-2010 cm^{-1} are suggested as bridge-bonded defective species, such as surface steps or particle edges. CO bridge-bonded to Pd(111) facets has assigned peaks in range 1900-1940 cm^{-1}.[67] The peaks assigned to three-fold CO adsorption on Pd(111) facets are distinguished in region 1800-1890 cm^{-1}.[67,68]The remaining bands in the region 1500-1700 cm^{-1} were more likely attributed to carbonate and bicarbonate species.[18,69,70] The changes in peak position and intensity of fresh and used catalysts can be attributed to the geometric and electronic modification of Pd atoms during the reaction, which is in agreement with XPS analysis shown in Figure 3.17. As shown in Figure 3.18, no significant difference in DRIFTS spectra is observed for fresh and aged catalyst suggesting, that geometric modification of Pd atoms did not occur with catalyst age.

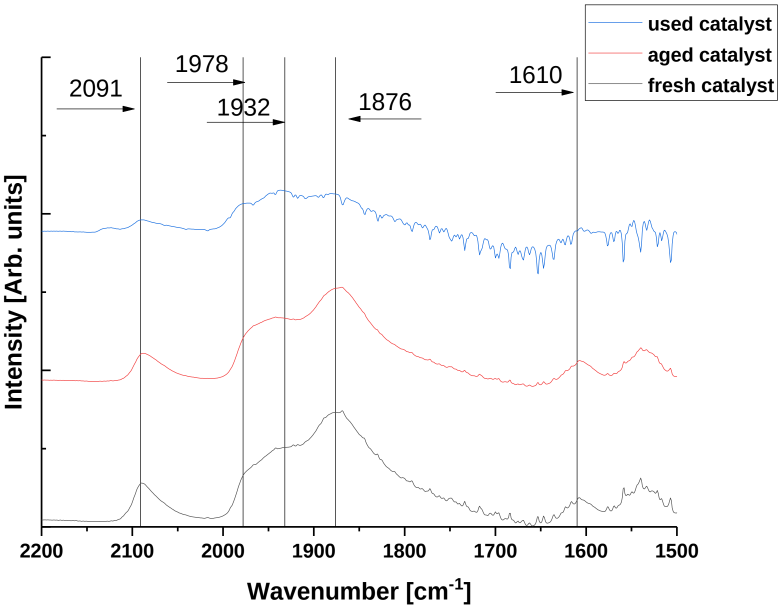

Figure 3.18: In situ DRIFTS of CO adsorption over fresh, aged and used 0.5wt.%Pd/TiO$_2$ at 293K.

X-Ray Absorption Near Edge Structure (XANES) and Extended X-Ray Absorption Fine Structure (EXAFS) spectrometry was carried out to investigate the structure and the oxidation state of the 0.5wt.%Pd/TiO$_2$ catalyst. These spectra are shown in Figure 3.19. The XANES results show the fresh and aged 0.5wt.%Pd/TiO$_2$ catalyst have almost the same near edge absorption feature. Both have higher average oxidation states than for the used catalyst. This means that there is a change in oxidation state of Pd during reaction, which is in keeping with the analysis by XPS and, in addition to particle agglomeration, can effect the reusability of the catalyst and lead to the increase in H$_2$O$_2$ degradation activity upon re-use. It can be seen from this analysis that the used catalyst displays a mixture of PdO and Pd^0, which corresponds with XPS results of used sample. Linear combination fitting (LCF) shows that the Pd speciation is very different between the fresh and used catalysts, with the fresh sample observed to have a contribution of about 1/4 from PdCl$_2$ and 3/4 of PdO, while the used sample is about 2/5 of PdO and 3/5 of Pd^0.

The EXAFS fitting of fresh and aged catalysts shows a contribution from Pd-Cl scattering in the first shell. The coordination number of Pd-O is around 3 and the Pd-Cl is less than 1. The aged sample has slightly less Cl than the fresh catalysts. There is no significant scattering path beyond Pd-Cl scattering, proving the presence of highly dispersed Pd species on an atomic scale. As shown in Table 3.7, there was no measurable Pd-Pd bond for fresh (2 days old sample) and aged (60 days old sample) catalyst. For fresh catalyst, there is existing Pd-O bond of 2.00 ± 0.01 Å and Pd-Cl bond of 2.30 ± 0.01 Å, indicating that monodisperse or isolated Pd atoms are predominant on the surface. Same bonds are existing on aged catalyst with slight increase in Pd-O bond to 2.01 ± 0.01 Å. For both fresh and aged catalyst STEM-HAADF images show a mean particle diameter of 0.7 nm, suggesting that sub-nano Pd clusters with few Pd atoms are present on the catalyst surface. However, no significant Pd-Pd scattering suggest that monodispersed or isolated Pd atoms are predominant on the surface. The coordination number of Pd-O is around 3.2 ± 0.2 and the Pd-Cl is less than 0.8 ± 0.2 in fresh catalyst. It is generally believed that the Pd-O coordination in the bulk of PdO is a square-like 4 oxygen coordination with the same bond length at 2.0 Å. The Pd-Cl scattering suggests that some of the oxygen atoms in the square-like coordination are replaced by Cl. The aged catalyst shows slightly lower Pd-Cl coordination number of 0.6 ± 0.2. For the used catalyst, a Pd-O bond of 1.99 ± 0.01 Å with a CN 1.5 ± 0.4 is determined. The Pd-Pd bond of 2.74 ± 0.01 Å is close to the Pd-Pd distance in Pd foil and CN of 5.4 ± 0.5 was a result of larger particles. This is in agreement with STEM-HAADF analysis showing larger Pd particles with mean diameter 3.88 nm.

Table 3.7: Tabulated Pd-Pd, Pd-Cl and Pd-O coordination numbers (N), bond distances (R), bond length disorder (σ^2), and threshold energy corrections (ΔE_0) for Pd nanoparticles on fresh, used and aged catalyst.

sample	Pd-O R [Å]	CN	Pd-Cl R [Å]	CN	Pd-Pd R [Å]	CN	σ^2 Pd-O	σ^2 Pd-Cl	σ^2 Pd-Pd	ΔE_o [eV]
PdO	2.01	4			-	-	-	-	-	-
$PdCl_2$	-	-	2.31	4	-	-	-	-	-	-
Pd foil	-	-	-	-	2.75	12	-	-	-	-
fresh	2. 0(1)	3.2(2)	2.3(1)	0.8(2)	-	-	0.003(1)	0.003 (1)		-0.9(2.1)
used	1.99(1)	1.5(4)	-	-	2.74 (1)	5.4(5)	0.003(2)	-	0.006(1)	1.9(0.7)
aged	2.01(1)	3.4(2)	2.3(1)	0.6(2)	-	-	0.003(1)	0.003(1)		0.7(1.2)

The number in parentheses indicates the statistical error: error for *R* is in two decimal places (e.g., 2.0 (1) ≡ 2.0 ± 0.01); error for CN is in one decimal place (e.g., 3.2 (2) ≡ 2.0 ± 0.2); error for σ^2 is in three decimal places (e.g., 0.003 (1) ≡ 0.003 ± 0.001); error for ΔE_o is as stated in parentheses (e.g., -0.9 (2.1) ≡ -0.9 ± 2.1)

Tian *et al.* reported that single site Pd catalysts supported on HAp are inactive towards the direct synthesis of H_2O_2 and it is sub-nano Pd clusters, with a few Pd atoms (two or three atoms) that are responsible for synthesis of H_2O_2.[18] The larger Pd particles (>2.5nm) with abundant Pd(111) facets are not favourable for H_2O_2 and are rather active for O_2 dissociation leading to H_2O formation.

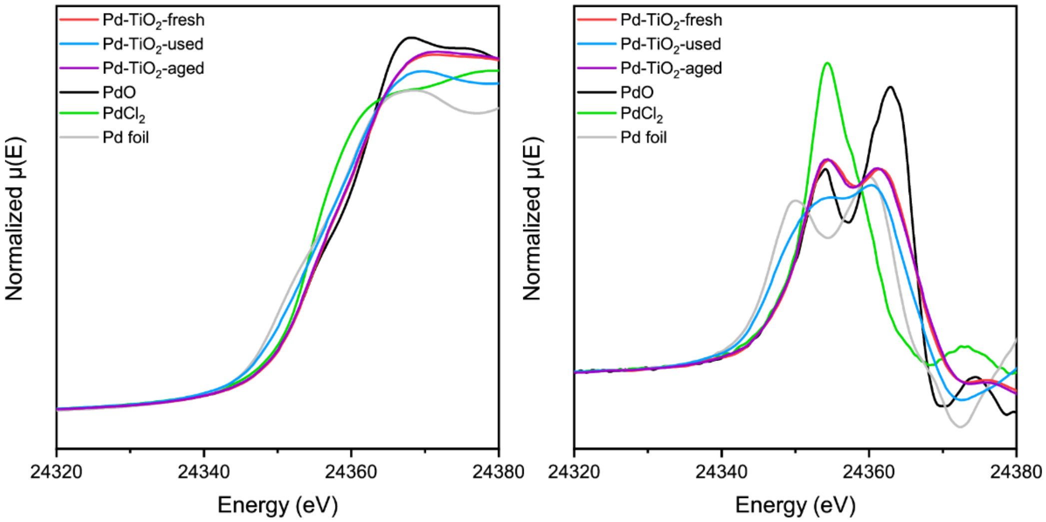

Figure 3.19: XANES (left) and EXAFS (right) spectra of fresh, aged and used 0.5wt.%Pd/TiO₂ catalyst.

Acknowledgment: The EXAFS characterisation was carried out by Dr Wang and his research team. We acknowledge the Diamond Light Source B18 beamline for the experiment sessions (SP17377, SP19072 and SP19850).

As shown in previous characterization of the freshly prepared and aged 0.5wt.%Pd/TiO_2, there was no significant chance in catalyst morphology or Pd oxidation state. EXAFS and XANES fittings showed very similar spectra, with the Pd-Cl coordination number slightly decreased from 0.8 ± 0.2 to 0.6 ± 0.2. It is not yet clear what is causing the change in catalyst activity over time; however, if the change in catalyst morphology occurred, it must have been in such a delicate merit that it was not clearly observed during catalyst characterization.

3.2.4 Effect of initial H_2O_2 concentration on catalyst synthesis and degradation activity of 0.5wt.%Pd/TiO_2

No H_2O_2 is present at the beginning of the standard synthesis reaction and a relatively small concentration (0.1-0.3 wt.%) is typically produced during a single standard reaction (0.5 h), comparable to that produced in the initial stages of the industrial route to H_2O_2 production (0.8 -1.9 wt.%), prior to extraction of H_2O_2 from the working solution.[1] To investigate the effect of a higher initial concentration of H_2O_2 in the reaction solution on catalyst activity, a series of experiments were carried out over 0.5wt.%Pd/TiO_2. As shown in Figure 3.20, the starting concentration of H_2O_2 has a significant effect on catalyst activity towards further H_2O_2 synthesis or degradation. No synthesis activity and low degradation activity are observed in the reaction with a starting concentration of H_2O_2 above 0.25 wt.%. Degradation of 16 mol_{H2O2} kg_{cat}^{-1} h^{-1} is obtained with 2wt.%H_2O_2 and 7 mol_{H2O2} kg_{cat}^{-1} h^{-1} with 0.5wt%.

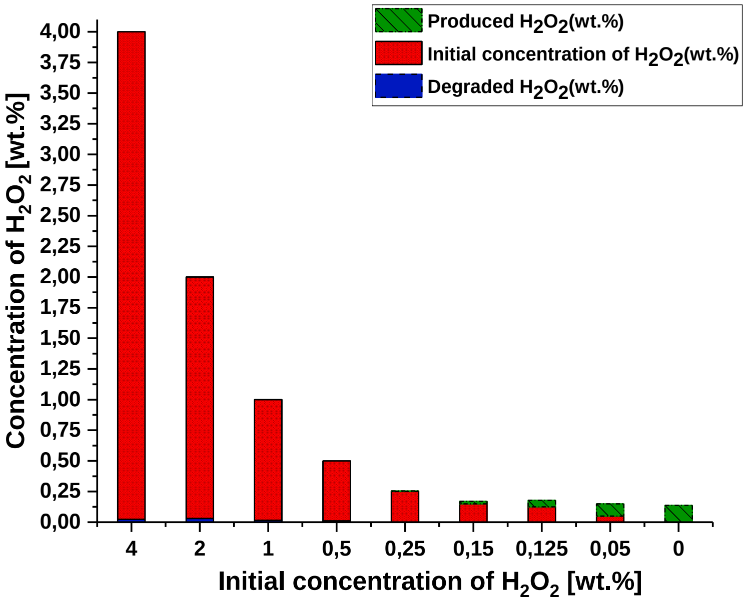

Figure 3.20: Initial H_2O_2 concentration study over 0.5wt.%Pd/TiO2. **Reaction conditions:** 0.01 g catalyst, x g of H_2O_2, (2.9-x) g of water, 5.6 g of methanol 2.9 MPa 5% H_2/CO_2, 1.1 MPa 25% O_2/CO_2, 0.5 h, ambient temperature, 1200 rpm.

At initial H_2O_2 concentrations of 0.25wt.% H_2O_2, no synthesis or degradation activity is observed; with decreasing initial concentration of H_2O_2, formation of H_2O_2 was achieved. Synthesis activity of 11 $mol_{H2O2}\ kg_{cat}^{-1}\ h^{-1}$ is obtained with 0.15wt.%H_2O_2 and this synthesis activity increases to 49 $mol_{H2O2}\ kg_{cat}^{-1}\ h^{-1}$ with only 0.05wt.% H_2O_2 in initial solution. As previously shown (Figure 3.14), after use in the H_2O_2 degradation reaction in the presence of 4wt.% of H_2O_2, Pd on the catalyst surface remains as Pd^{2+}. No synthesis activity over higher concentrations of H_2O_2 might be related to the stabilization of Pd as Pd^{2+}, and therefore a mixture of Pd^{2+} and Pd^0 might be required to obtain reasonable synthesis activity. As shown in Figure 3.21, low H_2 conversions are obtained when H_2O_2 varies from 0.25 – 4 wt.%, due to low degradation activity of catalyst and no visible synthesis activity, and therefore no H_2 selectivity was calculated. A small amount of H_2O_2 could be produced in these conditions; however, if this is the case then more H_2O_2 is degraded than produced. Interestingly, addition of small amounts of H_2O_2 (0.05-0.15 wt.%) increases the selectivity towards H_2O_2 from 23% up to 59%, and significantly decreases the H_2 conversion to 18% with 0.05wt.% H_2O_2 in starting solution. The addition of H_2O_2 might help maintain Pd as Pd^{2+}, which can explain an increase in H_2 selectivity. Choudhary *et al.* reported that the presence of larger amounts of H_2O_2 result in a drastic decrease in the net H_2O_2 formation over a 1wt.%Br–1wt.%F–5wt.%Pd/Al_2O_3 catalyst. No H_2O_2 formation was observed with the H_2O_2 concentration above 0.27 wt.%, and a further increase in H_2O_2 led to a significant increase in degradation activity.

They suggested that decrease in synthesis activity may be due to the oxidation of Pd species by H_2O_2 added to the reaction mixture.[38] In comparison; Piccinini *et al.* reported no net production of H_2O_2 in the presence of H_2O_2, due to increased degradation activity in the presence of higher H_2O_2 concentration.[46]

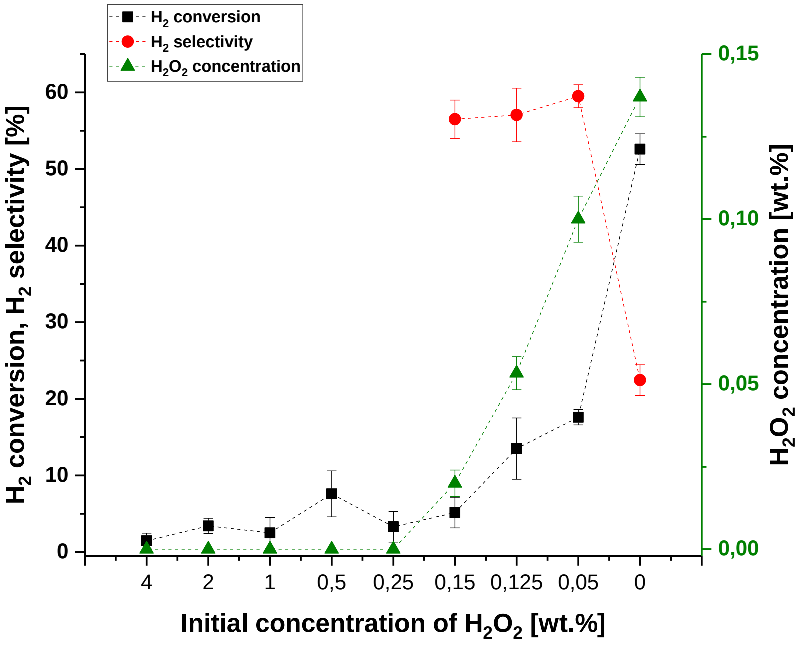

Figure 3.21: **Conversion and selectivity of the 0.5wt.% H_2O_2 with different H_2O_2 concentration in starting solution. Reaction conditions:** 0.01 g catalyst, x g of H_2O_2, (2.9-x) g of water, 5.6 g of methanol 2.9 MPa 5% H_2/CO_2, 1.1 MPa 25% O_2/CO_2, 0.5 h, ambient temperature, 1200 rpm.

3.2.5 Reusability of the 0.5wt.%Pd/TiO_2 catalysts and recalcination of the used catalyst

A crucial factor to consider in evaluating catalyst is its reusability. As previously shown in Table 3.4, 0.5wt.%Pd/TiO_2 exhibits increased degradation activity upon re-use, up to 331 mol_{H2O2} kg_{cat}^{-1} h^{-1}. To investigate potential factors responsible for this increase, catalytic samples were subjected to different treatments and then dried in a vacuum oven prior to re-use. The results of this study are summarised in Table 3.8. Upon the re-use of the catalyst, a slight decrease in synthesis activity is observed from 65 mol_{H2O2} $kg_{cat}^{-1}h^{-1}$ to 61 mol_{H2O2} $kg_{cat}^{-1}h^{-1}$. With subsequent re-use of the catalyst, synthesis activity decreases further to 56 mol_{H2O2} $kg_{cat}^{-1}h^{-1}$ and H_2O_2 degradation activity increased up to 448 mol_{H2O2} kg_{cat}^{-1} h^{-1}.

Table 3.8: Reusability study over 0.5wt.%Pd/TiO$_2$ catalyst.

Number of uses	**Productivity [mol$_{H2O2}$ kg$_{cat}^{-1}$ h^{-1}]**	**Degradation [mol$_{H2O2}$ kg$_{cat}^{-1}$ h^{-1}]**
1st use [a]	65	0
2nd use [a]	61	331
3rd use [a]	56	448
2nd use [b]	71	90
2nd use [c]	65	66
2nd use [d]	74	41

Reaction conditions: a) Synthesis reaction: 0.01 g catalyst, 2.9 g of water, 5.6 g of methanol, 2.9 MPa 5% H_2/CO_2, 1.1 MPa 25% O_2/CO_2, 0.5 h, ambient temperature, 1200 rpm **b) Degradation reaction:** 0.01 g catalyst, 0.68 g H_2O_2, 2.22 g of water, 5.6 g of methanol, 2.9 MPa 5% H_2/CO_2, 1.1 MPa 25% O_2/CO_2, 0.5 h, ambient temperature, 1200 rpm.

[a] Standard reaction conditions were applied during testing.

[b] Only 1.1 MPa 25%O_2/CO_2 was used in the initial reaction. Catalyst was then dried and re-used in reaction using standard reaction conditions.

[c] No reagent gases were used in the initial reaction (reaction was carried out at atmospheric pressure). Catalyst was then dried and re-used in reaction using standard reaction conditions.

[d] Catalyst was dispersed in water/methanol mixture as per standard reaction conditions for 0.5 h. Catalyst was then dried and re-used in reaction using standard reaction conditions.

Subjecting the catalyst to 1.1MPa of 25%O_2/CO_2 with stirring at 1200 rpm, and then re-using it results in an increase in synthesis activity to 71 mol$_{H2O2}$ kg$_{cat}^{-1}$ h^{-1} and a rise in degradation activity to 90 mol$_{H2O2}$ kg$_{cat}^{-1}$ h^{-1}. Treating the 0.5wt.%Pd/TiO$_2$ with 8.5g reaction solvent for 0.5 h, without stirring and then re-using it, increases the synthesis activity similarly as in to 74 mol$_{H2O2}$ kg$_{cat}^{-1}$ h^{-1} and also an increase in degradation activity (41 mol$_{H2O2}$ kg$_{cat}^{-1}$ h^{-1}) is observed. These results show that two different factors may affect re-usability of the 0.5wt.%Pd/TiO$_2$. Subjecting the catalyst to the solvent mixture and O_2/CO_2 gas mixture results in an increase in synthesis, and degradation activity; however, once H_2 is introduced to the mixture and the synthesis reaction took place, a significant increase in degradation activity is observed.

Reduction of Pd species from Pd^{2+} to Pd^0 during the synthesis reaction, as shown by XPS (Figure 3.14), may be a crucial factor responsible for the observed increase in the degradation activity of 0.5wt.%Pd/TiO$_2$ upon re-use. To counter the formation of Pd^0, the catalyst was subjected to a range of heat treatments after initial use in the direct synthesis reaction. As shown in Table 3.9, a near-identical synthesis activity is obtained with a catalyst that was re-calcined at 200 ºC; however, the effect on degradation activity is negligible, with high rates of degradation (350 mol$_{H2O2}$ kg$_{cat}^{-1}$ h^{-1}) observed. Increasing the calcination temperature to 300 ºC results in a minor decrease in catalyst activity to 57 mol$_{H2O2}$ kg$_{cat}^{-1}$ h^{-1}; however, more importantly, after this heat-treatment degradation activity in presence of 4 wt.%H_2O_2 is completely inhibited. With a further increase in calcination temperature, no degradation activity is observed, but significant decrease in synthesis activity (16 mol_{H2O2} kg_{cat}^{-1} h^{-1}) is obtained.

Table 3.9: Re-calcination of 0.5wt.%Pd/TiO_2 catalyst after use in standard reaction conditions.

0.5 wt.%Pd/TiO_2	**Productivity [mol_{H2O2} kg_{cat}^{-1} h^{-1}]**	**Degradation [mol_{H2O2} kg_{cat}^{-1} h^{-1}]**
1st use	65	0
2nd use [a]	61	331
2nd use, re-calcined at 200°C	64	350
2nd use, re-calcined at 300°C	57	0
2nd use, re-calcined at 400°C	16	0

Reaction conditions: a) Synthesis reaction: 0.01 g catalyst, 2.9 g of water, 5.6 g of methanol, 2.9 MPa 5% H_2/CO_2, 1.1 MPa 25% O_2/CO_2, 0.5 h, ambient temperature, 1200 rpm **b) Degradation reaction:** 0.01 g catalyst, 0.68 g H_2O_2, 2.22 g of water, 5.6 g of methanol, 2.9 MPa 5% H_2/CO_2, 1.1 MPa 25% O_2/CO_2, 0.5 h, ambient temperature, 1200 rpm.

[a] Standard reaction conditions were applied during initial testing. Catalyst was then dried and re-used in the reaction using standard reaction conditions.

As shown in Figure 3.22, a decrease in H_2 conversion from 53% to 42% and a corresponding increase in H_2 selectivity from 22% to 29% is observed when then catalyst was re-used after drying under vacuum at 25°C. After the catalyst was re-calcined at 200°C, an increase in H_2 conversion up to 57%, with selectivity being 22% ,as with the used fresh catalyst (1st use). Higher H_2 conversion can be attributed to slightly higher degradation activity of re-calcined catalyst at 200°C as shown in Table 3.9. An increase in the re-calcination temperature to 300°C results in a decrease in H_2 conversion and an increase in H_2 selectivity to 26%. The lowest H_2 conversion (38%) and H_2 selectivity is observed after 0.5 wt.% Pd/TiO_2 was re-calcined at 400 °C. XPS analysis was carried out to investigate the effect of re-calcination on Pd oxidation state and the results are summarised in Table 3.10. After initial use of the catalyst in the synthesis reaction (catalyst was dried after reaction, prior to analysis), a reduction of Pd from Pd^{2+} to Pd^0 is observed, with only 13% of surface Pd is observed in Pd^{2+} form. After re-calcination of the catalyst, an increase in Pd^{2+} content is observed with increasing temperature; when the re-calcination temperature was 400°C, all surface Pd was present in Pd^{2+} form.

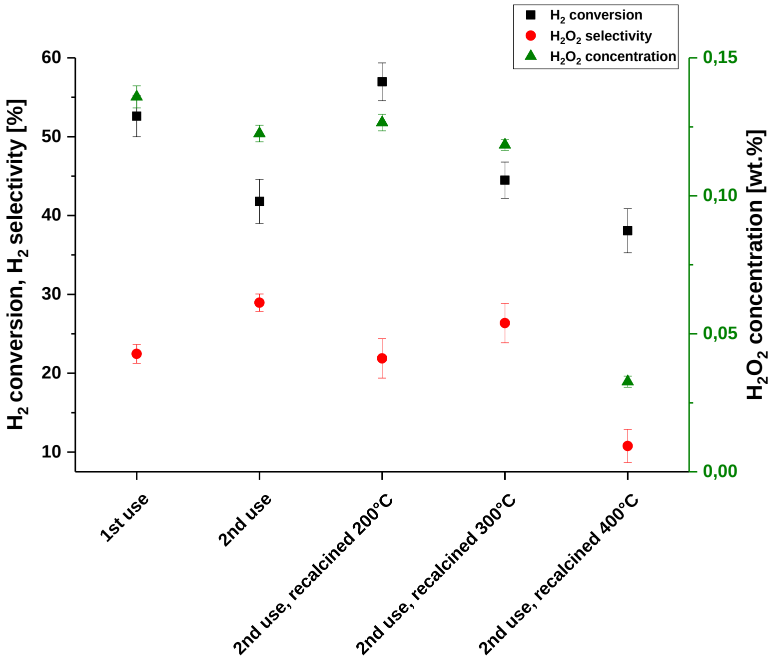

Figure 3.22: **Conversion and selectivity of the reused 0.5wt.% H_2O_2 with different re-calcination temperatures. Reaction conditions:** 0.01 g catalyst, 2.9 g of water, 5.6 g of methanol 2.9 MPa 5% H_2/CO_2, 1.1 MPa 25% O_2/CO_2, 0.5 h, ambient temperature, 1200 rpm.

Table 3.10: Quantified XPS data for the surface Pd atoms.

0.5 wt.%Pd/TiO_2	Concentration [%]	
	Pd^{2+}	Pd^0
Fresh	100	0
1st use (standard rection condition)	13.3	86.7
2nd use, re-calcined at 200°C	24.1	75.9
2nd use, re-calcined at 300°C	82.9	17.1
2nd use, re-calcined at 400°C	100.0	0

TEM images of the fresh catalyst (Figure 3.6) show no visible particles. TEM images of re-calcined catalysts (Figure 3.23) at 200 °C and 300 °C show mean particle diameter of 5.2 nm and 4.7 nm, with both catalysts showing a wide range in particle diameter from smaller particles (up to 3 nm) to larger nanoparticles of 10 nm. Catalysts re-calcined at 400°C show slightly higher mean particle diameter of 6.6 nm, with particles up to 13 nm. In comparison, 0.5wt.%Pd/TiO_2 used in standard reaction conditions after 20 min shows mean particle diameter of 5.8 nm. This shows that there was no significant particle agglomeration upon re-calcination of catalyst. Upon the re-use, an increase in degradation activity is observed, up to 331 mol_{H2O2} kg_{cat}^{-1} h^{-1} in presence of 4 wt.% H_2O_2. However, no degradation activity is observed upon re-use of the recalcined catalyst at 300 °C and 400 °C, with similar mean particle diameter as the used catalyst without recalcination. These results imply that larger Pd nanoparticles can exhibit no degradation activity towards H_2O_2 in presence of 4 wt.% H_2O_2 if the majority of Pd species is present as Pd^{2+}..

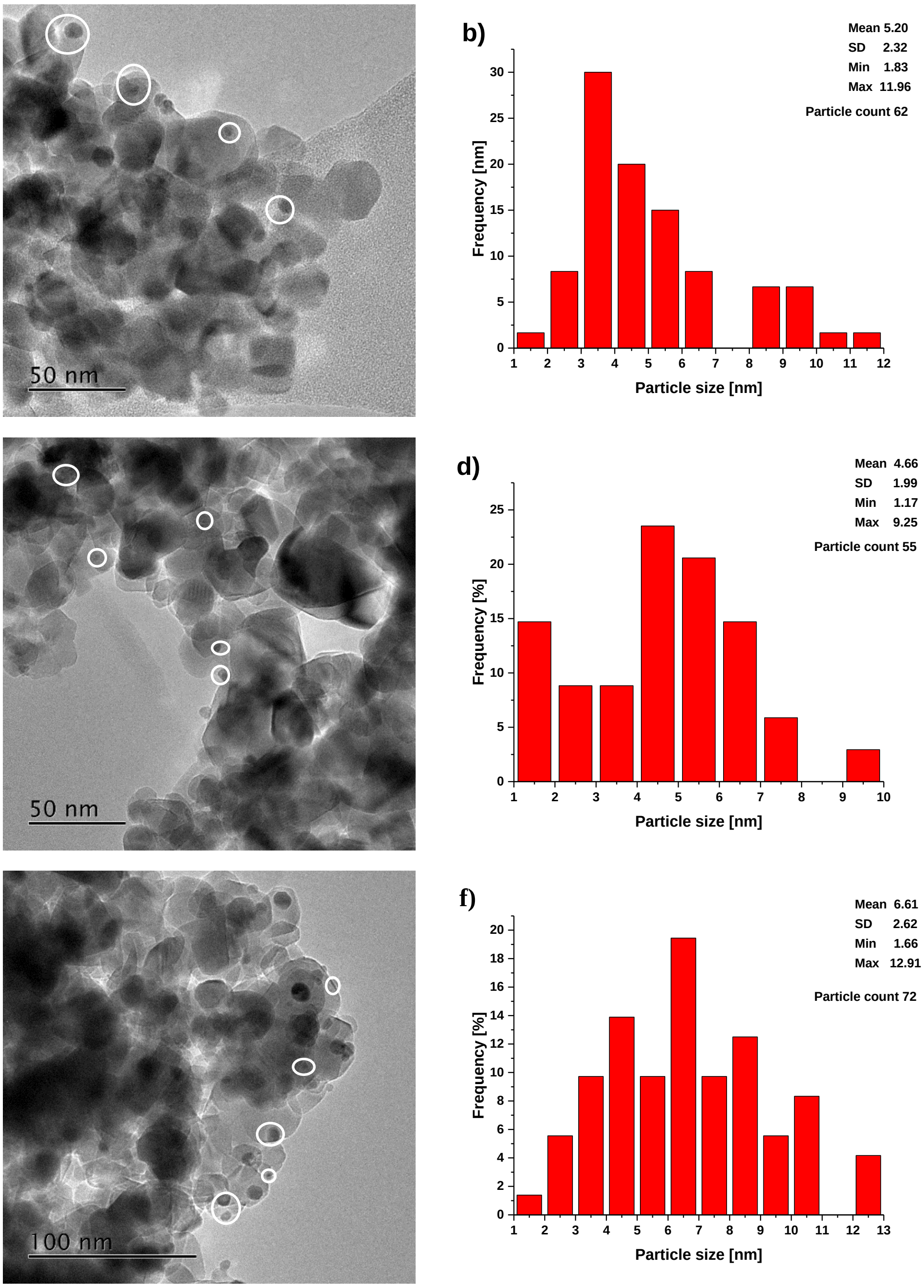

Figure 3.23: TEM images of used 0.5 wt.%Pd/TiO_2 catalyst recalcined at: a) 200 °C, c) 300 °C and e) 400 °C and particle diamter distribution of used 0.5 wt.%Pd/TiO_2 catalyst recalcined at: b) 200 °C, d) 300 °C and f) 400 °C.

These results show that the treatment of the catalyst prior to a reaction can have a significant effect on its performance and, with the right treatment, there was option to improve the synthesis activity the original activity of the catalyst can be retained.

3.2.6 Effect of calcination temperature on the activity of 0.5wt.%Pd/TiO_2 towards H_2O_2 synthesis and its subsequent degradation.

The heat treatment plays a crucial role in catalyst activity and stability. Edwards *et al.* reported, that catalysts initially calcined at temperatures lower than 400 °C are much more active than catalyst calcined at 400 °C when used for the first time.[22] However, on subsequent re-use, catalysts calcined at temperatures below 400 °C were much less active, due to loss of active metal species. Catalysts calcined at 400 °C were stable and showed no detectable leaching of metals.[71] Different calcination temperatures were applied to investigate the effect of the heat treatment on catalyst activity. As shown in Table 3.11, calcination temperature has a significant effect on catalyst performance. Calcination of the catalyst at 200 ºC results in synthesis activity of 89 mol_{H2O2} kg_{cat}^{-1} h^{-1}; however, a degradation activity of 146 mol_{H2O2} kg_{cat}^{-1} h^{-1} is obtained. This is in agreement with observations made by Edwards *et al.*, that lower calcination temperatures result in higher synthesis and degradation activity over a AuPd catalyst supported on acid pre-treated carbon.[22] Increasing the calcination temperature to 400 ºC decreases the degradation activity of a 0.5 wt.%Pd/TiO_2 catalyst to 0 mol_{H2O2} kg_{cat}^{-1} h^{-1} and decreased both H_2 conversion and selectivity towards H_2O_2. The decrease in selectivity could be mainly attributed to lower synthesis activity compared to the catalyst calcined at 200 °C, suggesting that both catalysts have similar degradation activity.

As shown in Table 3.11, a calcination temperature of 400 °C is required to prevent any H_2O_2 degradation activity and applying heat treatments with higher temperatures only result in a decrease in the synthesis activity. A dramatic decrease in H_2 conversion and increase in H_2O_2 selectivity is observed with increasing calcination temperature, with conversion only 0.9% and selectivity of 99.3% when catalyst was calcined at 800 ºC; however, minimal synthesis activity of 5 mol_{H2O2} kg_{cat}^{-1} h^{-1} is observed with this catalyst. Choudhary and co-workers reported that the H_2O_2 formation was strongly influenced by the calcination temperature, depending on Pd metal loading.[13] For catalysts with Pd metal loadings below 2.5wt.%, an increase in calcination temperature resulted in a decrease in synthesis activity and selectivity. A decrease in synthesis activity from 11 mol_{H2O2} kg_{cat}^{-1} h^{-1} to 7 mol_{H2O2} kg_{cat}^{-1} h^{-1} and selectivity of 30% to 20% was reported when calcination temperature increased from 400 ºC to 800 ºC. An increase in H_2O_2 degradation activity was observed by Choudhary *et al.* with increasing calcination temperature over 0.5wt.%Pd/Al_2O_3.[13]

Table 3.11: Effect of calcination temperature on the activity of 0.5wt.%Pd/TiO$_2$ towards H$_2$O$_2$ synthesis and its subsequent degradation.

Calcination temperature [°C]	Productivity [mol_{H2O2} kg_{cat}^{-1} h^{-1}]	Degradation [mol_{H2O2} kg_{cat}^{-1} h^{-1}]	Conversion [%]	Selectivity [%]
200	89	146	63.9	28.2
400	65	0	52.6	22.5
600	8	0	10.8	30.2
800	5	0	0.9	99.3

Reaction conditions: a) H_2O_2 synthesis: 0.01 g catalyst, 2.9 g of water, 5.6 g of methanol 2.9 MPa 5% H_2/CO_2, 1.1 MPa 25 %O_2/CO_2, 0.5 h, ambient temperature, 1200 rpm. **b) H_2O_2 degradation:** 0.01 g catalyst, 0.68 g H_2O_2, 2.9 of water, 5.6 g of methanol 2.9 MPa 5% H_2/CO_2, 0.5 h, ambient temperature, 1200 rpm.

ICP-MS analysis of post-reaction solutions, summarized in Table 3.12, shows no significant leaching of Pd after use of the 0.5wt.%Pd/TiO$_2$ catalyst, regardless of calcination temperature utilized. The highest leaching (0.3 % of total 0.5wt.% Pd, 17.8 ppb) is observed with the lowest calcination temperature. An increase in calcination temperature results in more stable catalyst and no leaching is observed when the catalyst was calcined at 400 °C. It was previously shown that homogeneous Pd can have catalytic activity, and therefore the may explain the higher degradation activity of catalyst calcined at 200 °C, due to higher amount of leached Pd.[43]

Table 3.12: The effect of calcination temperature on the leaching of Pd from 0.5wt.%Pd/TiO$_2$ during H$_2$O$_2$ synthesis.

Calcination temperature [°C]	Pd leached [%]	Pd leached [ppb]
200	0.3	17.82
400	0.24	13.84
600	0.04	2.38
800	0	0

Reaction conditions: 0.01 g catalyst, 2.9 g of water, 5.6 g of methanol 2.9 MPa 5% H_2/CO_2, 1.1 MPa 25% O_2/CO_2, 0.5 h, ambient temperature, 1200 rpm.

As previously shown, TEM image of 0.5wt.%Pd/TiO$_2$ calcined at 400 °C (Figure 3.24 a) shows no visible Pd particles due to good dispersion of Pd on catalyst surface, with Pd present below the detection limit of the equipment. This was confirmed by STEM-HAADF imaging in Figure 3.12. Images of the catalyst calcined at 600 °C and 800 °C show also no visible Pd particles, suggesting that due to low metal loading and good Pd dispersion particles are below detection limit of equipment. Choudhary *et al.*[13] and Tian *et al.*[18] both reported an increase in particle size with increasing calcination temperature, however this was observed with higher Pd metal loadings than 0.5wt.%. In comparison, Edwards *et al.* observed that calcination appeared to increase the metal dispersion with AuPd catalyst supported on C, and aid in dispersing the sub-nm clusters into dispersed atomical species.[22]

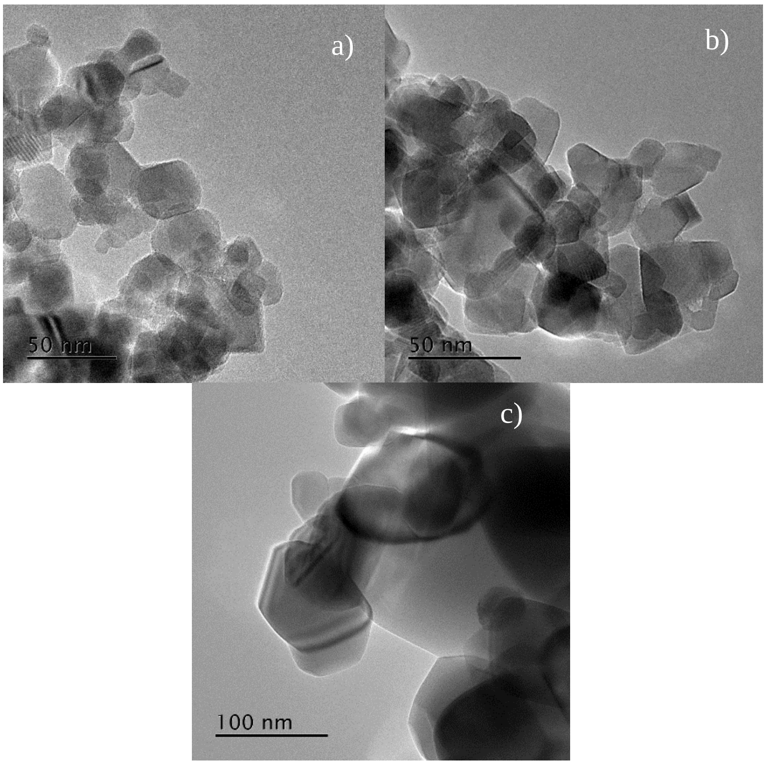

Figure 3.24: TEM images of fresh monometallic Pd catalysts with different calcination temperatures: a) 400 ºC; b) 600 ºC and c) 800 ºC

Tian *et al.* reported that catalysts consisting of monodispersed Pd atoms were inactive towards H_2O_2 synthesis and sub-nm particles are responsible for H_2O_2 formation.[18] Increased dispersion of Pd with increasing calcination temperature could therefore explain a decrease in synthesis activity observed in Table 3.10.

3.2.7 Effect of HCl concentration on catalytic activity 0.5wt.%Pd/TiO_2 towards the direct synthesis and subsequent degradation of H_2O_2.

Inorganic acids and halides are commonly used as additives in direct synthesis of H_2O_2.[24,72,73] The addition of halides, mainly Cl^- and Br^-, to the solvent or catalyst support can significantly increase selectivity of the catalyst. This increase in selectivity in the presence of halides is due to inhibiting hydrogenation of H_2O_2 by changing the catalyst surface charge and by poisoning the active sides of the catalyst on which dissociation of O_2 occurs, which leads to formation of H_2O.[5,15] Increasing the concentration of halides leads to greater dissolution of metal from support and therefore reduces longevity and reusability of the catalyst.[15] Acids have been proposed to inhibit the decomposition of H_2O_2 by preventing its deprotonation to more reactive forms (e.g., OOH^-).[15,74] Lunsford *et al.* proposed a catalytic cycle for H_2O_2 formation in acidified H_2O in which proton-electron transfer pathways are responsible for H_2O_2 formation.[75] The role of protons derived from acids are often described as promoters modifying reactivity of the Pd surface but are not participating directly in H_2O_2 formation.[45] Recently, Flaherty and co-workers reported that protic solvents participate directly in the proton transfer process and therefore in formation of H_2O_2.[15]

Typically, $PdCl_2$ has been used for preparation of the catalyst reported in this work. Small amounts of HCl were added ($4x10^{-2}$ M) into $PdCl_2$ solution to help dissolve and stabilize the metal precursor. The effects of chlorine concentration were next examined by adding aqueous solution of HCl to the solvent mixture when utilising $Pd(NO_3)_2$ as the Pd precursor. As shown in Table 3.13, no degradation activity of H_2O_2 (4wt.%) is observed when $Pd(NO_3)_2$ was used as the precursor, in the presence or absence of HCl (4.2 – 21 $x10^{-2}$ M). This indicates that the inhibition of H_2O_2 degradation, at relatively high concentrations, is not dependant on the choice of Pd precursor. An initial synthesis activity towards H_2O_2 of 0.5wt.%Pd/TiO_2 prepared using $Pd(NO_3)_2$ as a precursor in the absence of HCl is observed to be 46 mol_{H2O2} kg_{cat}^{-1} h^{-1}. Increasing HCl concentrations to $8.4x10^{-2}$ M in the solvent mixture resulted in an increase in catalyst synthesis activity to a maximum of 81mol_{H2O2} kg_{cat}^{-1} h^{-1}, with a corresponding decrease in H_2 conversion and increase in selectivity towards H_2O_2.This observation can be attributed to the blocking of active sites of the catalyst responsible for H_2O_2 degradation, and a subsequent rise in H_2 conversion due to lower degradation activity.

Increasing HCl concentration beyond $8.4x10^{-2}$ M results in significant increase in H_2 conversion (63.9%) and a drop in H_2O_2 selectivity to 25%. This suggest that addition of HCl at a concentration higher than 8.4 $x10^{-2}$ M results in an increase in H_2O_2 degradation compared to lower HCl concentration, considering that the drop in H_2 selectivity was observed despite the higher synthesis activity. This can be related to higher Pd leaching from the catalyst, as shown in Table 3.14. Unsupported Pd particles are active for synthesis of H_2O_2, which can explain why an increase in productivity of the catalyst was observed with higher Pd leaching.[57] Similar observation was made by Choudhary *et al.* who showed that selectivity and yield pass through the maximum with increasing concentration of the acid over Pd/Al_2O_3, and decreased with increasing concentration of acid due to significant leaching of Pd.[12] It should be noted that the synthesis activity of the catalyst utilizing $Pd(NO_3)_2$ as precursor was lower than the analogous catalyst utilising $PdCl_2$ even with addition of higher concentrations of HCl. A catalytic synthesis activity of 66 mol_{H2O2} kg_{cat}^{-1} h^{-1} was obtained with addition of $6.3x10^{-2}$ M HCl to the $Pd(NO_3)_2$ catalyst, while same synthesis activity was obtained over analogous catalyst using $PdCl_2$ as precursor with only $4x10^{-2}$ M HCl present. The observed increase in synthesis activity can be attributed to the presence of Cl^- anions, which may selectively poison active sites responsible for H_2O_2 hydrogenation, and also the presence of protons participating in proton-electron transfer.

Table 3.13: Effect of HCl concentration on catalytic activity 0.5wt.%Pd/TiO_2 towards the direct synthesis and subsequent degradation of H_2O_2.

Molarity of HCl solution [M]	**Productivity [$mol_{H2O2}\ kg_{cat}^{-1}\ h^{-1}$]**	**Degradation [$mol_{H2O2}\ kg_{cat}^{-1}\ h^{-1}$]**	**Conversion [%]**	**Selectivity [%]**
none	46	0	55.3	17.8
$4.2x10^{-2}$	55	0	54.4	20.3
$6.3x10^{-2}$	66	0	46.6	26.4
$8.4x10^{-2}$	67	0	44.8	29.8
$21x10^{-2}$	81	10	63.9	25.0
$PdCl_2$ as precursor	65	0	52.6	22.5

Reaction conditions: a) H_2O_2 synthesis: 0.01 g catalyst, 2.9 g of water, 5.6 g of methanol 2.9 MPa 5% H_2/CO_2, 1.1 MPa 25% O_2/CO_2, 0.5 h, ambient temperature, 1200 rpm. **b) H_2O_2 degradation:** 0.01 g catalyst, 0.68 g H_2O_2, 2.9 of water, 5.6 g of methanol 2.9 MPa 5% H_2/CO_2, 0.5 h, ambient temperature, 1200 rpm.

Table 3.14: The effect of HCl concentration on the leaching of Pd from 0.5wt.%Pd/TiO_2 during H_2O_2 synthesis.

Molarity of HCl solution [M]	**Pd leached [%]**	**Pd leached [ppb]**
none	0.28	16.15
$4.2x10^{-2}$	0.29	16.90
$6.3x10^{-2}$	0.33	19.05
$8.4x10^{-2}$	0.37	21.52
$21x10^{-2}$	0.76	43.82
$PdCl_2$ as precursor	0.24	13.84

Reaction conditions: 0.01 g catalyst, 2.9 g of water, 5.6 g of methanol 2.9 MPa 5% H_2/CO_2, 1.1 MPa 25% O_2/CO_2, 0.5 h, ambient temperature, 1200 rpm.

3.2.8 Effect of TiO_2 phase on activity of 0.5wt.%Pd/TiO_2 towards H_2O_2 synthesis and degradation.

Different phases of TiO_2 were used as a support for the 0.5wt.%Pd/TiO_2 catalysts prepared by a wet impregnation methodology and tested for the direct synthesis of H_2O_2, to investigate the effect of metal-support-interaction on catalyst synthesis and degradation activity towards H_2O_2. As shown in Table 3.15, both anatase and rutile supported catalysts show higher activity towards H_2O_2 synthesis than TiO_2 (P25) (70% anatase, 30% rutile). No degradation activity is observed when P25, anatase or rutile were used as a support. Both anatase and rutile are less affected by catalyst aging compared to the P25 analogue. The H_2O_2 synthesis activities for both catalysts are observed to be stable, in excess of 80 $mol_{H2O2}\ kg_{cat}^{-1}\ h^{-1}$ after 3 months since catalyst preparation, in comparison to the TiO_2 (P25) supported catalyst. In addition, no degradation activity is observed over the analogous anatase or rutile supported materials, even after extended storage periods. Han *et al.* reported that electron-deficient species are dominantly observed on rutile, resulting in higher synthesis activity and selectivity of Pd supported catalyst compared to anatase used as support.[20]

Table 3.15: Activity of Pd catalysts at ambient temperature made by wet impregnation using different supports.

	Fresh		**Tested after 90 days**	
TiO_2 phase	**Productivity** [$mol_{H2O2}\ kg_{cat}^{-1}\ h^{-1}$]	**Degradation** [$mol_{H2O2}\ kg_{cat}^{-1}\ h^{-1}$]	**Productivity** [$mol_{H2O2}\ kg_{cat}^{-1}\ h^{-1}$]	**Degradation** [$mol_{H2O2}\ kg_{cat}^{-1}\ h^{-1}$]
P25	65	0	70	97
Anatase	84	0	83	0
Rutile	94	0	105	0

Reaction conditions: a) H_2O_2 synthesis: 0.01 g catalyst, 2.9 g of water, 5.6 g of methanol 2.9 MPa 5% H_2/CO_2, 1.1 MPa 25% O_2/CO_2, 0.5 h, ambient temperature, 1200 rpm. **b) H_2O_2 degradation:** 0.01 g catalyst, 0.68 g H_2O_2, 2.9 g of water, 5.6 g of methanol 2.9 MPa 5% H_2/CO_2, 0.5 h, ambient temperature, 1200 rpm.

XPS analysis (Table 3.16) revealed that fresh 0.5wt.%Pd/anatase catalyst contains 97.3% of surface Pd in the form Pd^{2+}, and only 2.7% is present as Pd^0. The Pd^{2+}:Pd^0 ratio remained the same after aging the catalyst for three months. After use in the H_2O_2 synthesis reaction, reduction of Pd^{2+} to Pd^0 is observed, with only 45.3% of Pd presented as Pd^{2+}. The fresh 0.5wt.%Pd/rutile catalyst has almost all surface Pd (99.1%) present as Pd^{2+} and remain unchanged with catalyst age. Partial reduction of Pd species is observed after synthesis reaction, with 51.8% of Pd present as Pd^{2+}. Both 0.5 wt.%Pd/anatase and 0.5 wt.%Pd/rutile catalyst retained higher concentration of Pd^{2+} after synthesis reaction than 0.5 wt.%Pd/TiO_2.

Table 3.16: Quantified XPS data for the surface Pd atoms.

	Concentration [%]	
	Pd^{2+}	**Pd^0**
0.5 wt.%Pd/TiO_2		
Fresh	100	0
Aged	100	0
Used	13.3	86.7

0.5 wt.%Pd/anatase		
Fresh	97.3	2.7
Aged	96.2	3.8
Used	45.3	54.7
0.5 wt.%Pd/rutile		
Fresh	99.1	0.9
Aged	99.0	1.0
Used	51.8	48.2

X-Ray Absorption Near Edge Structure (XANES) and Extended X-Ray Absorption Fine Structure (EXAFS) spectroscopy were carried out to investigate the structure and the oxidation state of the 0.5wt.%Pd/anatase and 0.5wt.%Pd/rutile catalysts. XANES of the Pd K edge shows that both fresh catalysts have higher oxidation states than the used samples. Fresh catalysts are very likely to contain Pd^{2+} and used catalysts comprise a mixture of Pd^{2+} and Pd^0. This shows change in oxidation state of Pd during reaction, which was in keeping with the analysis by XPS, and can affect the reusability of the catalyst and lead to the increase in H_2O_2 degradation activity upon re-use. Linear combination fitting (LCF) suggests that the Pd species identified on fresh catalysts are PdO and $PdCl_2$ with contribution of 1/3 from $PdCl_2$ and 2/3 of PdO. Used 0.5wt.%Pd/anatase shows contributions of 52% from PdO and 48% from Pd^0, while used 0.5wt.%Pd/rutile catalyst showed slightly higher contribution from PdO of 57% and 43% from Pd^0, which is in agreement with the XPS analysis.

The EXAFS fitting results of fresh 0.5wt.%Pd/anatase and 0.5wt.%Pd/rutile catalysts show both Pd-O and Pd-Cl scattering in the first shell coordination, which is similar to 0.5 wt.%Pd/TiO_2 catalyst. The coordination numbers for Pd-O and Pd-Cl are 3.4 and 0.6 for 0.5wt.%Pd/anatase catalyst and 3.1 and 0.9 for 0.5wt.%Pd/rutile catalyst, respectively. The bond length for these two scattering paths is very similar to the Pd-O in PdO, at 2.01 Å, and Pd-Cl in $PdCl_2$, at 2.31 Å. The EXAFS fitting results of used 0.5wt.%Pd/anatase and 0.5wt.%Pd/rutile catalysts confirm that these two catalysts are partially oxidized Pd nanoparticles distributed on the support. The first shell coordination of Pd-O and Pd-Pd scattering path match well with Pd-O in PdO and Pd-Pd in Pd^0. The coordination number of each scattering path is much smaller than bulk PdO and Pd foil, indicating the nanosized nature of the Pd species. As summarised in Table 3.17, there is no measurable Pd-Pd bond for fresh 0.5wt.%Pd/anatase and 0.5wt.%Pd/rutile catalysts. For anatase catalysts, there is existing Pd-O bond of 2.02 ± 0.02 Å and Pd-Cl bond of 2.3 ± 0.02 Å. The same bonds are existing on rutile catalyst, with a slight increase in the Pd-O bond length to 2.03 ± 0.03 Å. The coordination number of Pd-O is around 3.4 ± 0.3 and the Pd-Cl is less than 0.6 ± 0.3 in the anatase supported catalyst. The catalyst supported on rutile shows a higher Pd-Cl coordination number of 0.9 ± 0.3. For the used anatase supported catalyst, a Pd-O bond of 1.99 ± 0.02 Å with a CN 1.9 ± 0.5 is determined, while the used rutile catalyst exhibits a Pd-O bond of 2.01 ± 0.02 Å with a CN 2.8 ± 0.8. The Pd-Pd bond of 2.75 ± 0.01 Å is the same as the Pd-Pd distance in Pd foil for both used catalysts. The catalyst supported on rutile showslower Pd-Pd CN (3.4 ± 0.9) compared to used anatase catalyst CN (5 ± 0.7).

Table 3.17: Tabulated Pd-Pd, Pd-Cl and Pd-O coordination numbers (N), bond distances (R), bond length disorder (σ^2), and threshold energy corrections (ΔE_0) for Pd nanoparticles on fresh and used catalyst supported on anatase and rutile.

sample	Pd-O		Pd-Cl		Pd-Pd		σ^2	σ^2	σ^2	ΔE_o
	R [Ȧ]	CN	R [Ȧ]	CN	R [Ȧ]	CN	Pd-O	Pd-Cl	Pd-Pd	[eV]
PdO	2.01	4			-	-	-	-	-	-
$PdCl_2$	-	-	2.31	4	-	-	-	-	-	-
Pd foil	-	-	-	-	2.75	12	-	-	-	-
0.5wt.%Pd/anatase										
fresh	2.02(2)	3.4(3)	2.3(2)	0.6(3)	-	-	0.003(1)	0.003 (1)	-	-0.6(2.5)
used	1.99(1)	1.9(5)	-	-	2.75 (1)	5(7)	0.003(2)	-	0.006(1)	1.9(0.5)
0.5wt.%Pd/rutile										
fresh	2.03(3)	3.1(3)	2.3(2)	0.9(3)	-	-	0.003(1)	0.003(1)		-0.7(2.3)
used	2.01(1)	2.8(8)	-	-	2.75(1)	3.4(9)	0.003(1)	0.005(1)	-	-2.9(1.4)

The number in parentheses indicates the statistical error: error for *R* is in two decimal places (e.g., 2.0 (1) ≡ 2.0 ± 0.01); error for CN is in one decimal place (e.g., 3.2 (2) ≡ 2.0 ± 0.2); error for σ^2 is in three decimal places (e.g., 0.003 (1) ≡ 0.003 ± 0.001); error for ΔE_o is as stated in parentheses (e.g., -0.9 (2.1) ≡ -0.9 ± 2.1)

Acknowledgment: The EXAFS characterisation was carried out by Dr Wang and his research team. We acknowledge the Diamond Light Source B18 beamline for the experiment sessions (SP17377, SP19072 and SP19850).

Both anatase and rutile supported catalysts show slightly higher levels of Pd leaching compared to the catalyst prepared on P25, after use in H_2O_2 synthesis reaction (Table 3.18). However, the amount of leached Pd is below 0.5% of the total Pd meatal loading for both catalysts.

Table 3.18: Total Pd leaching, as determined via ICP-MS, from 0.5wt.%Pd catalysts supported on different TiO_2 phases, during H_2O_2 synthesis reaction.

TiO_2 phase	**Pd leached [%]**	**Pd leached [ppb]**
P25	0.24	13.84
anatase	0.39	22.74
rutile	0.45	26.24

Reaction conditions: 0.01 g catalyst, 2.9 g of water, 5.6 g of methanol 2.9 MPa 5% H_2/CO_2, 1.1 MPa 25% O_2/CO_2, 0.5 h, ambient temperature, 1200 rpm.

Reusability of the catalysts was next investigated, with the used catalysts collected after use in a H_2O_2 synthesis reaction and the catalysts were dried under vacuum with the results summarised in Table 3.19. Re-use of the 0.5wt.%Pd/TiO_2 catalysts supported on P25 and rutile TiO_2 phases show no significant change in catalytic activity towards H_2O_2 synthesis, while the analogous catalyst supported on anatase TiO_2 shows a significant loss in synthesis activity, which cannot be explain by either metal leaching or increased degradation. Interestingly, catalytic activity of all catalysts towards H_2O_2 degradation drastically increased. This increase in degradation activity can be explained by partial reduction of Pd species, as shown by XPS analysis shown in Table 3.16. Increase in Pd-Pd CN of the used catalysts indicates an increase in Pd particle diameter from single atoms to highly dispersed Pd nanoclusters, which might also contribute to increased degradation activity upon re-use.

Table 3.19: Re-usability study over monometallic Pd catalysts at ambient temperature made by wet impregnation using different supports.

Catalyst	Productivity [mol_{H2O2} kg_{cat}^{-1} h^{-1}]		Degradation [mol_{H2O2} kg_{cat}^{-1} h^{-1}]	
	Fresh	**used**	**fresh**	**Used**
0.5 wt.%Pd/TiO_2 (P25)	65	61	0	321
0.5 wt.%Pd/anatase	84	42	0	135
0.5 wt.%Pd/rutile	94	90	0	257

Reaction conditions: a) H_2O_2 synthesis: 0.01 g catalyst, 2.9 g of water, 5.6 g of methanol 2.9 MPa 5% H_2/CO_2, 1.1 MPa 25% O_2/CO_2, 0.5 h, ambient temperature, 1200 rpm. **b) H_2O_2 degradation:** 0.01g catalyst, 0.68 g H_2O_2, 2.9 g of water, 5.6 g of methanol 2.9 MPa 5% H_2/CO_2, 0.5 h, ambient temperature, 1200 rpm.

3.2.9 Effect of support on the catalytic activity 0.5wt.%Pd towards H_2O_2 synthesis and degradation.

It has previously been shown that the nature of the support can significantly effect catalyst activity and selectivity.[4,12,13] The performance of the supported catalyst is generally governed by several factors, including metal particle size, shape, morphology, the dispersion of the metal particles, and the electronic state of the support.[37] It has been previously reported that the support can effect the electronic structure of the metal particles.[12] Hutchings and co-workers have previously reported a correlation between the activity of the catalyst and isoelectric points of the supports, with more acidic supports shown to aid in H_2O_2 stabilisation.[4] Different metal oxides were next used as supports to investigate the effects on catalyst activity. Prior to catalyst testing, all the bare supports were tested in the synthesis and degradation reaction, and no activity towards H_2O_2 formation and degradation is observed (as summarised in Table 3.20). As shown in Table 3.21, catalysts prepared on all phases of TiO_2 show the highest productivities among the chosen supports, and also are shown to be inactive towards H_2O_2 degradation in the presence of 4 wt.% H_2O_2. These catalysts also show much higher H_2 conversions, above 52%, compared to analogues prepared on other common oxide supports. Catalyst supported on TiO_2 (P25) show lowest selectivity 22.5%, while counterparts supported on rutile show selectivity of 35.3%. The analogous catalyst prepared on SiO_2 exhibits productivity of 52 mol_{H2O2} kg_{cat}^{-1} h^{-1} and no degradation activity towards H_2O_2. Compared to catalysts supported on TiO_2, lower H_2 conversion of 22.1% and selectivity towards H_2O_2 of 52.1% s obtained.

Table 3.20: H_2O_2 synthesis and degradation testing over supports materials at ambient temperature.

Support	**Productivity[a]** **[mol_{H2O2} kg_{cat}^{-1} h^{-1}]**	**Degradation[b]** **[mol_{H2O2} kg_{cat}^{-1} h^{-1}]**
TiO_2 (P25)	0	0
anatase	0	0
rutile	0	0
SiO_2	0	0
Al_2O_3	0	0
ZrO_2	0	0

Reaction conditions: a) H_2O_2 synthesis: 0.01 g catalyst, 2.9 g of water, 5.6 g of methanol 2.9 MPa 5% H_2/CO_2, 1.1 MPa 25% O_2/CO_2, 0.5 h, ambient temperature, 1200 rpm. **b) H_2O_2 degradation**: 0.01 g catalyst, 0.68 g H_2O_2, 2.9 g of water, 5.6 g of methanol 2.9 MPa 5% H_2/CO_2, 0.5 h, ambient temperature, 1200 rpm.

Both 0.5wt.%Pd/Al_2O_3 and 0.5wt.%Pd/ZrO_2 show significantly lower productivities comparing to other catalysts, but more importantly they show increasing degradation activity towards H_2O_2 in the presence of 4wt.%H_2O_2. Lower synthesis activity and increased degradation activity of these supported catalysts can be related to the more basic nature of the support, as it was previously reported that more acidic supports can promote direct synthesis of H_2O_2 and provide much lower degradation rates.[4,76,77] When Al_2O_3 and ZrO_2 was used as supports, H_2 conversions of 11% and 10.8% are achieved, respectively. Interestingly, these catalysts showed the highest selectivities ,even when H_2O_2 degradation activity was observed in presence of 4 wt.%H_2O_2.

Table 3.21: H_2O_2 synthesis and degradation testing over 0.5wt.% Pd supported catalysts at ambient temperature made by wet impregnation using different supports.

Support	**Productivity[a]** **[mol_{H2O2} kg_{cat}^{-1} h^{-1}]**	**Degradation[b]** **[mol_{H2O2} kg_{cat}^{-1} h^{-1}]**	**Conversion** **[%]**	**Selectivity** **[%]**

TiO_2 (P25)	64	0	53	23
anatase	84	0	59	29
rutile	94	0	55	35
SiO_2	52	0	22	52
Al_2O_3	25	50	11	54
ZrO_2	37	82	11	73

Reaction conditions: a) H_2O_2 synthesis: 0.01 g catalyst, 2.9 g of water, 5.6 g of methanol 2.9 MPa 5% H_2/CO_2, 1.1 MPa 25% O_2/CO_2, 0.5 h, ambient temperature, 1200 rpm. **b) H_2O_2 degradation**: 0.01 g catalyst, 0.68 g H_2O_2, 2.9 g of water, 5.6 g of methanol 2.9 MPa 5%H_2/CO_2, 0.5 h, ambient temperature, 1200 rpm.

3.2.10 Effect of reaction time on catalyst synthesis and degradation activity of 0.5wt.%Pd/TiO_2

Reaction time has a crucial role on catalyst performance. Low reaction times may result in low concentrations of H_2O_2 and, on the other hand, degradation of H_2O_2 can be more significant at extended contact times. To investigate the effect of reaction time on catalyst performance, a time-on-line study over 0.5wt.%Pd/TiO_2 was carried out. As shown in Figure 3.25, a concentration of 0.03wt.% of H_2O_2 is produced in the first two minutes, with H_2 conversion of 5.2% and selectivity of 74.3%. An 3-fold increase in H_2O_2 concentration is observed after 5 min with a corresponding increase in H_2 conversion up to 15.6%, and a decrease in selectivity towards H_2O_2 to 45.4%. A very small increase in H_2O_2 concentration is observed between 15 and 20 min, which corresponds to a minimal increase in H_2 conversion (from 50.5 to 52.9 %).

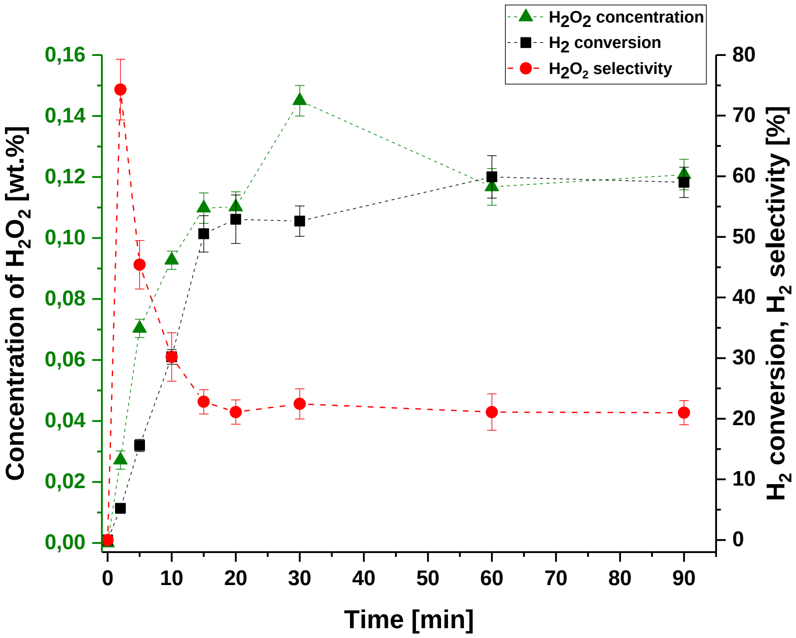

Figure 3.25: Effect of reaction time over 0.5wt.%Pd/TiO$_2$. Reaction conditions: 0.0 1g catalyst, 2.9 g of water, 5.6 g of methanol, 2.9 MPa 5% H$_2$/CO$_2$, 1.1 MPa 25% O$_2$/CO$_2$, various reaction times, ambient temperature, 1200 rpm

The concentration of H_2O_2 passes through a maximum of 0.14wt.% at 30 min. Further increase in the reaction time results in a decrease in H_2O_2 concentration to 0.12wt.% after 90 min. No significant change in H_2 conversion and selectivity is observed as the reaction time went from 60 to 90 min, indicating catalyst deactivation or insufficient concentration of reagent gases. After the reaction, the catalysts were collected and dried in vacuum oven for 16 h. Once dried, the catalysts were analysed by XPS and TEM.

XPS analysis (Table 3.22) shows that, once a catalyst is introduced into the reaction mixture with reagent gases (0 min), immediate partial reduction of Pd species from Pd^{2+} to Pd^0 is observed. The results in Table 3.22 shows that the content of Pd^{2+} species is generally decreasing between 2 and 20 min. After 30 min, the Pd^{2+} concentration decreases to 13.3%, and increases to 19.1% after 60 min, which can be attributed to increasing H_2O_2 concentration. These results suggest that Pd species are constantly in flux during reaction. It was previously reported by Choudhary *et al.* that H_2O_2 might oxidise reduced Pd species.[61]

Table 3.21: Quantified XPS data for the surface Pd atoms.

Reaction time [min]	**Concentration [%]**	
	Pd^{2+}	**Pd^0**
0	42.9	57.1
2	34.4	65.6
5	25.7	74.3
10	27.8	72.2
15	32.0	68.0
20	28.7	71.3
30	13.3	86.7
60	19.1	80.9

TEM analysis was carried out to investigate the change in particle diameter during the reaction. TEM images in Figure 3.26 show an increase in particle diameter with increasing reaction time and these results are summarised in Table 3.23. Fresh unused 0.5wt.%Pd/TiO$_2$ showed no particles on TEM images.

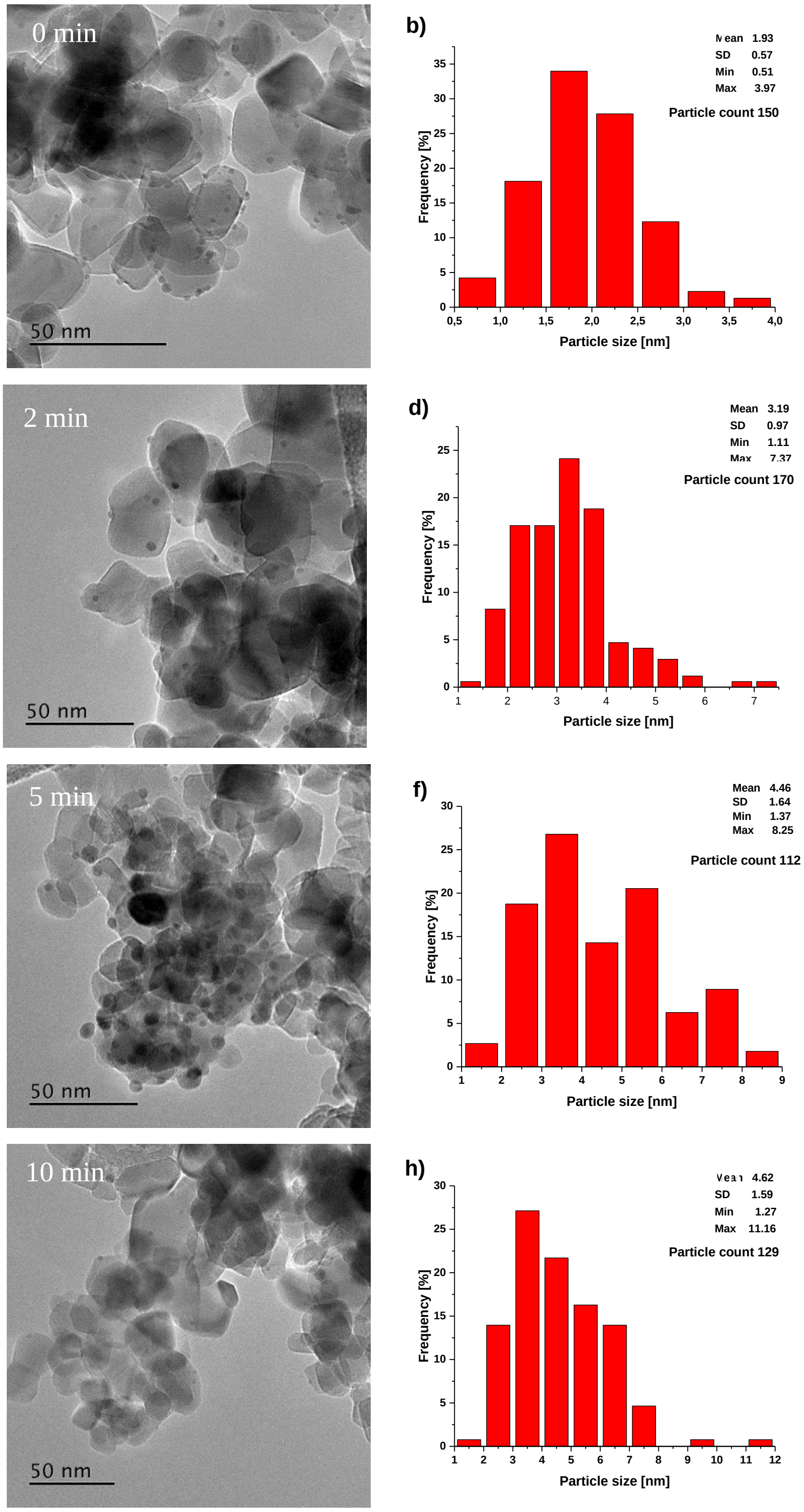
0 min
50 nm
b)
Mean 1.93
SD 0.57
Min 0.51
Max 3.97
Particle count 150
Frequency [%]
0
5
10
15
20
25
30
35
0,5
1,0
1,5
2,0
2,5
3,0
3,5
4,0
Particle size [nm]
2 min
50 nm
d)
Mean 3.19
SD 0.97
Min 1.11
Max 7.37
Particle count 170
Frequency [%]
0
5
10
15
20
25
1
2
3
4
5
6
7
Particle size [nm]
5 min
50 nm
f)
Mean 4.46
SD 1.64
Min 1.37
Max 8.25
Particle count 112
Frequency [%]
0
5
10
15
20
25
30
1
2
3
4
5
6
7
8
9
Particle size [nm]
10 min
50 nm
h)
Mean 4.62
SD 1.59
Min 1.27
Max 11.16
Particle count 129
Frequency [%]
0
5
10
15
20
25
30
1
2
3
4
5
6
7
8
9
10
11
12
Particle size [nm]

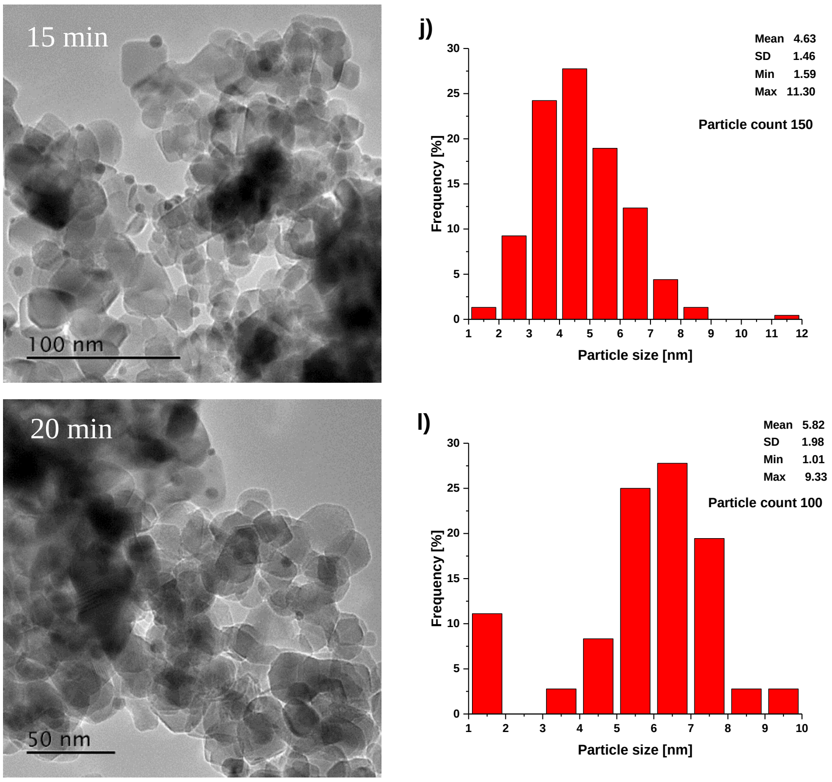

Figure 3.26: TEM images of used 0.5 wt.%Pd/TiO$_2$ at various reaction times: a) 0 min, c) 2 min, e) 5 min, g) 10 min, i) 15, k) 20 min and particle diameter distribution of used 0.5 wt.%Pd/TiO$_2$ catalyst at: b) 0 min, d) 2 min, f) 5 min, h) 10 min, j) 20 min, l) 20 min.

After 0 min (i.e. wetted and exposed to reactant gases, stirring turned on and immediately off to ensure well mixed mixture) the mean particle diameter is 1.9 nm with narrow particle diameter distribution, with more than 80% of particles below 2.5 nm. A further increase in reaction time to 2 min results in an increase in mean particle diameter to 3.2 nm, and a larger particle diameter distribution as shown in Figure 3.26 d). The mean particle diameter of 4.5 nm is observed after 5 min, and increases to 4.6 nm after 15 min. Particle size distribution diagrams show an increase in particle diameter with reaction time and also wider particle diameter distribution, with a small fraction of particles above 9 nm. After 20 min, the mean particle size increases to 5.8 nm, with less than 15% particles below 4 nm.

Table 3.23: Average particle diameter over 0.5wt.%Pd/TiO$_2$ upon re-use at different reaction times.

Reaction time [min]	**Average particle size [nm]**
fresh	no visible particles
0	1.9
2	3.2
5	4.5
10	4.6

15	4.6
20	5.82

Reaction conditions: a) Synthesis reaction: 0.01 g catalyst, 2.9 g of water, 5.6 g of methanol, 2.9 MPa 5% H_2/CO_2, 1.1 MPa 25% O_2/CO_2, various reaction time, ambient temperature, 1200 rpm **b) Synthesis reaction** - reuse: 0.01 g catalyst, 2.9 g of water, 5.6 g of methanol, 2.9 MPa 5% H_2/CO_2, 1.1 MPa 25%O_2/CO_2, 0.5 h, ambient temperature, 1200 rpm

Building on this work, the effect of the initial reaction time on 0.5wt.%Pd/TiO_2 was evaluated (Figure 3.27). First, the catalyst was used in an initial H_2O_2 synthesis reaction for different reaction times. Then the catalyst was removed from reaction mixture and dried under vacuum (25 ºC, 16 h). Once dried, the catalyst was re-used in a reaction using standard reaction conditions. A significant increase in catalyst synthesis activity, to 87 mol_{H2O2} $kg_{cat}^{-1}h^{-1}$, is observed after the catalyst was initially used in a 0 min reaction (i.e. wetted and exposed to reactant gases, stirring turned on and immediately off to ensure well mixed mixture). The results indicate that the catalyst is activated once subjected to reaction conditions. As shown in Table 3.22, immediate reduction of the Pd species is observed, with only 42.9 % of Pd remaining as Pd^{2+}, and an increase in mean Pd particle diameter to 1.93 nm is observed. Tian *et al.* reported that single site Pd catalysts are inactive for H_2O_2 formation, and 1.4 – 2.5 nm particles are desirable for highly selective and active catalyst.[18] It has been previously published that the H_2O_2 synthesis occurs on interfaces of Pd and PdO domains and therefore partial reduction of Pd might be beneficial to obtain higher synthesis activity.[31] A lower H_2 conversion of 42.3% is observed upon re-use after initial 0 min reaction compared to 52.6% obtained in standard reaction conditions and higher selectivity towards H_2O_2 of 39.3% is achieved over re-use, in comparison to standard reaction with selectivity of 22.5% (as shown in Figure 3.28). Up to an initial reaction time of 15 min, the enhancement in catalysts activity upon second use exceeded that observed over a standard rection (0.5 h) with no prior reaction. Interestingly, a dramatic increase in H_2O_2 degradation activity is already achieved after 0 min, suggesting that the change causing this increase in activity occurs immediately as the catalyst came into contact with the gas mixture. As shown in Figure 3.27, the highest degradation activity (441 mol_{H2O2} kg_{cat}^{-1} h^{-1}) is obtained after 0 min, and further decreases to approximately 330 mol_{H2O2} kg_{cat}^{-1} h^{-1} after 5 min. No significant change in degradation activity, in presence of 4wt.%H_2O_2, is observed with increasing reaction time in first use, and it is comparable with activity of re-used catalyst after 30 min reaction prior to catalyst re-use.

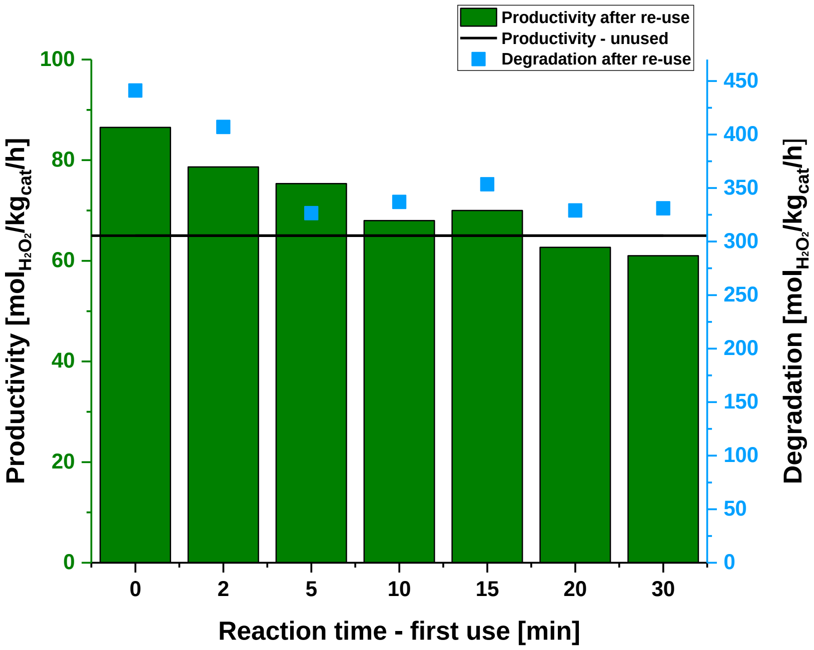

Figure 3.27: Effect of initial reaction time on catalyst re-usability over 0.5wt.%Pd/TiO2. Reaction conditions: a) Synthesis reaction: 0.01g catalyst, 2.9 g of water, 5.6 g of methanol, 2.9 MPa 5% H_2/CO_2, 1.1 MPa 25% O_2/CO_2, various reaction time, ambient temperature, 1200 rpm b) Synthesis reaction - reuse: 0.01 g catalyst, 2.9 g of water, 5.6 g of methanol, 2.9 MPa 5% H_2/CO_2, 1.1 MPa 25% O_2/CO_2, 0.5 h, ambient temperature, 1200 rpm c) Degradation reaction: 0.01 g catalyst, 0.68 g H_2O_2, 2.22 g of water, 5.6 g of methanol, 2.9 MPa 5% H_2/CO_2, 1.1 MPa 25% O_2/CO_2, 0.5 h, ambient temperature, 1200 rpm.

As shown in Figure 3.28, lower H_2 conversions are observed with the re-used catalyst, at any reaction time compared to fresh catalyst, with conversion passing through a maximum of 48.3% with first use at 15 min. Selectivities towards H_2O_2 are higher for all re-used catalyst compared to the fresh 0.5wt.%Pd/TiO_2. The highest selectivity towards H_2O_2 39.3% is achieved with re-used of a catalyst used in an initial 0 min reaction, and a further decrease in H_2 selectivity is achieved with increasing initial rection time. A decrease in selectivity correlates with increase in Pd mean particle diameter, while a similar distribution in Pd oxidation states is observed with reaction times of initial use between 2-20 min, as shown in Table 3.22. This suggest that changes in particle size, with combination of Pd oxidation state, have significant effect on catalyst activity.

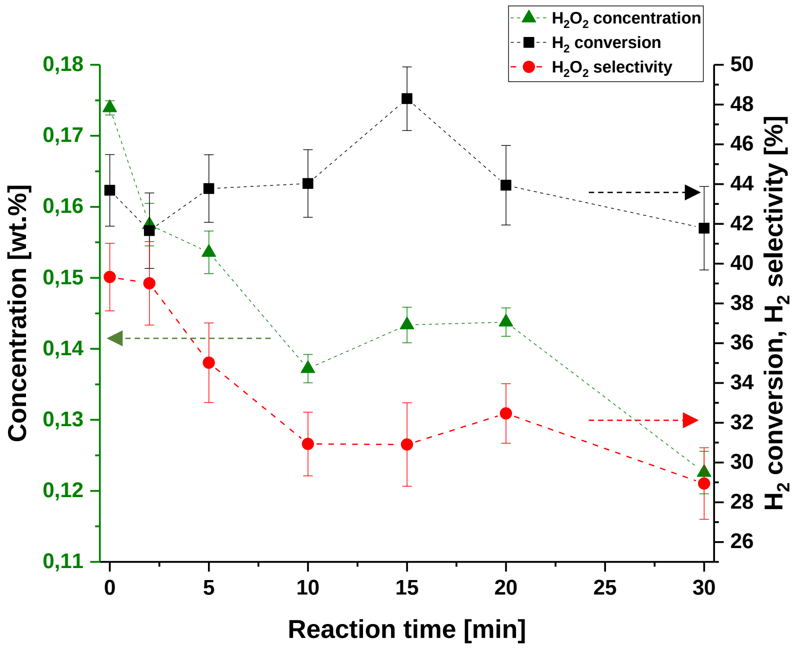

Figure 3.28: ***Effect of reaction time on catalyst re-usability over 0.5wt.%Pd/TiO2.*** **Reaction conditions: a) Synthesis reaction:** 0.01 g catalyst, 2.9 g of water, 5.6 g of methanol, 2.9 MPa 5% H_2/CO_2, 1.1 MPa 25% O_2/CO_2, various reaction time, ambient temperature, 1200 rpm **b) Synthesis reaction** - reuse: 0.01 g catalyst, 2.9 g of water, 5.6 g of methanol, 2.9 MPa 5% H_2/CO_2, 1.1 MPa 25% O_2/CO_2, 0.5 h, ambient temperature, 1200 rpm **c) Degradation reaction:** 0.01 g catalyst, 0.68 g H_2O_2, 2.22 g of water, 5.6 g of methanol, 2.9 MPa 5% H_2/CO_2, 1.1 MPa 25% O_2/CO_2, 0.5 h, ambient temperature, 1200 rpm.

3.2.11 Effect of reaction temperature on catalyst synthesis and degradation activity of 0.5wt.%Pd/TiO$_2$

To investigate the effect of low reaction temperatures on catalyst performance, a time-on-line study over 0.5wt.%Pd/TiO$_2$ was carried out at 2 °C. As shown in Figure 3.29, a concentration of 0.04wt.% of H_2O_2 is produced in the first two minutes with H_2 conversion of 9.2% and selectivity of 37.6%. In comparison with reaction carried out at ambient temperature, higher concentration of H_2O_2 is achieved. However, a significant drop in H_2 selectivity from 74.3% at ambient temperature to 37.6 %, is observed. An increase in reaction time results in an increase in H_2O_2 concentration within the whole time-online study. After 15 min, 0.1wt.% H_2O_2 is produced, and this concentration increases up to 0.18 wt.% after 30 min; concentration of 0.27 wt.% is achieved after 90 min at the end of the study. Interestingly, at ambient temperature, the maximum concentration of 0.15 wt.% is achieved after 30 min and further increases in reaction time resulting in concentration decrease. As expected, H_2 conversion increases with reaction time. However, H_2O_2 selectivity shows more interesting trend. The highest value of 37.6 was achieved during 2 min reaction and selectivity decreased to 24.1, and is slowly increasing to 30.1% up to 20 min reaction. Selectivity remains constant between

30 to 60 min at value of 36.7 %; further decrease to 32.8% is observed after 90 min. The results in Figures 3.25 and 3.29 suggest that, at ambient temperature, degradation of H_2O_2 is lower at the beginning of the reaction compared to reaction at 2 °C, but, with increasing reaction time, the synthesis of H_2O_2 is more selective at ambient temperature. Landon *et al.* was one of the first who identified low temperature and short reaction time to be a key factor that favour high selectivity to H_2O_2.[32]

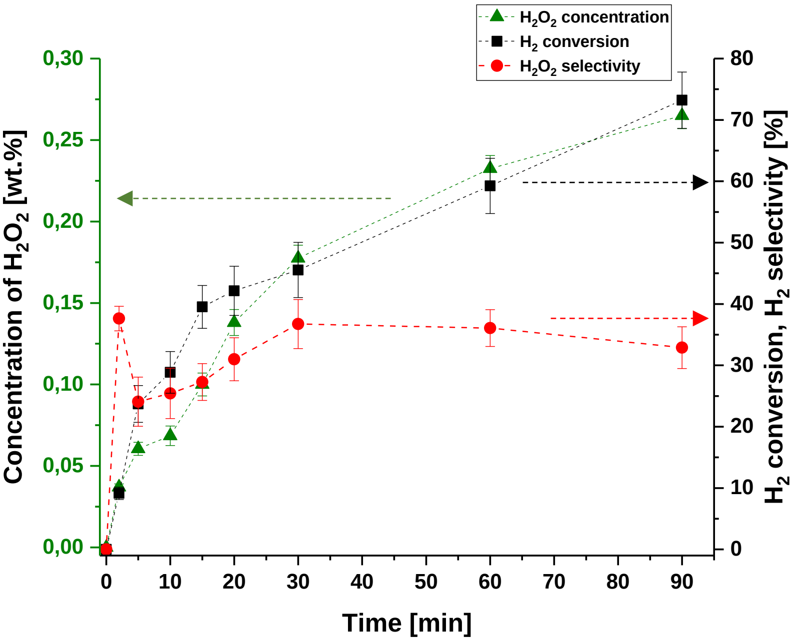

Figure 3.29: ***Effect of reaction time over 0.5wt.%Pd/TiO₂ at 2°C*.** **Reaction conditions:** 0.01 g catalyst, 2.9 g of water, 5.6 g of methanol, 2.9 MPa 5%H_2/CO_2, 1.1 MPa 25%O_2/CO_2, various reaction times, 2°C, 1200 rpm

3.2.12 Effect of gas replacement reactions on catalyst synthesis and degradation activity of 0.5wt.%Pd/TiO_2

One of the main limitations of the batch-style experimental set up is the low concentration of H_2 utilised. As shown in Section 3.2.10, no change in H_2 conversion or H_2O_2 concentration is observed at extended reaction times (beyond 60 min), suggesting deactivation of catalyst or insufficient concentration of reagent gases. Gas replacement reactions partially solve low H_2 concentration limitation by continually replacing H_2 at fixed time intervals. Gas replacement experiments were carried out to maximize the produced concentration of H_2O_2, with the results shown in Figure 3.30. After second gas replacement, a linear increase in the H_2O_2 concentration to 0.28 wt.% is achieved; less H_2O_2 was produced in a further 3 gas replacement reactions combined. After 5 gas replacement reactions, the H_2O_2 concentration is 0.38wt.%. For comparison, the H_2O_2 concentration 0.12wt.% was obtained after 60 min (same reaction time as two gas replacement reactions). No significant change in H_2O_2 concentration, H_2 conversion and H_2O_2 selectivity was observed in time on-line study (Figure 3.25) after 60 min which suggests, that this was caused by low concentration of reagent gases rather than deactivation of the catalyst as an increase in H_2O_2 concentration was observed even after 5th gas replacement (2.5 h reaction time). Freakley *et al.* at reported production of 0.35 wt.% H_2O_2 over the highly selective 2wt.%Sn-3wt.%Pd/TiO_2 subjected to sequential oxidation-reduction-oxidation (ORO) heat treatment after 3 gas replacements at 2 °C.[9] This is comparable with the concentration obtained over 0.5wt.%Pd/TiO_2 in this study, without need of high concentration of Pd and secondary metal, or requirement of extensive heat treatment cycles. This shows that high metal loadings and extensive heat treatment are not needed to achieve higher concentrations of H_2O_2, and gas replacement reactions present a possibility to significantly increase the H_2O_2 concentration in comparison to longer reaction times.

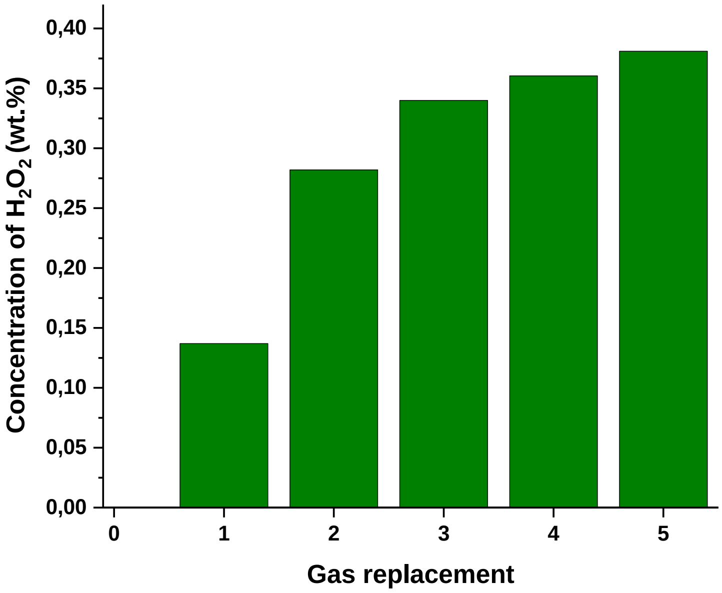

Figure 3.30: Effect of gas replacement reaction over 0.5wt.%Pd/TiO_2. Reaction conditions: 0.01 g catalyst, 2.9 g of water, 5.6 g of methanol, 2.9 MPa 5% H_2/CO_2, 1.1 MPa 25% O_2/CO_2, 0.5 h, ambient temperature, 1200 rpm

3.3 Conclusion

Within this Chapter, the role of catalyst design has been investigated to improve catalyst synthesis activity and selectivity towards H_2O_2, as well as inhibit degradation activity. The effect of the Pd metal loading on H_2O_2 synthesis and degradation activity was investigated.

The synthesis activity passed through a maximum of 65 mol_{H2O2} kg_{cat}^{-1} h^{-1} over 0.5wt.%Pd/TiO_2. More importantly, the 0.5wt.% Pd/TiO_2 catalyst showed no degradation activity towards H_2O_2 (in presence of 4 wt.% H_2O_2) in the absence of any promoters or additives and at ambient temperature.

Reaction conditions play a crucial role in catalyst performance and by optimising them an enhancement in catalyst synthesis activity and H_2O_2 selectivity, as well as decrease in H_2O_2 degradation activity, can be achieved. The effect of H_2/O_2 ratio, total pressure and solvent composition has been investigated on the synthesis and degradation activity over a 0.5 wt.%Pd/TiO_2 catalyst to determine the optimal reaction conditions and improve catalytic performance. The results showed that the optimal H_2:O_2 ratio is 1:1, which is in agreement with the reaction stoichiometry. At this optimum ratio, the productivity of the catalyst increased from 65 mol_{H2O2} kg_{cat}^{-1} h^{-1} (standard reaction condition) to 70 mol_{H2O2} kg_{cat}^{-1} h^{-1}. The effect of gas pressure was investigated using H_2:O_2 ratio 1:2. The highest activity of 75 mol_{H2O2} $kg_{cat}^{-1}h^{-1}$ was obtained at 650 psi, which was the maximum pressure that could be achieved in our reaction set-up. No degradation activity in the presence of 4 wt.% H_2O_2 was observed over the pressure range of 0 – 650 psi.

In the absence of CH_3OH, a synthesis activity of 32 mol_{H2O2} kg_{cat}^{-1} h^{-1} was achieved over 0.5 wt.%Pd/TiO_2; the introduction of CH_3OH resulted in a significant increase in H_2O_2 synthesis activity, up to 65 mol_{H2O2} $kg_{cat}^{-1}h^{-1}$ at a solvent composition of 75% CH_3OH. This can be attributed to higher solubility of H_2 and O_2 in the CH_3OH than H_2O. These results are summarised in Table 3.24 and highlight the need to consider reaction conditions in addition to catalyst design.

Table 3.24: Summary of optimal reaction conditions on synthesis activity of 0.5 wt.%Pd/TiO_2.

H_2/O_2 ratio	**Total pressure [psi]**	**CH_3OH content [%]**	**Productivity [mol_{H2O2} kg_{cat}^{-1} h^{-1}]**
1:1	580	66	70
1:2	650	66	75
1:2	580	75	67
	Standard reaction conditions		
1:2	580	66	65

Reaction conditions: a) H_2O_2 synthesis: 0.01 g catalyst, 0.5 h, ambient temperature, 1200 rpm.

STEM-HAADF analysis of the fresh 0.5wt.%Pd/TiO_2 catalyst showed sub-nanometres particles with an average particle diameter of 0.7 nm, with good Pd dispersion. After use in the H_2O_2 synthesis reaction, an increase in mean particle diameter to 3.9 nm was observed, suggesting the agglomeration of particles during the H_2O_2 synthesis reaction. According to XPS, fresh catalysts contain only Pd^{2+}. After use in the H_2O_2 synthesis reaction, a shift in Pd binding energy from 336.7 to 335 eV was observed, which suggests that surface Pd was reduced from Pd^{2+} to Pd^0 (Pd^{2+}:Pd^0 is 1:6.5). An increase in degradation activity towards H_2O_2, from 0 mol_{H2O2} kg_{cat}^{-1} h^{-1} to 331 mol_{H2O2} kg_{cat}^{-1} h^{-1}, upon re-use of the catalyst can be attributed to an increase in mean particle dimeter during reaction and partial reduction of Pd^{2+} to Pd^0 after the synthesis reaction.

No degradation activity was observed with the increasing concentration of H_2O_2 up to 16 wt.%, which is the maximum concentration achievable using reaction conditions described in this work. The starting concentration of H_2O_2 has a significant effect on catalyst activity towards further H_2O_2 synthesis. No synthesis activity was observed in the reaction with starting concentrations of H_2O_2 above 0.25 wt.% and, initial H_2O_2 concentrations of 0.25wt.%, no synthesis or degradation activity was observed. The addition of small amounts of H_2O_2 (0.05-0.15 wt.%) increased the selectivity towards H_2O_2 from 23% (no H_2O_2 present at the start of the reaction) up to 59 % with 0.05wt.% H_2O_2 in starting solution. The addition of H_2O_2 might help maintain Pd as Pd^{2+}, which can explain the increase in H_2 selectivity.

Re-calcination of a used 0.5 wt.%Pd/TiO_2 catalyst at 300 °C resulted in a decrease in catalyst synthesis activity, to 57 mol_{H2O2} kg_{cat}^{-1} h^{-1}, but more importantly inhibition of H_2O_2 degradation in presence of 4 wt.% H_2O_2. With further increase in the calcination temperature, no degradation activity was observed, but a significant decrease in synthesis activity (16 mol_{H2O2} kg_{cat}^{-1} h^{-1}) was obtained. When the re-calcination temperature was 400°C, all surface Pd was present in a Pd^{2+} form again.

To investigate the effect of reaction time on catalyst performance, a time-on-line study over the 0.5 wt.%Pd/TiO_2 catalyst was carried out. The concentration of H_2O_2 passed through a maximum of 0.14 wt.% at 30 min, and decreased with further reaction time. This can be attributed to particle agglomeration during the reaction, as well as reduction of Pd^{2+} to Pd^0. After 5 gas replacement reactions, a H_2O_2 concentration of 0.38wt.% was achieved. Freakley *et al*. at reported production of 0.35 wt.% H_2O_2 over the highly selective 2wt.%Sn-3wt.%Pd/TiO_2 subjected to subsequential oxidation-reduction-oxidation heat treatment after 3 gas replacements at 2°C.[9] The 0.5 wt.%Pd/TiO_2 catalyst testing showed, that to achieve higher concentrations of H_2O_2, high metal loadings and extensive heat treatment are not necessary.

The Figure 3.21 illustrates proposed schematic for direct synthesis of H_2O_2. Thought it is generally agreed that different active sites are present for formation and degradation of H_2O_2

the nature of these sites is still subject of discussions. The initial step of the reaction is adsorption of O_2 onto the catalyst surface to produce adsorbed intermediate. The key to H_2O_2 formation is for O-O bond to remain intact. The cleavage of the O-O bond leads to H_2O formation. In contrast, dissociative adsorption of H_2 on the catalyst surface is required. The adsorbed O_2 intermediate undergoes a proton-electron transfer to form hydroperoxyl followed by the proton-electron transfer to form H_2O_2. Cleavage of the O-O bond in O_2, H_2O_2 or OOH leads to H_2O formation.

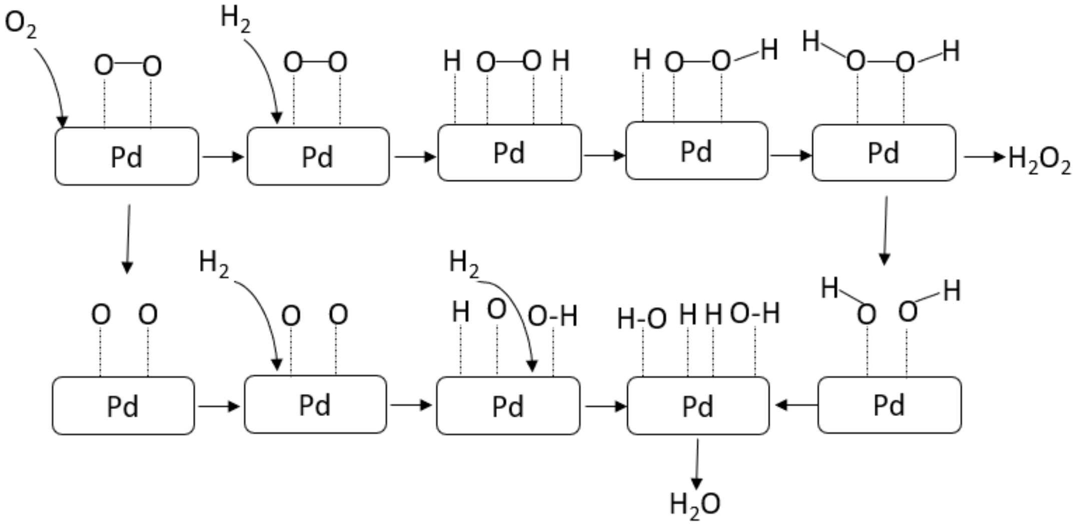

Figure 3.21: Proposed schematic for the direct synthesis of H_2O_2 on a Pd.

Pd oxidation state play an important role in the direct synthesis of H_2O_2 and is crucial to obtain high activity and selectivity of the catalyst. When higher concentration of H_2O_2 are present in the reaction solution prior the start of the reaction, no or low synthesis activity (depending on the H_2O_2 concentration) is observed over the 0.5 wt.%Pd/TiO_2 catalyst. This can be attributed to a stabilization of Pd as Pd^{2+} as only Pd^{2+} is present in the fresh catalyst and higher concentrations of H_2O_2 have been reported to help retain Pd^{2+}, suggesting that Pd^{2+} has low activity for both synthesis and degradation of H_2O_2. Upon re-use, partial reduction of Pd^{2+} to Pd^0 is observed resulting in increased degradation activity of the catalyst, which suggest that Pd^0 is highly active for both synthesis and degradation reaction. Once the catalyst is recalcined at 300°C, Pd^{2+} is mainly present on the catalyst surface which results in no degradation activity of the catalyst in the presence of 4 wt.% of H_2O_2. These observations suggest that a mixture of Pd^{2+} and Pd^0 is required to obtain higher concentration of H_2O_2 and minimise unwanted degradation pathways.

3.4 References

1 J. M. Campos-Martin, G. Blanco-Brieva and J. L. G. Fierro, *Angew. Chemie - Int. Ed.*, 2006, **45**, 6962–6984.

2 Evonik, *The Modern Chemist's Guide to Hydrogen Peroxide and Peracetic Acid*, 2018.

3 J. K. Edwards and G. J. Hutchings, *Angew. Chemie - Int. Ed.*, 2008, **47**, 9192–9198.

4 J. K. Edwards, S. J. Freakley, R. J. Lewis, J. C. Pritchard and G. J. Hutchings, *Catal. Today*, 2015, **248**, 3–9.

5 Y. Yi, L. Wang, G. Li and H. Guo, *Catal. Sci. Technol.*, 2016, **6**, 1593–1610.

6 V. R. Choudhary and P. Jana, *Catal. Commun.*, 2008, **9**, 1624–1629.

7 J. K. Edwards, E. Ntainjua N, A. F. Carley, A. A. Herzing, C. J. Kiely and G. J. Hutchings, *Angew. Chemie Int. Ed.*, 2009, **48**, 8512–8515.

8 S. Wang, D. E. Doronkin, M. Hähsler, X. Huang, D. Wang, J. D. Grunwaldt and S. Behrens, *ChemSusChem*, 2020, **13**, 3243–3251.

9 S. J. Freakley, Q. He, J. H. Harrhy, L. Lu, D. A. Crole, D. J. Morgan, E. N. Ntainjua, J. K. Edwards, A. F. Carley, A. Y. Borisevich, C. J. Kiely and G. J. Hutchings, *Science* 2015, **351**, 279–296.

10 S. Maity and M. Eswaramoorthy, *J. Mater. Chem. A*, 2016, **4**, 3233–3237.

11 A. S. K. Hashmi and G. J. Hutchings, *Angew. Chemie - Int. Ed.*, 2006, **45**, 7896–7936.

12 V. R. Choudhary and C. Samanta, *J. Catal.*, 2006, **238**, 28–38.

13 V. R. Choudhary and P. Jana, *Catal. Commun.*, 2008, **9**, 2371–2375.

14 D. A. Crole, S. J. Freakley, J. K. Edwards and G. J. Hutchings, *Proc. R. Soc. A Math. Phys. Eng. Sci.*,2016,**472.**

15 D. W. Flaherty, *ACS Catal.*, 2018, **8**, 1520–1527.

16 J. S. Adams, A. Chemburkar, P. Priyadarshini, T. Ricciardulli, Y. Lu, V. Maliekkal, A. Sampath, S. Winikoff, A. M. Karim, M. Neurock and D. W. Flaherty, *Science*, 2021, **371**, 626–632.

17 N. Gemo, S. Sterchele, P. Biasi, P. Centomo, P. Canu, M. Zecca, A. Shchukarev, K. Kordás, T. O. Salmi and J. P. Mikkola, *Catal. Sci. Technol.*, 2015, **5**, 3545–3555.

18 P. Tian, L. Ouyang, X. Xu, C. Ao, X. Xu, R. Si, X. Shen, M. Lin, J. Xu and Y.-F. Han, *J. Catal.*, 2017, **349**, 30–40.

19 S. Kim, D. W. Lee and K. Y. Lee, *J. Mol. Catal. A Chem.*, 2014, **391**, 48–54.

20 G. H. Han, G. P. Lee and K. Y. Lee, *Catal. Today*, 2020, **352**, 262–269.

21 A. Pashkova, R. Dittmeyer, N. Kaltenborn and H. Richter, *Chem. Eng. J.*, 2010, **165**, 924–933.

22 J. K. Edwards, J. Pritchard, M. Piccinini, G. Shaw, Q. He, A. F. Carley, C. J. Kiely and

G. J. Hutchings, *J. Catal.*, 2012, **292**, 227–238.

23 N. M. Wilson and D. W. Flaherty, *J. Am. Chem. Soc.*, 2016, **138**, 574–586.

24 Q. Liu and J. H. Lunsford, *Appl. Catal. A Gen.*, 2006, **314**, 94–100.

25 J. K. Edwards, A. Thomas, A. F. Carley, A. A. Herzing, C. J. Kiely and G. J. Hutchings, *Green Chem.*, 2008, **10**, 388–39.

26 E. N. Ntainjua, J. K. Edwards, A. F. Carley, J. A. Lopez-Sanchez, J. A. Moulijn, A. A. Herzing, C. J. Kiely and G. J. Hutchings, *Green Chem.*, 2008, **10**, 1162–1169.

27 J. K. Edwards, A. Thomas, B. E. Solsona, P. Landon, A. F. Carley and G. J. Hutchings, *Catal. Today*, 2007, **122**, 397–402.

28 V. R. Choudhary, C. Samanta and T. V. Choudhary, *Appl. Catal. A Gen.*, 2006, **308**, 128–133.

29 C. Samanta and V. R. Choudhary, *Chem. Eng. J.*, 2008, **136**, 126–132.

30 N. R. C. Fernandes MacHado and V. S. Santana, *Catal. Today*, 2005, **107**–**108**, 595–601.

31 L. Ouyang, P. F. Tian, G. J. Da, X. C. Xu, C. Ao, T. Y. Chen, R. Si, J. Xu and Y. F. Han, *J. Catal.*, 2015, **321**, 70–80.

32 P. Landon, P. J. Collier, A. F. Carley, D. Chadwick, A. J. Papworth, A. Burrows, C. J. Kiely and G. J. Hutchings, *Phys. Chem. Chem. Phys.*, 2003, **5**, 1917–1923.

33 M. Piccinini, J. K. Edwards, J. A. Moulijn and G. J. Hutchings, *Catal. Sci. Technol.*, 2012, **2**, 1908–1913.

34 S. J. Freakley, M. Piccinini, J. K. Edwards, E. N. Ntainjua, J. A. Moulijn and G. J. Hutchings, *ACS Catal.*, 2013, **3**, 487–501.

35 A. Santos, R. J. Lewis, G. Malta, A. G. R. Howe, D. J. Morgan, E. Hampton, P. Gaskin and G. J. Hutchings, *Ind. Eng. Chem. Res.*, 2019, **58**, 12623–12631.

36 J. K. Edwards, S. J. Freakley, A. F. Carley, C. J. Kiely and G. J. Hutchings, *Acc. Chem. Res.*, 2013, **47**, 845–854.

37 C. Samanta, *Appl. Catal. A Gen.*, 2008, **350**, 133–149.

38 V. R. Choudhary and P. Jana, *Appl. Catal. A Gen.*, 2009, **352**, 35–42.

39 Y. Voloshin and A. Lawal, *Chem. Eng. Sci.*, 2010, **65**, 1028–1036.

40 T. Moreno, J. García-Serna and M. J. Cocero, *Green Chem.*, 2010, **12**, 282–289.

41 Y. Voloshin, J. Manganaro and A. Lawal, *Ind. Eng. Chem. Res.*, 2008, **47**, 8119–8125.

42 X. Liang, Z. Mi, Y. Wang, L. Wang, X. Zhang and T. Liu, *Chem. Eng. Technol.*, 2004, **27**, 176–180.

43 D. P. Dissanayake and J. H. Lunsford, *J. Catal.*, 2003, **214**, 113–120.

44 V. Paunovic, V. V. Ordomsky, V. L. Sushkevich, J. C. Schouten and T. A. Nijhuis, *ChemCatChem*, 2015, **7**, 1161–1176.

45 Y. F. Han and J. H. Lunsford, *J. Catal.*, 2005, **230**, 313–316.

46 M. Piccinini, E. Ntainjua N., J. K. Edwards, A. F. Carley, J. A. Moulijn and G. J. Hutchings, *Phys. Chem. Chem. Phys.*, 2010, **12**, 2488–2492.

47 R. Battino, H. L. Clever and C. L. Young, *the Solubility of Gases in Liquids*, 1981, vol. 7.

48 R. Battino, T. R. Rettich and T. Tominaga, *J. Phys. Chem. Ref. Data*, 1983, **12**, 163–178.

49 K. C. Chao and H. Kim, *Hydrogen and deuterium: Solubility data series*, 1983, vol. 10.

50 J. Xia, M. Jo, Ä. Pe and G. Maurer, *J. Chem. Eng. Data*, 2004, **49**, 1756–1759.

51 V. R. Choudhary, C. Samanta and T. V. Choudhary, *Appl. Catal. A Gen.*, 2006, **308**, 128–133.

52 J. K. Edwards, B. Solsona, E. N. N, A. F. Carley, A. A. Herzing, C. J. Kiely and G. J. Hutchings, *Science* , 2009, **323**, 1037–1041.

53 S. Wang, K. Gao, W. Li and J. Zhang, *Appl. Catal. A Gen.*, 2017, **531**, 89–95.

54 S. Melada, R. Rioda, F. Menegazzo, F. Pinna And G. Strukul, *J. Catal.*, 2006, **239**, 422–430.

55 J. Gu, S. Wang, Z. He, Y. Han and J. Zhang, *Catal. Sci. Technol.*, 2016, **6**, 809–817.

56 D. Ding, X. Xu, P. Tian, X. Liu, J. Xu and Y. F. Han, *Cuihua Xuebao/Chinese J. Catal.*, 2018, **39**, 673–681.

57 S. Chinta and J. H. Lunsford, *J. Catal.*, 2004, 225, 249–255.

58 S. Melada, R. Rioda, F. Menegazzo, F. Pinna and G. Strukul, *J. Catal.*, 2006, **239**, 422–430.

59 M. Sankar, Q. He, M. Morad, J. Pritchard, S. J. Freakley, J. K. Edwards, S. H. Taylor, D. J. Morgan, A. F. Carley, D. W. Knight, C. J. Kiely and G. J. Hutchings, *ACS Nano*, 2012, **6**, 6600–6613.

60 J. K. Edwards, B. Solsona, E. N. N, A. F. Carley, A. a Herzing, C. J. Kiely and G. J. Hutchings, 2009, 1037–1041.

61 V. R. Choudhary, A. G. Gaikwad and S. D. Sansare, *Catal. Letters*, 2002, **83**, 235–239.

62 S. Biniak, R. Diduszko, W. Gac, M. Pakuła and A. Świątkowski, *React. Kinet. Mech. Catal.*, 2010, **101**, 331–342.

63 V. R. Choudhary and C. Samanta, *J. Catal.*, 2006, **238**, 28–38.

64 J. Brehm, R. J. Lewis, D. J. Morgan, T. E. Davies and G. J. Hutchings, *Catal. Letters*.

65 J. K. Edwards, A. F. Carley, A. A. Herzing, C. J. Kiely and G. J. Hutchings, *Faraday Discuss.*, 2008, **138**, 225–239.

66 Y. Voloshin and A. Lawal, *Appl. Catal. A Gen.*, 2009, **353**, 9–16.

67 A. Tereshchenko, A. Guda, V. Polyakov, Y. Rusalev, V. Butova and A. Soldatov,

Analyst, 2020, **145**, 7534–7540.

68 Q. Fan, S. He, L. Hao, X. Liu, Y. Zhu, S. Xu and F. Zhang, *Sci. Rep.*, 2017, **7**, 1–15.

69 D. G. Rethwisch and J. A. Dumesic, *Langmuir*, 1986, **2**, 73–79.

70 N. Macleod and R. M. Lambert, *Appl. Catal. B Environ.*, 2003, **46**, 483–495.

71 M. Haruta, N. Yamada, T. Kobayashi and S. Iijima, *J. Catal.*, 1989, **115**, 301–309.

72 V. R. Choudhary, C. Samanta and P. Jana, *Appl. Catal. A Gen.*, 2007, **332**, 70–78.

73 V. R. Choudhary, C. Samanta and T. V. Choudhary, *Catal. Commun.*, 2007, **8**, 1310–1316.

74 V. R. Choudhary, C. Samanta and T. V. Choudhary, *J. Mol. Catal. A Chem.*, 2006, **260**, 115–120.

75 S. Chinta and J. H. Lunsford, *J. Catal.*, 2004, **225**, 249–255.

76 S. Park, J. Lee, J. H. Song, T. J. Kim, Y. M. Chung, S. H. Oh and I. K. Song, *J. Mol. Catal. A Chem.*, 2012, **363**–**364**, 230–236.

77 E. Ntainjua N., J. K. Edwards, A. F. Carley, J. A. Lopez-Sanchez, J. A. Moulijn, A. a. Herzing, C. J. Kiely and G. J. Hutchings, *Green Chem.*, 2008, **10**, 1162.

Appnedix 1

Table S3.1: Productivity and reaction conditions of individual reactions of the monometallic Pd catalysts with various metal loadings.

Pd metal loading [wt.%]	**Batch**	**Productivity $[mol_{H_2O_2}\,kg_{cat}^{-1}\,h^{-1}]$**	**Catalyst mass [g]**	**Solvent mass [g]**	**Temperature [°C]**
0.0625	1	8	0.0100	8.51	25.3
		6	0.0099	8.51	25.8
		6	0.0102	8.49	25.5
	2	6	0.0099	8.51	25.8
		7	0.0101	8.50	26
		6	0.0100	8.50	25.4
	3	7	0.0101	8.51	24.3
		6	0.0099	8.50	24.8
		5	0.0098	8.49	24.8
0.125	1	23	0.0099	8.51	24.5
		24	0.0103	8.51	25
		24	0.0101	8.50	25.1
	2	23	0.0101	8.51	22.3
		23	0.0100	8.52	23.1
		22	0.0099	8.49	23
	3	24	0.0098	8.51	24.5
		23	0.0099	8.50	24.7
		23	0.0101	8.50	26
0.25	1	55	0.0099	8.50	25.3
		56	0.0102	8.52	25.6
		58	0.0099	8.50	26.1
	2	52	0.0098	8.51	24.5
		55	0.0101	8.52	25
		56	0.0100	8.51	25.1
	3	56	0.0103	8.50	26
		53	0.0099	8.51	26.1
		58	0.0099	8.52	26.1
0.5	1	65	0.0099	8.52	22.3
		64	0.0098	8.51	22
		65	0.0100	8.49	24

	2	63	0.0100	8.50	25.3
		66	0.0102	8.51	25.6
		65	0.0101	8.50	26
	3	66	0.0099	8.50	27
		67	0.0098	8.49	26.5
		62	0.0100	8.51	26.1
1	1	50	0.0101	8.50	22.3
		51	0.0101	8.50	23
		48	0.0099	8.49	23.5
	2	49	0.0098	8.52	25.6
		47	0.0102	8.51	25.6
		49	0.0098	8.50	25
	3	53	0.0100	8.51	26.3
		48	0.0101	8.51	25.7
		47	0.0099	8.49	25.8
2.5	1	32	0.0099	8.51	26
		36	0.0099	8.51	26.3
		36	0.0101	8.50	27
	2	33	0.0101	8.49	22.3
		36	0.0103	8.52	23
		35	0.0101	8.51	23.1
	3	37	0.0099	8.51	26.3
		33	0.0098	8.52	25.6
		38	0.0101	8.50	25.1
5	1	29	0.0101	8.50	24.3
		31	0.0100	8.49	24.4
		28	0.0100	8.49	24.4
	2	30	0.0098	8.51	25.6
		30	0.0103	8.50	26
		31	0.0100	8.50	26.1
	3	29	0.0100	8.51	23.1
		31	0.0101	8.52	22.9
		31	0.0100	8.51	24

Reaction conditions: 0.01g catalyst, 2.9 g of water, 5.6 g of methanol, 2.9 MPa 5%H_2/CO_2, 1.1 MPa 25%O_2/CO_2, 0.5 h, ambient temperature, 1200 rpm.

Table S3.2: Degradation and reaction conditions of individual reactions of the monometallic Pd catalysts with various metal loadings.

Pd metal loading [wt.%]	**Batch**	**Degradation [mol_{H2O2} kg_{cat}^{-1} h^{-1}]**	**Catalyst mass [g]**	**Solvent mass [g]**	**Conc. H_2O_2 [wt.%]**	**Temperature [°C]**
0.0625	1	0	0.0101	8.50	3.92	22.3
		0	0.0099	8.52	4	22.5
		0	0.0101	8.49	4.01	23
	2	0	0.0100	8.50	4.11	24
		2	0.0099	8.49	3.99	24.2
		0	0.0100	8.50	4.0	25.1
	3	0	0.0101	8.52	4.03	24.3
		0	0.0098	8.50	3.99	24.8
		0	0.0101	8.51	4.02	24.8
0.125	1	0	0.0010	8.51	4.00	24.5
		1	0.0099	8.52	4.02	25.3
		0	0.0101	8.50	4.08	25.2
	2	0	0.0098	8.51	3.95	22.4
		0	0.0100	8.50	3.97	23.1
		0	0.0100	8.50	4.11	23.4
	3	0	0.0098	8.51	3.99	26.7
		0	0.0099	8.48	4	27
		2	0.0103	8.49	4.05	26.4
0.25	1	0	0.0099	8.50	4.01	22.6
		0	0.0101	8.52	4.04	23
		0	0.0099	8.51	3.95	23.1
	2	0	0.0099	8.51	4	24.5
		0	0.0098	8.52	4.03	25
		0	0.0100	8.49	4.03	25.2
	3	0	0.0103	8.50	4.01	26.1
		0	0.0101	8.51	3.99	26.1
		0	0.0102	8.51	3.98	26.4
0.5	1	0	0.0099	8.50	4.15	22.9
		3	0.0100	8.51	4	23
		0	0.0100	8.49	4.12	23.1
	2	0	0.0100	8.50	3.95	25.3

		0	0.0101	8.52	3.99	26
		0	0.0101	8.50	4.1	26.1
	3	0	0.0099	8.50	4	26.1
		0	0.0099	8.21	4.01	26.5
		0	0.0100	8.51	4.03	26.9
1	1	122	0.0098	8.50	4	22.3
		131	0.0101	8.50	4.05	23.1
		133	0.0103	8.49	3.94	23.5
	2	116	0.0098	8.50	3.99	25
		123	0.0101	8.51	4.01	25.4
		137	0.0100	8.50	4.06	25.2
	3	124	0.0100	8.51	4.10	26.3
		135	0.0100	8.52	3.99	27
		114	0.0099	8.49	3.98	25.8
2.5	1	451	0.0098	8.52	4.01	26
		430	0.0099	8.51	4.03	26.1
		473	0.0101	8.49	4	27.1
	2	425	0.0102	8.49	4	22.4
		465	0.0103	8.52	4.06	23.1
		461	0.0101	8.51	3.91	23
	3	452	0.0100	8.53	4.01	26.1
		435	0.0098	8.52	4.06	25.6
		467	0.0101	8.50	3.99	25.4
5	1	608	0.0101	8.51	3.95	22.1
		600	0.0102	8.49	4	22.2
		628	0.0100	8.49	4.09	22.5
	2	607	0.0098	8.51	3.96	25.7
		599	0.0103	8.52	4.01	26.2
		635	0.0101	8.50	4.15	26.4
	3	610	0.0102	8.50	3.99	23.2
		626	0.0101	8.52	3.98	22.9
		590	0.0098	8.51	4.01	24

Reaction conditions:0.01g catalyst, 0.68 g H_2O_2, 2.22 g of water, 5.6 g of methanol, 2.9 MPa 5%H_2/CO_2, 1.1 MPa 25%O_2/CO_2, 0.5 h, ambient temperature, 1200 rpm.

Chapter 4

The Direct Synthesis of H_2O_2 Using Supported Bimetallic Catalysts.

4.1 Introduction

Pd based catalysts are at the centre of investigation and most of the important developments in the direct synthesis of H_2O_2 are based upon these catalysts.[1–6] Despite being highly active towards the direct synthesis of H_2O_2, most monometallic Pd catalysts are also activity for the subsequent degradation. The addition of Au into monometallic Pd catalyst resulted in a dramatic enhancement in catalyst activity towards H_2O_2 formation as well as H_2O_2 selectivity through a synergistic effect.[7,8] This enhancement in activity is mainly attributed to modification of Pd electronic structure and surface structure through a geometric effect and reconstruction of the surface composition.[8,9] The geometric effect is a dilution of surface Pd by secondary metal. Increasing surface ratio of Au-Pd results in size decrease of contiguous Pd ensembles to small Pd clusters or AuPd alloys on a catalyst surface, which have been reported to be more selective for the H_2O_2 formation.[46,8] The electronic modification of Pd by secondary metal can occur via direct charge transfer or by affecting the bond length.[46-47] By alloying Au and Pd, Au gains s, p electrons and loses d electrons, whereas Pd loses s, p electrons but gains d electrons.[46-48] Shifts in the d band centre away from the Fermi level is observed once Pd gains d electrons, which leads to weaker interaction between adsorbates and surface Pd atoms.[46] The Pd d band for Pd monomers surrounded by Au is much lower in energy than that for Pd monolayer or bulk Pd surfaces.[49] Pd has been found to adopt the lattice constant of Au, resulting in increase of Pd-Pd bond length. Both changes makes Pd more “atomic like” resulting in weaker binding of reactants and products compared to Pd in bulk.[46]

In recent studies, addition of secondary metal such as Sn, Ni, Sb and Zn was investigated to present cheaper alternatives to well established AuPd catalysts.[10–15] Hutchings and co-workers demonstrated that subjecting SnPd supported on TiO_2 to oxidation-reduction-oxidation (ORO) treatment resulted in highly active and selective catalysts under sub-ambient temperatures (2 ^{o}C).[12] It was suggested that, during heat treatment, the small Pd-rich particles responsible for H_2O_2 degradation are encapsulated in an SnO_x layer by generating strong metal support interactions (SMSIs). Li *et al.* investigated a series of PdSn nanocrystals with a hollow structure, using a facile solvent-thermal method that results in highly active and selective catalysts.[11] The enhancement of synthesis activity and inhibition of degradation is attributed to the ensemble effect of PdSn alloys, as well as the Pd/SnO_x and PdO/SnO_x interfaces. Addition of Ni and Sb has been also reported to increase the selectivity of the catalyst and synthesis activity via electronic modification of Pd or morphological medication of surface Pd.[13,16,17]

This Chapter is focused on bimetallic supported catalysts and how the addition of secondary metal (Au, Sn, Ni) affects synthesis and degradation activity towards H_2O_2. The bimetallic catalysts in this work show high synthesis activities at ambient temperature without use of any additives. It was also demonstrated that optimised SnPd and NiPd catalysts showed comparable synthesis activities to well established AuPd catalysts presenting cheaper alternative for the studied reaction. To maximise the concentration of H_2O_2 obtained during the reaction, different reaction conditions were also investigated.

4.2 Results and Discussion

Supported bimetallic catalysts were prepared using the standard wet impregnation technique using $PdCl_2$, $HAuCl_4$, $SnCl_2$ and $NiCl_2$ as metal precursors and TiO_2 as the support, as outlined in Chapter 2, Section 2.2.1. Each catalyst was prepared at least 3 times and each batch of catalyst was tested at least 3 times for H_2O_2 synthesis and degradation reaction. All H_2O_2 synthesis and degradation testing was carried out according to the procedures discussed previously in Chapter 2, unless otherwise stated. A summary of the testing conditions is given below:

- Blank degradation reactions, in the absence of a catalyst, were carried out on a regular basis to determine possible reactor contamination. In a case of contamination, the reactor was subjected to cleaning process using mineral acids followed by water and TiO_2 washing cycles. A subsequent blank degradation reaction was then carried out before continuing testing with catalyst.
- Standard reaction conditions for H_2O_2 synthesis: 0.01 g catalyst, 2.9 g of water, 5.6 g of methanol, 2.9 MPa 5% H_2/CO_2, 1.1 MPa 25% O_2/CO_2, 0.5 h, ambient temperature,1200 rpm.
- H_2O_2 degradation activity was determined from the amount of H_2O_2 that was degraded after the reaction under standard reaction conditions: 0.01 g catalyst, 0.68 g of 50 wt.% solution of H_2O_2, 2.22 g of water, 5.6 g of methanol, 2.9 MPa 5% H_2/CO_2, 0.5 h, ambient temperature, 1200 rpm.

4.2.1 Effect of metal loading on catalytic activity towards the direct synthesis and subsequent degradation of H_2O_2.

Metal loading of Pd can significantly effect catalysts synthesis and degradation activity towards H_2O_2, as well as H_2 conversion and selectivity by altering particle size, shape, morphology, metal dispersion, and electronic state of the catalyst.[4,6,18–23] As shown in Chapter 3, a decrease in Pd metal loading results in an increase in synthesis activity and H_2O_2 selectivity, and a significant decrease in degradation activity in presence of 4 wt.% H_2O_2. Enhancement in catalyst performance was reported when Pd was alloyed with a range of secondary metals (e.g. Au, Sn, Ni, Zn, Sb).[10,13–15,24] With the addition of the secondary metal, the alloyed nanoparticles offer enhanced catalytic activity and selectivity compared to the monometallic analogue.[8] To investigate the effect of the metal loading on H_2O_2 synthesis and degradation activity, a series of bimetallic catalysts were prepared with different Pd content with addition of secondary metal (Au, Sn and Ni). All catalysts were prepared by wet co-impregnation with a metal weight ratio for Pd to secondary metal that is equal to 1:1 and a total metal loading varying from 0.125 – 5 wt.%. No activity towards H_2O_2 formation or degradation was observed over bare TiO_2, which was used as the catalyst support.

As illustrated in Figure 4.1, 0.0625wt.%Pd/TiO_2 shows low H_2O_2 synthesis activity of 8 $mol_{H2O2}\ kg_{cat}^{-1}\ h^{-1}$. Addition of the same amount of Au (0.0625wt.%Au-0.0625wt.%Pd/TiO_2) increases H_2O_2 synthesis activity more than 3 times, achieving activity of 27 $mol_{H2O2}kg_{cat}^{-1}h^{-1}$, while the monometallic Pd counterpart (0.125wt.%Pd/TiO_2) exhibited a marginally lower synthesis activity of 23 $mol_{H2O2}\ kg_{cat}^{-1}\ h^{-1}$. This demonstrates how the synthesis activity of the catalyst can be enhanced by addition of the same weight loading of Au to monometallic Pd catalyst. Even larger enhancement in synthesis activity was observed with 0.25wt.% metal loading, where AuPd (1:1 weight ratio) shows an increase in synthesis activity to 83 $mol_{H2O2}\ kg_{cat}^{-1}\ h^{-1}$, significantly higher than the 56 $mol_{H2O2}\ kg_{cat}^{-1}\ h^{-1}$ obtained with monometallic 0.25wt.%Pd/TiO_2 catalysts.

Both monometallic Pd catalysts and bimetallic AuPd catalysts show a volcano trend for activity towards H_2O_2 synthesis with metal loading; the synthesis activity for both the monometallic Pd and bimetallic AuPd catalysts passes through a maximum of 65 and 90 $mol_{H2O2}\ kg_{cat}^{-1}\ h^{-1}$, respectively, with a total metal loading of 0.5 wt.%. In comparison, synthesis activity of 64 $mol_{H2O2}\ kg_{cat}^{-1}\ h^{-1}$ is obtained with well-studied 2.5wt.%Au-2.5wt.%Pd/TiO_2 catalyst previously prepared by Edwards *et al.*, which is an established catalyst for direct synthesis of H_2O_2 and used as benchmark within our research group.[26] Further increase in metal loading results in decreased synthesis activity. In contrast, Brehm *et al.* reported increase in H_2O_2 synthesis activity with increasing metal loading of AuPd catalysts prepared by an “excess chloride” co-impregnation procedure (use of acidified $PdCl_2$ solution as Pd precursor).[27] The increase in synthesis activity of the AuPd catalysts when compared to monometallic counterparts was attributed to the development of Pd domains of mixed oxidation state, and an increased control of nanoparticle size compared to Au- or Pd- rich analogues. Despite a higher concentration of Cl^- anions added during the “excess chloride” co-impregnation procedure, lower synthesis activities were achieved; for example, 56 mol_{H2O2} kg_{cat}^{-1} h^{-1} was reported by Brehm *et al.* over 0.25 wt.%Au – 0.25 wt.%Pd/TiO_2, while the preparation method used in this thesis resulted in synthesis activity of 90 mol_{H2O2} kg_{cat}^{-1} h^{-1} with the same AuPd analogue. As shown in Figure 4.1, catalysts with low metal loading prepared in this work show significantly higher synthesis activity compared to catalysts with higher metal loading, resulting in more effective use of precious metals and therefore a decrease in catalyst cost.

No significant enhancement in H_2O_2 synthesis activity is observed over 0.25wt.%Sn-0.25wt.%Pd/TiO_2, with an activity of 62 mol_{H2O2} kg_{cat}^{-1} h^{-1} compared to 0.5 wt.%Pd/TiO_2 with synthesis activity of 65 mol_{H2O2} kg_{cat}^{-1} h^{-1}. However, an increase in synthesis activity is observed compared to the monometallic 0.25 wt.%Pd/TiO_2 (56 mol_{H2O2} kg_{cat}^{-1} h^{-1}), suggesting an enhancement in synthesis activity per mol of Pd due to presence of Sn. The enhancement in performance of the SnPd catalyst is attributed to formation of SnO_x which is suggested to absorb O_2 without bond cleavage and encapsulation of small Pd rich particles responsible for H_2O_2 degradation by SnO_x,as well as modification of Pd electronic structure by Sn or isolating Pd nanoparticles with Sn.[10–12] As shown in Figure 4.1, the 0.5 wt.%Sn – 0.5 wt.%Pd/TiO_2 catalyst shows higher synthesis activity than 0.5 wt.%Au – 0.5 wt.%Pd/TiO_2 or 0.5 wt.%Pd/TiO_2 catalyst. With a further increase in metal loading, similar enhancement in synthesis activity was observed with SnPd catalysts as for AuPd analogues, which presents a cheaper alternative to well established AuPd catalysts.

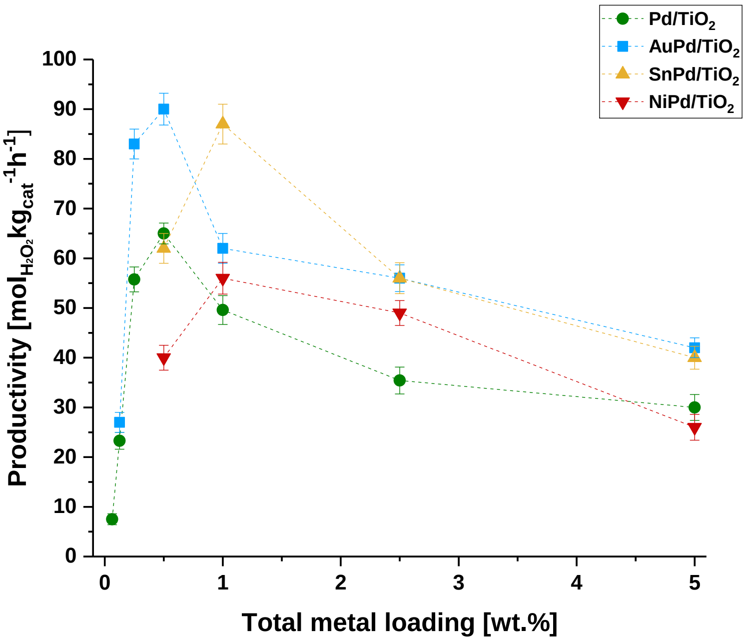

***Figure 4.1: Synthesis activity of the bimetallic (1:1 weight ratio) AuPd, SnPd, NiPd and monometallic Pd catalysts with various metal loadings*.** **Reaction conditions:** 0.01 g catalyst, 2.9 g of water, 5.6 g of methanol, 2.9 MPa 5%H_2/CO_2, 1.1 MPa 25%O_2/CO_2, 0.5 h, ambient temperature, 1200 rpm

In contrast, a decrease in H_2O_2 synthesis activity (to 40 $mol_{H2O2}\ kg_{cat}^{-1}\ h^{-1}$) is obtained with Ni incorporation into the 0.25wt.%Pd/TiO_2 catalyst (0.25wt.%Ni-0.25wt.%Pd/TiO_2), which is significantly lower than the synthesis activity obtained over a 0.25wt.%Pd/TiO_2 catalyst. However, the increase in H_2O_2 synthesis activity to 56 $mol_{H2O2}\ kg_{cat}^{-1}\ h^{-1}$ and 49 $mol_{H2O2}\ kg_{cat}^{-1}\ h^{-1}$ with increasing 1:1 metal loading to 1 wt.% and 2.5wt.%, respectively, suggests that the addition of Ni to a Pd catalyst can indeed enhance synthesis activity when higher loadings are used. SnPd and NiPd catalysts reach maxima of 87 and 56 $mol_{H2O2}\ kg_{cat}^{-1}\ h^{-1}$, respectively, over 1 wt.% total metal loading; as with AuPd and Pd-only catalysts, a further increase in metal loading results in a decrease in synthesis activity.

It can be observed in Figure 4.2 that, at metal loadings below 0.5wt.%, no H_2O_2 degradation activity is observed over monometallic Pd catalysts, as discussed in Chapter 3, Section 3.2.1. However, the bimetallic AuPd catalysts started to exhibit a relatively low degradation activity of 24 $mol_{H2O2}\ kg_{cat}^{-1}\ h^{-1}$ with 0.125 wt.% Au – 0.125 wt.% Pd/TiO_2 catalyst, and degradation increases 4 -fold over 0.25wt.%Au-0.25wt.%Pd/TiO_2. In contrast with synthesis activity data, further increases in metal loading dramatically increased the degradation activity of all catalysts. The greatest degradation activity (609 $mol_{H2O2}kg_{cat}^{-1}h^{-1}$) is obtained over the

5wt.%Pd/TiO_2 catalyst, which is significantly higher than degradation activity, 417 mol_{H2O2} kg_{cat}^{-1} h^{-1}, of the AuPd counterpart.

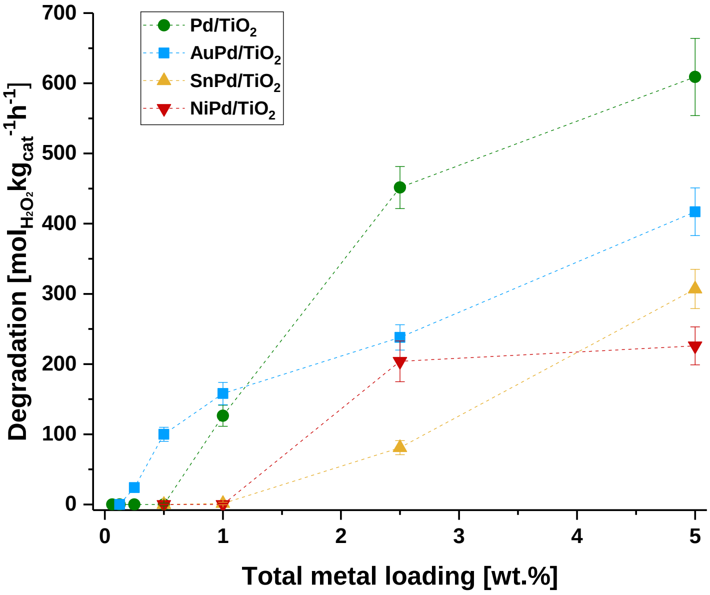

***Figure 4.2: Degradation activity of the bimetallic (1:1 weight ratio) AuPd, SnPd, NiPd and monometallic Pd catalysts with various metal loadings*. Degradation reaction conditions:** 0.01 g catalyst, 0.68 g H_2O_2, 2.22 g of water, 5.6 g of methanol, 2.9 MPa 5% H_2/CO_2, 1.1 MPa 25% O_2/CO_2, 0.5 h, ambient temperature, 1200 rpm.

No degradation activity is observed with SnPd and NiPd catalysts up to 1 wt.% total metal loading. Both SnPd and NiPd show an increase in degradation activity towards H_2O_2 with further increasing metal loading; however, the degradation activities are significantly lower than the activities obtained with monometallic Pd and AuPd counterparts. These observations suggests that, at low metal loadings, addition of Au enhances both, synthesis and degradation activity (0.25wt.%Au-0.25wt.%Pd/TiO_2). In contrary, the enhancement in degradation activity become less significant with higher metal ladings (above 2.5 wt.%) when compared to monometallic Pd catalysts, while increase in synthesis activity towards H_2O_2 is still observed. Both SnPd and NiPd catalysts show significantly lower H_2O_2 degradation activities than the monometallic Pd or AuPd series. It is important to mention that 1.25wt.%Sn-1.25wt.%Pd/TiO_2 shows degradation activity towards H_2O_2 only 81 mol_{H2O2} kg_{cat}^{-1} h^{-1}, which is more than 2.5 times less than the degradation activities obtained with other catalyst at this metal loading, i.e. it is the best performing catalyst.

As shown in Figure 4.3, combining Au with Pd does not only enhance the synthesis activity of the catalyst (compared to monometallic Pd counterpart) but also increases selectivity towards H_2O_2. The introduction of Au into the Pd catalyst results in a change of the surface structure of the catalysts, by geometric effects, through reconstructing the surface composition, as well as modification of electronic structure of Pd.[7,9] H_2 conversions over monometallic Pd catalysts and AuPd catalysts show almost identical trends, with the exception of 0.125 wt.% metal loading. The higher concentration of H_2O_2 obtained over AuPd catalysts compared to the monometallic Pd counterparts is therefore due to higher H_2O_2 selectivity of these catalysts. For comparison, 0.25wt.%Au-0.25wt.%Pd/TiO_2 shows H_2 selectivity of 35%, while selectivity of 28% is obtained with 0.25wt.%Pd/TiO_2, and decreases to 23% with an increase in metal loading up to 0.5wt.%Pd/TiO_2. Edwards *et al.* reported significantly higher H_2O_2 selectivity of 61 % with 2.5wt.%Au-2.5wt.%Pd/TiO_2 at 2°C.[28,29] It was previously published that lower reaction temperatures (1-2°C) are more favourable for achieving higher selectivity towards H_2O_2.[30] This work is focusing on using reaction temperatures of 20 °C, which presents industrially more applicable option and therefore lower H_2O_2 selectivities are obtained compared to studies conducted at low temperatures. As shown in Figure 4.3, SnPd/TiO_2, generally shows higher H_2O_2 selectivities compared to the monometallic Pd and AuPd counterparts. A H_2O_2 concentration of 0.12 wt.% was achieved with 0.25wt.%Sn-0.25wt.%Pd/TiO_2, which was comparable with concentration of 0.14 wt.% achieved over 0.5wt.%Pd/TiO_2 but significantly lower than 0.18 wt.% obtained over 0.25wt.%Au-0.25wt.%Pd/TiO_2. However, a much lower H_2 conversion of 27.5% and higher H_2O_2 selectivity of 44.1% are obtained over the 0.25wt.%Sn-0.25wt.%Pd/TiO_2 catalyst, while both monometallic Pd and AuPd counterparts demonstrate conversion of 52.6 % and 51.2 %, respectively.

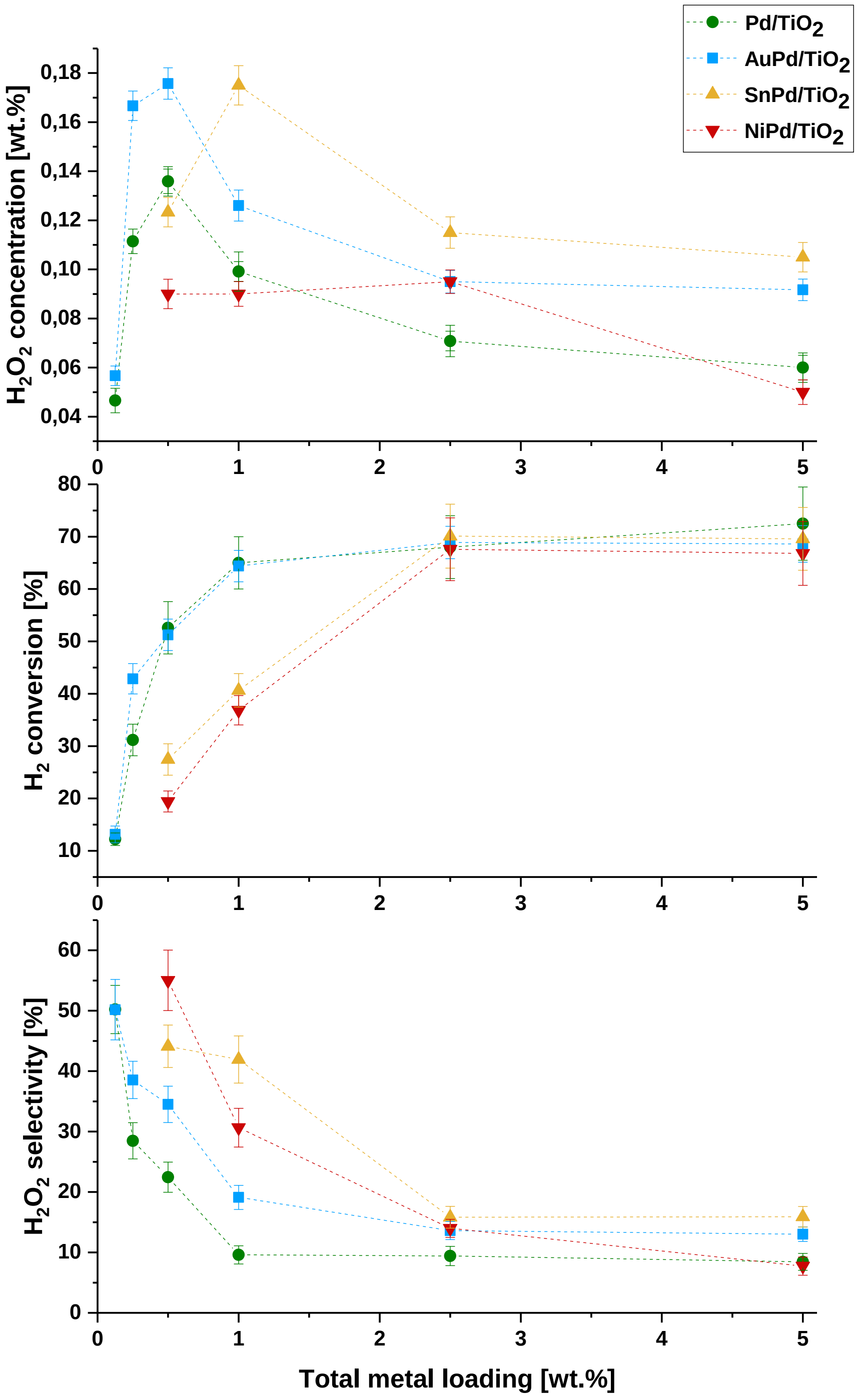

Figure 4.3: H_2O_2 concentration, H_2 conversion and selectivity of the bimetallic (1:1 weight ratio) AuPd, SnPd and NiPd and monometallic Pd catalysts with various metal loadings. **Reaction conditions:** 0.01 g catalyst, 2.9 g of water, 5.6 g of methanol, 2.9 MPa 5% H_2/CO_2, 1.1 MPa 25% O_2/CO_2, 0.5 h, ambient temperature, 1200 rpm

Despite the decrease in synthesis activity of the 0.25wt.%Ni-0.25wt.%Pd/TiO_2 catalyst compared to the monometallic Pd analogue, the NiPd catalyst shows a significant increase in H_2O_2 selectivity, to 55%, which was the highest selectivity amongst all the catalyst presented in this study. All investigated series show that H_2O_2 concentration passes through a maximum between 0.5 wt.% (Pd, AuPd) and 1 wt.% (SnPd,NiPd) metal loading and a further increase in total metal loading results in a decrease in H_2O_2 concentration. An increase in H_2 conversion is observed with a metal loading up to 2.5 wt.%, reaching the maximum conversion around 67% for all studied series of catalysts. No significant change in H_2 conversion is observed with further increase in metal loading. As expected H_2O_2 selectivity shows the exact opposite trend, with a decreasing tendency up to 2.5 wt.% metal loading and no significant change with further increase in total metal loading. Exceptional to this trend were NiPd catalysts, which show a decrease in H_2O_2 selectivity from 14% (obtained with 1.25wt.%Ni-1.25wt.%Pd/TiO_2) to 7.7% with 2.5wt.%Ni-2.5wt.%Pd/$TiO_{2.}$

Transmission electron microscopy (TEM) characterization was carried out to investigate the average particle diameter of catalysts with different AuPd metal loadings with an Au:Pd ratio of 1: 1 (by weight), with TEM micrographs shown in Figure 4.4. Only few larger particles around 10 nm were observed for the 0.25wt.%Au- 0.25wt.%Pd/TiO_2 catalyst and therefore it was difficult to calculate mean particle diameter. It is highly possible that smaller particles were below detection limit of the TEM equipment, due to low metal loading and good metal dispersion. Similarly, no visible particles are observed over the 0.5wt.%Pd/TiO_2 catalyst, again possibly due to low metal loading and good Pd dispersion; STEM-HAADF of 0.5wt.%Pd/TiO_2 (Chapter 3, Section 3.2.3) confirmed good Pd dispersion and mean particle diameter of 0.7 nm. TEM analysis (Figure 4.4 b) of 1.25 wt.%Au - 1.25wt.%Pd/TiO_2 shows well dispersed particles, with an average particle diameter of 2.9 nm. Analysis by energy dispersive X-ray spectroscopy (Figure 4.6 a and b) shows that larger particles (> 6 nm) are Au rich (strong Au signal and weak Pd signal is observed), and smaller particles contain more Pd (small Pd particles exhibit weak Pd signal). As shown in Figure 4.5 a), 80% of analysed particles are below 4 nm. TEM micrographs (Figure 4.4 c) of 2.5 wt.%Au - 2.5wt.%Pd/TiO_2 show a good dispersion of nanoparticles, with an average particle diameter of around 3.2 nm, and 13 % particles larger than 4 nm. The mean particle diameter of these catalyst could be even smaller, as it is highly possible that there are particles present on the catalyst below detection limit of the equipment. Similarly, as with the 1.25 wt.%Au - 1.25wt.%Pd/TiO_2 catalyst, larger particles are Au rich while smaller particles contain more Pd (Figure 4.6 c and d). Edwards *et al.* also reported correlation between particle size and composition of AuPd catalysts supported on TiO_2, with the larger particles being Au rich and smaller particles being Pd rich.[24,29] In comparison, 2.5 wt.%Au - 2.5 wt.%Pd/TiO_2 prepared by Edwards *et al.* using wet co-impregnation method showed a mean particle diameter above 5 nm, with wider particle size distribution compared to catalysts prepared in this section.[24] This can be attributed to use of excess of the solvent during catalyst preparation, resulting in better metal dispersion.

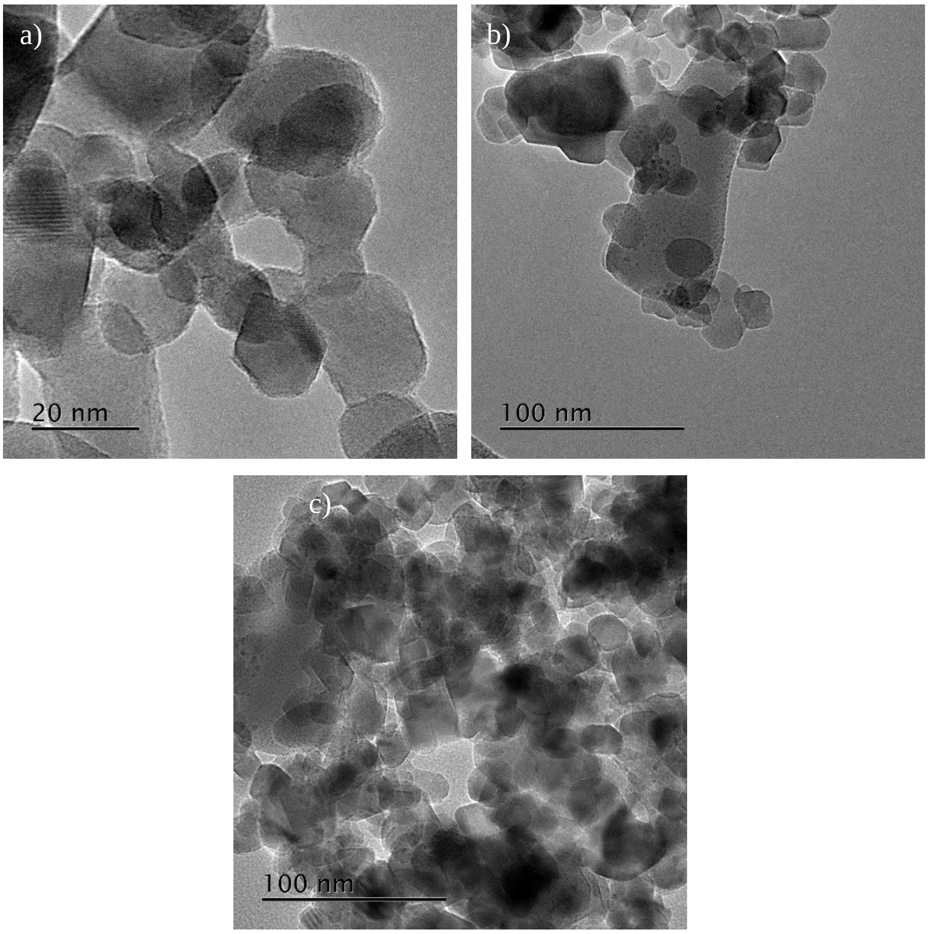

Figure 4.4: TEM images of fresh AuPd catalysts with different metal loading: a) 0.25wt.%Au -0.25wt.%Pd/TiO_2; b) 1.25wt.%Au -1.25wt.%Pd/TiO_2; c) 2.5wt.%Au -2.5wt.%Pd/TiO_2.

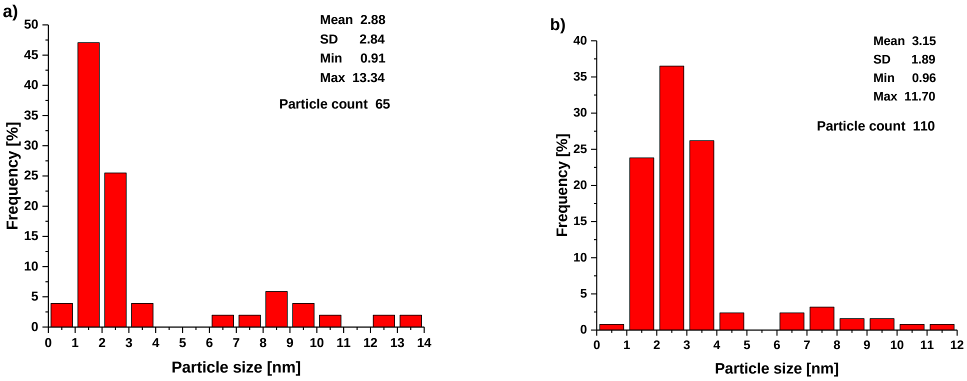

Figure 4.5**: **Particle diameter distribution of fresh AuPd catalysts with different metal loading: a) 1.25wt.%Au -1.25wt.%Pd/TiO_2; b) 2.5wt.%Au -2.5wt.%Pd/TiO_2.

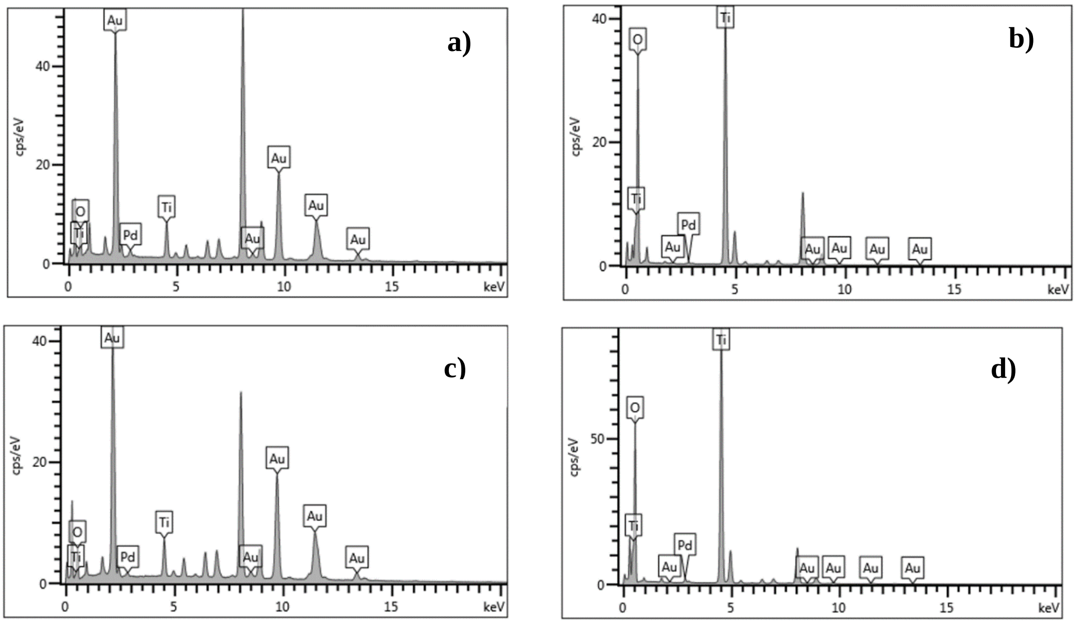

Figure 4.6: EDX images of fresh AuPd catalysts with different metal loading: a) 1.25wt.%Au - 1.25wt.%Pd/TiO_2 – large particle; b) 1.25wt.%Au -1.25wt.%Pd/TiO_2 – small particles; c) 2.5wt.%Au - 2.5wt.%Pd/TiO_2 – large particle; d) 2.25wt.%Au -2.25wt.%Pd/TiO_2 – small particles.

4.2.2 Effect of metal ratio on catalytic activity towards the direct synthesis and subsequent degradation of H_2O_2

As shown in Section 4.2.1, combining Pd with a secondary metal can significantly enhance the synthesis activity and selectivity of the catalyst compared to monometallic Pd counterparts. All the previously studied catalysts were prepared with a 1:1 ratio (by weight) of Pd to secondary metal. To further investigate how metal composition effects the catalyst activity and selectivity, a series of bimetallic catalyst were prepared by wet impregnation with varying Pd: secondary metal ration, and total metal loading fixed to 0.5 wt.%. As shown in Figure 4.7, monometallic Au, Sn and Ni (0.5wt.%/TiO_2) catalysts show very low synthesis activity towards H_2O_2. A small amount of Pd combined with Au results in significant enhancement in catalytic activity compared to monometallic catalyst with same metal loading. An optimal Au:Pd ratio is 1:1 (by weight) with synthesis activity 90 mol_{H2O2} kg_{cat}^{-1} h^{-1}. The Au:Pd ratio 1:1 (by weight) was previously reported to be the optimal one in many studies.[7,27,31] Both the 0.375 wt.% Au – 0.125 wt.% Pd/TiO_2 and 0.125 wt.% Au – 0.375 wt.% Pd/TiO_2 catalysts show identical synthesis activities (80 mol_{H2O2} kg_{cat}^{-1} h^{-1}). Pritchard *et al.* showed the effect of Au: Pd ratio on catalyst activity over a series of 1wt.% catalyst supported on C, prepared by sol immobilization.[32] Similar, to this study, no significant difference in catalyst activity was observed between 2:1 and 1:3 Au: Pd ratios (by weight), with maximum synthesis activity(188 mol_{H2O2} kg_{cat}^{-1} h^{-1}) obtained over 1:1.85 Au:Pd ratio. Brehm *et al.*

conducted a similar study over a series of 1wt.%dAuPd catalyst supported on TiO_2, in which 1:1 (by weight) ratio resulted in the highest synthesis activity.[27] Han *et al.* reported that alloying Pd with Au results in surface and electron modification of Pd, which is responsible for enhanced reactivity and selectivity for the direct synthesis of H_2O_2.[9]

The 0.5 wt.% $SnPd/TiO_2$ catalysts with different Sn: Pd ratios show similar synthesis activities as the monometallic 0.5 wt.% Pd counterpart. As shown in Figure 4.7, the monometallic Sn catalyst shows negligible H_2O_2 synthesis activity, and synthesis activity increases with introduction of Pd. No significant difference in synthesis activity is observed with increase in Pd content from 0.25 wt.% to 0.5 wt.%. In comparison, Li *et al.* reported a study in which significant enhancement in synthesis activity was observed over hollow $SnPd/TiO_2$, prepared by a facile solvent-thermal method, compared to monometallic Pd catalysts.[11] The highest synthesis activity was achieved over a Sn:Pd ratio of 1:4.5 (by weight), and, the activity was almost 5 times higher than of the monometallic Pd counterpart. The enhancement activity was attributed to an existence of a PdO species, the ensemble effect of hollow SnPd nanocrystals, and an interface effect of Pd and PdO with $SnO_{x.}$

On the other hand, all the 0.5 wt.% NiPd catalysts with different Ni:Pd ratio in this study showed lower H_2O_2 synthesis activities than the monometallic Pd counterparts, with a decrease in H_2O_2 synthesis activity observed with increasing Ni content. This is an interesting observation as Ni was previously reported to enhance synthesis activity of catalyst upon combining with Pd.[10,13] However, these studies utilized significantly higher total metal loadings, above 5 wt.%. As shown in Figure 4.1, there was an enhancement in synthesis activity of the NiPd catalysts compared to monometallic Pd counterparts at higher metal loadings (2.5wt.%). Maity *et al.* reported that the presence of Ni in NiPd alloys enhanced the synthesis activity of the catalyst by modifying the electronic structure of Pd.[13] It was also stated that micron size Pd and NiPd particles showed no activity towards synthesis of H_2O_2 and therefore particles in nano scale (8-30 nm) were required for active catalyst. It was reported by Han *et al.* that the addition of Ni to Pd increases the dispersion of the metals, which could explain the lower synthesis activity of 0.5 wt.% NiPd catalyst, as it was previously shown in this work (Chapter 3, Section 3.2.3 and Chapter 4, Section 4.2.1) that catalysts at this metal loading were composed of small particles below 1 nm. [16]

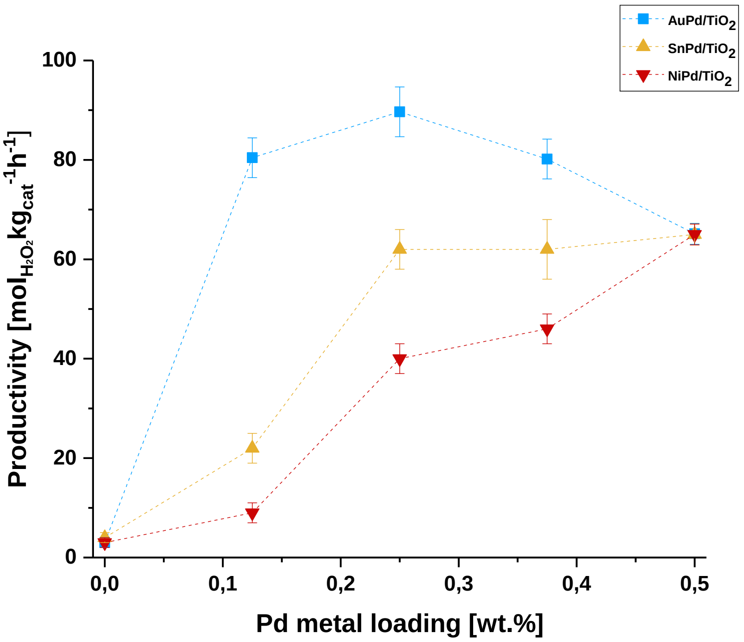

Figure 4.7**: Synthesis activity of the bimetallic 0.5wt.% AuPd, SnPd and NiPd catalysts supported on TiO$_2$ with varying metal ratio**. **Reaction conditions:** 0.01 g catalyst, 2.9 g of water, 5.6 g of methanol, 2.9 MPa 5% H_2/CO_2, 1.1 MPa 25% O_2/CO_2, 0.5 h, ambient temperature, 1200 rpm

Figure 4.8 shows, that no H_2O_2 degradation activity was observed over SnPd and NiPd catalysts. Low degradation activity (of 8 mol$_{H2O2}$ kg$_{cat}$$^{-1}$ h^{-1}) was also observed over monometallic 0.5 wt.% Au/TiO$_2$ catalysts; however, once Pd is combined with Au, an increase in the degradation activity is observed as shown in Figure 4.8. The lowest degradation activity amongst AuPd catalysts tested in this study, 100 mol$_{H2O2}$ kg$_{cat}$$^{-1}$ h^{-1}, is observed for 0.25wt.%Au-0.25wt.%Pd/TiO$_2$; both the 0.375 wt.% Au - 0.125 wt.%Pd/TiO$_2$ and 0.125wt.% Au – 0.375 wt.% Pd/TiO$_2$ catalysts exhibit slightly higher degradation activities. This demonstrates that addition of Au to Pd not only enhances synthesis activity but also affects degradation activity, which was also shown by Pritchard *et al.*[32] Brehm *et al.* reported an increase in H_2O_2 degradation activity with increasing Pd:Au ratio of 1 wt.% AuPd/TiO$_2$ catalysts, prepared by an “excess-chloride” co-impregnation procedure.[27]

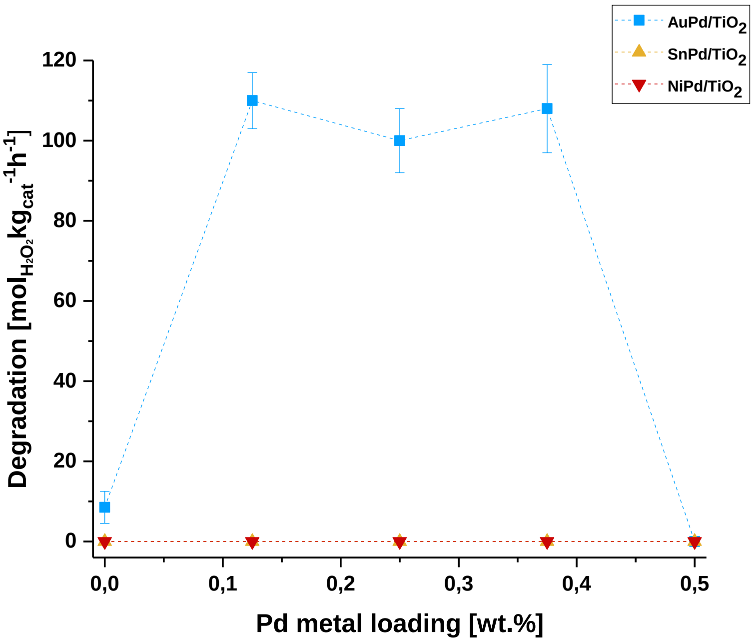

***Figure 4.8: Degradation activity of the bimetallic 0.5wt.% AuPd, SnPd and NiPd catalysts supported on TiO_2 with varying metal ratio*. Reaction conditions: Degradation reaction:** 0.01 g catalyst, 0.68 g H_2O_2, 2.22 g of water, 5.6 g of methanol, 2.9 MPa 5% H_2/CO_2, 0.5 h, ambient temperature, 1200 rpm.

As shown in Figure 4.9, the addition of secondary metals can significantly affect H_2 conversion and H_2O_2 selectivity compared to monometallic Pd catalysts. Monometallic Au, Sn and Ni catalysts (0.5 wt.%/TiO_2) show minimal H_2 conversion and H_2O_2 selectivities close to 100 %, which is attributed to very low activity of these catalysts. Introduction of Pd at low loadings (0.375 wt.% X – 0.125wt.%Pd/TiO_2 where X=Au, Sn, Ni) results in a significant increase in H_2 conversion for the AuPd and SnPd catalyst, to 26 and 21 %, respectively. In comparison, the 0.125 wt.% Pd /TiO_2 catalyst shows H_2 conversion of 12 %, a relatively low H_2 conversion of 4% was observed over NiPd catalyst with this metal ratio. A H_2O_2 selectivity of 61 % is achieved over the 0.375wt.% Au – 0.125 wt.%Pd/TiO_2 catalyst, which is the highest selectivity achieved. Further increase in Pd content results in an increase in H_2 conversion, and a decrease in H_2O_2 selectivity, for AuPd and SnPd catalysts. Both 0.125 wt.%Au – 0.375 wt.%Pd/TiO_2 and 0.125 wt.%Sn – 0.375 wt.%Pd/TiO_2 show higher H_2 conversions than 0.5 wt.% Pd %/TiO_2, with comparable H_2O_2 selectivities to the monometallic counterpart. The 0.5wt.%NiPd/TiO_2 series of catalysts shows small differences in H_2O_2 selectivity with varying Ni: Pd ratio, with the highest selectivity (43.2%) achieved over the 0.25 wt.%Ni – 0.25 wt.%Pd/TiO_2 catalyst. As previously discussed in Section 4.2.1, a decrease in H_2O_2 synthesis activity occurs over the 0.5 wt.%NiPd/TiO_2 catalysts when compared to the monometallic Pd counterpart; however, as shown in Figure 4.9, the lower H_2O_2 synthesis activity is compensated with lower H_2 conversion and higher H_2O_2 selectivity. The blocking of active sites by Ni could explain lower synthesis activity and lower conversion compared to the monometallic Pd counterparts, and results in higher H_2 selectivity. Lee *et al.* reported blocking of large Pd ensembles by added Ni, resulting in an increased ethylene selectivity in the hydrogenation of acetylene.[33]

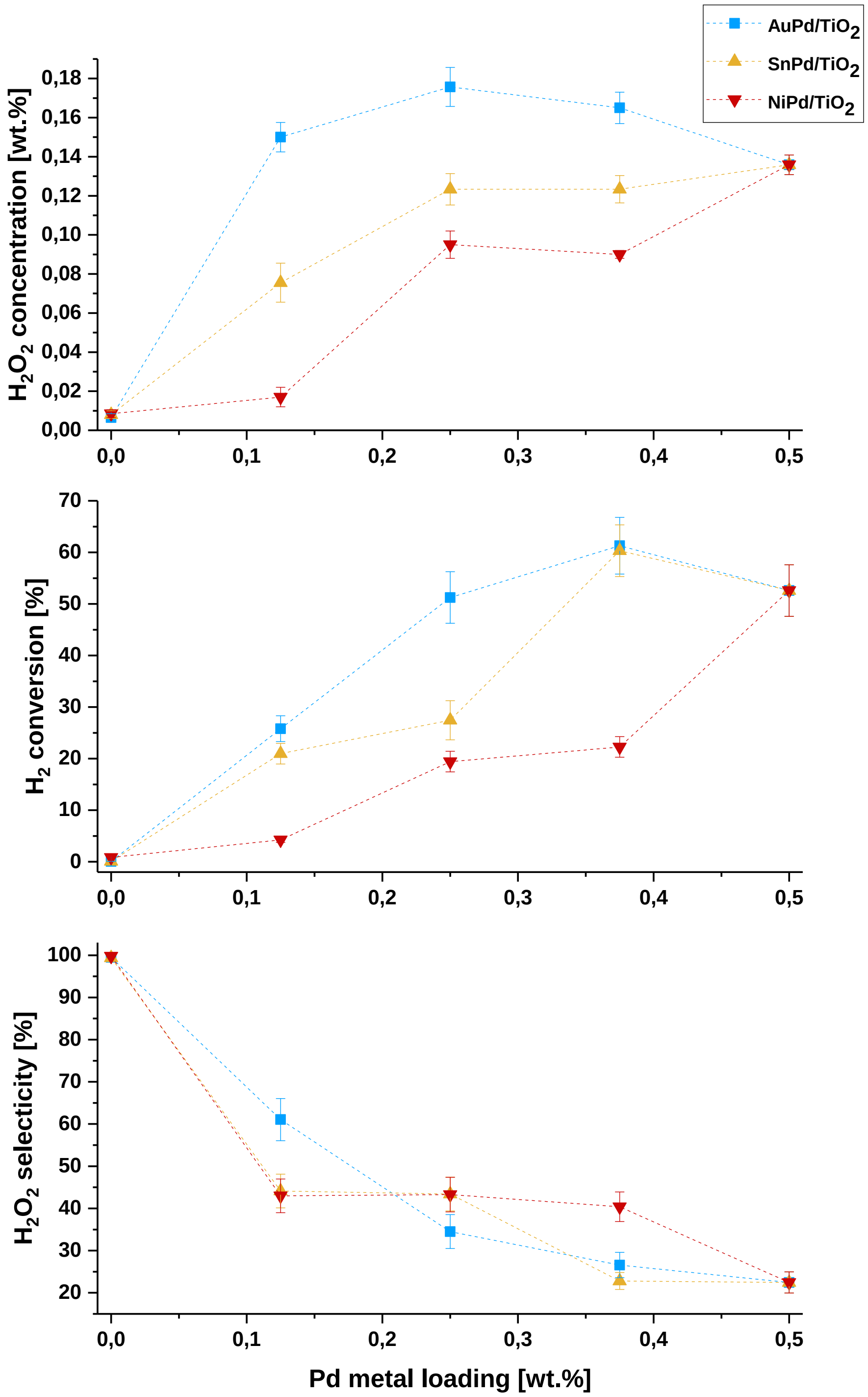

***Figure 4.9: H_2O_2 concentration, H_2 conversion and selectivity of the bimetallic 0.5wt.% AuPd, SnPd and NiPd catalysts supported on TiO_2 with varying metal ratio*.** **Reaction conditions:** 0.01 g catalyst, 2.9 g of water, 5.6 g of methanol, 2.9 MPa 5%H_2/CO_2, 1.1 MPa 25%O_2/CO_2, 0.5 h, ambient temperature, 1200 rpm

TEM characterization was carried out to investigate the effect of Au:Pd ratio on particle diameter distribution. Monometallic 0.5 wt.%Au/TiO_2 catalyst shown in Figure 4.10 a) exhibit mean particle diameter of 13 nm, with a wide particle distribution (from 4 to 21 nm) as shown in Figure 4.11. A decrease in mean particle diameter to 9.1 nm is observed for the 0.375 wt.% Au – 0.125 wt.%Pd/TiO_2 catalyst, and narrower particle diameter distribution. Further decrease in Au content to 0.25 wt.% Au – 0.25 wt.%Pd/TiO_2 results in only a few visible particles, around 10 nm, and therefore it was not possible to calculate a mean particle diameter; it is highly likely that many smaller particles are below the detection limit of the equipment. Similar correlation between Pd content and particle size was observed by Santos *et al.*, who reported a decrease in mean particle size with increasing Pd content over a series of 1 wt.% AuPd/TiO_2 catalysts prepared by modified impregnation.[31]

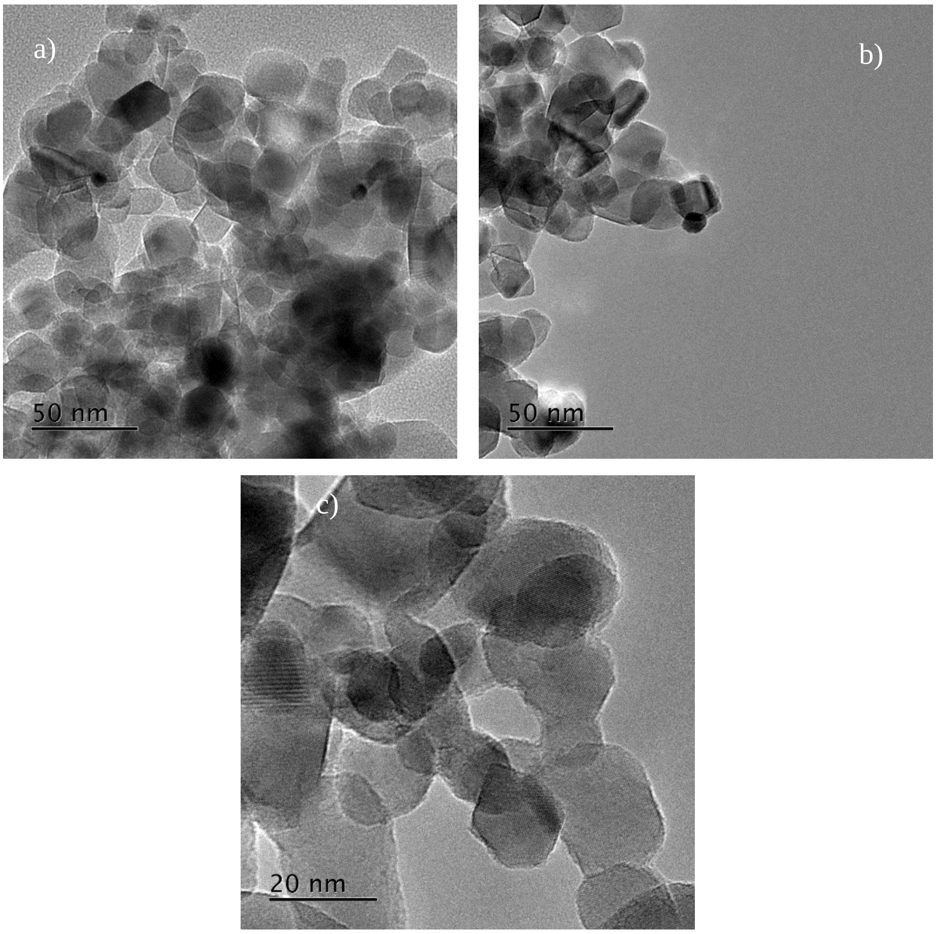

Figure 4.10**: TEM images of fresh AuPd catalysts with different Au:Pd ratio:** a) 0.5wt.%Au/TiO_2; b) 0.375wt.%Au -0.125wt.%Pd/TiO_2; c) 0.25wt.%Au -0.25wt.%Pd/TiO_2

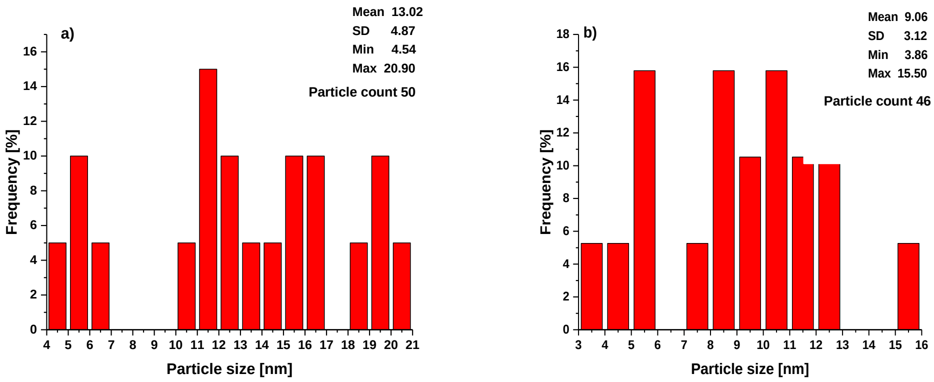

***Figure 4.11*: Particle size distribution of fresh AuPd catalysts with different metal ratio:** a) 0.5wt.%Au /TiO_2; b) 0.375wt.%Au - 0.125wt.%Pd/TiO_2.

4.2.3 Reusability of the AuPd, SnPd and NiPd catalysts supported on TiO_2 towards the direct synthesis of H_2O_2

To further investigate the stability of AuPd, SnPd and NiPd catalysts, the catalysts were investigated over repeat H_2O_2 synthesis experiments, with the results are summarised in Table 4.1. Catalysts were collected after a standard H_2O_2 synthesis reaction and dried in a vacuum oven for 16 h at 25°C, and then re-tested again using standard H_2O_2 synthesis reaction conditions. Both the 0.25 wt.%Au-0.25 wt.% Pd/TiO_2 and 0.25 wt.%Sn-0.25 wt.% Pd/TiO_2 catalysts show a significant decrease in H_2O_2 synthesis activity on second use, while the 0.25 wt.%Ni-0.25 wt.% Pd/TiO_2 catalyst shows an increase in H_2O_2 synthesis activity. A significant increase in degradation activity is observed for the 0.25 wt.%Sn-0.25 wt.% Pd/TiO_2 and 0.25 wt.%Ni-0.25 wt.% Pd/TiO_2 catalysts in the presence of 4 wt.% H_2O_2, from 0 mol_{H2O2} kg_{cat}^{-1} h^{-1} upon first use to 88 mol_{H2O2} kg_{cat}^{-1} h^{-1} and 200 mol_{H2O2} kg_{cat}^{-1} h^{-1}, respectively, upon reuse. The degradation activity of the 0.25 wt.%Au-0.25 wt.% Pd/TiO_2 remained unchanged.

Table 4.1: Synthesis and degradation activity of the re-used Pd, AuPd, SnPd and NiPd catalysts supported on TiO_2

Catalyst	**Productivity [mol_{H2O2} kg_{cat}^{-1} h^{-1}]**		**Degradation [mol_{H2O2} kg_{cat}^{-1} h^{-1}]**	
	Fresh	**used**	**Fresh**	**Used**
0.5 wt.% Pd/TiO_2	65	61	0	321
0.25 wt.%Au-0.25 wt.% Pd/TiO_2	90	53	100	102
0.25 wt.%Sn-0.25 wt.% Pd/TiO_2	62	32	0	88
0.25 wt.%Ni-0.25 wt.% Pd/TiO_2	40	48	0	200

Reaction conditions: a) H_2O_2 synthesis: 0.01 g catalyst, 2.9g of water, 5.6g of methanol 2.9 MPa 5% H_2/CO_2, 1.1 MPa 25% O_2/CO_2, 0.5 h, ambient temperature, 1200 rpm. **b) H_2O_2 degradation:** 0.01 g catalyst, 0.68 g H_2O_2, 2.9 g of water, 5.6 g of methanol 2.9 MPa 5% H_2/CO_2, 0.5 h, ambient temperature, 1200 rpm.

A decrease in H_2 conversion is also observed upon catalyst re-use, with the exception of the 0.25 wt.%Ni-0.25 wt.%Pd/TiO_2 catalyst, which shows no significant change in H_2 conversion. All catalysts show an increase in selectivity towards H_2O_2 with 0.25 wt.%Sn-0.25 wt.%Pd/TiO_2 showing the highest increase, from 43.4 % to 61.7 %, upon re-use. The 0.25 wt.% Sn – 0.25 wt.% Pd/TiO_2 catalyst also shows the lowest increase in degradation activity upon reuse, which can explain the increase in H_2O_2 selectivity.

Table 4.2: H_2 conversion and selectivity of the re-used Pd, AuPd, SnPd and NiPd catalysts supported on TiO2

Catalyst	**H_2 conversion (%)**		**H_2O_2 selectivity (%)**	
	Fresh	**Used**	**Fresh**	**Used**
0.5 wt.% Pd/TiO_2	52.6	41.8	22.5	28.9
0.25 wt.%Au-0.25 wt.% Pd/TiO_2	51.2	26.4	34.5	38.0
0.25 wt.%Sn-0.25 wt.% Pd/TiO_2	27.5	12.1	43.4	61.7
0.25 wt.%Ni-0.25 wt.% Pd/TiO_2	19.4	19.8	43.3	47.1

Reaction conditions: a) H_2O_2 synthesis: 0.01 g catalyst, 2.9 g of water, 5.6 g of methanol 2.9 MPa 5% H_2/CO_2, 1.1 MPa 25% O_2/CO_2, 0.5 h, ambient temperature, 1200 rpm. **b) H_2O_2 degradation:** 0.01 g catalyst, 0.68 g H_2O_2, 2.9 g of water, 5.6 g of methanol 2.9 MPa 5% H_2/CO_2, 0.5 h, ambient temperature, 1200 rpm.

4.2.4 Effect of reaction time on catalyst synthesis activity of AuPd and SnPd catalysts supported on TiO_2

As shown in Sections 4.2.1 and 4.2.2, combining Au and Sn with Pd enhances the catalytic activity towards H_2O_2 synthesis, as well as increasing H_2 selectivity, compared to the monometallic Pd counterpart. Therefore, catalyst performance as a function of reaction time was next studied, with an aim to maximize the use of the hydrogen gas fed to reactor, with a focus on the 0.25wt.%Au–0.25wt.%Pd/TiO_2 and 0.25wt.%Sn– 0.25wt.%Pd/TiO_2 catalysts. It should be noted that the reactant gas was not continually introduced to the reactor. For comparison, time online studies using 0.25wt.%Pd/TiO_2 and 0.5wt.%Pd/TiO_2 were also carried out to observe the effect of secondary metal addition.

As shown in Figure 4.12, after 2 min all catalysts produce similar H_2O_2 concentration (around 0.02 wt.%); however, a significant difference in H_2O_2 concentration is observed with an increase in reaction time. After 10 min, a concentration of 0.11 wt.% is achieved over the AuPd catalyst, which surpassed monometallic Pd catalysts; 0.06 wt.% H_2O_2 is produced over 0.25wt.%Pd/TiO_2 and 0.09 wt.% produced over the 0.5 wt.%Pd/TiO_2 analogue. The SnPd counterpart produces a H_2O_2 concentration of 0.08 wt.%, which was higher than obtained over 0.25 wt.%Pd/TiO_2, further highlighting the enhanced activity that can be achieved by combining Sn and Pd.

All catalysts show an increase in concentration of H_2O_2 up to 60 min, with the exception of 0.5 wt.%Pd/TiO_2, which passes through a maximum of 0.15 wt.% after 30 min. After 60 min, both the 0.25 wt.%Au-0.25 wt.%Pd/TiO_2 and 0.25 wt.%Pd/TiO_2 catalysts produce 0.21 wt.% of H_2O_2; however, a further increase in reaction time to 90 min results in a decrease in H_2O_2 concentration for 0.25 wt.%Au-0.25 wt.%Pd/$TiO_{2.}$ An increase in H_2 conversion suggests increased degradation. The result can be attributed to partial reduction of Pd^{2+}, as it is shown in Table 4.4. In comparison, both the 0.25 wt.%Sn-0.25 wt.%Pd/TiO_2 and 0.25 wt.%Pd/TiO_2 catalysts show an increase up to 90 min, with H_2O_2 concentration of 0.15 wt.% and 0.22 wt.%, respectively. Crole *et al.* reported a time study using a 2.5 wt.%Au – 2.5 wt.%Pd/TiO_2 catalyst prepared by wet impregnation, in which the majority of H_2O_2 was produced after 15 min (0.9 wt.%) and the maximum concentration (0.12 wt.%) was reached after 40 min.[34] In comparison to the catalyst prepared by Crole *et a.*, the 0.25 wt.%Au-0.25 wt.%Pd/TiO_2 catalyst in this work is more active and selective towards H_2O_2 at 10 times lower metal loading.

Higher H_2O_2 selectivities are achieved over bimetallic catalysts compared to both monometallic Pd catalysts, showing that combining Pd with a secondary metal not only increases synthesis activity of the catalyst but also increases the H_2O_2 selectivity. A H_2O_2 selectivity of 43 % is observed over the 0.25 wt.%Au-0.25 wt.%Pd/TiO_2 catalyst with a reaction time between 5 and 20 min, with a drop in selectivity to 34 % after 30 min. A further increase in reaction time results in a decrease in H_2O_2 selectivity to 25 % after 90 min. The drop in H_2O_2 selectivity can be attributed to an increase in degradation activity, as the H_2O_2 degradation will be more significant at higher H_2O_2 concentrations.[12,35] Similarly, the 0.25 wt.%Sn-0.25 wt.%Pd/TiO_2 catalyst shows a H_2O_2 selectivity of 43 % from 5 to 30 min, which dropped significantly to 26% after 60 min. In comparison, the 0.25 wt.%Pd/TiO_2 catalyst shows a more narrow distribution of H_2O_2 selectivities compared to bimetallic catalysts. Higher H_2O_2 selectivity is observed after 90 min in comparison to the bimetallic catalysts.

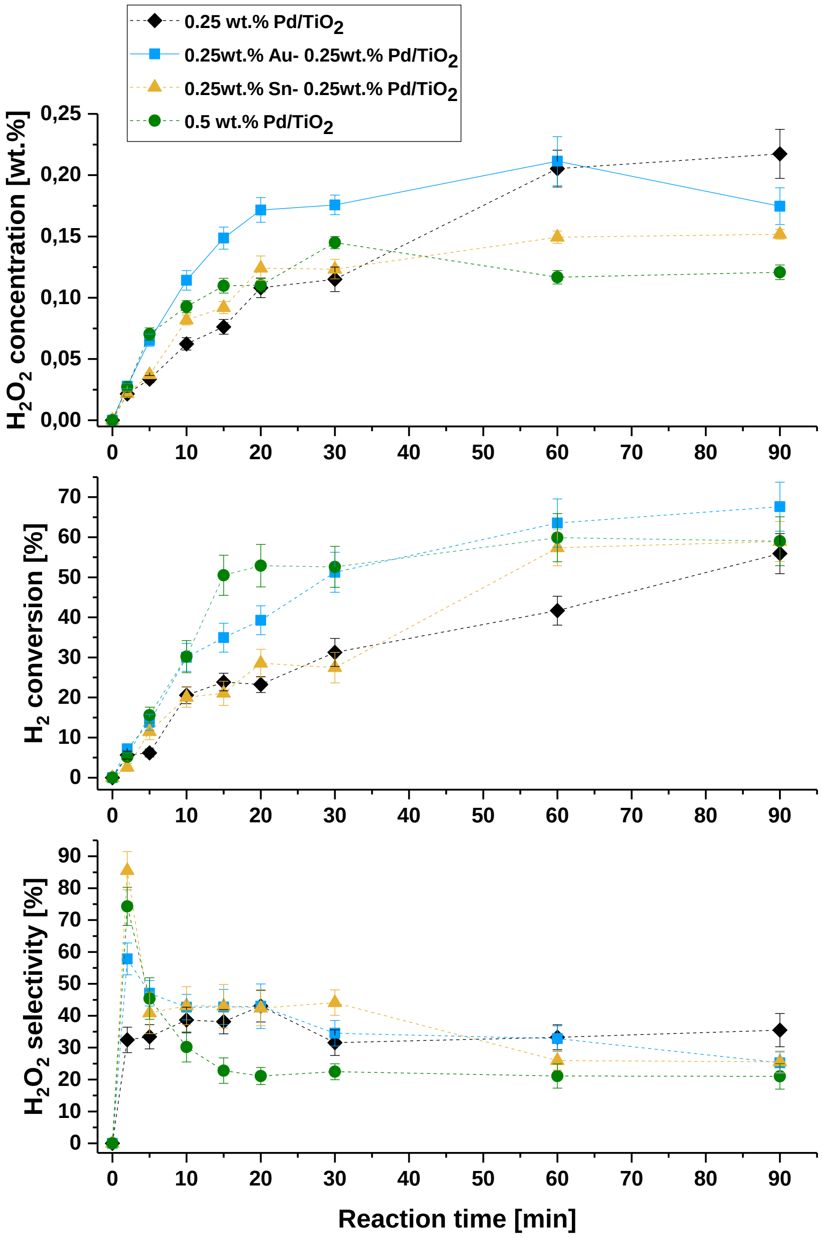

Figure 4.12: ***Effect of reaction time on catalyst activity towards direct synthesis of H_2O_2, H_2 conversion and H_2O_2 selectivity over Pd, AuPd and, SnPd supported catalysts at ambient temperature.*** **Reaction conditions:** 0.01 g catalyst, 2.9 g of water, 5.6 g of methanol 2.9 MPa 5% H_2/CO_2, 1.1 MPa 25% O_2/CO_2, ambient temperature, 1200 rpm.

Time-on-line studies were used to calculate initial rates of H_2O_2 synthesis. Calculated reaction rates at 30 min show no significant difference in activity between the 0.25wt.%Pd/TiO_2, 0.5wt.%Pd/TiO_2, and 0.25wt.%Sn-0.25wt.%Pd/TiO_2 catalysts. Initial rate of H_2O_2 synthesis are calculated at a reaction time where the contribution of H_2O_2 degradation is considered to be negligible (5 min). As shown in Table 4.3, 0.5wt.%Pd/TiO_2, and 0.25wt.%Sn-0.25wt.%Pd/TiO_2 catalysts have identical initial rates of synthesis (4597 $mol_{H_2O_2}mol_{Pd}^{-1}h^{-1}$) once the amount of H_2O_2 produced in reaction is normalised per mol of Pd used. In comparison, the 0.25wt.%Au-0.25wt.%Pd/TiO_2 catalyst shows an initial rate of reaction almost twice the Pd and SnPd catalysts tested.

Table 4.3: Initial rate of synthesis reaction over studied supported catalysts at ambient temperature.

Catalysts	**Rate of reaction** **[$mol_{H_2O_2}mol_{Pd}^{-1}h^{-1}$]**	**H_2O_2 concentration** **[wt.%]**
0.25wt.%Pd/TiO_2	4086	0.03
0.5wt.%Pd/TiO_2	4597	0.07
0.25wt.%Au-0.25wt.%Pd/TiO_2	8173	0.07
0.25wt.%Sn-0.25wt.%Pd/TiO_2	4597	0.04

Reaction conditions: 0.01 g catalyst, 2.9 g of water, 5.6 g of methanol 2.9 MPa 5% H_2/CO_2, 1.1 MPa 25% O_2/CO_2, 5 min, ambient temperature, 1200 rpm.

XPS analysis (Table 4.4) shows that partial reduction of Pd^{2+} to Pd^0 occurs with all the studied catalysts upon use. Both Pd^{2+} and Pd^0 species play an important role in H_2O_2 formation and subsequent degradation. H_2 is easily activated on Pd^0 sites, which is essential for the formation of H_2O_2.[5] However, Pd^0 sites are also active for O_2 dissociation, which leads to formation of H_2O. On the other hand, O_2 is stable on the surface of PdO and therefore formation of H_2O does not occur. It was suggested by several authors that a small fraction of the nanoparticles must exist as reduced Pd^0 in order to form H_2O_2, but a higher fraction of Pd^0 will result in increased degradation of H_2O_2.

Only Pd^{2+} is present on 0.25 wt.%Pd/TiO_2 after calcination; the introduction of secondary metal can change the surface structure of the catalyst by electronic modification of Pd atoms, or reconstructing the surface composition, and therefore affecting the oxidation state of Pd[5,36,9,11] A significant reduction in the Pd^{2+} : Pd^0 ratio is observed for all catalysts after 2 min of reaction; however, the reduction of Pd was most pronounced in the Pd-only catalyst, with only 31.8% of Pd species remaining as Pd^{2+}.

XPS analysis of the 0.25 wt.%Au-0.25 wt.%Pd/TiO_2 catalyst shows that, after calcination, Pd species are present as Pd^{2+}. Compared to 0.25 wt.%Pd/TiO_2, higher content of Pd^{2+} is present on 0.25 wt.%Au-0.25 wt.%Pd/TiO_2 catalyst throughout the time online study, with 60% Pd^{2+} after 30 min. This could explain the higher H_2O_2 selectivities compared to the monometallic Pd catalyst, as it has been reported before that Pd^0 offers higher activity towards H_2O_2 hydrogenation and decomposition than the corresponding PdO catalyst.[38,39] In contrast, the 0.25 wt.%Sn-0.25 wt.%Pd/TiO_2 catalyst show a lower content of Pd^{2+}; however, higher H_2O_2

selectivities are obtained over the 0.25 wt.%Sn - 0.25 wt.%Pd/TiO_2 catalyst compared to monometallic 0.25 wt.%Pd/TiO_2. An increased metal dispersion, changes in particle diameter, and particle structure, lead to the isolation of Pd in smaller particles that can affect catalyst activity and selectivity, and may be the cause for the enhanced performance of the PdSn catalyst. [11,13,16,33] In addition, SnO_x can activate O_2 without breaking the O-O bond, and therefore H_2O_2 can be selectively produced at the Pd/SnO_x or PdO/SnO_x interface.[11] Further work will need to be conducted to determine which of these factors is key in dictating catalyst performance.

Table 4.4: Quantified XPS data for the surface Pd atoms.

Reaction time [min]	Concentration [%]					
	0.25 wt.%Pd/TiO_2		**0.25wt.%Au-0.25wt.%Pd/TiO_2**		**0.25wt.%Sn-0.25wt.%Pd/TiO_2**	
	Pd^{2+}	**Pd^0**	**Pd^{2+}**	**Pd^0**	**Pd^{2+}**	**Pd^0**
fresh	100	0	100	0	69.7	30.3
2	31.8	68.2	60	40	39.4	60.6
5	36.8	63.2	60	40	33.3	66.6
10	35	65	62.5	37.5	35.1	64.9
15	30	70	62.5	37.5	17.4	82.6
20	25	75	66.7	33.3	25.6	74.4
30	29.4	70.6	60	40	15.1	84.9
60	29.4	70.6	57.1	42.9	13.2	86.8
90	35.7	64.3	40	60	28.6	71.4

4.2.5 Gas replacement reactions over AuPd and SnPd catalysts supported on TiO_2

Gas replacement studies were carried out to maximize the concentration of H_2O_2, with the results shown in Figure 4.13. One of the main limitations of the of the direct synthesis of H_2O_2 is the low concentration of H_2 that can be used without exceeding lower explosive limit. Gas replacement reactions partially solve low H_2 concentration limitations by continually replacing H_2 at fixed time intervals. All studied catalysts show an increase in H_2O_2 concentration up to 4 reagent gas replacements. The highest concentration of H_2O_2, 0.53 wt.%, is achieved with the 0.25wt.%Au-0.25wt.%Pd/TiO_2 catalyst after 4 gas replacements, and no further increase is achieved with additional gas replacements. Comparable concentrations of

H_2O_2, 0.49 wt.%, were produced over the 0.25wt.%Sn-0.25wt.%Pd/TiO_2 catalyst after 4 replacements.

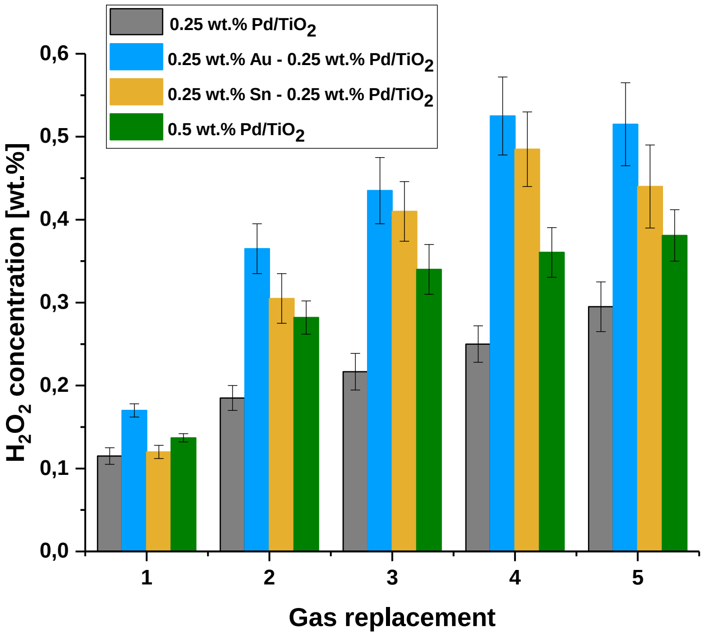

Figure 4.13: ***H_2O_2 direct synthesis gas replacement reactions over Pd, AuPd and SnPd supported catalysts*.** **Reaction conditions:** H_2O_2 synthesis: 0.01 g catalyst, 2.9 g of water, 5.6 g of methanol 2.9 MPa 5% H_2/CO_2, 1.1 MPa 25% O_2/CO_2, ambient temperature, 1200 rpm.

For comparison, 0.53 wt.% H_2O_2 was produced over the highly selective 2wt.%Sn-3wt.%Pd/TiO_2 when subjected to a sequential heat treatment that consisted of an oxidative (500°C, 3 h, air), reductive (200°C, 2 h, 5% H_2/Ar) and final oxidative (400°C, 4 h, air) step, after 5 gas replacements at 2 °C.[12] Crole *et al.* reported H_2O_2 selectivity of 95 % over a 0.5 wt.%Pd – 4.5 wt.%Ni/TiO_2 catalyst after 5 gas replacement reaction, in H_2O_2 as solvent, and with a reaction temperature of 20°C, with only 0.075 wt.% H_2O_2 produced.[40]

XPS analysis of post reaction catalysts was carried out to investigate changes in Pd oxidation state over the course of multiple gas replacements. As shown in Table 4.5, a fluctuation in Pd oxidation state is observed between gas replacement. These small changes might be caused by partial oxidation of Pd species with higher concentrations of produced H_2O_2, and subsequent reduction by replaced H_2 during the gas replacement. Both 0.25wt.%Au-0.25wt.%Pd/TiO_2 and 0.25wt.%Sn-0.25wt.%Pd/TiO_2 catalysts show a significant reduction of Pd^{2+} species after 5 gas replacements, which correlates well with the decrease in H_2O_2 concentration after 5 gas replacements. In comparison, no significant reduction of Pd^{2+} species is observed over the 0.25 wt.%Pd/TiO_2 catalyst after 5 gas replacements, with a further increase in H_2O_2 concentration after this replacement.

Table 4.5: Quantified XPS data for the surface Pd atoms.

Gas replacement	Concentration [%]					
	0.25 wt.%Pd/TiO_2		0.25wt.%Au-0.25wt.%Pd/TiO_2		0.25wt.%Sn-0.25wt.%Pd/TiO_2	
	Pd^{2+}	Pd^0	Pd^{2+}	Pd^0	Pd^{2+}	Pd^0
fresh	100	0	100	0	69.7	30.3
1	29.4	70.6	60	40	15.1	84.9
2	25.0	75.0	50	50	20.6	79.4
3	40	60	50	50	19.4	80.6
4	33.3	66.7	60	40	23.1	76.9
5	35.7	64.3	25	75	15.2	84.8

4.2.6 Effect of metal ratio on the catalyst synthesis and degradation activity

In Section 4.2.1 of this Chapter, all bimetallic catalysts were prepared by wet co-impregnation and with a 1:1 (by weight) Pd: X raio (X = Au, Sn, Ni). It has been previously shown that higher ratios of secondary metal to Pd can significantly enhance synthesis activity and selectivity of the catalyst by modifying the electronic or geometric structure of Pd.[11,12,40] In this Section, different amounts of Au, Sn or Ni were added to 0.25 wt.%/TiO_2 to prepare catalysts with different secondary metal to Pd ratios and investigate the effect on the catalyst synthesis and degradation activity.

As shown Figure 4.14, the highest synthesis activity over AuPd catalysts, 90 mol_{H2O2} kg_{cat}^{-1} h^{-1} is achieved over a 0.25 wt.%Au – 0.25 wt.Pd/TiO_2 catalyst (1:1 ratio by weight); further increasing Au content results in a decrease in synthesis activity as well as degradation activity. A decrease in synthesis activity from 56 mol_{H2O2} kg_{cat}^{-1} h^{-1} to 40 mol_{H2O2} kg_{cat}^{-1} h^{-1} is observed when Ni was added to Pd with 1:1 ratio; however, increasing Ni content beyond 0.25 wt% lead to an increase in synthesis activity to 64 mol_{H2O2} kg_{cat}^{-1} h^{-1} . As with the AuPd series, further increasing Ni content results in a decrease in synthesis activity. Similarly, Crole *et al.* reported that an increase in Ni content from 4 wt.% to 4.75 wt.% in 5 wt.% NiPd/TiO_2 catalysts resulted in a significant drop in synthesis activity as well as degradation activity of the catalyst.[40] A more interesting trend was observed over the SnPd catalyst series. A small increase in synthesis activity was obtained by increasing Sn: Pd ratio from 1:1 to 3:1 (by weight); however, a significant increase in synthesis activity to 104 and 111 mol_{H2O2} kg_{cat}^{-1} h^{-}

[1], was achieved by increasing Sn:Pd ratio to 6:1 and 9:1, respectively. Freakley *et al.* have previously reported that H_2O_2 synthesis activity passed through a maximum of 68 mol_{H2O2} kg_{cat}^{-1} h^{-1} with 2:3 Sn:Pd ratio (by weight).[12] No degradation activity in the presence of 4 wt.% H_2O_2 was obtained over 0.25 wt.%Pd/TiO_2 and any NiPd and SnPd catalyst investigated in this study. While the AuPd catalysts offer high activity towards H_2O_2 degradationat low Au: Pd ratios (100 mol_{H2O2} kg_{cat}^{-1} h^{-1} at Au:Pd =1:1), this metric was substantially decreased through the addition of more Au (6 mol_{H2O2} kg_{cat}^{-1} h^{-1} at Au:Pd =9:1).

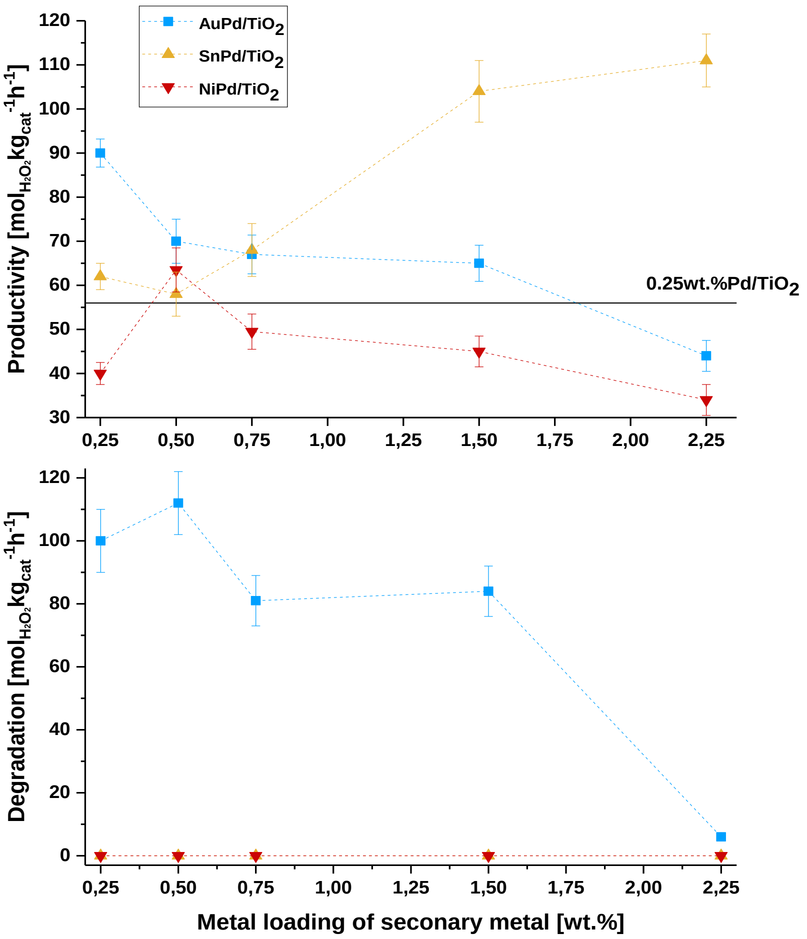

Figure 4.14: Synthesis and degradation activity of the bimetallic AuPd, SnPd and NiPd catalysts supported on TiO_2 with fixed 0.25 wt.%Pd contents and varying wt.% of secondary metal. Reaction conditions: 0.01 g catalyst, 2.9 g of water, 5.6 g of methanol, 2.9 MPa 5% H_2/CO_2, 1.1 MPa 25% O_2/CO_2, 0.5 h, ambient temperature, 1200 rpm. Solid black line in the Figure represents synthesis activity of 0.25 wt.%Pd/TiO_2.

As illustrated in Figure 4.15, a decrease in H_2 conversion is observed with increasing Au and Ni content, which is in agreement with the decreasing synthesis activity of these catalysts, and in the case of AuPd catalysts also with decreasing degradation activity. In comparison, an opposite trend in H_2 conversion is observed with SnPd catalysts; H_2 conversion increases with

Sn content even up to 2.25 wt.% Sn, showing that SnPd catalyst are more active compared to AuPd and NiPd counterparts.

H_2O_2 selectivity over the AuPd catalysts passes through a maximum of 57% with 6:1 Au:Pd ratio (by weight), while the NiPd catalysts show a similar increase in H_2O_2 selectivity up to Ni:Pd ratio of 9:1 (63%). The H_2O_2 selectivtiy of the SnPd catalysts also increases to 52% with a Sn: Pd ratio of 9:1.

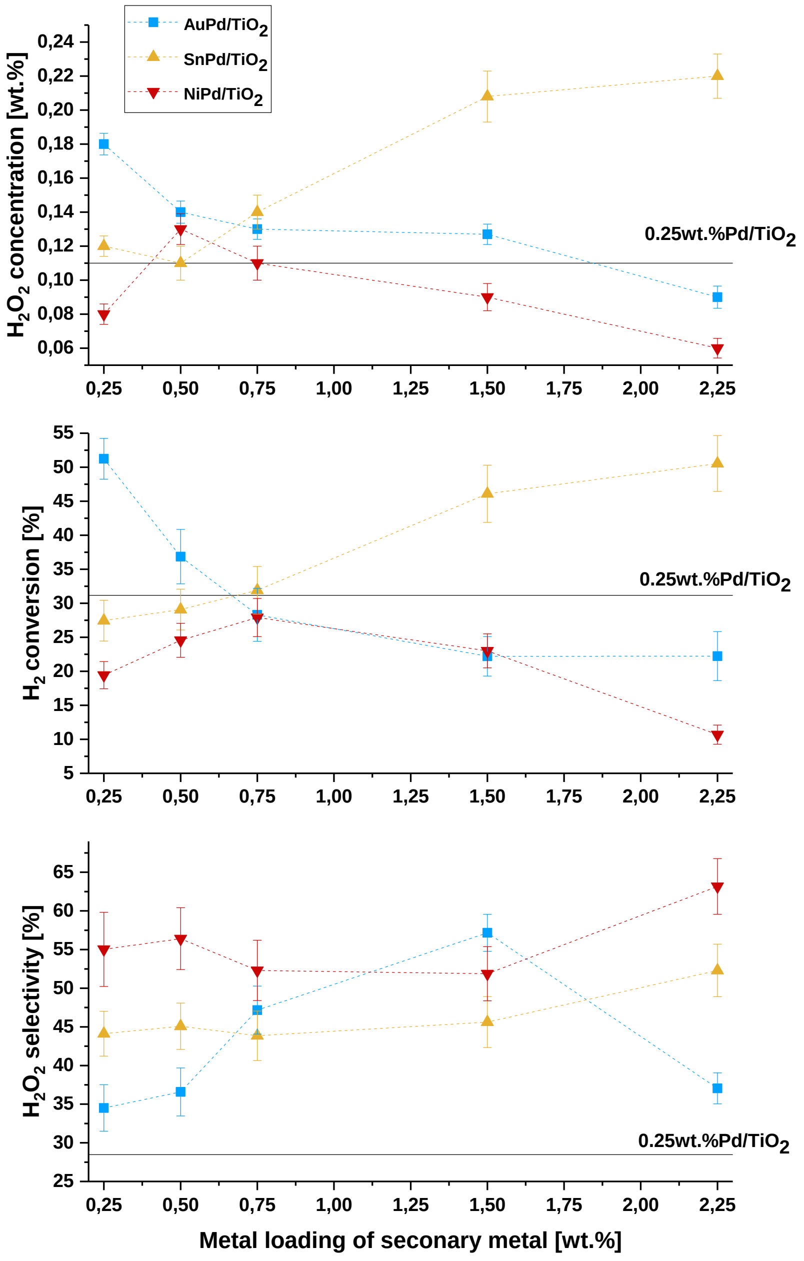

Figure 4.15: Concentrations of H_2O_2, H_2 conversion and H_2O_2 selectivity of the bimetallic AuPd, SnPd and NiPd catalysts supported on TiO_2 with varying secondary metal to Pd ratio obtained in synthesis reaction. **Reaction conditions:** 0.01 g catalyst, 2.9 g

of water, 5.6 g of methanol, 2.9 MPa 5% H_2/CO_2, 1.1 MPa 25% O_2/CO_2, 0.5 h, ambient temperature, 1200 rpm. Straight line in the Figure represents H_2 conversion and selectivity of 0.25 wt.%Pd/TiO_2.

4.2.7 Further investigation of the 2.25 wt.% Sn – 0.25 wt.%Pd/TiO$_2$ catalyst

As shown is Section 4.2.6, the 2.25 wt.% - 0.25 wt.%Pd/TiO_2 catalyst shows a significant increase in both catalyst activity and H_2O_2 selectivity compared to the 0.25 wt.%Sn – 0.25 wt.%Pd/TiO_2 analogue. A time-on-line study was carried out to maximize the use of hydrogen gas fed to reactor. Gas replacement reactions were also carried out to maximise the H_2O_2 concentration obtained over this catalyst. Freakley *et al.* reported that subjecting 2 wt.%Sn – 3 wt.% Pd/TiO_2 to extensive heat treatment, consisting of oxidative, reductive, and oxidative steps results in highly selective catalyst towards H_2O_2.[12,40] Therefore, a series of heat treatments were carried out to investigate the effect on catalyst synthesis activity and reusability.

4.2.7.1 Effect of reaction time on synthesis activity of 2.25 wt.% Sn – 0.25 wt.%Pd/TiO$_2$ catalyst

Time-on-line studies were carried out with the 2.25 wt.% Sn- 0.25wt.%Pd/TiO_2 catalyst to maximize the H_2 feed and H_2O_2 concentration achieved over this catalyst. As shown in Figure 4.16, a H_2O_2 concentration of 0.11 wt.% is produced after 5 min of reaction, which is higher than the concentration obtained with the 0.25 wt.%Sn – 0.25 wt.%Pd/TiO_2 catalyst after 15 min reaction. After 30 min, the H_2O_2 concentration increases to 0.25 wt.%, which is double the concentration achieved by the 0.25 wt.%Sn – 0.25 wt.%Pd/TiO_2 analogue over the same reaction time. H_2O_2 concentration passes through a maximum of 0.27 wt.% after 60 min, and increasing reaction time beyond this time resulted in decrease in H_2O_2 concentration. Negligible changes in H_2 conversion after 60 min suggest possible deactivation of the catalyst, or limited availability of the H_2 in solvent system.

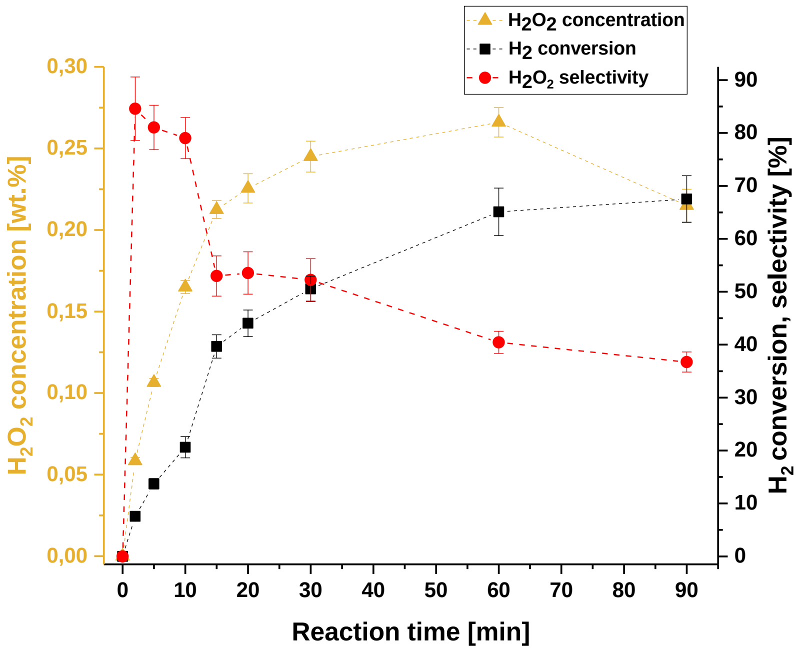

Figure 4.16: ***Time-on-line study over 2.25 wt.%Sn–0.25 wt.Pd/TiO_2 at ambient temperature.*** Reaction conditions: 0.01 g catalyst, 2.9 g of water, 5.6 g of methanol 2.9 MPa 5% H_2/CO_2, 1.1 MPa 25% O_2/CO_2, ambient temperature, 1200 rpm.

H_2 conversion over the 2.25 wt.% Sn – 0.25 wt.%Pd/TiO_2 catalyst is increasing with time, to 68% after 90 min reaction. High H_2O_2 selectivities (above 80%) are obtained within the first 10 min of the study, where the rate of H_2O_2 degradation is lower due to low concentrations of H_2O_2. A significant drop in selectivity is observed after 15 min to 53%. A further decrease in H_2O_2 selectivity with increasing reaction time is observed beyond 15 min. In comparison with the time-on-line study of the 0.25 wt.%Sn-0.25 wt.%Pd/TiO_2 catalyst, presented in Figure 4.12, higher H_2O_2 selectivities are obtained over 2.25 wt.%Sn-0.25 wt.%Pd/TiO_2 in the studied reaction time range.

It has been previously reported that low reaction temperatures result in a higher H_2O_2 selectivity as lower rates of H_2O_2 degradation are observed.[23,41,42] To investigate the effect of the reaction temperature on synthesis activity and selectivity for 2.25 wt.% - 0.25wt.%Pd/TiO_2, a time-on-line study at 2 °C was carried out and results are shown in Figure 4.17. A similar trend in H_2 conversion and H_2O_2 selectivity is observed during the time-on-line study at 2°C and ambient temperature; however, significantly lower H_2O_2 concentrations are achieved at 2 °C during the first 30 min. After 30 min, 0.11 w.% of H_2O_2 is produced, which represents less than half of the concentration produced at ambient temperature (0.25wt.%) within the same reaction time. After 60 min, a comparable H_2O_2 concentration is achieved at both temperatures studied. An increase in H_2O_2 concentration is observed up to

180 min, with 0.41 wt.% of H_2O_2 produced. A further increase in reaction time results in a decrease in H_2O_2 concentration. In comparison, maximum H_2O_2 concentration obtained at room temperature is only 0.27 wt.%.

An increase in H_2 conversion (up to 79 %) is observed up to 180 min and remains unchanged up to 210 min suggesting limited H_2 in the reaction mixture. After 15 min, H_2O_2 selectivity in the time online study obtained at 2°C surpasses selectivity obtained at ambient temperature, demonstrating a positive effect of the low reaction temperature.

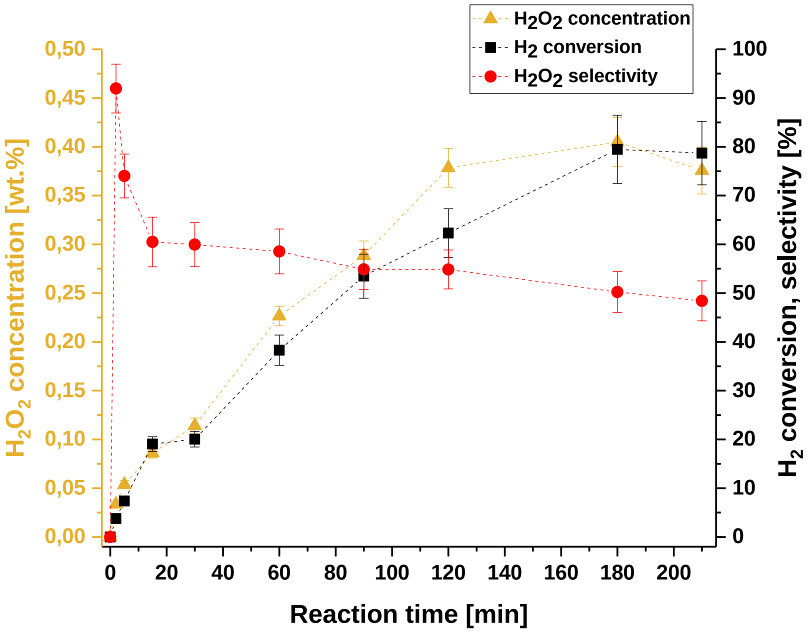

Figure 4.16: ***Time-on-line study over 2.25 wt.%Sn–0.25 wt.Pd/TiO_2 at 2°C.*** Reaction conditions: 0.01 g catalyst, 2.9 g of water, 5.6 g of methanol 2.9 MPa 5% H_2/CO_2, 1.1 MPa 25% O_2/CO_2, 2°C, 1200 rpm.

4.2.7.2 Effect of gas replacement reaction on synthesis activity of 2.25 wt.%Sn-0.25wt.%Pd/TiO_2

Gas replacement reactions were also carried out to maximise the H_2O_2 concentration obtained over the 2.25wt.%Sn- 0.25wt.%Pd/TiO_2 catalyst. As shown in Figure 4.17, H_2O_2 concentration is doubled after the 2nd gas replacement; however, a significantly lower increases in H_2O_2 concentration is observed after following gas replacements. An increase in H_2O_2 concentration is observed even after 5th gas replacement, resulting in H_2O_2 concentration of 0.69 wt.%, which is more than double the maximum concentration obtained after 60 min on-stream at ambient temperature; and almost double the concentration obtained after 210 min on-stream at 2°C with the same catalyst. During the on-stream reaction, the gas is not continuously charged, while in the gas replacement reaction the gas is re-charged with each replacement. This suggests that no change in H_2 conversion occurs beyond a certain point in an on-stream reaction, caused by low concentration of H_2 in system rather than deactivation of the catalyst. In contrast the 0.25 wt.%Sn-0.25 wt.%Pd/TiO_2 catalyst shows an increase in H_2O_2 concentration up to 3 gas replacement, but H_2O_2 concentration decreases after the 5th replacement.

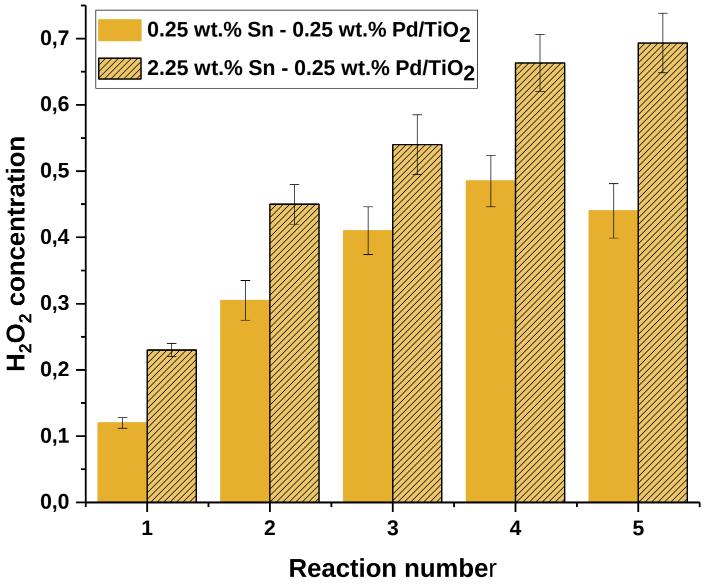

Figure 4.17: ***H_2O_2 direct synthesis top up reactions over* 2.25wt.%Sn- 0.25wt.%Pd/TiO_2 *at ambient temperature.*** Reaction conditions:0.01 g catalyst, 2.9 g of water, 5.6 g of methanol 2.9 MPa 5% H_2/CO_2, 1.1 MPa 25% O_2/CO_2, ambient temperature, 1200 rpm.

4.2.7.3 Effect of heat treatment on synthesis activity and reusability of 2.25wt.%Sn – 0.25 wt.%Pd/TiO_2

The 2.25 wt.%Sn – 0.25 wt.%Pd/TiO_2 catalyst was subjected to ORO heat treatment to investigate the effect of different heat treatments on catalyst activity and reusability. The highest synthesis activity of 111 mol_{H2O2} kg_{cat}^{-1} h^{-1} is achieved when 2.25 wt.%Sn-0.25 wt.%Pd/TiO_2 was calcined at 400 °C; as shown in Table 4.6, reduction (200 °C, 5% H_2/Ar) of a calcined catalyst (OR) and additional oxidation (400 °C, static air) of the oxidised-reduced catalyst (ORO) results in a decrease in catalyst activity. An increase in degradation activity in the presence of 4 wt.% H_2O_2 is observed, to 41 mol_{H2O2} kg_{cat}^{-1} h^{-1}, after catalyst reduction, and is decreased back to 0 mol$_{H2O2}$ kg$_{cat}^{-1}$ h^{-1} after subsequent calcination of the reduced catalyst at 400 ^{o}C. O_2 can be easily dissociated on Pd^0 sites but is more stable on the surfaces of PdO, and therefore the higher degradation activity towards H_2O_2 over reduced form of the catalyst compared to re-oxidised form can be attributed to higher content of Pd^0 on the surface.[5,43] A significant decrease in synthesis activity and an increase in degradation activity over the 2.25 wt.%Sn – 0.25 wt.%Pd/TiO_2 catalyst is observed after re-use of the catalyst with all the studied heat treatments. The highest synthesis activity is shown after re-use of the catalyst subjected to OR heat treatment, and the lowest degradation activity upon re-use is obtained with only calcined catalyst (O). The decrease in synthesis activity can be attributed to a reduction of Pd^{2+} species as well as possible morphological changes of particles during the synthesis reaction.

Table 4.6: Re-usability of the 2.25 wt.%Sn-0.25 wt.%Pd/TiO$_2$ catalysts at ambient temperature made by wet impregnation subjected to different heat treatments.

Heat treatment	Productivity [mol$_{H2O2}$ kg$_{cat}^{-1}$ h^{-1}]		Degradation [mol$_{H2O2}$ kg$_{cat}^{-1}$ h^{-1}]	
	fresh	**used**	**fresh**	**used**
O	111	30	0	87
OR	100	59	41	214
ORO	92	39	0	154

Reaction conditions: 0.01 g catalyst, 2.9 g of water, 5.6 g of methanol 2.9 MPa 5% H_2/CO_2, 1.1 MPa 25% O_2/CO_2, 5 min, ambient temperature, 1200 rpm.
Heat treatment: O (400 ^{o}C, 3 h, static air), OR (400 ^{o}C, 3 h, static air; 200 ^{o}C, 2 h, 5% H_2/Ar), ORO (400 ^{o}C, 3 h, static air; 200 ^{o}C, 2 h, 5% H_2/Ar; 400 ^{o}C, 3 h, static air),

The effect of the ORO heat treatment on H_2 conversion and selectivity of 2.25 wt.%Sn- 0.25 wt.%Pd/TiO_2 is summarised in Table 4.7. The highest H_2 conversion is obtained over the catalyst subjected to an OR heat treatment, which can be related to increased degradation activity of this catalyst. Pd^0 can break the O_2 bond, which leads to formation of H_2O, consuming H_2. Both O and ORO treatments result in higher H_2O_2 selectivity than the reduced catalyst, subjected to OR treatment, because of the higher Pd^{2+} content. A lower H_2O_2 degradation rate is associated with PdO compared to reduced Pd^0 species.[5,44,45] Upon the re-use of the catalysts, a decrease in H_2 conversion and selectivity was exhibited with all the heat treatments.

Table 4.7: Re-usability of the 2.25 wt.%Sn-0.25 wt.%Pd/TiO$_2$ catalysts at ambient temperature made by wet impregnation subjected to different heath treatments.

Heat treatment	H_2 conversion [%]		H_2O_2 selectivity [%]	
	fresh	**used**	**fresh**	**used**
O	50.5	19.3	52.2	41.3

OR	67.4	37.8	29.9	29.7
ORO	38.7	20.5	49.5	39.2

Reaction conditions: 0.01 g catalyst, 2.9 g of water, 5.6 g of methanol 2.9 MPa 5% H_2/CO_2, 1.1 MPa 25% O_2/CO_2, 5 min, ambient temperature, 1200 rpm.
Heath treatment: O (400 ºC, 3 h, static air), OR (400 ºC, 3 h, static air; 200 ºC, 2 h, 5% H_2/Ar), ORO (400 ºC, 3 h, static air; 200 ºC, 2h, 5% H_2/Ar; 400 ºC, 3 h, static air),

Results in Table 4.6 and Table 4.7 showed that the best performing catalyst are calcined only, and additional heat treatment steps resulted in an increase in degradation activity or decrease in synthesis activity and H_2O_2 selectivity. Additional heat treatment steps did not improve the performance of the catalyst upon the reuse.

4.2.8 Effect of total metal loading with fixed Sn:Pd ratio

As shown in this Chapter, a Sn:Pd metal ratio of 9:1 (2.25 wt.%Sn – 0.25 wt.%Pd/TiO_2) results in a significant increase in activity and selectivity compared to the 1:1 ratio (by weight). To further investigate this effect, catalysts with different total metal loading were prepared by wet impregnation, with the fixed Sn:Pd metal ratio (by weight) of 9:1. Figure 4.18 illustrates that the synthesis activity passes through a maximum of 111 $mol_{H2O2}\ kg_{cat}^{-1}\ h^{-1}$ with a Sn metal loading of 2.5 wt.%, and decreases with further increase in catalyst metal loading. No degradation activity is observed in the presence of 4 wt.% H_2O_2 up to a total metal loading of 7.5 wt.%. As shown in Figure 4.19, an increase in H_2 conversion is observed with metal loading. A significant increase in H_2 conversion, from 3.5% to 50.5 % is obtained with increase in total metal loading from 1.25 wt.% to 2.5 wt.%, which is in agreement with the significant increase in synthesis activity of the catalyst. In comparison, H_2O_2 selectivity decreases with increasing total metal loading up to 7.5 wt.%. High selectivities of 92% and 85% are obtained with lower total metal loadings of 0.625 wt.% and 1.25 wt.%, respectively. A significant drop in H_2O_2 selectivity, to 52 %, is observed with a further increase in total metal loading to 2.5 wt.%.

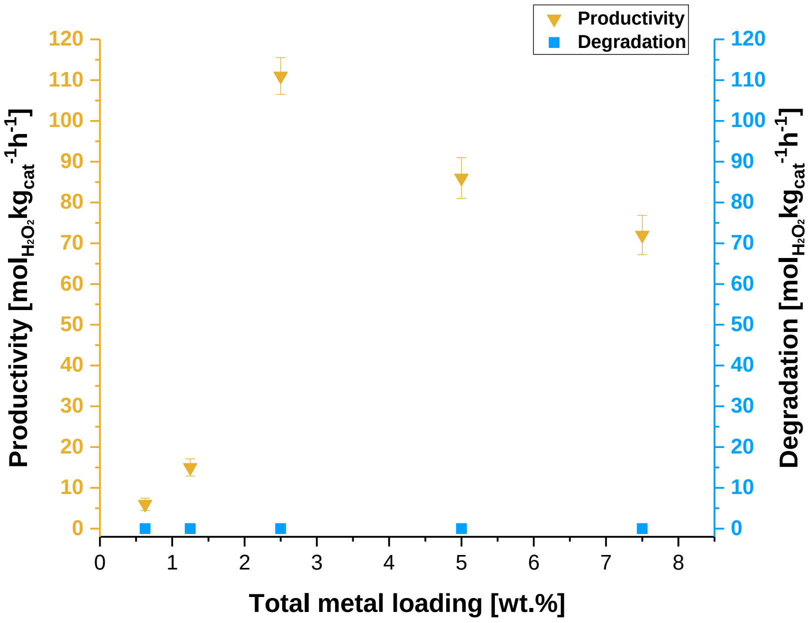

Figure 4.18: ***Effect of total metal loading on synthesis and degradation activity of the catalyst with fixed Sn:Pd metal ratio (9:1) at ambient temperature.*** Reaction conditions:0.01 g catalyst, 2.9 g of water, 5.6 g of methanol 2.9 MPa 5% H_2/CO_2, 1.1 MPa 25% O_2/CO_2, ambient temperature, 0.5 h, 1200 rpm.

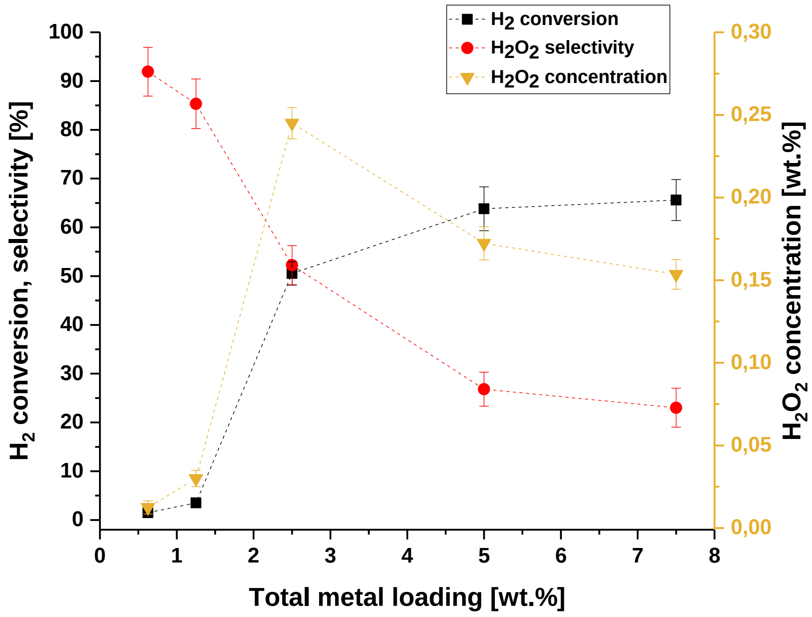

Figure 4.19: ***Effect of total metal loading on H_2 conversion and H_2O_2 selectivity of the catalyst with fixed Sn:Pd metal ratio (9:1) at ambient temperature.*** Reaction conditions:0.01 g catalyst, 2.9 g of water, 5.6 g of methanol 2.9 MPa 5% H_2/CO_2, 1.1 MPa 25% O_2/CO_2, ambient temperature, 0.5 h, 1200 rpm.

4.3 Conclusions

The effect of the addition of secondary metals (Au, Sn, Ni) in to a Pd catalyst, on catalytic performance towards H_2O_2 synthesis and degradation, was investigated in this Chapter. The addition of Au to Pd increases the synthesis activity up to 0.5 wt.% metal loading, with a synthesis activity of 90 mol_{H2O2} kg_{cat}^{-1} h^{-1}, and optimal Au:Pd determined to be 1:1. Addition of Sn results also in an enhancement in synthesis activity, with optimal metal loading of 1 wt.% and synthesis activity of 87 mol_{H2O2} kg_{cat}^{-1} h^{-1}. In comparison, addition of Ni showed at low concentrations a decrease in synthesis activity, but a further increase in Ni loading results in an enhancement in synthesis activity. The addition of Au, Sn and Ni also results in an enhancement in H_2O_2 selectivity. The enhancement in catalysts activity and selectivity is attributed to modification of the Pd electronic structure and ensemble effect of Pd-X (X=Au,Sn,Ni) particles evidenced by the XPS and TEM. Time-on-line studies were carried out to maximize the use of H_2 in gas feed. A H_2O_2 concentration of 0.21 wt.% was produced after 60 min with 0.25 wt.%Au – 0.25 wt.%Pd/TiO_2, and 0.15 wt.% with 0.25 wt.%Sn-0.25 wt.%Pd/TiO_2. Gas replacement reactions were carried out to maximise H_2O_2 concentration and, after 4 gas replacement, 0.53 wt.% of H_2O_2 is produced over 0.25 wt.%Au – 0.25 wt.%Pd/TiO_2, and 0.49 wt.% over 0.25 wt.%Sn – 0.25 wt.%Pd/TiO_2.

Different amounts of Au, Sn or Ni were added to a 0.25 wt.%/TiO_2 catalyst to prepare catalysts with different secondary metal to Pd ratios and investigate the effect on the synthesis and degradation activity. The optimal Au:Pd ratio is 1:1 with synthesis activity of 90 mol_{H2O2} kg_{cat}^{-1} h^{-1}; a decrease in synthesis activity occurs with increasing Au:Pd ratio, a decrease in degradation activity was also observed with increasing Au content. The maximum synthesis activity of the NiPd/TiO_2 catalyst was 64 mol_{H2O2} kg_{cat}^{-1} h^{-1}, with a 2:1 Ni:Pd ratio. The SnPd/TiO_2 series showed an increase in synthesis activity with increasing Sn:Pd ratio, with a maximum synthesis activity of 111 mol_{H2O2} kg_{cat}^{-1} h^{-1} achieved with 9:1 ratio.

The best performing catalyst, 2.25 wt.%Sn – 0.25 wt.%Pd/TiO_2, was further investigated through a time-on-line study and gas replacement reactions. Time-on-line studies were carried out at two different temperatures: 2 °C, which is a favourable temperature for direct synthesis of H_2O_2, and ambient temperature, which is more desirable temperature for industrial applications. A H_2O_2 concentration of 0.27 wt.% was produced after 60 min at ambient temperature, and decreased with further increase in reaction time. An increase in H_2O_2 concentration is observed even after 180 min at 2 °C, up to 0.41 wt.%. A maximum H_2O_2 concentration is observed of 0.69 wt.%, achieved after 5 gas replacement reaction over this catalyst. As the 9:1 Sn:Pd ratio shows to be optimal, a series of SnPd catalysts with this ratio and different metal loading were prepared. The 2.5 wt.% Sn loading was found to be best.

4.4 References

1 W. Weber and T. Assiertons, *US Pat., Pat. 1108752.*

2 D. P. Dissanayake and J. H. Lunsford, *J. Catal.*, 2003, **214**, 113–120.

3 J. S. Adams, A. Chemburkar, P. Priyadarshini, T. Ricciardulli, Y. Lu, V. Maliekkal, A. Sampath, S. Winikoff, A. M. Karim, M. Neurock and D. W. Flaherty, *Science*, 2021, **371**, 626–632.

4 N. M. Wilson and D. W. Flaherty, *J. Am. Chem. Soc.*, 2016, **138**, 574–586.

5 L. Ouyang, P. F. Tian, G. J. Da, X. C. Xu, C. Ao, T. Y. Chen, R. Si, J. Xu and Y. F. Han, *J. Catal.*, 2015, **321**, 70–80.

6 P. Tian, L. Ouyang, X. Xu, C. Ao, X. Xu, R. Si, X. Shen, M. Lin, J. Xu and Y.-F. Han, *J. Catal.*, 2017, **349**, 30–40.

7 J. K. Edwards and G. J. Hutchings, *Angew. Chemie - Int. Ed.*, 2008, **47**, 9192–9198.

8 J. K. Edwards, S. J. Freakley, A. F. Carley, C. J. Kiely and G. J. Hutchings, *Acc. Chem. Res.*, 2013, **47**, 845–854.

9 Y. F. Han, Z. Zhong, K. Ramesh, F. Chen, L. Chen, T. White, Q. Tay, S. N. Yaakub and Z. Wang, *J. Phys. Chem. C*, 2007, **111**, 8410–8413.

10 S. Wang, D. E. Doronkin, M. Hähsler, X. Huang, D. Wang, J. D. Grunwaldt and S. Behrens, *ChemSusChem*, 2020, **13**, 3243–3251.

11 F. Li, Q. Shao, M. Hu, Y. Chen and X. Huang, *ACS Catal.*, 2018, **8**, 3418–3423.

12 S. J. Freakley, Q. He, J. H. Harrhy, L. Lu, D. A. Crole, D. J. Morgan, E. N. Ntainjua, J. K. Edwards, A. F. Carley, A. Y. Borisevich, C. J. Kiely and G. J. Hutchings, *Science*, 2015, **351**, 279–296.

13 S. Maity and M. Eswaramoorthy, *J. Mater. Chem. A*, 2016, **4**, 3233–3237.

14 D. Ding, X. Xu, P. Tian, X. Liu, J. Xu and Y. F. Han, *Cuihua Xuebao/Chinese J. Catal.*, 2018, **39**, 673–681.

15 S. Wang, K. Gao, W. Li and J. Zhang, *Appl. Catal. A Gen.*, 2017, **531**, 89–95.

16 S. Han, Y. Liu, J. Li, R. Li, F. Yuan and Y. Zhu, *Catal. 2018, 8.*

17 D. Ding, X. Xu, P. Tian, X. Liu, J. Xu and Y. F. Han, *Cuihua Xuebao/Chinese J. Catal.*, 2018, **39**, 673–681.

18 N. Gemo, S. Sterchele, P. Biasi, P. Centomo, P. Canu, M. Zecca, A. Shchukarev, K. Kordás, T. O. Salmi and J. P. Mikkola, *Catal. Sci. Technol.*, 2015, **5**, 3545–3555.

19 S. Kim, D. W. Lee and K. Y. Lee, *J. Mol. Catal. A Chem.*, 2014, **391**, 48–54.

20 G. H. Han, G. P. Lee and K. Y. Lee, *Catal. Today*, 2020, **352**, 262–269.

21 A. Pashkova, R. Dittmeyer, N. Kaltenborn and H. Richter, *Chem. Eng. J.*, 2010, **165**, 924–933.

22 J. K. Edwards, J. Pritchard, M. Piccinini, G. Shaw, Q. He, A. F. Carley, C. J. Kiely and G. J. Hutchings, *J. Catal.*, 2012, **292**, 227–238.

23 Q. Liu and J. H. Lunsford, *Appl. Catal. A Gen.*, 2006, **314**, 94–100.

24 J. K. Edwards, E. Ntainjua N, A. F. Carley, A. A. Herzing, C. J. Kiely and G. J. Hutchings, *Angew. Chemie Int. Ed.*, 2009, **48**, 8512–8515.

25 J. K. Edwards, A. F. Carley, A. A. Herzing, C. J. Kiely and G. J. Hutchings, *Faraday Discuss.*, 2008, **138**, 225–239.

26 J. K. Edwards, A. Thomas, A. F. Carley, A. A. Herzing, C. J. Kiely and G. J. Hutchings, *Green Chem.*, 2008, **10**, 388–39.

27 J. Brehm, R. J. Lewis, D. J. Morgan, T. E. Davies and G. J. Hutchings, *Catal. Letters,2021*.

28 J. K. Edwards, B. E. Solsona, P. Landon, A. F. Carley, A. Herzing, C. J. Kiely and G. J. Hutchings, *J. Catal.*, 2005, **236**, 69–79.

29 J. K. Edwards and G. J. Hutchings, *Angew. Chemie - Int. Ed.*, 2008, **47**, 9192–9198.

30 P. Landon, P. J. Collier, A. F. Carley, D. Chadwick, A. J. Papworth, A. Burrows, C. J. Kiely and G. J. Hutchings, *Phys. Chem. Chem. Phys.*, 2003, **5**, 1917–1923.

31 A. Santos, R. J. Lewis, G. Malta, A. G. R. Howe, D. J. Morgan, E. Hampton, P. Gaskin and G. J. Hutchings, *Ind. Eng. Chem. Res.*, 2019, **58**, 12623–12631.

32 J. Pritchard, L. Kesavan, M. Piccinini, Q. He, R. Tiruvalam, N. Dimitratos, J. A. Lopez-Sanchez, A. F. Carley, J. K. Edwards, C. J. Kiely and G. J. Hutchings, *Langmuir*, 2010, **26**, 16568–16577.

33 J. H. Lee, S. K. Kim, I. Y. Ahn, W. J. Kim and S. H. Moon, *Korean J. Chem. Eng.*, 2012, **29**, 169–172.

34 D. A. Crole, S. J. Freakley, J. K. Edwards and G. J. Hutchings, *Proc. R. Soc. A Math. Phys. Eng. Sci.*, 2016, **472.**

35 Y. Voloshin, J. Manganaro and A. Lawal, *Ind. Eng. Chem. Res.*, 2008, **47**, 8119–8125.

36 D. W. Flaherty, *ACS Catal.*, 2018, **8**, 1520–1527.

37 V. R. Choudhary, A. G. Gaikwad and S. D. Sansare, *Catal. Letters*, 2002, **83**, 235–239.

38 V. R. Choudhary, C. Samanta and T. V. Choudhary, *Appl. Catal. A Gen.*, 2006, **308**, 128–133.

39 V. R. Choudhary and P. Jana, *Catal. Commun.*, 2008, **9**, 1624–1629.

40 D. A. Crole, R. Underhill, J. K. Edwards, G. Shaw, S. J. Freakley, G. J. Hutchings and R. J. Lewis, *Philos. Trans. R. Soc. A Math. Phys. Eng. Sci.*

41 B. E. Solsona, J. K. Edwards, P. Landon, A. F. Carley, A. Herzing, C. J. Kiely and G. J. Hutchings, *Chem. Mater.*, 2006, **18**, 2689–2695.

42 M. Piccinini, E. Ntainjua N., J. K. Edwards, A. F. Carley, J. A. Moulijn and G. J. Hutchings, *Phys. Chem. Chem. Phys.*, 2010, **12**, 2488–2492.

43 V. R. Choudhary, C. Samanta and P. Jana, *Appl. Catal. A Gen.*, 2007, **332**, 70–78.

44 V. R. Choudhary and P. Jana, *Appl. Catal. A Gen.*, 2009, **352**, 35–42.

45 V. R. Choudhary, C. Samanta and T. V. Choudhary, *J. Mol. Catal. A Chem.*, 2006, **260**, 115–120.

46 F. Gao and D. W. Goodman, *Chem. Soc. Rev.*, 2012, **41,** 8009-8020.

47 C.W. Yi, K. Luo, T. Wie, and D.W.Goodman, *J. Phys. Chem.,* 2005, **109**, 18535-18540.

48 A.M. Venezia, V. La Parola, G. Deganello, B. Pawelec, and J.L.G. Fierro, *Jour. of Cat.*, 2003, **215**, 317-325.

49 D.W. Yuan, X. G. Gong and R.Q. Wu, *J. Phys. Chem. C,* 2008, **112,** 1539**.**

Chapter 5

Conclusion and future work

5.1 Conclusions for Chapter 3.

Currently most industrially produced H_2O_2 is by an anthraquinone auto oxidation process (AO process).[1,2] This process has been industrially used for several decades due to the high yield of H_2O_2 per cycle. The main disadvantages of the AO process are its use of complex organic solvents as the working solution, deactivation of the hydrogenation catalyst, and the need for the continual replacement the anthraquinone H_2 carrier, due to over hydrogenation.[2,3] The anthraquinone process is only economically viable via large scale production and highly concentrated solutions of H_2O_2 (70 wt. %) are obtained, despite most applications use solutions with low concentration of H_2O_2, around 2 to 8 wt. %.[4]

The direct synthesis of H_2O_2 from hydrogen and oxygen in the presence of a catalyst potentially offers an environmentally friendly, more atom-efficient alternative to the current commercial production and in addition it overcomes the extensive disadvantages of the anthraquinone process. However, it also presents some significant challenges for industrial application. In particular the subsequent degradation of H_2O_2 to H_2O via decomposition and hydrogenation often result in low H_2O_2 concentration and selectivity. In order to operate in safe conditions, the reaction is carried out below the lower explosive limit (5 v/v % for H_2 in O_2), which means the reagent gases have to be diluted in inert gases such as N_2 or CO_2 and therefore the amount of reagent gases is limited.[5–7]

Within this thesis, the role of catalyst design has been investigated in improving catalyst synthesis activity and selectivity towards H_2O_2, as well as inhibiting catalyst degradation activity. Previous studies have focussed on the use of higher metal loadings (typically 5 wt.%).[8,9] In Chapter 3, the effect of the Pd metal loading on H_2O_2 synthesis and degradation activity was investigated. The results showed that the synthesis activity towards H_2O_2 passed through a maximum of 65 $mol_{H2O2}\ kg_{cat}^{-1}\ h^{-1}$ with 0.5wt.%Pd/TiO_2. In comparison, synthesis activity of 64 $mol_{H2O2}\ kg_{cat}^{-1}\ h^{-1}$ was obtained with well-studied 2.5wt.%Au-2.5wt.%Pd/TiO_2 catalyst previously prepared by Edwards *et al.*, which is an established benchmark catalyst for direct synthesis of H_2O_2.[10] This shows that high metal loadings are not required to obtain active catalyst for direct synthesis, and indeed decreasing catalyst metal loading was shown to result in more effective utilisation of H_2, while also significantly decreasing the cost of the catalyst.

More importantly, the 0.5wt.% Pd/TiO_2 catalyst showed no degradation activity towards H_2O_2 (in presence of 4 wt.% H_2O_2) in the absence of any promoters or additives and at ambient temperature. In comparison, the well-established 2.5wt.%Au-2.5wt.%Pd/TiO_2 catalyst exhibits a degradation activity of 417 mol_{H2O2} kg_{cat}^{-1} h^{-1}, and the 5 wt.%Pd/TiO_2 catalyst exhibits a degradation activity of 609 mol_{H2O2} kg_{cat}^{-1} h^{-1}.

Reaction conditions play a crucial role in catalyst performance and, by optimising them, an enhancement in catalyst synthesis activity and H_2O_2 selectivity, as well as decrease in H_2O_2 degradation activity, can be achieved. The effect of H_2/O_2 ratio, total pressure, and solvent composition has been investigated on the synthesis and degradation activity over a 0.5 wt.%Pd/TiO_2 catalyst to determine the optimal reaction conditions and improve catalytic performance. The results showed that the optimal H_2:O_2 ratio is 1:1, which is in agreement with the reaction stoichiometry. At this optimum ratio, the productivity of the catalyst increased from 65 mol_{H2O2} kg_{cat}^{-1} h^{-1} (standard reaction condition) to 70 mol_{H2O2} kg_{cat}^{-1} h^{-1}. The results further suggested that at low H_2:O_2 ratios the reaction is limited by the amount of H_2 present in reactor. On the other hand, high H_2:O_2 ratio can affect the Pd oxidation state during the reaction, as well as change H_2O_2 hydrogenation rate. At high H_2/O_2 ratios Pd was expected to be present as Pd^0 due to reduction of surface PdO by H_2, which was reported to be more active towards H_2O_2 hydrogenation and decomposition than the corresponding PdO catalyst. [6,9,11] No degradation activity was observed over the whole range of different H_2 amounts.

The effect of gas pressure was investigated next using a H_2:O_2 ratio 1:2. The highest activity of 75 mol_{H2O2} $kg_{cat}^{-1}h^{-1}$ was obtained at 650 psi, which was the maximum pressure that could be achieved in our reaction set-up. Due to this limitation a pressure of 580 psi (4 MPa) was further used. These results indicate that the reaction rate is controlled by the amount of H_2 and O_2 available in reaction solution, which can be increased with increasing pressure in reactor set up.[12,13] No degradation activity in presence of 4 wt.% H_2O_2 was observed in the pressure range of 0 – 650 psi.

The effect of solvent (CH_3OH/H_2O) composition on the 0.5 wt.%Pd/TiO_2 catalyst activity was further investigated. In the absence of CH_3OH, a synthesis activity of 32 mol_{H2O2} kg_{cat}^{-1} h^{-1} was achieved over 0.5 wt.%Pd/TiO_2. The introduction of CH_3OH resulted in a significant increase in H_2O_2 synthesis activity up to 65 mol_{H2O2} $kg_{cat}^{-1}h^{-1}$ at a solvent composition of 75% CH_3OH. This can be attributed to higher solubility of H_2 and O_2 in the solvent, as H_2 is far more soluble in CH_3OH than in H_2O. However, a significant decrease in synthesis activity, to 27 mol_{H2O2} kg_{cat}^{-1} h^{-1}, was achieved in a pure methanol solvent. The degradation data showed a more interesting trend. In the absence of CH_3OH, a degradation activity of 84 mol_{H2O2} kg_{cat}^{-1} h^{-1} was obtained in the presence of 4wt.% H_2O_2. With increasing content of CH_3OH, a decrease in degradation was observed and no degradation activity was detected when the concentration of CH_3OH was 50 wt.% or higher. It was suggested that CH_3OH generates hydroxymethyl intermediates on palladium surfaces that efficiently transfer protons and electrons to oxygen to form H_2O_2 and CH_2O, resulting in increased H_2O_2 selectivity.[14] Increasing the amount of CH_3OH increases reagent gas solubility, which results in a higher rate of H_2O_2 formation, up to 80 wt.% of CH_3OH. Use of CO_2 as a diluent was had a beneficial effect on H_2O_2 selectivity due to the formation of carbonic acid.[5,15] As such the presence of H_2O is still required for the formation of carbonic acid, and therefore this can explain the drop in H_2O_2 productivity in pure CH_3OH.[16] The low solubility of reagent gases in H_2O compared to organic solvents is most often emphasised as the main reason to employ alcohols as co-solvents. Recent studies suggest that the role of solvent should be observed in broader context, such as the potential interaction of solvent functional groups and catalyst.[14,17,18]

By optimizing these reaction parameters, it was shown that high rates of H_2O_2 synthesis can be achieved with the 0.5wt.%Pd/TiO_2 catalyst. These results are summarised in Table 5.1 and highlight the need to consider reaction conditions in addition to catalyst design.

Table 5.1: Summary of optimal reaction conditions on synthesis activity of 0.5 wt.%Pd/TiO_2.

H_2/O_2 ratio	**Total pressure [psi]**	**CH_3OH content [%]**	**Productivity [mol_{H2O2} kg_{cat}^{-1} h^{-1}]**
1:1	580	66	70
1:2	650	66	75
1:2	580	75	67
	Standard reaction conditions		
1:2	580	66	65

Reaction conditions: a) H_2O_2 synthesis: 0.01 g catalyst, 0.5 h, ambient temperature, 1200 rpm.

Scanning transmission electron microscopy – high-angle annular dark-field (STEM-HAADF) analysis of the 0.5wt.%Pd/TiO_2 catalyst was carried out to investigate morphology of the catalyst. The fresh sample indicates sub-nanometres particles with average particle size 0.7 nm, with good Pd dispersion. STEM-HAADF analysis of the catalyst after use in the H_2O_2 synthesis reaction revealed an increase in mean particle size to 3.9 nm which suggests the agglomeration of particles during the H_2O_2 synthesis reaction; however, some small sub-nanoparticles are also still observed on the sample.

X-ray photoelectron spectroscopy (XPS) was carried out to investigate any change in Pd oxidation state after use in the H_2O_2 synthesis reaction. In the fresh catalyst, Pd species were present as Pd^{2+}. After use in the H_2O_2 synthesis reaction, a shift in Pd binding energy from

336.7 to 335 eV was observed, which suggests that surface Pd was reduced from Pd^{2+} to Pd^0 (Pd^{2+}:Pd^0 is 1:6.5). An increase in degradation activity towards H_2O_2, from 0 mol_{H2O2} kg_{cat}^{-1} h^{-1} to 331 mol_{H2O2} kg_{cat}^{-1} h^{-1}, was observed upon re-use of the catalyst. This can be related to increased mean particle size of the used catalyst, as shown by STEM-HAADF and partial reduction of Pd^{2+} to Pd^0 after synthesis reaction, as well as loss of Cl species, as evidence by XPS analysis. The addition of Cl promoters can increase selectivity of the catalyst, due to inhibiting hydrogenation of H_2O_2 by changing the catalyst surface charge and by poisoning the active sites of the catalyst on which dissociation of O_2 occurs.[12,18]It has been previously reported that catalysts with a high content of Pd^0 are more active for H_2O_2 degradation than those with a higher Pd^{2+} content.[18–20] There was no significant change in the activity of the catalyst towards H_2O_2 synthesis upon the re-use; however, the increase in degradation activity suggest that gross H_2O_2 synthesis activity is likely to be higher but, because of the increased degradation activity, the final H_2O_2 concentration is similar to the concentration obtained with fresh catalyst.

X-Ray absorption near edge structure (XANES) and Extended X-Ray absorption fine structure (EXAFS) were carried out to investigate the structure and the oxidation state of the 0.5wt.%Pd/TiO_2 catalyst. XANES results showed that the Pd species in the fresh catalyst has a higher average oxidation state than the used catalyst. This means that there was a change in oxidation state of Pd during reaction, which was in keeping with the analysis by XPS. Linear combination fitting (LCF) showed that the Pd speciation is very different between the fresh and used catalysts, with the fresh sample observed to have a contribution of about 1/4 from $PdCl_2$ and 3/4 of PdO, while the used sample is about 2/5 of PdO and 3/5 of Pd^0. The EXAFS fitting of the fresh catalyst showed a contribution from Pd-Cl scattering in the first shell. The coordination number of Pd-O is around 3 and the Pd-Cl is less than 1. There is no significant scattering path beyond Pd-Cl scattering, proving the presence of highly dispersed Pd species on an atomic scale. For the used catalyst, a Pd-O bond of 1.99 ± 0.01 Å with a coordination number 1.5 ± 0.4 was determined. The Pd-Pd bond of 2.74 ± 0.01 Å was close to the Pd-Pd distance in Pd foil, and the coordination number of 5.4 ± 0.5 was a result of larger particles.

Observing no H_2O_2 degradation activity in the presence of 4 wt.% H_2O_2 over a monometallic Pd catalyst is a relatively unusual, particularly in the absence of additives as halides or acids. For industrial application it would be necessary for H_2O_2 degradation activity to remain low even in the presence of high H_2O_2 concentrations and therefore a series of H_2O_2 degradation experiments were carried out with increasing H_2O_2 concentration. No degradation activity was observed with increasing concentration of H_2O_2 up to 16 wt.%, which is the maximum concentration achievable using reaction conditions described in this work.

To investigate the effect on catalyst activity of higher initial concentration of H_2O_2 in the reaction solution, a series of experiments were carried out over a 0.5wt.%Pd/TiO_2 catalyst. The starting concentration of H_2O_2 was shown to have a significant effect on catalyst activity towards further H_2O_2 synthesis. No synthesis activity and low degradation activity were observed in the reaction with H_2O_2 starting concentrations 0.25 wt.% or higher. Synthesis activity of 11 $mol_{H2O2}\ kg_{cat}^{-1}\ h^{-1}$ was obtained with 0.15wt.%H_2O_2, and this synthesis activity increased to 49 $mol_{H2O2}\ kg_{cat}^{-1}\ h^{-1}$ with only 0.05wt.% H_2O_2 in initial solution. The addition of small amount of H_2O_2 (0.05-0.15 wt.%) increased the selectivity towards H_2O_2 from 23% (no H_2O_2 present at the start of the reaction) up to 59%, and significantly decreased the H_2 conversion to 18% with 0.05wt.% H_2O_2 in starting solution. The addition of H_2O_2 might help maintain Pd as Pd^{2+}, which can explain the increase in H_2O_2 selectivity.

The reduction of Pd species from Pd^{2+} to Pd^0 during the synthesis reaction, as shown by XPS, may be a crucial factor responsible for the observed increase in degradation activity of the 0.5wt.%Pd/TiO_2 catalyst upon re-use. To counter the formation of Pd^0, the catalyst was subjected to a range of heat treatments after initial use in the direct synthesis reaction. Applying a re-calcination temperature of 300 ºC resulted in a decrease in catalyst synthesis activity to 57 $mol_{H2O2}\ kg_{cat}^{-1}\ h^{-1}$, as well as complete inhibition of H_2O_2 degradation in presence of 4 wt.% H_2O_2. With further increase in calcination temperature, no degradation activity was observed, but significant decrease in synthesis activity (16 $mol_{H2O2}\ kg_{cat}^{-1}\ h^{-1}$) was obtained. After initial use of the catalyst in the synthesis reaction (the catalyst was dried after reaction prior analysis) a reduction of Pd from Pd^{2+} to Pd^0 was observed, with only 13% of surface Pd in the Pd^{2+} form. After re-calcination of the catalyst, an increase in Pd^{2+} content was observed with increasing temperature. When the re-calcination temperature was 400ºC, all surface Pd was present in Pd^{2+} form. TEM images of the re-calcined catalyst at 300ºC show a significant increase in particle size compared to the fresh catalyst. A mean particle diameter of 4.7 nm, with wide range in particle diameter from smaller particles (up to 3 nm) to larger nanoparticles of 10 nm, was observed. Catalysts re-calcined at 400ºC show slightly higher mean particle diameter, of 6.6 nm, with particles up to 13 nm; however, no degradation activity was observed upon re-use of recalcined catalyst at 300ºC and 400ºC, with similar mean particle diameter as used catalyst without recalcination. These results imply that even larger Pd nanoparticles can exhibit no degradation activity towards H_2O_2 in the presence of 4 wt.% H_2O_2 if the majority of Pd species is present as Pd^{2+}.

The use of a support influences the formation of H_2O_2 as well as competing degradation reactions.[21] Different metal oxides were next used as supports for a monometallic Pd catalyst. Prior to catalyst testing, all the bare supports were tested in synthesis and degradation reaction and no activity towards H_2O_2 formation and degradation was observed. As shown in Table

5.2, catalysts prepared on all phases of TiO_2 showed the highest productivities among the chosen supports and also were shown to be inactive towards H_2O_2 degradation in presence of 4 wt.% H_2O_2. The analogous catalyst prepared on SiO_2 exhibited productivity of 52 mol_{H2O2} kg_{cat}^{-1} h^{-1} and no degradation activity towards H_2O_2. Both the 0.5wt.%Pd/Al_2O_3 and 0.5wt.%Pd/ZrO_2 catalysts showed significantly lower productivities comparing to other catalysts, but more importantly they showed increasing degradation activity towards H_2O_2 in presence of 4wt.% H_2O_2. Lower synthesis activity and increased degradation activity of these supported catalysts can be related to the more basic nature of the support, as it was previously reported that more acidic supports can promote direct synthesis of H_2O_2 and provide much lower degradation rates.[6,21,22]

Table 5.2: H_2O_2 synthesis and degradation testing over 0.5wt.% Pd supported catalysts at ambient temperature made by wet impregnation using different supports.

Support	**Productivity[a] [mol_{H2O2} kg_{cat}^{-1} h^{-1}]**	**Degradation[b] [mol_{H2O2} kg_{cat}^{-1} h^{-1}]**	**Conversion [%]**	**Selectivity [%]**
TiO_2 (P25)	64	0	53	23
anatase	84	0	59	29
rutile	94	0	55	35
SiO_2	52	0	22	52
Al_2O_3	25	50	11	54
ZrO_2	37	82	11	73

Reaction conditions: a) H_2O_2 synthesis: 0.01 g catalyst, 2.9 g of water, 5.6 g of methanol 2.9 MPa 5% H_2/CO_2, 1.1 MPa 25% O_2/CO_2, 0.5 h, ambient temperature, 1200 rpm. **b) H_2O_2 degradation**: 0.01 g catalyst, 0.68 g H_2O_2, 2.9 g of water, 5.6 g of methanol 2.9 MPa 5% H_2/CO_2, 0.5 h, ambient temperature, 1200 rpm.

To investigate the effect of reaction time on catalyst performance, a time-on-line study over the 0.5wt.%Pd/TiO_2 catalyst was carried out. The concentration of H_2O_2 passed through a maximum of 0.14wt.% at 30 min, and decreased with increasing reaction time. This can be attributed to particle agglomeration during the reaction, as well as reduction of Pd^{2+} to Pd^0. No significant change in H_2 conversion and selectivity was observed with increase in reaction time beyond 60 min, indicating catalyst deactivation or insufficient concentration of reagent gases.

Gas replacement reactions partially solve low H_2 concentration limitations by continually replacing H_2 at fixed time intervals. After a 5 gas replacement reaction, a H_2O_2 concentration of 0.38wt.% was achieved. In comparison, H_2O_2 concentration of 1-2 wt.% is obtained during initial stages of AO process, which is further increased up to 70 wt.% by distillation and purification. Freakley *et al*. at reported production of 0.35 wt.% H_2O_2 over the highly selective

2wt.%Sn-3wt.%Pd/TiO_2 subjected to ORO treatment after 3 gas replacements at 2°C.[23] This demonstrates that to achieve higher concentrations of H_2O_2, high metal loadings and extensive heat treatment are not necessary.

5.2 Conclusions for Chapter 4.

In the Chapter 4, the effect of the addition of secondary metals (Au, Sn, Ni) to a Pd catalyst are investigated on catalytic performance towards H_2O_2 synthesis and degradation. It has been shown that the addition of Au to Pd increased synthesis activity up to 0.5 wt.% metal loading, with a synthesis activity of 90 $mol_{H2O2}\ kg_{cat}^{-1}\ h^{-1}$, in comparison to 0.5 wt.%Pd/TiO_2 with synthesis activity of 65 $mol_{H2O2}\ kg_{cat}^{-1}h^{-1}$. The optimal Au: Pd ratio was determined to be 1: 1. The addition of Sn also resulted in an enhancement in synthesis activity, with optimal metal loading of 1 wt.% (1:1 weight ratio) and synthesis activity of 87 $mol_{H2O2}kg_{cat}^{-1}h^{-1}$. In comparison, the addition of Ni at low concentrations initially led to a decrease in synthesis activity, but a further increase in Ni loading (1:1 weight ratio) results in an enhancement in synthesis activity. The addition of Au, Sn and Ni also resulted in an enhancement in H_2O_2 selectivity. The enhancement in catalysts activity and selectivity is attributed to modification of the Pd electronic structure and ensemble effect of Pd-X (X=Au,Sn,Ni) particles.

Time-on-line studies were carried out to maximize the utilisation of H_2 in the gas feed. A H_2O_2 concentration of 0.21 wt.% was produced after 60 min with 0.25 wt.%Au – 0.25 wt.%Pd/TiO_2, as well as 0.25wt.%Pd/TiO_2, and 0.15 wt.% with 0.25 wt.%Sn-0.25 wt.%Pd/TiO_2. However, a further increase in reaction time to 90 min results in a decrease in H_2O_2 concentration over the 0.25 wt.%Au-0.25 wt.%Pd/TiO_2 catalyst, which can be attributed to the partial reduction of Pd^{2+}, as shown by XPS. In comparison, both the 0.25 wt.%Sn-0.25 wt.%Pd/TiO_2 and 0.25 wt.%Pd/TiO_2 catalysts show an increase in H_2O_2 concentrations up to 90 min, achieving 0.15 wt.% and 0.22 wt.% H_2O_2, respectively. The initial rate of H_2O_2 synthesis was calculated at a reaction time where the contribution of H_2O_2 degradation is considered to be negligible (5 min). As shown in Table 5.3, the 0.5wt.%Pd/TiO_2, and 0.25wt.%Sn-0.25wt.%Pd/TiO_2 catalysts have identical initial rates of synthesis, of 4597 $mol_{H_2O_2}mol_{Pd}^{-1}h^{-1}$. In comparison, the 0.25wt.%Au-0.25wt.%Pd/TiO_2 catalyst showed an initial rate of reaction almost twice that of the optimal Pd-only and SnPd catalysts tested in this study.

Table 5.3: Initial rate of synthesis reaction over studied supported catalysts at ambient temperature.

Catalysts	**Rate of reaction [$mol_{H_2O_2}mol_{Pd}^{-1}h^{-1}$]**	**H_2O_2 concentration [wt.%]**
0.25wt.%Pd/TiO_2	4086	0.03
0.5wt.%Pd/TiO_2	4597	0.07
0.25wt.%Au-0.25wt.%Pd/TiO_2	8173	0.07
0.25wt.%Sn-0.25wt.%Pd/TiO_2	4597	0.04

Reaction conditions: 0.01 g catalyst, 2.9 g of water, 5.6 g of methanol 2.9 MPa 5% H_2/CO_2, 1.1 MPa 25% O_2/CO_2, 5 min, ambient temperature, 1200 rpm.

Gas replacement reactions were carried out to maximise the H_2O_2 concentration. After 4 gas replacements, 0.53 wt.% of H_2O_2 was produced over the 0.25 wt.%Au – 0.25 wt.%Pd/TiO_2 catalyst and 0.49 wt.% over the 0.25 wt.%Sn – 0.25 wt.%Pd/TiO_2 analogue. For comparison, 0.53 wt.% H_2O_2 was produced over the previously reported highly selective 2wt.%Sn-3wt.%Pd/TiO_2 that had beensubjected to a sequential heat treatment that consisted of an oxidative (500°C, 3 h, air), reductive (200°C, 2 h, 5% H_2/Ar) and final oxidative (400°C, 4 h, air) step, after 5 gas replacements, under near-identical reaction conditions. [23]

Different amounts of Au, Sn or Ni were added to a 0.25 wt.% Pd/TiO_2 catalyst to prepare catalysts with different secondary metal to Pd ratios and investigate the effect on the catalyst synthesis and degradation activity. The optimal Au: Pd ratio was 1: 1, with a synthesis activity of 90 $mol_{H2O2}kg_{cat}^{-1}h^{-1}$ and degradation activity towards H_2O_2 of 100 $mol_{H2O2}\,kg_{cat}^{-1}\,h^{-1}$ reported. A decrease in synthesis activity was observed with increasing Au: Pd ratio as well as a decrease in degradation activity was also observed with increasing Au content. The maximum synthesis activity of 64 $mol_{H2O2}\,kg_{cat}^{-1}\,h^{-1}$ for the 0.5 wt.% Ni – 0.25 wt.% Pd/TiO_2 catalyst was obtained with a 2:1 Ni:Pd ratio. The SnPd/TiO_2 series showed an increase in synthesis activity with increasing Sn:Pd, ratio with maximum synthesis activity of 111 $mol_{H2O2}\,kg_{cat}^{-1}\,h^{-1}$ achieved with 9:1 ratio. No degradation activity was observed over any of the NiPd and SnPd catalysts in this series.

The best performing catalyst, 2.25 wt.%Sn – 0.25 wt.%Pd/TiO_2, was further investigated through a time-on-line study and gas replacement reactions. Time-on-line studies were carried out at two different temperatures: 2 °C, which is favourable temperature for direct synthesis of H_2O_2; and ambient temperature, which is more desirable temperature for industrial applications. H_2O_2 concentration of 0.27 wt.% was produced after 60 min at ambient temperature, and decreased with further increase in reaction time. An increase in H_2O_2 concentration was observed even after 180 min at 2 °C, up to 0.41 wt.%, highlighting the key role in reaction conditions in achieving optimal catalyst performance. The maximum H_2O_2

concentration observed in this Chapter was 0.69 wt.%, achieved after 5 gas replacement reaction over this catalyst. As a 9:1 Sn:Pd ratio was optimal, a series of SnPd catalysts with this ratio and different metal loading were prepared and results are summarised in Table 5.4. The 2.25 wt.%Sn – 0.25 wt.%Pd/TiO_2 showed the highest synthesis activity in this study.

Table 5.4: Effect of total metal loading on catalyst activity for fixed Sn:Pd metal ratio (9:1) at ambient temperature.

Metal loading [wt.%]	**Productivity[a] [mol_{H2O2} kg_{cat}^{-1} h^{-1}]**	**Degradation[b] [mol_{H2O2} kg_{cat}^{-1} h^{-1}]**	**Conversion [%]**	**Selectivity [%]**
0.625	6	0	2	92
1.25	15	0	4	85
2.5	111	0	51	52
5	86	0	64	27
7.5	72	0	66	23

Reaction conditions: a) H_2O_2 synthesis: 0.01 g catalyst, 2.9 g of water, 5.6 g of methanol 2.9 MPa 5% H_2/CO_2, 1.1 MPa 25% O_2/CO_2, 0.5 h, ambient temperature, 1200 rpm. **b) H_2O_2 degradation**: 0.01 g catalyst, 0.68 g H_2O_2, 2.9 g of water, 5.6 g of methanol 2.9 MPa 5% H_2/CO_2, 0.5 h, ambient temperature, 1200 rpm.

5.3 Future work

Currently, many research groups are utilising semi-batch and flow reactors for the direct synthesis of H_2O_2, instead of batch reactors.[13,24,25] The main advantage of these reactor set ups is limited contact between catalyst, H_2O_2 and H_2, as well as continuous flow of reagent gases, which overcomes the limitation of the batch reactors by replacing the H_2 and O_2 used in the reaction with fresh gas. The future work could concentrate on using catalysts prepared in this work in the semi-batch or flow reactors. As these are more complicated reactor set ups, extensive work will have to be dedicated to optimising different reaction conditions to maximise the synthesis activity and selectivity of the catalysts, and decreasing their degradation activity.

To further investigate the mechanism of direct synthesis as well as improve catalyst design, a more detailed characterisation of the catalysts is required. Especially, characterisation of the catalysts *in situ* during the reaction would present a great deal of information about changes on catalyst surface during the reaction. *In situ* X-Ray Absorption Spectroscopy could determine electronic and structural state of Pd nanoparticles under reaction conditions. The STEM-HAADF microscopy can provide more information about structural changes before and after reaction, and therefore having access to high resolution microscopy immediately after experiments are carried out could be also extremely beneficial.

Use of trimetallic catalyst is another area this work could explore. As shown in Chapter 4, addition of Au to monometallic Pd catalyst enhances the synthesis activity of the catalyst, as well as its degradation activity in presence of 4 wt.% H_2O_2. The results suggest that the increase in H_2O_2 selectivity was due to increased synthesis activity. On the other hand, addition of Sn shows smaller enhancements in synthesis activity, but no degradation activity suggesting that an increase in H_2O_2 selectivity is due to decreased degradation activity. Addition of both metals, Au and Sn, to monometallic Pd catalyst could result in unique catalysts with high synthesis but no degradation activity. A preliminary study was carried out in this work by preparing series of trimetallic AuSnPd catalysts supported on TiO_2 with the fixed content of AuPd, 0.125 wt.%Au-0.125 wt.%Pd/TiO_2, and increasing the amount of Sn. Table 5.5 shows highly active catalysts with no degradation activity in presence of 4 wt.% H_2O_2 can be prepared by combining Au, Sn and Pd. Further optimisation of the metal ratios can result in highly active catalysts.

Table 5.5: H_2O_2 synthesis and degradation testing over trimetallic catalyst at ambient temperature.

Catalyst	**Productivity**[a] **[$mol_{H2O2}\ kg_{cat}^{-1}\ h^{-1}$]**	**Degradation**[b] **[$mol_{H2O2}\ kg_{cat}^{-1}\ h^{-1}$]**
0.125wt.%Au-0.125wt.%Pd-0.125wt.%Sn/TiO_2	52	11
0.125wt.%Au-0.125wt.%Pd-0.25wt.%Sn/TiO_2	41	16
0.125wt.%Au-0.125wt.%Pd-0.5wt.%Sn/TiO_2	47	7
0.125wt.%Au-0.125wt.%Pd-0.75wt.%Sn/TiO_2	66	0
0.125wt.%Au-0.125wt.%Pd-1.5wt.%Sn/TiO_2	85	0
0.125wt.%Au-0.125wt.%Pd-2.25wt.%Sn/TiO_2	19	0

Reaction conditions: a) H_2O_2 synthesis: 0.01 g catalyst, 2.9 g of water, 5.6 g of methanol 2.9 MPa 5% H_2/CO_2, 1.1 MPa 25% O_2/CO_2, 0.5 h, ambient temperature, 1200 rpm. **b) H_2O_2 degradation**: 0.01 g catalyst, 0.68 g H_2O_2, 2.9 g of water, 5.6 g of methanol 2.9 MPa 5% H_2/CO_2, 0.5 h, ambient temperature, 1200 rpm.

Different protocols can be followed, during preparation of trimetallic catalysts by wet impregnation, as showed in Table 5.6. A one step method refers to standard methodology in which all the metal precursors are mixed before support is added; in two step preparation, the 2.25 wt.%Sn/TiO_2 was prepared first, following methodology described in Chapter 2, and then the catalyst was dried on air (uncalcined) or calcined at 400°C. In the second step, the Au and Pd precursors are mixed and, once the temperature reaches 65°C, the 2.25 wt.%Sn/TiO_2 was added. Once the catalyst was dried (16h, 95°C), it was then calcined at 200°C or 400°C. As shown in Table 5.6, the different steps in preparation can have significant effect on catalyst synthesis activity and therefore future investigation is needed.

Table 5.6: H_2O_2 synthesis and degradation testing over 0.125wt.%Au-0.125wt.%Pd-2.25wt.%Sn/TiO_2 prepared by two step impregnation.

Catalyst	**Productivity[a]** **[mol_{H2O2} kg_{cat}^{-1} h^{-1}]**	**Degradation[b]** **[mol_{H2O2} kg_{cat}^{-1} h^{-1}]**
One step	19	0
Uncalcined – calcined 400°C	24	0
Calcined 400°C – calcined 200°C	117	0
Calcined 400°C – calcined 400°C	46	0

Reaction conditions: a) H_2O_2 synthesis: 0.01 g catalyst, 2.9 g of water, 5.6 g of methanol 2.9 MPa 5% H_2/CO_2, 1.1 MPa 25% O_2/CO_2, 0.5 h, ambient temperature, 1200 rpm. **b) H_2O_2 degradation**: 0.01 g catalyst, 0.68 g H_2O_2, 2.9 g of water, 5.6 g of methanol 2.9 MPa 5% H_2/CO_2, 0.5 h, ambient temperature, 1200 rpm.

Edwards *et al.* reported that acid pre-treatment of a carbon support can switch off sequential degradation of H_2O_2, and therefore achieve a high selectivity.[8] Pre-treatment of different supports with acids, or different solvents, can have similar effects resulting in highly active and selective catalysts. It is possible to prepare solid acids by adding different functional groups on the support.[26] Supports with different functional group can replace additives and promoters, presenting a cheaper reusable alternative that is easily separated from product and does not produce additional waste. Use of more structured supports could be also interesting alternative in which Pd nanoparticles could be incorporated within structure or located inside the structure. This may stop Pd particles from migrating on the surface and agglomerating into bigger nanoparticles.

5.4 References

1 Q. Chen, *Chem. Eng. Process. Process Intensif.*, 2008, **47**, 787–792.

2 J. M. Campos-Martin, G. Blanco-Brieva and J. L. G. Fierro, *Angew. Chemie - Int. Ed.*, 2006, **45**, 6962–6984.

3 Evonik, *The Modern Chemist's Guide to Hydrogen Peroxide and Peracetic Acid*, 2018.

4 C. Samanta, *Appl. Catal. A Gen.*, 2008, **350**, 133–149.

5 J. K. Edwards, S. J. Freakley, A. F. Carley, C. J. Kiely and G. J. Hutchings, *Acc. Chem. Res.*, 2013, **47**, 845–854.

6 J. K. Edwards, S. J. Freakley, R. J. Lewis, J. C. Pritchard and G. J. Hutchings, *Catal.*

Today, 2015, **248**, 3–9.

7 A. Santos, R. J. Lewis, G. Malta, A. G. R. Howe, D. J. Morgan, E. Hampton, P. Gaskin and G. J. Hutchings, *Ind. Eng. Chem. Res.*, 2019, **58**, 12623–12631.

8 J. K. Edwards, B. Solsona, E. N. N, A. F. Carley, A. a Herzing, C. J. Kiely and G. J. Hutchings,*Science*, 2009, **323,**1037–1041.

9 V. R. Choudhary and P. Jana, *Appl. Catal. A Gen.*, 2009, **352**, 35–42.

10 J. K. Edwards, E. Ntainjua N, A. F. Carley, A. A. Herzing, C. J. Kiely and G. J. Hutchings, *Angew. Chemie Int. Ed.*, 2009, **48**, 8512–8515.

11 V. R. Choudhary, C. Samanta and T. V. Choudhary, *Appl. Catal. A Gen.*, 2006, **308**, 128–133.

12 Y. Yi, L. Wang, G. Li and H. Guo, *Catal. Sci. Technol.*, 2016, **6**, 1593–1610.

13 S. J. Freakley, M. Piccinini, J. K. Edwards, E. N. Ntainjua, J. A. Moulijn and G. J. Hutchings, *ACS Catal.*, 2013, **3**, 487–501.

14 J. S. Adams, A. Chemburkar, P. Priyadarshini, T. Ricciardulli, Y. Lu, V. Maliekkal, A. Sampath, S. Winikoff, A. M. Karim, M. Neurock and D. W. Flaherty, *Science*, 2021, **371**, 626–632.

15 J. K. Edwards, A. Thomas, A. F. Carley, A. A. Herzing, C. J. Kiely and G. J. Hutchings, *Green Chem.*, 2008, **10**, 388–39.

16 M. Piccinini, E. Ntainjua N., J. K. Edwards, A. F. Carley, J. A. Moulijn and G. J. Hutchings, *Phys. Chem. Chem. Phys.*, 2010, **12**, 2488–2492.

17 V. Paunovic, V. V. Ordomsky, V. L. Sushkevich, J. C. Schouten and T. A. Nijhuis, *ChemCatChem*, 2015, **7**, 1161–1176.

18 D. W. Flaherty, *ACS Catal.*, 2018, **8**, 1520–1527.

19 M. Sankar, Q. He, M. Morad, J. Pritchard, S. J. Freakley, J. K. Edwards, S. H. Taylor, D. J. Morgan, A. F. Carley, D. W. Knight, C. J. Kiely and G. J. Hutchings, *ACS Nano*, 2012, **6**, 6600–6613.

20 S. Melada, R. Rioda, F. Menegazzo, F. Pinna and G. Strukul, *J. Catal.*, 2006, **239**, 422–430.

21 E. Ntainjua N., J. K. Edwards, A. F. Carley, J. A. Lopez-Sanchez, J. A. Moulijn, A. a. Herzing, C. J. Kiely and G. J. Hutchings, *Green Chem.*, 2008, **10**, 1162.

22 S. Park, J. Lee, J. H. Song, T. J. Kim, Y. M. Chung, S. H. Oh and I. K. Song, *J. Mol. Catal. A Chem.*, 2012, **363**–**364**, 230–236.

23 S. J. Freakley, Q. He, J. H. Harrhy, L. Lu, D. A. Crole, D. J. Morgan, E. N. Ntainjua, J. K. Edwards, A. F. Carley, A. Y. Borisevich, C. J. Kiely and G. J. Hutchings,*Science*, 2015, **351**, 279–296.

24 D. A. Crole, R. Underhill, J. K. Edwards, G. Shaw, S. J. Freakley, G. J. Hutchings and R. J. Lewis, *Philos. Trans. R. Soc. A Math. Phys. Eng. Sci.*,2020, **378.**

25 P. Tian, X. Xu, C. Ao, D. Ding, W. Li, R. Si, W. Tu, J. Xu and Y. F. Han, *ChemSusChem*, 2017, **10**, 3342–3346.

26 P. Gupta and S. Paul, *Catal. Today*, 2014, **236**, 153–170.